AGRO-GEOPHYSICAL ASSESSMENTS OF SPATIAL VARIABILITY IN AGRICULTURAL SOIL PROPERTIES IN IBADAN, SOUTHWESTERN NIGERIA

BY

ABAYOMI ADESOLA, OLAOJO

B.Sc. Geology, M.Sc. Applied Geophysics (Ibadan)

Matric No.: 128278

A Thesis in the Department of Geology,
Submitted in the Faculty of Science
in partial fulfillment of the requirements for the Degree of

DOCTOR OF PHILOSOPHY
of the

UNIVERSITY OF IBADAN

September 2021

CERTIFICATION

I certify that this work was carried out by Mr. A.A. Olaojo (128278) in the Department of Geology, University of Ibadan, Ibadan

…….

Supervisor

M.A. Oladunjoye

B.Sc. (Ado-Ekiti), M.Sc., Ph.D. (Ibadan)

Department of Geology,

University of Ibadan, Nigeria

DEDICATION

This research is solely dedicated to my late father, Mr. Jacob Adebayo OLAOJO (ACA) who passed unto glory on 11th June, 2018 (23:50pm). His relentless efforts, enthusiasm and jokes will be missed. He is the pillar on whom I rest for comfort.

ACKNOWLEDGEMENTS

I sincerely appreciate the Almighty God for HIS infinite mercy upon me and divinely ordering my steps at various stages of this research. I am eternally grateful for the uncommon strength received when I was sapped, and I am greatly indebted for the knowledge, wisdom and understanding of the research concept.

I am highly favoured to have Dr. M.A. Oladunjoye as my supervisor, mentor and encourager. He contributed immensely to the success of this work; he was available during the field inspection which I considered a rare privilege that can be accorded to a research student. He was available at all the stages of this research, contributing immensely to the success of this innovative work. I pray that the dews of heaven continue to shower on you and your entire household.

The sincere efforts of the Head of Deparment, Prof. O.A. Okunlola are well appreciated for the value added to the proposal and the final stages of the presentation. Many thanks to Prof O.A. Ehinola (the former Head of Department) for his support and admonition are second to none. The efforts and contribution of Dr. A.S. Olatunji are highly appreciated, adding value to this research content. The encouragement together with warmth support of Dr. I.A. Oyediran is a pivot to ease the research stress for every research student most especially during seminar. All the efforts of my teachers and lecturers right from the undergraduate days to this present moment are greatly valued, on whose shoulders I stood to acquire wealth of knowledge, wisdom and understanding of geological complexes. I say a big thank you; these include late Prof. A.A. Elueze, Prof. A.I. Olayinka, Prof. G.O. Adeyemi, late Prof. A.F. Abimbola, Prof. M.N. Tijani, Prof. M.E. Nton, late Dr. I.M. Akaegbobi, Dr. O.A. Boboye, Dr. A.T. Bolarinwa, Dr. A.A. Omitogun, Dr. O.C. Adeigbe, Dr. O.O. Osinowo and Dr. M.A. Adeleye. I pray that the Lord Almighty in His infinite mercy crowns and rewards your hard work in Jesus name.

The support received from my parents, late Mr. J.B. Olaojo and Mrs C.B. Olaojo cannot be quantified at every stage of my career, and I pray that your labour of love shall be rewarded and pray everlasting rest for my dad. Good wishes and prayers of my siblings are appreciated, namely; Engr. A.A. Olaojo, Mrs A.A. Ajayi, Mr A.A. Olaojo (ACA) and Mr.

O.A. Olaojo. I would be an ingrate without mentioning the names of my friends who have been supportive during this research, namely; ‘Yemi Oyerinde, Dr. Saheed Adejumo, Adefehinti Afolabi, ‘Seun Sanuade, Dr. Maaruf Hussain and Afebu Kenneth. The wonderful and ever dynamic field team is greatly honoured for their relentless efforts during the tedious and stressful data acquisition; the field team includes ‘Yomi, Afo, Ken, Segun, Kuti, Pastor Johnson, Nnadi Chibuike and Ocheja Busayo. The unflinching support received from the host community (CRIN) is enormous, as observed when the staff of the Institute went on strike and I was allowed into the research farms to continue the data acquisition. Some of the members of the host community who facilitated the usage of the farms and data gathering include Dr. Olubamiwa (Ag. Director of CRIN), Mr. Sobowale, Mr. Oka-Irabor, Mr. Akanbi, Mr. Francis and the security outfit of the institute.

My profound appreciation also goes to Dr. R.A. Isibor, the former Acting Head, Department of Earth Sciences, Ajayi Crowther University Oyo, for granting the permission to embark on field work despite the tight restriction on staff movement out of the university. Many thanks to Prof. O. Oshin, Dr. Fasiku, Mr. Falana, Mrs. Kehinde and Mr. Adelowo for their advice and assistance rendered; useful hints on the laboratory analysis and release of helpful resources. The concern of Revd S.Ade Ayoola and Revd Ayo Olanrewaju is quite overwhelming, am grateful for having you as my spiritual mentors; thanks for your prayers and words of encouragement.

To my loving and caring wife, Mrs. O.R. Olaojo, as well as Ayomipo and Adesewa Olaojo (my children), I thank you for your patience and endurance in the course of this financial and mental tasking research. I know that I have deprived you of the leisure and adequate financial up keep but when I was down you really motivated me to continue and that the end is near. I thank you for understanding that research has its few short comings and ample merits, I pray that we shall enjoy the benefits together in good health and sound mind in Jesus Christ name.

ABSTRACT

Agricultural soil nutrients variability assessment for sustainable crop production has usually been through soil geochemical/chemical analyses which are laborious and expensive, thus necessitating the need for faster and cheaper alternatives. The application of geophysical methods to resolve this has gained acceptability globally. However, there is paucity of data from Nigeria on the application of geophysical investigation for soil properties variability determination. Therefore, this investigation was designed to use geophysical methods to assess the physical properties that can substitute for geochemical analysis of agricultural soil nutrients in Ibadan, southwestern Nigeria.

The investigation was at the research farms of the Cocoa Research Institute of Nigeria, Ibadan. The Apparent Electrical Conductivity (EC_a) and Volumetric Water Content (VWC) of the soils were determined using resistivity earth-meter and VG-meter-200 moisture-meter. The 912 (cocoa farm) and 700 (kola field) points were classified into zones of Low ECa (LEC_a), Moderate ECa (MEC_a) and High EC_a, (HEC_a) on which other investigations were based. Thermal Conductivity (TC), Volumetric Heat Capacity (VHC) and Thermal Diffusivity (TD) at 90 (Cocoa farm) and 67 (Kola field) points were determined by KD2PRO analyser. The EC_a, VWC, TC, VHC and TD were assessed in both wet and dry seasons. Falling and constant head permeability tests were conducted on duplicated ten cored soil samples per farmland for water infiltration assessment. Soil textural classes were established in the cocoa (54-sample) and kola (42-sample) farms using Bouyoucos method. Soil (20-sample/farmland) were analysed for pH, Electrical Conductivity (EC), organic carbon, total nitrogen, available phosphorus, acidity, Na, Mg, K, Ca and Cation Exchangeable Capacity (CEC) using standard soil science procedures. Soil mineralogy (6-sample/farmland) was determined using X-ray diffractometer. All investigations were limited to the root zone (0.3 m).

The soils EC_a, VWC, TC, VHC and TD were 10-545 µS/cm; 2-69%; 0.700-2.715 W/mk; 0.760-4.578 mJ/m^3k and 0.351-1.994 mm^2/s, respectively. The soils were categorised into LEC_a (1-49 µS/cm), MEC_a (50-99 µS/cm), and HEC_a (>100 µS/cm). The HEC_a had high TC (1.668-2.148 W/mk), high VHC (2.604-2.721mJ/m^3k), and low TD (0.622-0.835

mm^2/s), while LEC_a had inverse distribution, indicating that heat energy retained in soils aided mobility of ions. Soils' permeability ranged from $6.2x10^{-6}$-$3.97x10^{-3}$ cm/sec across the field. Infiltration rate was low (HEC_a), moderate (MEC_a) and rapid (LEC_a) accounting for the moisture variation. Texturally, the soils were sandy loam (HEC_a/MEC_a/LEC_a), loamy sand (MEC_a/LEC_a) and sandy clayey loam (HEC_a). The soils' pH, EC, organic carbon, total nitrogen, available phosphorus, acidity, Na, Mg, K, Ca, CEC ranged from 6.1-7.6; 30-180 µS/cm; 0.270-1.667%; 0.03-0.17%; 3.50-12.71 mg/kg; 0.32-1.20 cmol/kg; 0.15-0.42 cmol/kg; 0.25-2.84 cmol/kg; 0.13-1.33 cmol/kg; 0.46-5.84 cmol/kg and 1.92-10.33 cmol/kg, respectively. The saturation of basic cations in HEC_a (81.38-87.73%), MEC_a (73.24-81.82%) and LEC_a (71.80-77.87%) indicate that HEC_a had more nutrients than others. Kaolinite (4.7-41.2%), microcline (6.8-24.6%) and quartz (14.3-67.2%) were the main minerals in the soils. The HEC_a had low quartz (22.5-41.3%) and microcline (9.85-15.05%), but high kaolinite (31.1-37.6%).

Soil physical properties from geophysical methods were effective in evaluating the spatial agricultural soil nutrient variability. This method can therefore be adopted for cost effective agro-soil evaluation.

Keywords: Electrical conductivity, volumetric water content, thermal properties, soil permeability

Word count: 498

TABLE OF CONTENTS

LIST OF FIGURES

LIST OF TABLES

CHAPTER ONE

INTRODUCTION

1.1 Background to the Study

Soil is developed from the parent rock material which is influenced by the climatic condition, topography and living organisms acting on it; and tends to exhibit varying textural classes based on the mineral composition of the parent rocks (McCauley *et al.*, 2005; Botta, 2015 and Jaja, 2016). Thin sectioning of rock serves as an avenue to investigate the optical properties of mineral present in order to determine the possible rock type. Mineral identification is based on the fact that minerals in rock exhibit specific texture and colour which is deduced from their optical properties. The rock's mineralogy dictates the mineral contents and colour of soil being derived from it which in turn influences the soil nutrient capacity.

Agricultural practices have evolved from primitive means of farming to mechanized form, despite this improvement; agricultural fields are underutilised which invariably affects production. Agricultural production causes changes in soil which vary in space and time; this requires a continuous and precise spatial evaluation of physical and chemical properties of the soil. Conventional farming practices often treat an agricultural field evenly, disregarding the intrinsic variability of soil and crop conditions between and within fields; uniform management is not the most effective management plan (Corwin and Lesch, 2005a and Moral *et al.,* 2010).

Site-specific management or precision agriculture ensures that the rate of application of variables on an agricultural field is effectively managed such that uniform application of input is discouraged in order to address potential yield-limiting factors within the farm zones (Fraisse *et al*., 2001). Precision agriculture involves crop management with respect to spatial variability (Costa *et al.,* 2014; Carvalho *et al.*, 2016 and Khadka *et al.*, 2018). Corwin and Lesch (2005a) reported that spatial variation observed in crops is due to

complex interaction of biological factor (earthworm, pest and microbes), anthropogenic factor (soil compaction, leaching effect), edaphic factor (soil texture, nutrients, salinity and organic matter), climatic factor (rainfall, temperature and relative humidity) and topographic factor (elevation and slope).

Tremendous effort has been achieved in the field of geophysics as a useful tool in precision agricultural practices which has been reported to be cost effective, efficient and rapid approach of evaluating the soil attributes in order to evaluate its productive capabilities (Allred and Smith, 2010 and Corwin and Lesch, 2013). The dominant geophysical techniques employed in agricultural soil appraisal include resistivity, electromagnetic and ground-penetrating radar (Corwin *et al*., 2003; Samouëlian *et al.*, 2005; Brevik *et al.*, 2006; Lambot *et al.*, 2008; Oleschko *et al.*, 2008; Cassiani *et al.*, 2009; Allred and Smith, 2010; Moral *et al.*, 2010 and Ekwue and Bartholomew, 2011). The cost of geochemical assessment is enormous, a comprehensive soil assessment may be difficult to achieve due to the necessity of many soil samples which invariably limits denser sampling and results in the production of less accurate assessment maps due to cost of analysis (Moral *et al.*, 2010 and Costa *et al.*, 2014). Indirect approach via apparent electrical conductivity (EC_a) serves as an alternative for dense sampling and provides an avenue to lower the cost, coupled with good correlation with soil variables (Costa *et al.* 2014). Soil electrical conductivity is useful in assessing soil mineralogy, soil texture, nutrient, temperature, field holding capacity, chemical properties, soil moisture; these variables play vital role in plant's development.

Soil apparent electrical conductivity has wide applications in agronomy and soil science (Ekwue and Batholomew, 2011; Corwin and Lesch, 2013; Molin and Faulin, 2013 and Siqueira *et al.*, 2014). Soil unit consists of a three-phase system: solid (minerals and organic matter), air and water (Schoonover and Crim, 2015). With respect to electric current conduction, soil-water is the most important phase (Amidu and Olayinka, 2006 and Amidu and Dunbar, 2007). Flow of electrical charges through a material enables conduction of charged particles; soil also displays electrical properties based on its physical and chemical properties such as texture, water content (Samouëlian *et al.*, 2005). Soil electrical conductivity (EC) in agriculture field assessment has transformed from soil salinity tool to mapping the spatial variability of soil physico-chemical properties in analyzing soil quality, transport model and site specific management (Corwin and Lesch, 2005b).

Field acquisition of soil apparent electrical conductivity (EC_a) is simple and inexpensive which can be correlated with the other soil properties such as soil texture, cation exchange capacity, drainage conditions, organic matter level, salinity, water holding capacity, temperature and elevation (Grisso *et al.*, 2009 and Siqueira *et. al.*, 2014). Efforts have been made to characterize the physical and chemical soil variability over the years using apparent electrical conductivity (EC_a) in delineating management zones (Corwin *et al.*, 2006 and Costa *et al.,* 2014). Fraisse *et al.* (2001) reported that soil management zones can be delineated for site-specific management using geostatistical interpolation method to generate spatial distribution of soil attributes from series of point measurements.

Electrical conductivity of soil depends on soil mineralogy, particle size distribution, porosity, salinity level, cation exchange capacity (CEC), distribution of pore size, connectivity of the pore, water content and temperature (Corwin and Lesch, 2005a; Khattak and Hussain, 2007; Bai *et al.,* 2013; Brillante *et al.,* 2015 and Hawkin *et al.,* 2017). Moore *et al.* (2008) reported that electrical conductivity (EC) depends on the mobility of charged ions which rest solely on their ionic sizes and charges, both the ionic mobility and EC depend on temperature variation having effect on water viscosity. Electrical conductivity of soil takes place via bulk and surface conductions in the interconnected pore spaces and surface charges of soil (Sriraam *et al.,* 2016). Rise in soil temperature leads to an increase in kinetic energy agitating the water molecules (Friedman, 2005; Bai *et al.,* 2013 and Curado *et al.,* 2013).

Productivity of crops is dependent on soil moisture, soil texture, temperature, chemical properties, field holding capacity, soil nutrients, biological factor, anthropogenic factor, climatic factor, topographic factor and edaphic factor (Corwin and Lesch 205; Lipiec *et al.*, 2013; Chen *et al.*, 2015 and Dong *et al.*, 2016). Rise in soil's temperature tends to decrease the viscosity of its water content, thereby increasing the mobility of the ions due to dissociation of molecules in it. Electrical conductivity of subsurface materials is influenced by temperature variation (Brevik *et al.*, 2004; Amidu and Dunbar, 2007; USDA, 2011 and Bai *et al.*, 2013).

Soil thermal properties (thermal conductivity, thermal diffusivity and specific heat) are of great magnitude in civil/electrical engineering projects and agriculture (Abu-Hamdeh, 2001; Dec *et al.*, 2009, and Oladunjoye and Sanuade, 2012) where heat is

being conveyed via the soil mass. Variability of soil temperature in different soil types is due to the soil structure and texture despite same amount of solar energy received and this plays a crucial role in seed growth (Tessy and Renuka, 2008) and soil moisture greatly affect thermal properties (Shein and Mady, 2016). Biological processes involving water and nutrient uptake by plant root, germination, organic matter decomposition and entire plant growth are temperature dependent (Dec *et al*., 2009).

Soil texture is a vital tool influencing the relationship between soil and water, gas exchange, CEC, organic matter content and plant nutrient required for its growth (Khattak and Hussain, 2007 and Ritchey *et al.*, 2015). Soil texture is derived from the percentage composition of clay, silt and sand (Wayne *et al.*, 2007; Botta, 2015 and Ritchey *et al.*, 2015). Soil texture is a vital property which is not wholly subjected to change, thus maintaining its attributes, it is related to drainage capability and it's potential to store soil nutrient which in turn influence crop productivity (Jaja, 2016).

Adewole and Adeoye (2014) reported that Africa's rainfall pattern is torrential which is responsible for the leaching of soil nutrient beyond root zone and discourage blanket use of fertilizer which may be injurious to plant. Plant essential nutrients are hydrogen, oxygen, carbon, nitrogen, phosphorus, potassium, calcium, iron, magnesium, sulphur, manganese, zinc, boron, copper, chlorine, and molybdenum; and they have to be available for plant consumption in adequate proportion in order not to limit crop growth (FAO, 2008). Electrical conductivity (EC) has been reported by USDA (2011) to be a functional tool in soil productivity assessment, such that high EC value has been linked with high concentrations of P, K, Ca, Mg, Mn, Zn, and Cu and nitrate. Soil pH is the measure of hydrogen ions concentration in soil solution, measuring soil acidity or alkalinity (Botta, 2015). Soil pH affects the microbial activities, availability and balance of necessary soil nutrient for plant uptake (Wodaje and Abebaw, 2014; Botta, 2015; Olorunfemi *et al.*, 2018 and Qing *et al.*, 2018).

The clay minerals play vital role in their ability to adsorb cations onto their surfaces and determine the quantity of cation exchange capacity sites. Soil properties are determined by the nature and proportion of clay fraction, it comprises clay minerals, crystalline mineral such as quartz, iron, aluminium oxide and hydroxide, and organic compounds (Al-Ani and Sarapää, 2008). X-ray diffraction (XRD) studies had been found useful for both qualitative and quantitative assessment of geological samples

(Elueze *et al.,* 2015; Zhou *et al.,* 2018 and Bolarinwa *et al.,* 2019), environmental studies (Oyediran and Adeyemi, 2012), thin films (Widjonarko, 2016). Exchangeable cations are electro-statically bound or attached to the clay surface, although few anions are in a diffuse layer due to electrostatic repulsion (Al-Ani and Sarapää, 2008).

1.2 Problem Statement

Visual inspection of the cacao and kola research farms at Cocoa Research Institute of Nigeria (CRIN) revealed that the pod production rate of cacao plants varied significantly from one tree to another that were grown at same period. Conspicuous uneven growth rate of kola nut crops was also noticed despite the fact that they were planted at the same time. There is no clear distinction of surface soil distribution on which these crops were cultivated, thus, prompting the need to investigate the possible source(s) of essential soil attributes at the root zone responsible for the varying performances of these crops. The use of geochemical assessment of agricultural soil has been the norm in Nigeria, which is time consuming coupled with cumbersome laboratory analyses. To date, adapting geophysical approach to determine agricultural soil productivity and its long-term performance is scarce in this country, and the number of publications on this subject is rare in Nigeria. This study would serve as guide on the applicability of physical parameters to evaluate agricultural field with a target of increasing productivity.

1.3 Justification of the Study

Assessing the soil nutrients inconsistency via soil geochemical/chemical analyses for sustainable agricultural crop production are laborious and expensive, thus necessitating the need for faster and cheaper alternatives. The application of geophysical methods to resolve this has gained acceptability globally. However, there is paucity of data from Nigeria on the application of geophysical investigation for soil properties variability determination.

This research arose from the observations made on some of the cacao trees producing fewer cocoa pods as compared with others having higher number of pods; the cacao trees within the farm were planted at same season or time (Fig. 1.1). The trees that were producing fewer pods during rainy season were completely dried up in the dry period, this resulted in cutting down of some of these trees by the farm manager with a

Figure 1.1: A representation of withered and healthy cacao trees during dry season

focus of planting new cacao around this section (Fig. 1.2). It was also discovered that some of the kola trees were characterized with stunted growth with respect to other kola trees cultivated at same period (Figs. 1.3 and 1.4).

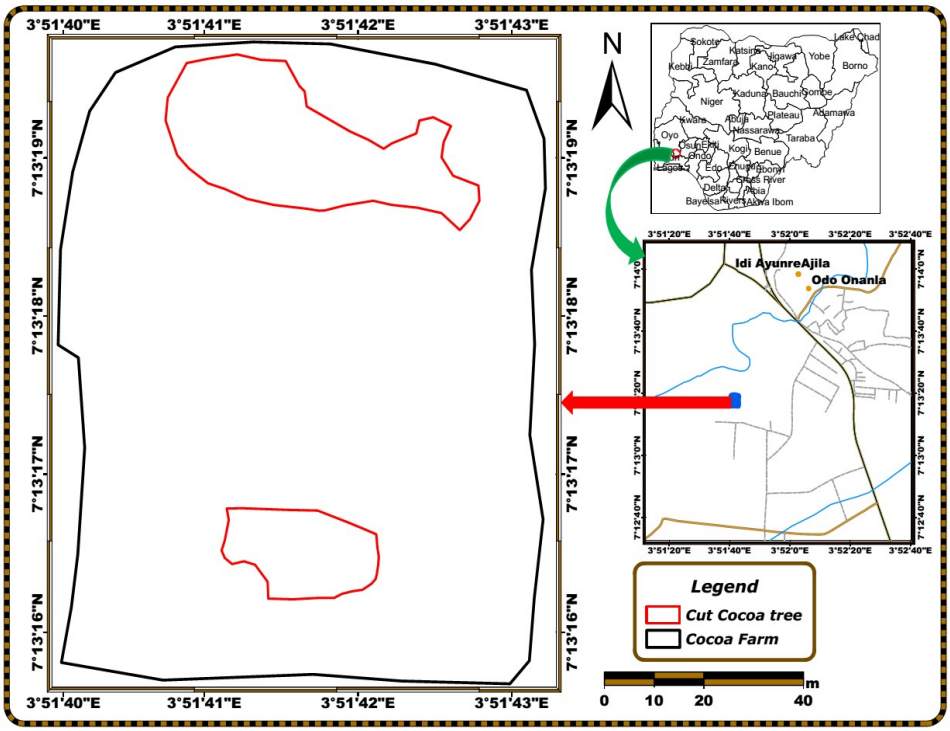

Figure 1.2: Segments of cacao farm with the cut section of unproductive cacao trees.

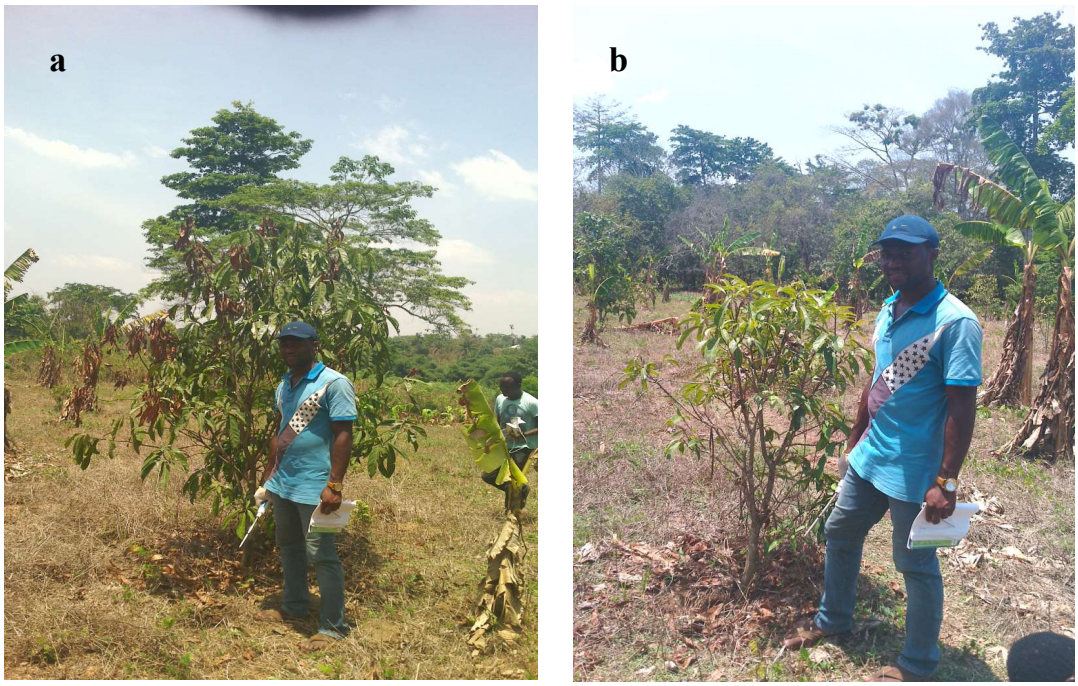

Figure 1.3: Differential growth rates (**a**-healthy growth; **b**-stunted growth) of kola trees

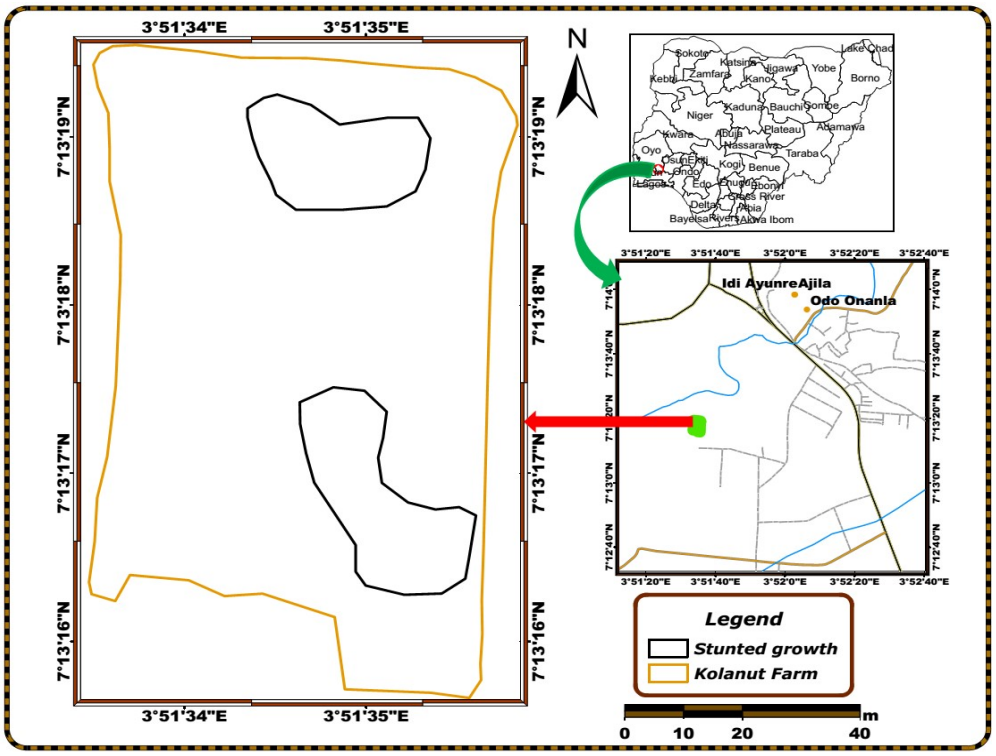

Figure 1.4: The sections with stunted growth of kola trees.

1.4 Aim and Objectives of the Study

Aim

This study is aimed at evaluating agricultural soil using physical parameters to evaluate its productivity status.

Objectives

(i) To establish the rock type underlying the research farms.

(ii)To test the effectiveness of electrical resistivity technique, in establishing the inconsistency of soil properties across the crop fields.

(iii) To determine the soil thermal properties at different crop fields.

(iv) To establish the influence of soil permeability on productivity.

(v) To establish the soils textural classification within the field.

(vi) Establishment of geochemical analysis as a corroborative tool to geophysical technique.

(vii) To ascertain the mineralogical components of soil in the productive and non-productive regions.

(viii) To delineate soil productivity zones in the research farms.

1.5 Significance of the Study

The essence of this study is to determine the efficacy of soil apparent electrical conductivity survey in characterising soil spatial variability, serving as a useful proxy to geochemical determination of soil attributes, speed of data acquisition, and coverage of more data stations which will be costlier in geochemical assessment. To infer the soil's moisture content, soil's textural variation, permeability and soil's thermal variation based on the soil apparent electrical conductivity. Also to discourage uniform treatment of agricultural fields being the practice in convectional farming, which is cost effective by making resourceful use of agrochemicals and maximizing production output of crops.

1.6 Scope of the Study

This research is centered on evaluating the physical parameters responsible for decline in productivity rate of some cash crops grown at Cocoa Research Institute of Nigeria (CRIN); both geophysical and geochemical methods were adopted for this work. The following approaches were used to achieve the set goals.

(i) Reconnaissance survey of the study area was established.

(ii) Review of relevant works.

(iii) Geo-referencing of the study area on the base map using Global Positioning System (GPS) to establish its geometry.

(iv) Detailed electrical resistivity surveying and soil moisture distribution assessment while some stations were selected for thermal properties estimation, soil textural classification, geochemical and mineralogical appraisal analyses based on the results of the electrical conductivity of the subsurface soil within the study area.

(v) Interpretation of the acquired data.

(vi) Detailed reporting of the findings.

1.7 Location and Accessibility of the Study Area

The research farms lie within Cocoa Research Institute of Nigeria, Ibadan (Fig. 1.5), two farms were engaged for the study, these include cacao farm which lies between Latitudes 7˚13′15.9″N and 7˚13′19.6″N, and Longitudes 3˚51′40.1″Eand 3˚51′43″E whereas the kola plot is situated between Latitudes 7˚13′15.7″N and 7˚13′19.9″N, and Longitudes 3˚51′33.5″E and 3˚51′35.8″E.

The research farms are accessible by road from the gate of the institute which leads to the study area, consequently made the accessibility of the study area easier. The area extent of the portion studied in the cacao farm is 7,722 m^2 while kola farm is 6,300 m^2. The cacao field was established in 2000 while kola plantation was established in 2010.

1.8 Relief and Drainage System of the Study Area

The topography within the study vicinity is gentle and nearly flat with some exposure of rocks at the office complex and around the kola farm. The topographical height above the sea level varies between 116m and 136 m at the cacao farm whereas it ranges from 120 m to 138 m for the kola plot. Idi-Ayunre environ is drained by Odo-Ona Kekere River flowing northeast-southwest direction and network of rivers around Idi-Ayunre displayed dendritic drainage pattern. Odo-Ona Kekere River is slow flowing and its volume varies with season, having the highest volume of water during the peak of the rainy season (April to October) and a reduction in volume during the

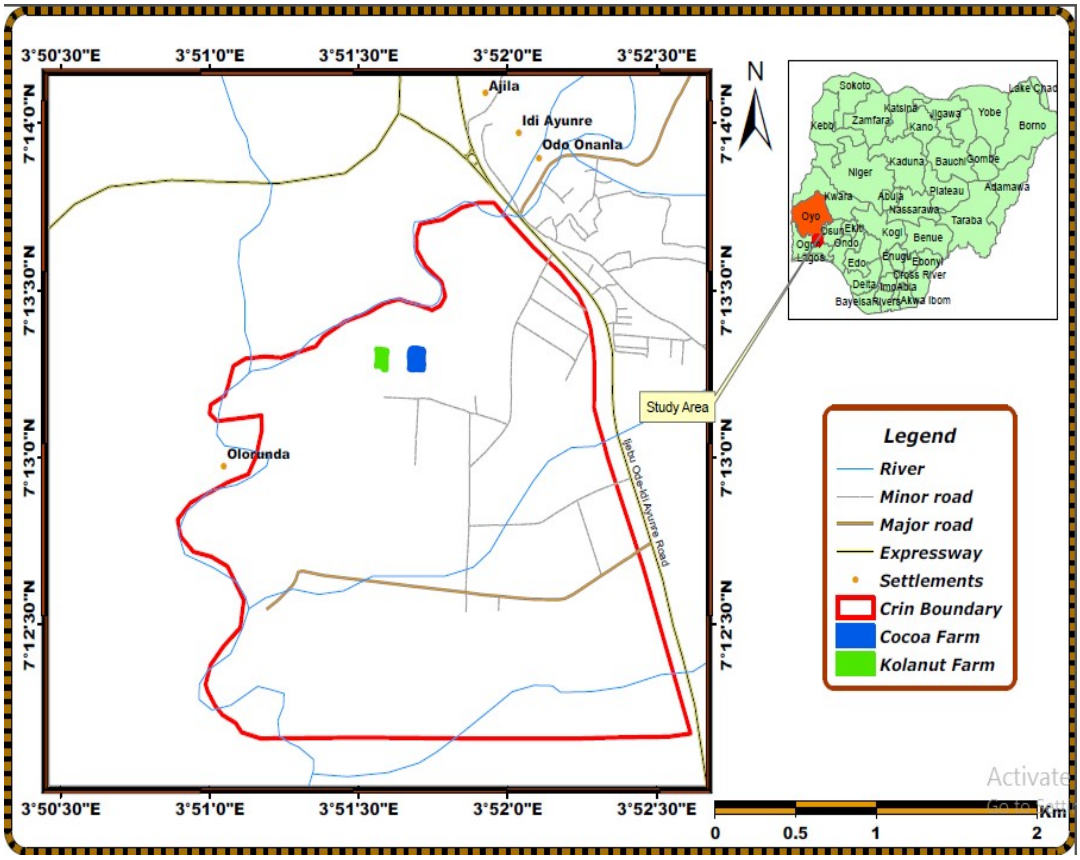

Figure 1.5: Location map of the study area

dry season (November to March). The mean monthly rainfalls in Ibadan for August 2016 and March 2017 are 157.5 mm and 166.8 mm respectively (NIMET 2016-2017).

1.9 Climate and Vegetation

The study area lies in the tropical rainforest belt; it has two distinct seasons, the wet and the dry climate, the rainy season stretches from month of April to October whereas the dry spell covers November to March (Adelekan and Bolarinwa, 2009). Maximum - rainfall occurs between June and September, with August break spanning between late July and early August for a period of two to three weeks (Adelekan and Bolarinwa, 2009; Chineke *et al*., 2010 and Adepitan *et al.,* 2017). The average yearly minimum and maximum temperature are about 21ºC and 30ºC (Ayanlade *et al.,* 2018). Climate of an area is dependent on the natural vegetation in such location and also edaphic and topographic factors influencing it (Fashae *et al.,* 2017)

Ibadan falls within the Guniea Savannah (Odekunle, 2004 and Adepitan *et al.,* 2017); the vegetation cover is mainly rainforest species such as mahogany, obeche and iroko. However, the effect of vegetation especially roots of trees and low-lying shrubs aids in disintegration of rock masses. This rainforest vegetation is gradually being reduced in the study area due to research and residential usage of the land.

1.10 Soil Profile

Formation of soil starts with the breakdown of rock into regolith, the horizon is developed from continuous weathering of the rock leading to the development of vertical section of soil known as soil profile (Gregory *et al.,* 2009), varying in colour, texture and structure. Soil profile is generated from the weathering product of the parent rock (primary mineral) and its mineral content is dependent on the primary mineral constituents. The weathering product generated is dependent on the interaction between the parent rock and water, organic ligand, soil microbes and root of plants; this suggests that biological weathering is of great significance in the formation of soil profile (Wilson, 2004).

White et al. (2001) reported the weathering rate of feldspar in the granitic regoliths, they revealed that plagioclase feldspar weathers to kaolinite at a depth of less than 6 m in the granitic rock while k-feldspar remains intact and stable in the bedrock but it also weathers into kaolinite. The kinetic rate constant at which the meteoric water penetrates the plagioclase feldspar in the regolith is in the folds of two to three times

compared to the k-feldspar. Wilson (2004) made known that rock forming minerals that crystallised at lower temperatures such as quartz, muscovite and k-feldspar are more resistant to weathering than the earlier formed minerals namely olivine, pyroxene, amphibole, biotite and plagioclase feldspar in the discontinuous and continuous reaction series that are susceptible to weathering. Wilson (2004) also reported that biotite can be altered to kaolinite and it can also be weathered in soil via the uptake of potassium (k) from the interlayer by plant or by the action of organic acid decomposing it.

1.11 Brief History of Cocoa Research Institute of Nigeria (CRIN)

Cocoa Research Institute of Nigeria (CRIN) was a substation of West African Cocoa Research Institute (WACRI) and it was established in 1947 in Ibadan and became autonomous in 1964 by Nigerian Research Institute Act No33. The Institute is meant to conduct research and development on cacao, kola, cashew and tea. Activities of the research Institute are centred on genetic improvement of the mandate crops, control of pest and diseases affecting these crops, effective crop utilization, integration of these crops into Nigerian cropping system, and adaptation of research findings coupled with improve technologies into agricultural practice.

Mandate crops of the Institute were grown in the main station, substation and experimental stations in Idi-Ayunre (Ibadan), Owena, Onisere and Ibule (Ondo state), Ochaja and Kabba (kogi state), Uhonmora (Edo state), Ibeku (Abia state), Ajassor and Okondi (Cross Rivers), Mambilla and Mayo-Selbe (Taraba state) and Ugbenu (Anambra state).

1.12 Review of Previous Works

Soil is regarded as the natural body of solids (minerals and organic matter), liquid and gases occurring on land surface, it occupies space and consisting of layers that are discernible from the previous material due to additions, losses, energy transfer and transformation of matter to sustain rooted plants (Schoonover and Crim, 2015). Horizon boundaries are determined from soil colour, distribution of root, soil texture, its structure, consistence of the horizon, effervescence, reactivity and rock fragment. The horizons are denoted with letters and it includes O, A, B, C and R (Fig. 1.6).

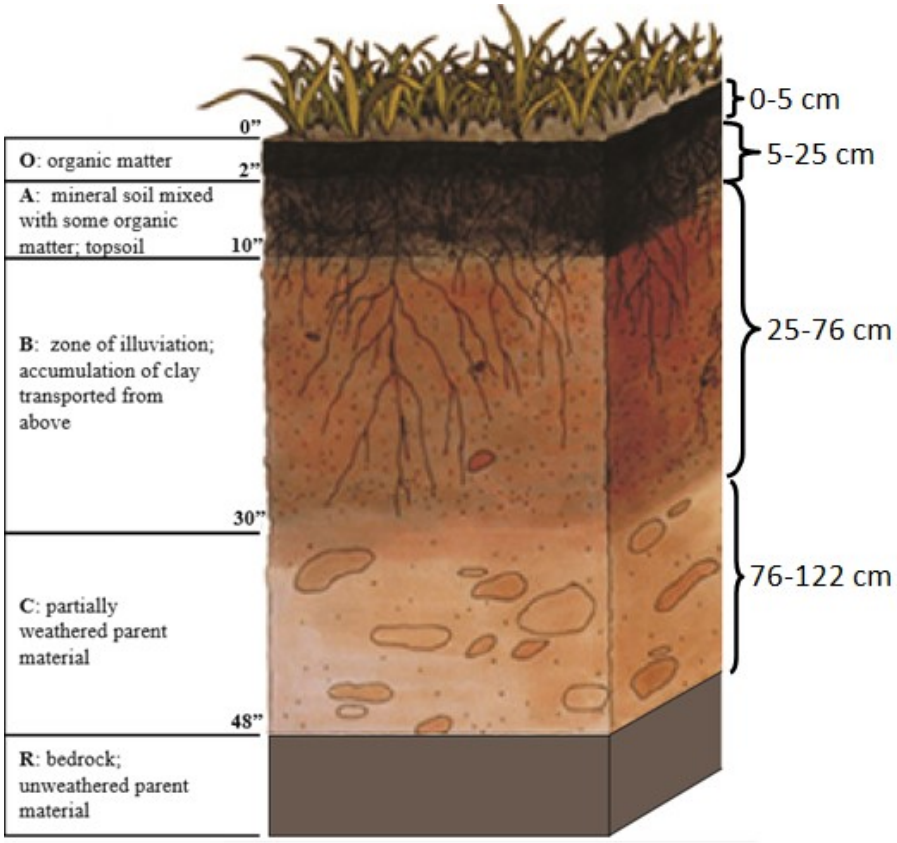

Figure 1.6: Typical soil horizons identified in a soil (adapted from Schoonover and Crim, 2015)

O-horizon: it is the uppermost layer consisting of organic matter usually present in forested areas but it may have been eroded in the grassland or cultivated ground as a result of persistent erosion or constant tillage (Schoonover and Crim, 2015). Botta (2015) reported that the layer is characterised with the accumulation of plant litter as the source of organic debris.

A-horizon: this is the mineral layer formed below the soil surface; it is known for the accumulation of organic matter and liable to tillage activities. The horizon is enriched with organic matter and has high level of biological activities; it is dark in nature due to accumulation of organic matter from above (Botta, 2015 and Schoonover and Crim, 2015). Thickness of this layer is being controlled by the landscape and the nature of soil type (Botta, 2015)

B-horizon: it is known as zone of accumulation of leached nutrient which is directly below A-horizon. Materials received in this layer include clay particles, aluminium and iron oxides, decay organic matter (humus), carbonate, gypsum and silicates; it has lighter colour than the overlying horizons (Schoonover and Crim, 2015). The moisture content in B-horizon is higher than the A-horizon due to presence of more clay content (Botta, 2015).

C-horizon: it is characterised with pedogenic weathering, that is, it has partially weathered rock material and it is the transition between soil and bedrock. There is possibility of the upper portion of C-horizon undergoing weathering and becoming part of the overlying B-horison, invariably it is the source of the A and B horizons (Botta, 2015 and Schoonover and Crim, 2015).

R-horizon: is directly below the C-horizon, it is usually the bedrock occasionally broken up by the roots of trees (Schoonover and Crim, 2015).

Soil electrical conductivity (EC) is defined as the ability of soil to conduct electrical current or attenuate its flow (Hawkins *et al*., 2017), they also stated the factors influencing the measurement of soil EC to be water content, porosity, texture of soil, level of salinity, cation exchange capacity and temperature. Corwin and Lesch (2005a) suggested various physical ways of measuring soil salinity; these include visual observation of crop in the field, electrical conductivity extracted from soil solution, electromagnetic induction-EMI, electrical resistivity and time domain reflectometry-TDR.

Corwin and Lesch (2003) made known that extraction of soil solution is time consuming, laborious and expensive for the determination of EC_e, thus focus is shifted to EC_a which measures the conductance of soil solution, solid soil particles and exchangeable cations between the interface of solid-liquid of clay minerals and air (Fig. 1.7). The purpose of EC assessment in agricultural field is to measure the soil's salinity which depends on the amount and type of soluble salts in solution, texture of the soil (its clay content and mineralogy), porosity, moisture content, water holding capacity and its temperature (Bozkurt *et al.*, 2009; Grisso *et al.*, 2009; Ekwue and Bartholomew, 2011; USDA, 2011; Hawkins *et al.*, 2017 and Medéiros *et al.,* 2018).

Allred and Smith (2010) reviewed the application of geophysics in agricultural investigation due to its low cost, rapid data gathering and continuity in time and space when compared with the aged long traditional practices. Dominant methods engaged in agricultural practices include electrical resistivity, ground penetrating radar (GPR) and electromagnetic induction (EMI). Also emerging methods in recent times involve magnetometry, airborne EMI, spontaneous potential and seismic. All the stated methods are viable in conducting precision agricultural practices, horizontal spatial distribution of soil properties could be produced from ECa map via resistivity or EMI, which is useful in partitioning the field into management zones.

Apparent soil electrical conductivity was used in characterising soil spatial variability on Westlake farms in California situated on clay loam. Geonics dual dipole EM38 was used in measuring the EC_a; and soil samples sites were selected from the EC_a and physicochemical analysis was conducted on the soil samples. Some of the soil attributes correlates with the EC_a (Corwin and Lesch, 2005b).

Corwin and Lesch (2005a) discussed the application of apparent electrical conductivity on agricultural soil. Use of EC_a is regarded as a quick, reliable, ease of data acquisition but may not be related to crop yield. They concluded that it is an efficient and effective agricultural soil quality assessor which is reliable in site specific management of farmland.

Eluwole (2016) carried out in-situ soil resistivity measurement as a tool in predicting maize yield on an experimental plot at Ekiti State University. He employed Wenner configuration for the resistivity measurement, also evaluated the moisture content, soil texture, pH and parameters were statistically analysed. Zones with high resistivity were

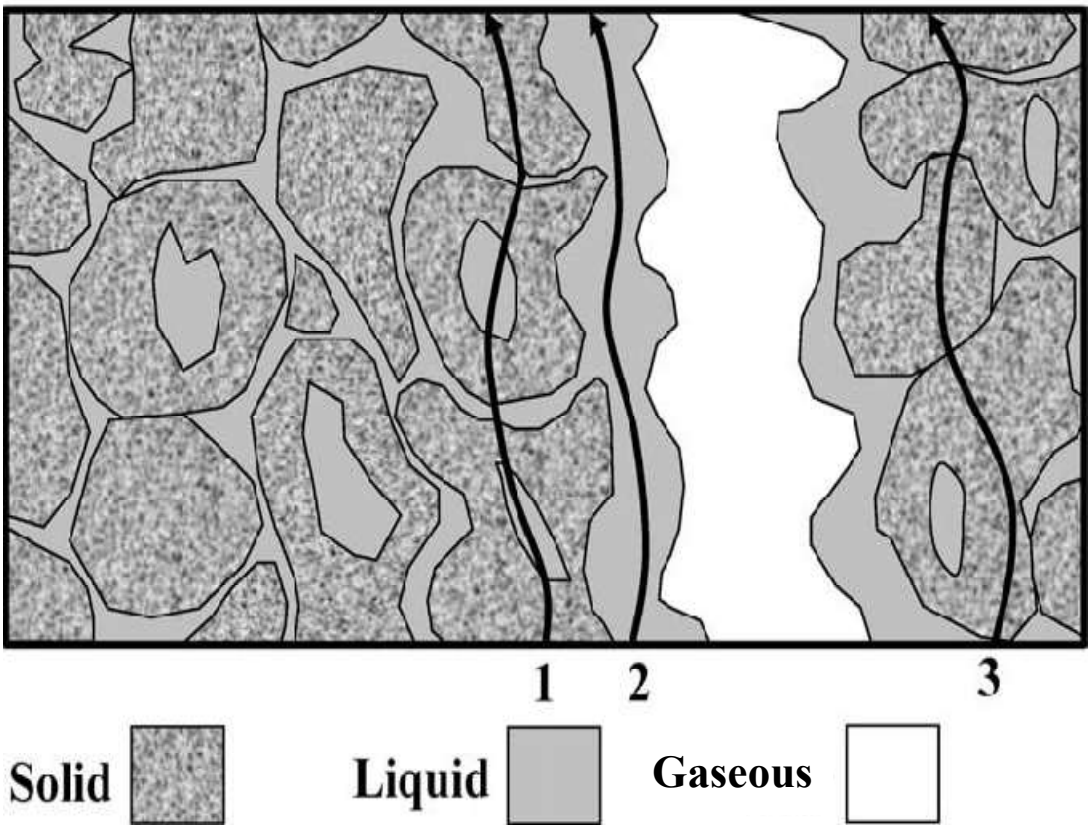

Figure 1.7: Three electrical conductance pathways for the ECa measurement (Modified after Corwin and Lesch, 2005a)

characterised with low moisture content and the yield is low to average whereas high maize yield sections were characterised with low resistivity and high moisture content. The textural class of soil with high yield is sandy loam while loamy sand is peculiar to the low to average yield segment. He concluded that soil resistivity could be useful index for soil properties.

Evaluating the variability of soil moisture with a target of determining its influence on soil EC_a was carried out on two experimental fields in Brazil. It was confirmed that EC_a reading is a good quality evaluator of soil moisture which depends on soil texture; also there is direct relationship between clay content and soil EC_a. They opined that soil EC_a is an effective indicator of soil variability especially in highly variable soil texture (Molin and Faulin, 2013).

Costa *et al.* (2014) verified the effect of soil moisture on electrical conductivity and also the interaction between EC_a and soil attributes were examined on a farm land in Brazil. EC_a was measured using hand held Landmapper ERM 02, gravimetric method for soil moisture and physicochemical assessment of the soil attributes. They noted that a strong correlation exist between EC_a and soil moisture, that is, the higher the EC_a value, the higher the moisture content. Positive correlation was derived from the interaction of EC_a with pH, Ca, Mg, CEC, organic matter, clay and silt while negative interaction with sand content, sulphur, K, P, Fe. They concluded that moisture content influenced the EC_a values and EC_a is a reliable tool in mapping soil spatial attributes.

Relationship between moisture content and electrical conductivity was analysed; and how it affects plant transpiration and growth in the experimental farm in Suwon, Korea. Electrical conductivity and rate of transpiration were measured at varying moisture content. The authors observed that transpiration rate is higher with increase in soil moisture content at EC between 2.5 and 4.5 dS/m whereas decrease in rate of transpiration was noted when treated with moisture content of EC greater than 4.5 dS/m due to an increase in water stress invariably affecting fruit productivity (Shin and Son, 2015).

Siqueira *et al.* (2014) assessed the spatial variability of soil EC_a and moisture content and the influence of soil texture on the mentioned variables in Spain. Electromagnetic induction equipment (EM 38) was used in measuring EC_a at 40 sampling points through two orientations; vertical and horizontal dipole positions and soil samples

were taken at the location between 0 and 30 cm depth. Soil texture was established using particle size analysis involving sieve-pipette method and gravimetric method for soil water content. A strong correlation coefficient was generated from the interaction of EC_a with soil water content and also positive correlation exists between EC_a and clay & silt content. They concluded that kriging the data set has helped in modeling the EC_a, water content and textural variations in the soil.

Mapping the spatial unpredictability of soil is essential for effective soil management; Behera *et al.* (2016) worked on spatial changeability of soil in oil palm plantation situated in Goa, India. They measured the physicochemical properties of 128 soil samples from different plantations taking from a depth of 0-20 cm and 20-40 cm. Geostatistical analysis was used in evaluating the data which aided in delineating soil management zones for site specific nutrient application especially fertilizer input.

Guo *et al.* (2015) engaged electromagnetic technique to map out spatial variation in soil salinity around rice growing coastal area in China. They employed EM 38 to record EC_a data and 19 soil samples were collected up to a depth of 80 cm. Their result showed a positive correlation between the measured EC value in the laboratory and field EC_a; and concluded that EMI survey is cost effective and efficient in characterizing the spatial unevenness of soil salinity.

Medéiros *et al.* (2018) studied the apparent electrical conductivity in two texturally (sandy clay loam and sandy loam) different sugarcane fields with an attempt to ensure site specific management zones. The study was carried out at two locations (Vicosa and Ponte Nova) in Brazil. A portable landmapper EMR-02 was used for resistivity data acquisition and soil samples were taken from the fields; soil moisture content and particle size distribution were determined using thermo-gravimetric method and Embrapa pipette method respectively. They concluded that EC_a mapping cannot wholly replace the chemical soil sampling approach of estimating soil attributes but it can be used in mapping soil spatial attributes that is, defining the management sections from which soil sampling can be executed.

Peralta *et al.* (2013) engaged soil apparent electrical conductivity in delineating the management zones on some agricultural fields in southeastern Pampas, Argentina. Veris 3100 sensor was used in measuring the EC_a, also georeferencing the investigated points and ArcGIS v9.3.1 was used in map production. Soil samples were taken with

core and analysed for gravimetric water content, particle size distribution and chemical analyses. Regions of low EC_a are characterised with low content of organic matter, soil moisture, clay content, cation exchange capacity and vice versa. They made known that the distribution of EC_a within a field can be used in designing sampling zone for efficient site-specific management.

Carvalho *et al.* (2016) studied the soil properties and yield of cocoa in determining the management zone in Bahia, Brazil. 120 sampling points were investigated; soil samples were collected at depth of 0-20 cm, particle size and chemical analyses were performed on them. Yield per cacao plant were extrapolated from the pod per plant. They established that the methods helped in delineating the management zone for effective cocoa production in the farm.

Dec *et al.* (2009) examined the influence of soil management on the thermal properties of soil in Harstl/Goettingen, Germany. Undisturbed silt loam samples were taken at depth of 0-30 cm and 30-60 cm prior and after compaction. The authors concluded that soil compaction and water content influenced the thermal properties, such that soils with high water content and well compacted were characterised with high thermal conductivity and high heat capacity are characterised with low thermal diffusivity.

Ekwue *et al*. (2015) carried out thermal conductivity on twenty six agricultural soils in Trinidad with a focus on determining the effect of bulk density and water content on it. KD2 thermal analyzer was used and thermal conductivity was measured both in the field and laboratory. The authors concluded that thermal conductivity rises with an increase in water content; it is high in sand than clay soil subjected to same water content and bulk density.

Lipiec *et al*. (2013) had a general review on the effect of heat stress and drought on the growth of plant and its yield. Increase in ambient temperature leads to an increase in soil temperature coupled with a low humidity in soil and air affect the root growth, plant's transpiration, photosynthesis and the water usage of plant.

Effect of temperature on the productivity of maize plant grown on silt loam in Iowa was examined by Hatfield and Prueger (2015). They reported that its effect on plant productivity is dependent on the species of plant and it tends to affect the grain yield rather than the vegetative growth.

Relationship between the thermal properties and porosity of sand and clay materials was studied by Goto and Matsubayashi (2009). The test was conducted on sediments recovered from the eastern flank of Juan de Fuca ridge. They observed that thermal diffusivity of clay is lower than that of the sandy material which is strongly influenced by distribution of porosity.

Barry-Macaulay *et al.* (2014) carried out thermal studies on some soils and rock samples in Melbourne, Australia with a target of determining the effect of soil moisture content, mineralogy and the density on these earth materials. KD2Pro thermal analyser was used to measure the thermal properties of soils and a steady state divided bar device was engaged for the rocks. They reported that thermal conductivity and volumetric heat capacity increase with an increase in water content and density. They opined that thermal properties are being influenced by the water content, density, mineralogy and particle size distribution.

Soil is a permeable unit due to the presence of interconnected pore spaces that allows flow of fluid from high to low energy region. Asadullah *et al.* (2014) carried out hydraulic conductivity test on sandy loam soil using constant and falling head permeability techniques in Pakistan. Three soil columns of 8.5 cm in length were filled with different percentages of texture. Primary purpose of the test was to determine the suitability of textural class for drainage. The authors concluded that hydraulic conductivity and porosity were influenced by soil texture and its structure; hydraulic conductivity is high in medium to coarse textured soil material whereas it decreases in fine texture. Falling head is more precise than constant head technique the test conducted on sandy loam soil.

Nijp *et al.* (2017) worked on modifying the traditional constant head permeameter used in detrmining the saturated hydraulic constant on undisturbed soil. Modified constant head permeameter by Wageningen was used to overcome the flow resistance in the tubing system leading to under estimation of saturated hydraulic conductivity. They agreed that modified gadget estimates the highly permeable soil unit without bias.

Kool *et al.* (2019) examined the hydraulic conductivity and porosity of tilled and non-tilled soil which was carried out on bare loam soil site. The study area is situated in the Agronomy and Agricultural Engineering farm, Boone Iowa, USA. Core samples were collected and subjected to gravity drain at atmospheric pressure to determine the volumetric water content and pressure was used to ascertain the bulk density and

constant head method for saturated hydraulic conductivity. The authors opined that tilled soil can reduce the soil bulk density favouring hydraulic conductivity and water retention in soil. Also as the bulk density of soil increases, the pore volume within the soil decreases permitting water retention than soil of low bulk density.

Hossain and Cohen (2012) revised the relationship between electrical properties, porosity, permeability and elastic properties using experimental and theoretical approaches on sixteen greensand samples from North Sea. They affirmed that there was linear relationship between permeability and electrical properties; also there was direct interaction between electrical and elastic properties provided that the clay micro porous is established.

Elhakim (2016) estimated permeability using in situ falling head method, pump testing, laboratory grain size distribution and cone penetration test. In situ falling head method measured the detailed permeability of soil profile against depth than through pump testing and both techniques recorded decrease in permeability with depth. Permeability coefficient was empirically determined from cone penetration test and grain size distribution. The author opined that permeability is over estimated from those that were generated using formula and there is need to calibrate the empirically generated permeability using the real field measured data. He also found that there is no generalized method for soil permeability estimation for all soil types because each method of measurement has its limitation and short comings.

Fernando (2008) conducted permeability test on Hazelwood ash retention overlying an aquifer system beneath it in Australia. The study was executed on a metre thick clay liner designed for the purpose of preventing leachate from infiltrating the aquifer system. Permeability was determined using double ring method, laboratory test and sol percolation test. He concluded that the permeability readings determined from both the soil percolation and laboratory test were within similar range; soil percolation test is useful in determining the permeability coefficient of a thin permeable layer.

Gleeson *et al.* (2011) mapped the regional permeability of near surface geologic unit underlying soil layers with a focus on saturated lithologies. Quantifying the regional scale permeability involves introduction of numerical model into hydraulic observation, stream flow, thermal and chemical observations in North America. Aquifer maps were compared with permeability maps to establish its reliability. They were able to predict the geological materials from their permeability values, thereby resolving the heterogeneity in permeability.

Rahman *et al.* (2017) studied the influence of pore and grains distribution on fluid accommodation and electrical properties of soils are dependent on these factors. Samples were taken from sandstone (two), limestone (two) and carbonate rocks (one) in Australia; they were imaged using high resolution x-ray micro computed tomography. The images were used in analyzing the porosity, distribution of pores and grain size. They concluded that micro structure strongly influenced fluid accommodation in rocks.

Li *et al.* (2014) measured the resistivity and relative permeability at the same time from core plugs in the pay zone of oil well operated by Saudi Aramco. Unsteady state displacement method was used in measuring the oil and water relative permeability in the pay zone of a carbonate rock. An attempt was also made to compare the result with that generated from resistivity log and laboratory resistivity measurement. Encouraging results were derived from the inferred relative permeability from resistivity log which was close to relative permeability determined from unsteady state approach.

Kirkby *et al.* (2016) observed the relationship between permeability and electrical resistivity in fractures that were filled with electrically conductive fluid in Australia; and model the relationship between them with the aid of random resistor. They noted that the apertures control electrical resistivity and permeability, an increase in rock aperture results in greater permeability leading to decrease in electrical resistivity of the medium.

Wayne *et al.* (2007) reported that agricultural field management and crop production were being driven by the soil textural class. Rate at which water moves through the soil determines the ease of its movement or retention capability of nutrient in it, invariably, texture of a soil determines amount of water made available to plant, its aeration, organic matter content in it and cation exchange capacity.

Mukungurutse *et al.* (2018) worked on pedological characterization and classification of soil in Lupane district in Zimbabwe in order to establish a plan and develop soil management scheme for productivity enhancement. The farm was situated within the sandstone terrain and the study was conducted using topographic map, aerial photographs followed by detailed soil survey using six representative profile pits. Soil samples were subjected to textural classification, pH test and cation exchange capacity (CEC). Pearson's correlation coefficient and regression assessments were conducted

using Microsoft excel package. The dominant soil particle was sand followed by clay and silt contents, the textures include sandy clay, clay, loamy sand, sandy clay loam and sand. The authors concluded that the sandy horizon is prone to low nutrient retention, organic matter and water holding capacity because of low clay fraction in it. They also affirmed that extremely acidic soil is attributed to leaching of bases resulting in low CEC. Relationship between CEC and %clay was positive, they concluded that areas of low CEC, soil acidity should be enhanced with the use of organic matter to improve on its nutrient retention and inorganic fertilizer can be used as soil amendment on slope section.

Khadka *et al.* (2018) carried out soil sampling around Chunbang farm in Nepal with the focus of assessing its fertility status. A total of twenty-seven soil samples were collected at depth of 0-20 cm based on soil variability in the farm. Minitab-17 software was used in determining its variability and ArcGIS software was used in producing soil fertility/productivity map because of its ability to relate one sampling point to another (krigging). The authors examined the soil texture, colour, structure, pH, organic matter, total N, available P_2O_5, k_2O, Ca, Mg, S, B, Fe, Zn, Cu and Mn. The observed colours are yellowish brown and brown with granular and sub-angular structure which favour agricultural production. High acidity (pH: 4.75) was responsible for the presence of toxic Al and Mn. It also has low concentration of organic matter, Ca, S, B, Zn, the status of K is between medium and high, while concentrations of P, Cu, Mn, Fe, are high. They concluded that nutrients were not made available to the plants because of the acidic nature of the soil and the use of organic matter, crop rotation, mulching, and planting of cover crop and systematic application of fertilizer should be adopted for effective farm management.

Physicochemical assessment was conducted on soil near microbiology laboratory in the main campus of university of Ilorin by Oyeyiola and Agbaje (2013) with a target of determining its suitability for microbial development and plant growth. Six soil samples were collected within an interval of two weeks; the test performed on the soil include pH, water holding capacity, organic matter, moisture content and soil texture. The texture is loamy sand which supports plant and microbial growth, also moisture content, organic matter and pH were reported to be within the range that will support plant and microbial growth.

Musa *et al.* (2016) examined soils from ruminant farms in Malaysia for the physicochemical attributes that support the presence of B. pseudomallei. One hundred and eighty soil samples from sixty farms were collected for their research and they were analysed for texture, organic matter, water content, pH, CEC, C, S, N, Fe, Cu, Mn & Zn. Data were analysed using Microsoft excel and Mac-JMP software. They confirmed that B. pseudomallei flourish in soil with high clay content than high sand fraction due to the ability of clay to retain water and soil nutrient, also Fe favours the survival of this bacterium because it aids respiration.

Inthavong *et al.* (2011) studied the rice yield in Savannakhet province of Laos through spatial evaluation of water availability and fertility of the assessed soil. The research is targeted at quantifying the spatial variation of water content, soil fertility and management practices toward productivity increase. The authors integrated the soil data acquired by the soil survey and land classification centre (SSLCC) with rainfall data, the sandy texture (sand, sandy loam and loamy sand) was classified to be above 80% while clayey loam and loam was less than 20% and soil nutrients were also estimated using Janssen *et al.* (1990) equation. GIS software was used in interpolating the data and the yield data were collected from the farmers. The investigated area was classified as low fertile section as deduced from the organic content, CEC, available P and K_2O. Correlation analysis showed that the yield was greatly influenced by N and P and to a lesser extent by K. they concluded that the productivity could be improved with increase fertilizer application, together with improved availability of water to the rice farm.

Environmental studies involving physicochemical assessment and nitrogen fertilization was carried out by Tkaczyk *et al.* (2018) in eastern Poland to determine the yield of winter wheat. The study was carried out on 45 farms. The approach adopted involves interviewing the farmers on yield, particle size analysis and chemical analysis of soil taken at depth of 0-20 cm. High yield of the winter wheat was observed on sandy loam than that obtained from loamy sand while highest yield was noted on silty soil due to low proportion of sand particle in it, therefore yield is dependent on particle size variation. The soil pH is not contributing to the yield but better yield was obtained on soils with neutral and slightly alkaline concentration. Available P, K and Mg concentrations were not having significant effect on yield of the winter wheat whereas nitrogen fertilization had effect on its yield.

Amos-Tautua *et al.* (2014) assessed the physicochemical properties of soils within a waste dumpsite located along Yenagoa-Tombia road, Bayelsa Nigeria. Concentration of Pb, Cr and Cd and soil fertility of the dumpsite were examined with a focus of determining the suitability of the soil for crop production. Soil samples were taken at two depth interval (0-10 cm and 10-20 cm) after the removal of dump material and also from the control section which is 100 m away from the dump section. Particle size distribution was done using Bouyoucos hydrometer method, pH, CEC, Ca, Mg, k, Na, N, available P, organic matter, Pb, Cr, Cd were determined from soil samples. Sand fraction was high while clay and silt quantities are lower in the dump field whereas the control section has an inverse particle size distribution with respect to soli particle size in the dumpsite. Soils within the dumpsite are susceptible to nutrient leaching due to high fraction of sand whereas high clay content in the soil of the control segment has low permeability and high nutrient retention. pH concentration of soil solution was classified between moderately acidic and neutral aiding nutrient solubility and mobility in soil. Concentration of chemical elements analysed were considered appropriate for crop production by FAO while Pb, Cr and Cd were below the maximum permissible level proposed for agricultural soil by WHO. They concluded that dump field can be converted for agricultural purpose.

Soil fertility status was evaluated by Khattak and Hussain (2007) in Galliyat region of Pakistan, the research was centred on soil management for sustainability of crop production. Composite soil samples were taken from 74 stations at depth of 0-30 cm. Textural analysis reveals that soils in the study location are loamy (sandy loam, loam, silty loam) which are favourable for crop production but there is possibility of nutrient leaching should in case the organic matter level is not maintained. pH values indicate neutral to slightly alkaline, low EC value was attributed to leaching of nutrient, there is sufficient concentration of K, Cu, Fe, Mn and low concentration of N, P and Zn.

Soil is regarded as the home for soil nutrients especially the cations, the presence of clay and organic matter which have negative charges tend to attract the positively charged soil nutrient and repel the similar like charges that is negatively charged nutrients via leaching.

Wodaje and Abebaw (2014) examined the physicochemical properties of soil used in cultivating garlic in east Gojjam region of Ethiopia. Soil samples were taken from

depth 0 to 20 cm, air dried and made to pass through 2 mm sieve. Analyses conducted on the samples include pH, moisture content, electrical conductivity, organic matter/carbon, cation exchange capacity (CEC). pH meter and EC meter were used in determining the pH values and EC measurement, whereas moisture content analysis was carried out in the laboratory using loss in weight through oven dry of soil sample at 105^0C for 24 hours. Organic carbon content of the soil was resolved using Walkley and Black method and CEC was evaluated using Raman and Sathiyanarayanan technique. The authors confirmed that the soils were classified as non-saline from its EC and the pH falls within the neutral category. They reported that soils of high EC have high organic matter and high CEC, and concluded that the study is a useful evaluator of soil nutrient capacity.

Olorunfemi *et al*. (2018) evaluated the soil physicochemical and fertility condition of long-term land use and cover changes of a vegetative forest district. The study was conducted in Ekiti state. A total of 105 samples were collected from 35 locations at depth up to 30 cm from cropland, natural forest and plantation areas. Contents of organic carbon, organic matter, CEC, base saturation, Al^{3+} saturation, soil pH, particle size distribution, water holding capacity, total porosity, and bulk density were examined. Natural forest has highest water holding capacity because of its lowest sand content and highest clay content while plantation zone has the least water holding capacity due to high proportion of sandy material and less of clay. The study reported zone with high water holding capacity has high contents of available phosphorus, organic carbon/matter, organic nitrogen, CEC, base saturation but has least exchangeable sodium percentage and less aluminium saturation percentage. The authors concluded that land use management is a good indicator of soil fertility status assessment

Watanabe *et al.* (2015) compared the physicochemical properties of soils under different land use system within southwestern Nigeria. 55 soil samples were collected from different soil series in IITA, soil pits were dug up to a maximum of 1.5 m deep. pH, organic carbon, total nitrogen, exchangeable cations (Ca, Mg, K and Na), exchange acidity, and available phosphorus. They reported high concentration of organic carbon, total nitrogen, calcium, magnesium, acidity together with less bulk density and compactness in the surface and upper horizons (0-50 cm) of forest reserve while available phosphorus, potassium, bulk density, pH, compactness were on the

high in the cropland. Available phosphorus and potassium were lower in the surface horizon of forest reserve due to application of fertilizer in cropland where organic carbon and total nitrogen were higher in the surface horizon of the forest reserve than the cropland. Soil acidity was prominent in all horizons of forest reserve than the cropland due to base consumption and organic acid which was derived from decomposition of litter. They concluded that continuous crop farming coupled with appropriate fertilizer management and conservation of soil will improve fertility status of soil.

Adebowale and Odesanya (2015) assessed the fertility status of soil in kola plantation in Ogun state, soil samples were taken from different depths (0-15 cm, 15-30 cm and 30-45 cm), air dried and made to pass through 2 mm sieve size. Physico-chemical test carried out include textural class, pH, total nitrogen, available phosphorus, exchangeable cations (K, Na, Mg and Ca). Dominant textural class is sandy loamy and organic carbon content varied across the study area. The content of magnesium was low in all the study area while available phosphorus is adequate in all the soils. The authors opined that there is need for soil management practice to ensure maximum productivity in the study location.

Arévalo-Gardini *et al.* (2015) examined the physico-chemical properties in soil of cacao agroforestry management system in Amazon precinct of Peru. Soil management showed both chemical and physical analyses were tending toward equilibrium within six years of its management. There was an increase n soil organic matter, phosphorus, potassium and magnesium. They concluded that soil fertility can be improved through adequate soil management.

CHAPTER TWO

LITERATURE REVIEW AND THEORETICAL FRAMEWORK

2.1 Nigerian Basement Complex

Nigeria has a territorial coverage area of 923,768 km^2 and it could be divided into two major geological setting; firstly, the Precambrian rocks which covered more than half of Nigeria comprising igneous and metamorphic rocks while the remaining portion is made up of formation of thick Cretaceous and young sediment overlying the Precambrian rocks (Fig. 2.1). The basement complex terrain accounts for about 60% of the Nigeria land area (Akande, 2006). Precambrian rocks of Nigeria are found within the Pan-African mobile belt and it has been affected by Pan–African orogeny about 600 Ma. It lies between West African Craton and Congo Craton and later intruded by Younger granite in the Jos plateau (Obaje, 2009). Pan African belt emerged from continental-continental plate impact involving passive continental margin of West African craton and the active Pharusian continental margin (Dada, 2006), with the Benioff zone dipping westward led to production of volcanic and plutonic rocks while new arc was formed; ultramafic and mafic rocks pierced through the thin crust in the Ife-Ilesha area, although there is some quantity of crustal contamination around this zone (Rahaman, 2006). A corroborative assertion was reported by Ocan (2006) that operation of Wilson cycle in the east of West African craton resulted in continental-continental collision (600 Ma). Two models were reported by different schools of thought;

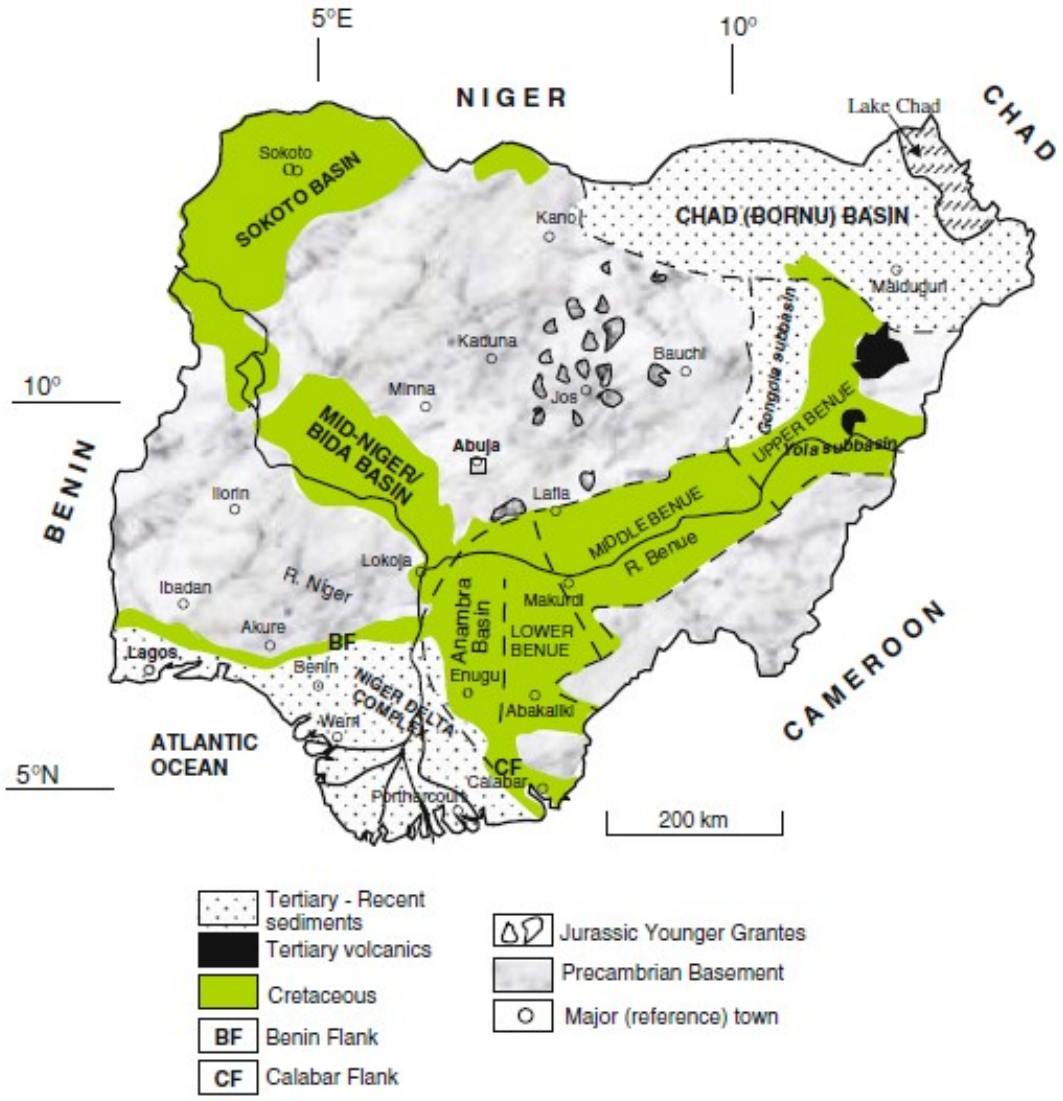

Figure 2.1: Geological map of Nigeria showing the sedimentary basins, Jurassic younger granites and the basement complex (Adapted from Obaje, 2009)

ensialic (crustal extension and continental rifting responsible for thinning of crustal plate housing sediment deposition) was responsible for the formation of schist belt and older basement being reactivated and ensimatic (that sediments were deposited in marginal back arc basins) in which sediments were deformed and metamorphosed and older basement was reactivated (Ocan, 2006). Regional metamorphism, migmatization coupled with extensive granitization and gneissification occurred during Pan African deformation producing homogeneous gneisses and syntectonic granites; the last episode of this deformation was accompanied by granite and granodiorite and marked by fracturing (Obaje, 2009). Structural geology of Nigeria was due to NW-SE compressional forces acting on the rock body leading to dominant structures of NNE-SSW and there are two major fractures in western Nigeria, these include Anka-Yauri-Iseyin and Kalangi-Zungeru-Ifewara belts extending southwards to the coastline (Dada, 2006).

The Nigeria basement complex had been subjected to various orogenic events and dated using K-Rb, Rb-Sr and Pb-Pb techniques on rocks of older granites together with whole rock sample (Ocan, 2006). Obaje (2009) reported that it has poly cyclic episode and bears the imprint of four events, namely:

(1) Liberian: 2700 Ma

(2) Eburnean: 2000 Ma

(3) Kibaran: 1100 Ma

(4) Pan-African: 600 Ma

Ocan (2006) and Rahaman (2006a) proposed the following suite of rocks:

- Migmatite-Gneiss-Quartzite Complex
- Slightly Migmatized to Unmigmatized paraschists and metaigneous rock or Newer/Younger metasediment or Schist belts rocks
- Charnockitic, Gabbroic and Dioritic rocks
- Members of the Older Granite suite
- Metamorphosed and Unmetamorphosed calc-alkaline volcanic and hypabyssal rocks
- Unmetamorphosed dolerite dykes, syenite dykes

2.1.1 Migmatite-Gneiss-Quartzite Complex

This complex is the widespread rock units within the Nigeria Basement Complex. It is the most prevailing rock unit in the southwestern and northern Nigeria consisting of different rocks assemblage such as migmatite, paragneisses, orthogneisses and presence of basic and ultra basic metamorphosed rock (Dada, 2006, Rahaman, 2006a and Obaje, 2009). Rock suite in this complex experienced three major orogenies; Liberian, Eburnean and Pan African (Akande, 2006, Rahaman, 2006a and Obaje, 2009). Biotite and banded gneiss together with the older metasediments were classified to be in the same lithology (Ocan, 2006). Migmatite gneiss complex in Kaduna, Ibadan and Ile-Ife shown a well defined Pan African lower intercept age as determined from U-Pb (Dada 2006). Ocan (2006) reported that the heterogeneous assemblage of this complex include grey gneiss which is the oldest; mafic to ultramafic components such as amphibolites, biotite schist and biotite-hornblende schist; felsic fraction varies in texture including aplite, granite, pegmatite and granite gneiss.

Origin of grey gneiss, mafic-ultramafic and felsic fractions are magmatic rocks of granodioritic to tonalite component, basic dyke of metamorphic source, and metamorphic or magmatic source respectively (Rahaman, 2006a). The grey gneisses are in locations such as Ibadan, Ile-Ife and Odo-Ogun areas. In recent time, aeromagnetic data (Balogun, 2019) around Ilorin and satellite imagery via landat and shuttle radar topographic mission (Ajigo *et al.*, 2019) around Ibillo-Okene axis were used to study the structural disposition of this complex, NE-SW and ENE-WSW directions were observed. The magnetic high and low contrast coincided with the azimuth of rocks on the geologic map (Balogun, 2019) and the structural pattern is important in hydrogeological and geotechnical applications (Ajigo *et al.*, 2019). The petrological and chemical details revealed that migmatite, banded and granite gneisses around Ekiti were derived from the sedimentary protolith (greywacke) from continental environment (Ayodele 2015).

Quartzites being the most prominent with excellent outcrops along Ibadan-Iseyin axis; calc-silicate (numerous occurrences in Ikare axis) and garnet-sillimanite-corderite noticed in Ikare axis. This complex is found in Abuja, Keffi, Bauchi, Akwanga, Kaduna, Okenne, Ajaokuta, Funtua and Egbe in northern Nigeria; Obudu and Oban massif region in eastern Nigeria while in western Nigeria it was found in Ikerre, Akure, Ibadan and Ile-Ife (Obaje, 2009). The economic viability of quartzite suggests

that it is a useful rock aggregate as against migmatite gneiss based on their physical and mechanical property (Afolagboye *et al*., 2016).

2.1.2 Schist Belts

The structural trends of the metasediments are mostly preserved in the N-S which is prominent in western half of Nigeria and imprints of the schist are infolded into migmatite-gneiss complex (Rahaman, 2006a and Obaje, 2009). Seventeen schist belts have been established in the Nigeria basement complex (Rahaman, 2006b) and it is sometime refers to as the younger or newer metasediments comprising pelitic to semi-pelitic schists, metaconglomerate, quartzite, calc-silicate rocks, mafic to ultramafic rock, banded iron formation and marble (Ocan, 2006 and Rahaman, 2006a). Dada (2006) classified the belt into two groups, the group 1 is regarded as older metasediments consisting of marble, quartzites, metavolcanics and mica schist and it is conspicuously developed in southwestern Nigeria whereas the other group has varying quantity of amphibolites and it ranges from psammitic to pelitic metasediments.

Rahaman (2006a) stated that rocks of the schist belt were of sedimentary origin except the mafic to ultamafic rocks were assigned different ages such Archaean, Kibaran and Pan African; and the belt was characterized with controversial evolution (ensialic and ensimatic processes). The belt is Upper Proterozoic rock with a rift-like structure which was considered to be fault controlled trending NNE (Obaje 2009) and gold mineralization was associated with this fault system (Rahaman, 2006a). Anka fault zone was defined by the relationship between the pelitic and amphibolites schist (Danbatta and Garba, 2007).

Economic resources in this belt include gold, marble, banded iron formation, talc, asbestos and manganese (Rahaman, 2006a; Danbatta, 2010 and Akinola and OlaOlorun 2021). Igue marble deposit is found in the Igarra schist belt, occurred as lenses and has similar composition as that of the Obajana marble (Akinola and OlaOlorun 2021). Notable good examples of this belt are found in Iseyin-Oyan river (Archean banded gneiss-quartzite), Ilesha (massive amphibolites, amphibolites schist, pelitic rock, talc-tremolite, quartz schist, ferruginous quartzite and quartzite) and Igarra-Kaba-Lokoja (marble, metapelites and quartzite), Anka, Maru, Kusheriki, Kazaure, Zungeru, Kushaka, Birnin-Gwari, Igue, Karaukarau, Okolom-Dogondaji, Malele, Bin Yauri, Komu, Keffi-Akwanga, Agate and Ofiki-Budo Are (Akande, 2006;

Dada, 2006; Okunlola, 2006; Rahaman, 2006a; Obaje, 2009 and Akinola and OlaOlorun 2021).

2.1.3 Charnockitic, Gabbroic and Dioritic Rocks

Olarewaju (2006) made known that a quartz-feldspar-hypersthene-iron ore bearing rock is regarded as charnockite. It can be of igneous (massive and homogenous) or metamorphic origin (strongly foliated). They were emplaced during Pan African event and occur as cores, in the margins of granitic intrusion and sometimes found in the migmatite gneisses as intrusion but absent in the schist belts (Ocan, 2006, Olarewaju, 2006 and Rahaman, 2006b). Ayodele and Akinyemi (2014) also classified the charnockites on the basis of their texture to be coarse grained porphyritic charnockite, fine to medium grained charnockite and fine grained charnockite which in an agreement with Olanrewaju (2006).

Nigerian charnockite occurs within the amphibolites facies having dark-greenish to greenish grey colouration; it is deficient in water during consolidation due to low water activity from its magmatic source or resulting from high carbondioxide fraction (Olarewaju, 2006). Dominance of carbondioxide to water seems to be the appropriate model for igneous charnockitic rocks and it is a low pressure type (5-6 Kbar) revealing absence of garnet (Olarewaju, 2006). These groups of rocks include gneissic charnokite, foliated charnokite and non-foliated charnokite based on their structure; they are found in Ikere Ekiti, Toro, Awo, Osuntedo, Yelwa, Wasimi, Iyin Ekiti, Idanre, Ado-Ekiti, Oke-Patara, Uro Elemo, Ilupeju Ekiti, Otun Ekiti and Akure (Ocan, 2006; Olarewaju, 2006 and Ayodele and Akinyemi, 2014).

2.1.4 Members of Older Granite Suite or Pan African Granitoids

It is distinguished from Jurassic anorogenic peralkaline Younger granites on the basis of texture and morphology (Dada, 2006). Pan African granitoids are formed from plate collision leading to the rework of the pre-existing rock during Pan African orogeny (Rahaman, 2006a; Omosanya *et al*. 2012). This rock group was classified as intrusive igneous rock rather than being a product of metasomatic transformation of pre-existing rocks and the textural description of porphyritic was used as against porphyroblastic texture signifying metamorphic origin (Ocan, 2006). It intrudes into the schist belts

and migmamtite gneiss complex, noted for lack associated mineralization and some of the mineralizing fluids may be remobilized due to thermal effect on it (Obaje, 2009). Members include migmatitic granite, granite gneiss, early pegmatite and fine-grained granite, porphyritic granite, deformed pegmatite and undeformed pegmatite, biotite granite, biotite muscovite granite, syenite, serpentinites and anorthosites (Dada, 2006, Ocan, 2006 and Obaje, 2009). Older granite found within the Bauchi axis was named Bauchite due to the presence of fayalite (olivine) and pyroxene occurring with feldspar, mica and quartz (Obaje, 2009). Bauchite trends in the north east-south west direction, they are texturally similar to the porphyritic granite occurring at Buli hill, Irku, Lushi, Yelwa, Fadam Mada, Inkil and Sabon Kaura (Haruna, 2016). Pegmatites occurring parallel to the basement are important source of tantalite, gold and gemstone as a result of mineralizing fluid (Rahaman, 2006b).

2.1.5 Acid and Basic Dykes

They cut across older granite, schist belt and migmatite during Late to Post tectonic Pan African episode, basic dykes (<500 Ma) are the youngest rock unit in basement while felsic dykes are the oldest (580-535 Ma) (Dada, 2006; Rahaman, 2006a; Obaje, 2009 and Olatunji and Jimoh, 2016). Acid dykes are associated with the older granite such as syenite dyke, aplite dyke, microgranite, muscovite bearing pegmatite, tourmaline bearing pegmatite and beryl bearing pegmatite whereas mafic dykes are less common such as lamprophyric dyke, dolerite dyke, felsites (Rahaman, 2006a and Obaje, 2009). These dykes exhibit cross cutting feature on older basement rock, this suggests that they were formed later after the formation of the older basement, that is relative age determination (Rahaman, 2006a).

2.2 Younger Granites

They cover a length of 1600 km and a width of 200 km between north of Niger and south central Nigeria, it is Ordovician in Adrar-Bóus north of Niger while it is Late Jurassic in central Nigeria. Hydrothermal alteration process was responsible for the mineralization (Akande, 2006) and they are enriched in wolframite, zinc, scheelite, columbite and alluvial-cassiterite (Obaje, 2009 and Rahaman, 2006a). Rocks in this area trend in NE-SW, N-S, E-W, NNE-SSW and over fifty complexes are found in Nigeria (Obaje, 2009; Szentes, 2009 and Aga and Haruna, 2019). Younger granites are

typical example of ring complexes across the globe with features including elliptical to circular or saucer-shape emplacement (Akande, 2006 and Rahaman, 2006a). Major rock types in this complex are granite and rhyolite which account for 90% of coverage while intermediate and mafic rocks occupy less than 1% of the entire area (Rahaman, 2006b). It has been reported that younger granites found in uplifted areas were subjected to erosion as confirmed by the rhyolitic rocks lying directly on the basement (metamorphic); exposure of the complex due to erosion account for the plutonic mode rather than volcanic origin (Obaje, 2009). Varieties of granites include peralkaline granites and related syenite, peraluminous biotite alkali feldspar granite and biotite syenogranite, and metaluminous fayalite and hornblende bearing granites and porphyris.

2.3 Tertiary to Recent volcanic Rocks

They are basaltic in nature, found mostly in Biu plateau, Longuda plateau and Jos plateau with scattered occurrence in the Benue trough (Rahaman, 2006b) while the largest occurence are found in Biu plateau with area extent of 5,000 km^2 (El-Nafaty, 2015). They belong to the Pliocene to Quaternary periods, mineral composition includes olivine, pyroxene, feldspar, magnetite and exhibit fine grained texture(El-Nafaty, 2015). Volcanic rocks include trachyte, basalt, rhyolite but basalt is the major volcanic (Kasidi, 2019); ranged from grey to dark grey.

2.4 Sedimentary Basins in Nigeria

The sedimentary basins ranged in age from Cretaceous to Tertiary, these include; the Dahomey basin, Sokoto basin, Niger Delta basin, Benue trough, Anambra basin, Chad basin and Bida/Nupe basin (Obaje 2009; Rahaman 2006c).

Benue Trough

It has an area extent of 120, 000 km^2 extending in the NNE-SSW direction, formed from tectonic rifting. It has thick pile of sediments of about 6,000 m pre-dated to be mid-Santonian. The trough has series of anticlines such as Abakaliki anticlinorium, Giza anticline, Lamurde anticline; and synclines such as Afikpo syncline, Dadiya syncline, Obi syncline (Obaje 2009). It is segregated into Lower, Middle and Upper

Benue tough and it is a failed arm of aulacogen during the Cretaceous that occurred beneath the Niger Delta.

Benkhelil et al., (1998) reported the evolutionary phases of the trough and they are stated below:

(i) The formation of the northern basin started in the early Jurassic (microconglomerate and fanglomerate deposits)

(ii) The second episode of the rifting occurred between Neocomian and early Albian (continental and lacustrine deposits)

(iii) The folding and faulting that occurred in Santonian.

Stratigraphic successions (Abdullahi *et al.,* 2019) of Benue trough include:

a) Lower Coal Formation (coal, sandstone and shale)

b) Bassange Formation (sandstone and ironstone)

c) Nkporo Formation (shale and mudstone)

d) Awgu Formation (shale and limestone)

e) Eze-Aku Formation (black shale, siltstone and sandstone)

f) Asu River Group (shale, limestone and sandstone)

Bornu Basin

It is also regarded as Chad basin which was formed from divergence of plate, related to the opening of south Atlantic. The sediments were deposited unconformably on the Precambrian Basement Complex ranging in age from Paleozoic to Quaternary and it has thickness above 3,600 m (Obaje 2009). The thermal gradient of the basin is 5.9^0C/100 m in Chad basin of Nigeria (Kurowska and Schoeneich, 2010). Stratigraphically, the basin consists of sediments dated from the folloeing ages:

(1) Paleozoic (arenaceous sediment)

(2) Lower Cretaceous (continental intercalaire arenaceous sediment)

(3) Middle Cretaceous (limestone)

(4) Upper Cretaceous (sandstone)

The stratigraphic successions in the Bornu basin include:

(i) Chad Formation (continental), Pliocene to Pleistocene

(ii) Fika shale (marine), Turonian to Coniacian

(iii) Gongila Formation (marine), Turonian

(iv) Bima sandstone (continental) Albian to Turonian

Sokoto Basin

The area extent of the basin is estimated to be 59,570 km^2 (Bonde *et al.,* 2014). The basin does not exceed 1 km in thickness around the northwestern section and a thermal gradient of the basin is 0.9-7.6^{0}C/100 m (Kurowska and Schoeneich, 2010). Bonde *et al*., (2014) reported that an increase in sedimentation was noted in the northern segment of the basin as deduced from aeromagnetic studies. Obaje (2009) reported that the sediments in this basin were unconformably deposited on the Precambrian basement, these include:

(i) Gwandu Formation (clay and sandstone), Eocene in age.

(ii) Sokoto Group- Dange, Kalambaina and Gamba Formations (shale, clayey limestone and laminated shale), Paleocene in age.

(iii) Rima Group- Taloka, Dukamaje and Wurno (friable sandstone, shale, limestone, and mudstone), Maastrichtian in age.

(iv) Ilo and Gundunmi Formations (grits and clays), Pre-Maastrichtian in age.

Bida Basin

It is also known as Mid-Niger basin, trending in the NW-SE direction. The basin extended from Kontagora to slightly beyond Lokoja containing post orogenic molasse and thin marine sediments that were not folded. Its origin is connected to the movement in the southeastern Nigeria and Benue trough during Santonian orogenic event (Obaje *et al.*, 2011). It was classified into two folds, namely; northern and Lokoja or southern Bida basin. The basin is characterised with rifting and drifting of the faulted blocks before the opening of the Atlantic Ocean (Obaje, 2009). It is situated in the north western part of Anambra basin filled with Upper Cretaceous sedimentary rock. Obaje *et al*., (2011) made known that the maximum thickness of Bida basin varied between 3.5 km and 4.7 km at the central portion and decreases outward to the flanks. The thermal gradient of the basin is 2.0-2.5^{0}C/100 m (Kurowska and Schoeneich, 2010).

Stratigraphic successions of the Formations in this basin ranged in age from Campanian to Maastrichtian.

a) Lokoja sub-basin

(i) Agbaja (ironstone, sandstone and claystone)

(ii) Patti Formation (shale, siltstone, claystone and sandstone)

(iii) Lokoja sandstone (sandstone and conglomerate)

b) Bida sub-basin

(i) Batati ironstone (ferruginous claystone and siltsone with minor occurnce of shale)

(ii) Enagi siltstone (siltstone)

(iii) Sakpe ironstone (ironstone)

(iv) Bida sandstone (Jima member-(quartzose sandstone, siltstone and claystone), Doko member- (arkoses and quartzose sandstone).

Dahomey Basin

The Dahomey basin formerly known as Benin basin is a combination of inland, coastal and offshore basin (Oli *et al*., 2019). It extends from southeast of Ghana to Togo, Benin republic and terminates in the southwestern part of Nigeria. Okitipupa ridge separates the Dahomey basin from the Niger Delta (Obaje, 2009). Notable mineral resources include gemstones, kaolin, sand, bitumen, limestone, feldspar, bentonite, phosphate and gypsum (Oli *et al.,* 2019)

Lithostratigraphic succession

(i) Benin Formation (sand)

(ii) Ilaro Formation (coarse sand)

(iii) Oshoshun Formation (phosphate and shale)

(iv) Akinbo Formation (shale)

(v) Ewekoro Formation (limestone)

(vi) Abeokuta Group

a. Araromi Formation (shale, siltstone and limestone), Maastrichtian in age.
b. Afowo Formation (marine sand and sandstone, shale and siltstone), Turonian in age
c. Ise Formation, Neocomian to Albian

Niger Delta Basin

It is situated between Benue Trough and south Atlantic Ocean. The basin is defined by the Okitipupa ridge in the west and Calabar flanks in the east. It belongs to the Cenozoic era and its evolution started in the early Tertiary. It pro-graded over the subsiding continental-oceanic lithospheric plate and the average thickness of sediment in this basin is 12 km with an area extent of 140, 000 km^2 (Obaje, 2009). It is subdivided into Akata Formation (shale), Agbada Formation (intercalation of shale and

sand) and Benin Formation (sand). The structural features include growth fault and roll over anticline, they are well observed in the Agbada Formation and die out in the Akata Formation (Rahaman 2006c).

Anambra Basin

It is an inland sedimentary basin bounded by Abakaliki anticlinorium in the east, Benin hinge line in the south western direction and Niger Delta basin in the southern part (Ekine and Onuoha, 2010). The basin is formed via continuous subsidence and the sedimentation has not been affected by major tectonic event.

Stratigraphic successions (Obaje *et al.*, 2013) include:

(i) Nsukka Formation

(ii) Ajali Sandstone

(iii) Mamu Formation

(iv) Nkporo Shale

(v) Pre-Santonian sediment

2.5 Geology of the Study Area

The Cocoa Research Institute of Nigeria lies within the migmatite-gneiss complex and schist. The study location falls within the migmatite-gneiss terrain, as extracted from the geologic map, orienting in the north-south direction (Fig. 2.2).

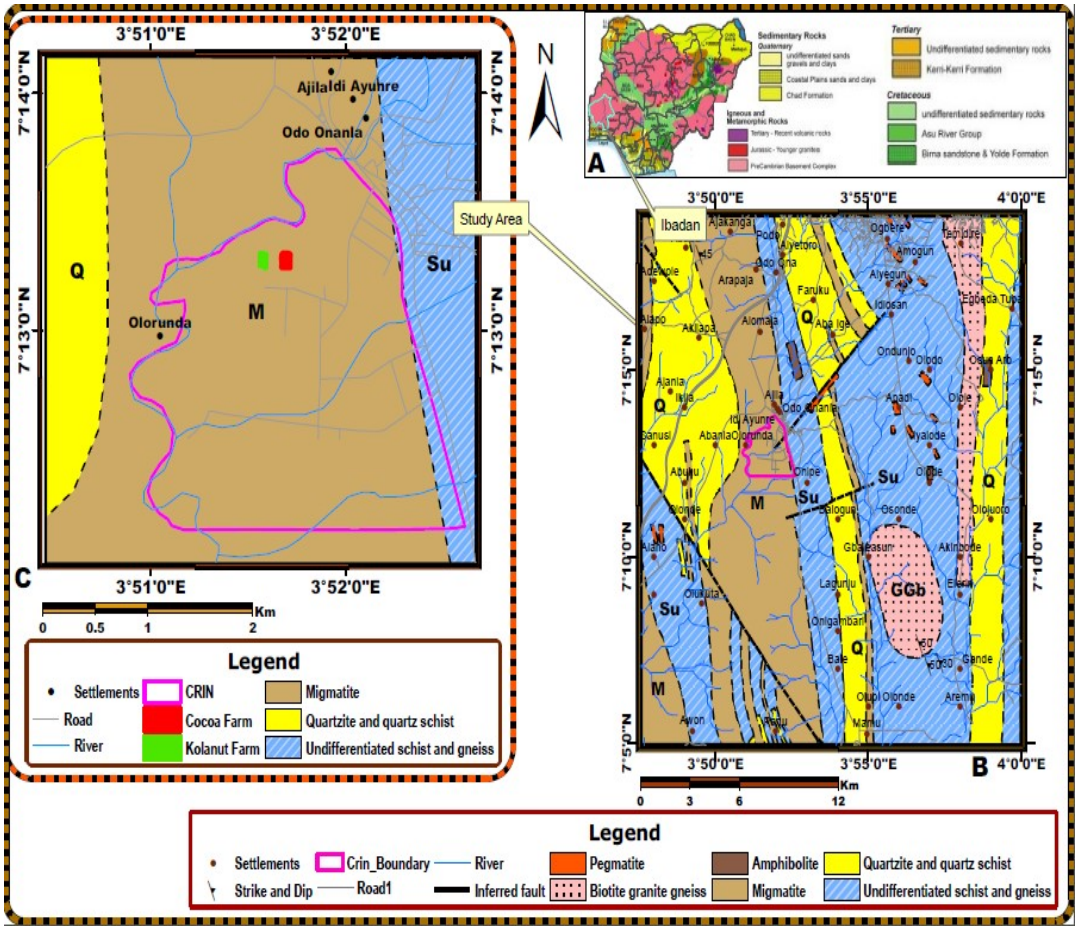

Figure 2.2: The study area is situated within migmatite gneiss complex (After NGSA 2009)

2.6 Electrical Resistivity Method

Reynold (1997) made know that development of electrical resistivity methods was dated back to early 1900s and the ease of use of computers to process and evaluate the data had made the methods to be widely used since 1970s. Resistivity surveying is centered on the passage of current through the electrode and distribution of electrical potential in the ground due to the current flow which depends on the electrical resistivity and distribution of the adjoining soils as well as rocks. Electrical resistivity surveying is an essential geophysical technique in environmental applications, search for suitable groundwater source and monitor groundwater pollution; to locate sub-surface cavities, faults and fissure in engineering surveys and suitable in archaeology for mapping out the extent of relics of earliest artifact. In recent times, it has found application in agricultural practices (Corwin and Lesch, 2005a&b and Allred and Smith, 2010), soil apparent electrical conductivity (EC_a) depends on salinity of soil, cation exchange capacity (CEC), clay content, pore size and its distribution, clay minerals, soil organic matter and soil temperature (Molin and Faulin, 2013, Hawkins *et al.,* 2017 and Medéiros *et al.,* 2018).

2.6.1 Basic Principle of Electrical Resistivity

In the delineation of geological units within the earth, various geophysical techniques are usually employed; either singly or in combination. Resistance (R) is that property of a conductor which opposes the flow of electric current when a voltage is applied across the two ends and its unit is Ohm (Ω). Resistance is the ratio of the potential difference (V) to the resulting current flow (I) as defined by Ohm's Law:

$$V = IR \qquad (2.1)$$

Where:

V = Potential difference in volt across the conducting body

I = current flowing in the conductor (Amperes)

R = Resistance of the conductor (Ohms)

The resistance of a conductor depends on the atomic structure of the material or its resistivity (measured in Ohm-m), and this is the property of a material that measures its ability to conduct electricity. A material regarded as a good conductor has a low

resistivity and the one with a high resistivity behaves as a bad conductor. Greek symbol ρ (rho) is the commonly used symbol for electrical resistivity.

2.6.2 Resistivity of Rocks and Minerals

The relevance of this technique stems from the existence of a resistivity contrast between layers, which helps in the detection of subsurface effects produced by flow of current in the ground. The apparent resistivity measured reflects significantly the underground properties in the area of investigation. Effective resistivity of a rock (the resistivity of the rock and its pore water) can be expressed in terms of the resistivity and volume of the pore water present according to the empirical formula given by Archie (1942).

$$\rho = a\emptyset^{-m}S^{-n}\rho_w \quad \text{...(2.2)}$$

Where,

Ø = porosity

S = the water saturation

a, m and n = Empirical constants that have to be determined for each case

$0.5 \leq a \leq 2.5$, $1.3 \leq m \leq 2.5$ and $n \approx 2$

ρ = effective rock resistivity

ρ_w = resistivity of the pore water

The resistivity of a material can be defined as the resistance of conducting cylinder with a cross sectional area (A) and unit length (L) (Fig. 2.3).

$$\rho \propto \frac{A}{L} \quad \text{..(2.3)}$$

$$\rho = R\,\frac{A}{L} \quad \text{..(2.4)}$$

ρ = Resistivity in Ohm-metres

R = Electrical resistance

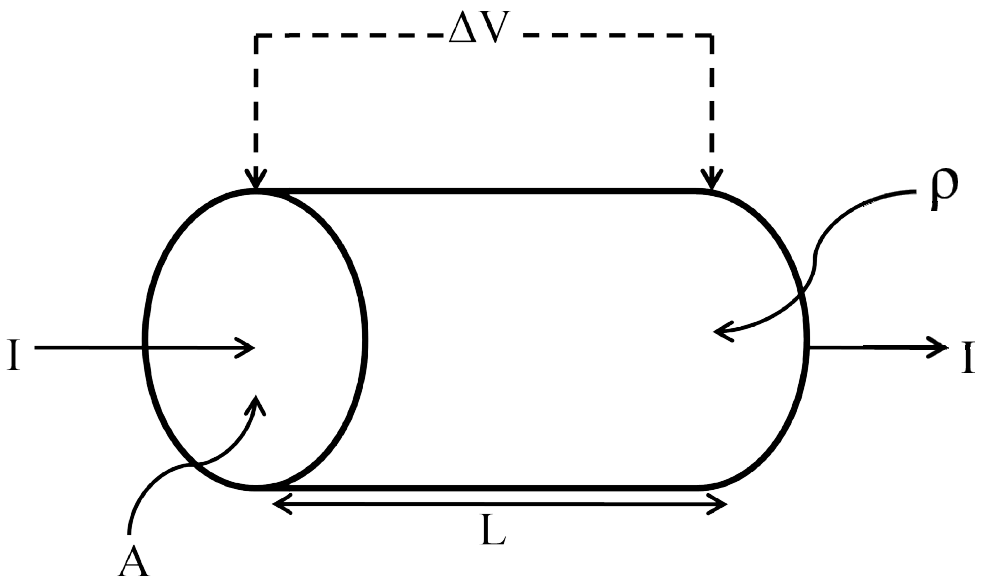

Figure 2.3: Flow of electric current through a conducting cylinder (adapted from Allred *et al.,* 2008)

L = Length

A = Cross-Sectional Area

Resistivity of a rock is a function of porosity and chemical properties of the water filling the pore spaces rather the conductivity of the mineral grains that the rock itself is composed. Therefore, massive rocks such as gneisses are poor conductors except when they are fractured; gravels and clean sands have relatively lower resistivity if filled with water, whereas sands saturated with saline water have the lowest resistivity. Loke (2000) highlighted a list of resistivity values for some rocks and chemicals (Table 2.1). Loke (2000) indicated that metals, such as iron, have extremely low resistivity values, presence of potassium chloride (KCl) and sodium chloride (NaCl) in soil solution tends to increase the electrical conductivity of the soil medium whereas weak electrolytes such as acetic acid slightly influence the conductivity, and hydrocarbon is non-conductive.

2.6.3 Apparent Electrical Resistivity (ρ_a) and Conductivity (σ_a)

Resistivity surveys data are presented and interpreted in the form of values of apparent resistivity (ρ_a). Apparent resistivity of earth material is regarded as the resistivity of an electrically homogeneous and isotropic half-space which is a function of the measured relationship between the applied current and the potential difference taking into cognizance the particular arrangement and spacing of electrodes. The computed resistivity value obtained from a completely homogeneous ground or medium which is half-spaced and it would give same result when examined in same way (Milsom, 2003). In heterogeneous media, the resistivity will vary with change in electrode spacing or movement of the whole array while spacing is fixed. The resistivity (ρ) measured in a homogeneous and isotropic layer is given by

$$\rho = K\frac{V}{I} \quad \text{..... (2.5)}$$

K = Geometric factor

V = Potential difference

I = Applied current

Table 2.1: Resistivities of some common rocks, minerals and chemicals (After Loke, 2000)

Material	Resistivity (Ωm)	Conductivity (Siemen/m)
Granite	$5x10^3$ -10^6	10^{-6} – $2x10^{-4}$
Basalt	10^3 -10^6	10^{-6} – 10^{-3}
Slate	$6x10^2$ – $4x10^7$	$2.5x10^{-3}$ – $1.7x10^{-3}$
Marble	10^2 – $2.5x10^8$	$4x10^{-9}$ - 10^{-2}
Quartz	10^2 – 2 x 10^8	5 x 10^{-9} – 10^{-2}
Sandstone	8-4 x 10^3	210^{-4} – 0.125
Shale	-	5 x 10^{-4} – 0.05
Limestone	50-$4x10^2$	2.5 x 10^{-3} – 0.02
Clay	1-100	0.01 -1
Alluvium	10-800	1.25 x 10^{-3} – 0.1
Groundwater (fresh)	10-100	0.01 – 0.1
Sea water	0.2	5
Iron	$9.074x10^{-8}$	$1.102x10^7$
0.01 M Potassium chloride	0.708	1.413
0.01 M Sodium chloride	0.843	1.185
0.01 M Acetic acid	6.13	0.163
Xylene	$6.998x10^{16}$	$1.429x10^{-17}$

Apparent resistivity (ρ_a) is an expression of Ohm's law involving the ratio of measured voltage (V) to the current applied (I) in the medium, muiltplied by the appropriate geometric factor (k) which depends on the electrode configuration. The analysis of the apparent resistivity (ρ_a) variations makes it possible to draw conclusion on the subsurface conditions. Inverse relationship exists between electrical resistivity (ρ) and conductivity (σ).

$$\rho = \frac{1}{\sigma} \quad \text{.....(2.6)}$$

2.6.4 Generalized Four Electrodes Method For Electrical Resistivity Survey

The physical parameters measured in the field from a generalized four electrode system, A, M, N, B are;

(i) Current I (ampere) flowing between current electrodes A (source) and B (sink).

(ii) Potential difference (ΔU) between the measuring electrodes, M and N.

(iii) Distance between the electrodes.

A collinear arrangement of current and potential electrodes (Fig. 2.4) can be used to establish the geometric factor which is vital in determining the resistivity of subsurface horizon. Current electrodes A and B act as source and sink respectively while the electrodes M and N, measure potential due to each;

At the measuring electrode M potential due to source A,

$$U_m = +\frac{\rho I}{2\pi AM} \quad \text{.....(2.7)}$$

While potential due to sink B

$$U_m = -\frac{\rho I}{2\pi B} \quad \text{.....(2.8)}$$

Similarly, the resultant potential at N due to source A,

$$U_n = +\frac{\rho I}{2\pi A} \quad \text{.....(2.9)}$$

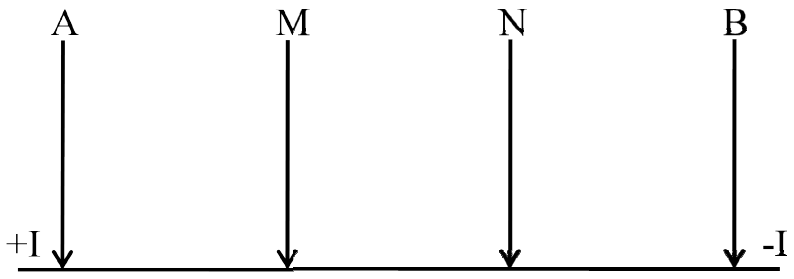

Figure 2.4: A generalized four-electrode system

And potential at N due to sink B

$$U_n = -\frac{\rho I}{2\pi BN} \ldots\ldots\ldots\ldots\ldots\ldots\ldots\ldots\ldots\ldots\ldots\ldots\ldots\ldots\ldots\ldots\ldots\ldots\ldots(2.10)$$

Potential difference Δu between the electrodes is

$$\Delta U = U_m - U_n \ldots\ldots\ldots\ldots\ldots\ldots\ldots\ldots\ldots\ldots\ldots\ldots\ldots\ldots\ldots\ldots\ldots(2.11)$$

$$\Delta U = \left(\frac{\rho I}{2\pi AM} - \frac{\rho I}{2\pi BM}\right) - \left(\frac{\rho I}{2\pi AN} - \frac{\rho I}{2\pi BN}\right) \ldots\ldots\ldots\ldots\ldots\ldots\ldots\ldots\ldots\ldots\ldots(2.12)$$

$$\Delta U = \frac{\rho I}{2\pi}\left(\left(\frac{1}{AM} - \frac{1}{BM}\right) - \left(\frac{1}{AN} - \frac{1}{BN}\right)\right) \ldots\ldots\ldots\ldots\ldots\ldots\ldots\ldots\ldots\ldots\ldots(2.13)$$

$$\rho = \frac{\Delta u}{I}\left(\frac{2\pi}{\left(\frac{1}{AM} - \frac{1}{BM} - \frac{1}{AN} + \frac{1}{BN}\right)}\right) \ldots\ldots\ldots\ldots\ldots\ldots\ldots\ldots\ldots\ldots\ldots\ldots\ldots\ldots\ldots\ldots\ldots\ldots(2.14)$$

$$\rho = \frac{\Delta U}{I} K = RK \ldots\ldots\ldots\ldots\ldots\ldots\ldots\ldots\ldots\ldots\ldots\ldots\ldots\ldots\ldots\ldots\ldots\ldots\ldots\ldots\ldots\ldots(2.15)$$

$$\text{Where } K = \frac{2\pi}{\left(\frac{1}{AM} - \frac{1}{BM} - \frac{1}{AN} + \frac{1}{BN}\right)} \ldots\ldots\ldots\ldots\ldots\ldots\ldots\ldots\ldots\ldots\ldots\ldots\ldots\ldots\ldots\ldots\ldots(2.16)$$

Where K is the geometric factor and K is different for each electrode configuration.

2.6.5 Electrode Configurations

The most commonly used electrode dispositions in resistivity method are Schlumberger, Wenner, and dipole-dipole.

(i) **Wenner array**

It comprises four electrodes in line, separated by comparable intervals or spacing, denoted ‘a’ and the electrodes are separated from one another by equal distance that is the distance between the adjacent electrodes are equal and the potential electrode is separated from the adjoining electrode by a space which is equal to one-third of the partition of the current electrode (Fig. 2.5).

AM = MN = NB = a (Wenner spacing)

$$K = \left(\frac{2\pi}{\left(\frac{1}{a} - \frac{1}{2a} - \frac{1}{2a} + \frac{1}{a}\right)}\right) \ldots\ldots\ldots\ldots\ldots\ldots\ldots\ldots\ldots\ldots\ldots\ldots\ldots\ldots\ldots\ldots\ldots\ldots\ldots(2.17)$$

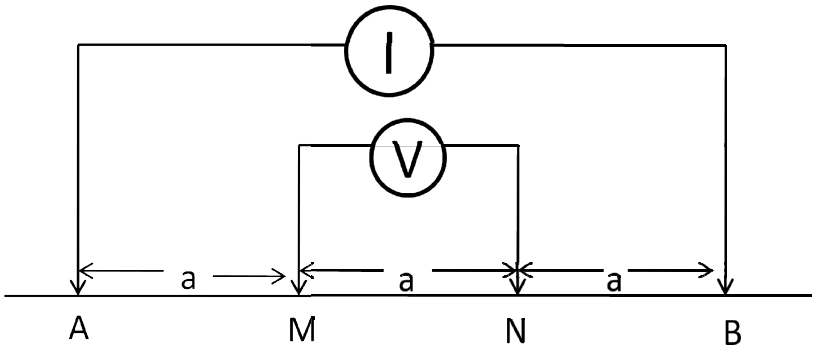

Figure 2.5: A Wenner array

$$K = \frac{2\pi}{(\frac{2}{a} - \frac{1}{a})} = 2\pi a \quad \text{.......................................(2.18)}$$

Recall that $\rho = RK$ and $V = IR$ (Ohm's law).................(2.19)

$$\therefore R = \frac{V}{I} \; (\Omega) \quad \text{...(2.20)}$$

$$\rho = 2\pi a \frac{V}{I} = 2\pi a R \quad \text{..(2.21)}$$

Edwards (1977) developed the idea of EFFECTIVE DEPTH, Z_E, and the space within the subsurface of a homogeneous earth contributing 50% of the signal. For the Wenner array, the centre of this effective depth is given by

$$Z_E = 0.519 * a \quad \text{..(2.22)}$$

Where "a" is the spacing between adjacent electrodes

(ii) **Schlumberger array**

It consists of four electrodes arranged in such a manner that the central (potential) electrodes remain unchanging, whereas the external (current) electrodes are adjusted to vary the distance ‘a’. The spacing ‘b’ is adjusted when it is considered necessary because of declining sensitivity of measurement. Current electrodes are spaced much more apart than the potential electrodes (Fig. 2.6). Apparent resistivity measurements are made by keeping the potential electrodes permanent about the mid-point of the array at the same time as the current electrodes are systematically spaced in opposite directions.

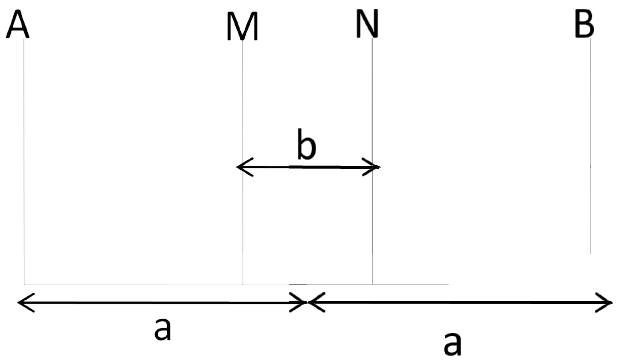

Figure 2.6: A Schlumberger array

$$K = \frac{2\pi}{\left(\frac{1}{\frac{a-b}{2}} - \frac{1}{\frac{a+b}{2}} - \frac{1}{\frac{a+b}{2}} + \frac{1}{\frac{a-b}{2}}\right)} \quad \text{.....(2.23)}$$

$$K = \frac{\pi}{\left(\frac{a^2}{b} - \frac{b}{4}\right)} \quad \text{.....(2.24)}$$

One constraint on use of the Schlumberger arrangement is that the spread of electrode AB must be at least 5 times MN separation; AB > 5 * MN

Effective depth (Z_E) range according to Edwards (1977) is about

$$Z_E = 0.190 * L \quad \text{.....(2.25)}$$

Where "L" is distance AB

(iii) **Dipole- dipole array**

Dipole-dipole arrangement is a member of the family of arrays using dipoles (closely spaced electrode pairs) to measure the curvature of the potential field. Potential electrodes are closely spaced and distanced from the current electrodes, which are also jointly closed (Fig. 2.7). The distance between the two pairs is constantly maintained at the centre.

AB= current dipole

MN= potential dipole

$$AM = a + \frac{c}{2} - \frac{b}{2} \quad \text{.....(2.26)}$$

$$BM = a - \frac{c}{2} - \frac{b}{2} \quad \text{.....(2.27)}$$

$$AN = a + \frac{c}{2} + \frac{b}{2} \quad \text{.....(2.28)}$$

$$BN = a - \frac{c}{2} + \frac{b}{2} \quad \text{.....(2.29)}$$

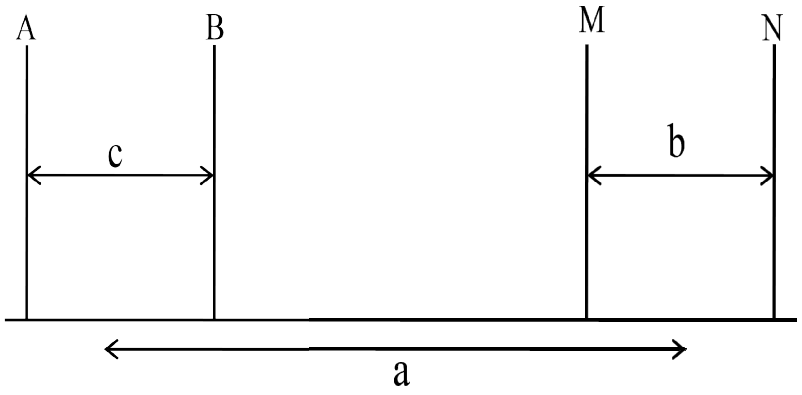

Figure 2.7: A Dipole-dipole array

$$K = \left(\frac{2\pi}{\left(\left(\frac{1}{a+\frac{c}{2}-\frac{b}{2}}\right)-\left(\frac{1}{a-\frac{c}{2}-\frac{b}{2}}\right)-\left(\frac{1}{a+\frac{c}{2}+\frac{b}{2}}\right)+\left(\frac{1}{a-\frac{c}{2}+\frac{b}{2}}\right)\right)}\right) \ldots\ldots\ldots\ldots (2.30)$$

$$\therefore K = \pi\left(\left(\frac{a^3}{b^2}\right) - a\right) \ldots\ldots\ldots\ldots\ldots\ldots\ldots\ldots\ldots\ldots (2.31)$$

Additional electrode arrays include pole-dipole, pole-pole, gradient, square (Milsom, 2003) and the configuration engaged in the course of this study is Wenner.

2.6.6 Advantages of Electrical Resistivity Method

Electrical resistivity method is one of the most broadly used geophysical techniques in investigating the nature of the subsurface material because of its flexibility, relatively rapid and the cost of data acquisition is minimal. The equipment is light and portable coupled with the possibility of quantitative modeling using computer software.

2.6.7 Limitations of Electrical Resistivity Method

Resolution and accuracy of electrical resistivity method may be affected by some inherent limitations such as ambiguity from its interpretation; analysis of resistivity data must be validated with geological concept. For greater depth of penetration to be achieved, utmost electrical power together with electrode layout and lengthy proportion of cable are required. A times the survey requires large electrode spacing for greater depth of investigation which is hindered in the developed areas. For these reasons, it is always worthwhile to use several paired geophysical methods in an integrated exploration program rather than relying on a solitary exploration method. Variation in resistivity of near-surface material may mask its variation from deeper layer, thereby generating a constraint in data interpretation.

2.7 Theory of Water Movement in Soil and Soil Moisture Measurement

Soil is a porous system consisting of air, liquid, and soil phases. The soil solution constitutes the dissolved minerals and organic materials. Soil properties together with the variables such as hydraulic, bulk density, pressure potential, and water content vary in time and position.

2.7.1 Soil Water Potential

Percolation of water in the soil is due to the forces acting on it. Gravitational force and weight of the overburden tend to ensure vertical movement of soil, also the force of attraction between water molecules and solid matrix surface, therefore, the ions in the soil water exhibit attractive force that oppose the movement of the soil solution. Kinetic energy is neglected as a result of the low-velocity flow field in the pores of the soil; the flow process is due to the potential energy of a unit water quantity in the force field. This is invariably responsible for the flow of water from regions of higher potential to low potential areas.

Soil water potential aids the understanding of the transport processes in soil and the assessment of water energy state in soil. Total soil potential is the work done per unit quantity of pore water to move reversibly and isothermally (equal temperature) an infinitesimal water quantity from a collection of pore water at a particular elevation and atmospheric pressure to the body of soil water.

$$\psi_t = \psi_g + \psi_p + \psi_o \qquad (2.32)$$

Where t = total potential

g = gravitational potential

p = pressure potential

o = osmotic pressure

2.7.2 Soil Water Retention

Soil water retention is based on the interaction of volumetric water content (θ) and pressure potential (h) which is controlled by the soil texture and structure.

At equilibrium when the soil is saturated, h = 0.

At critical value, when the pore is filled with air, the potential head in air entry is h_E

$h_E \leq h \leq 0$ (saturated and unsaturated conditions)

Reduction in h leads to a reduction in θ

Effective water content in soil is less than the total pore space in it because of the presence of the entrapped air in the void.

2.7.3 Basic Flow Equation

Water movement through a porous medium which is either saturated or unsaturated soil obeys Darcy's law.

$$q = -K\nabla H \quad \text{.....(2.33)}$$

Where q = volumetric flux density or Darcy velocity

k = soil hydraulic conductivity

H = soil water potential head

2.7.4 Soil Water Content

Soil water content is expressed in terms of either gravimetric or volumetric. Gravimetric water content (θ_g) is expressed as the mass of water divided by the soil mass. This is achieved by measuring the initial weight of the soil sample (M_{wet}), then it is dried to remove moisture and the weight of the dried soil sample is measured.

$$\theta_g = \frac{\text{Mass}_{water}}{\text{Mass}_{dry}} = \frac{\text{Mass}_{wet}\text{-Mass}_{dry}}{\text{Mass}_{dry}} \quad \text{.....(2.34)}$$

Volumetric water content (θ_v) of soil is expressed as the volume of water per unit volume of soil, which is, the mass divided by its density (ρ).

$$\theta_V = \frac{\text{Volume}_{water}}{\text{Volume}_{soil}} = \frac{\frac{M_{water}}{\rho_{water}}}{\frac{M_{soil}}{\rho_{soil}}} = \frac{M_{water}}{M_{soil}} * \frac{\rho_{soil}}{\rho_{water}} \quad \text{.....(2.35)}$$

$$\theta_V = \theta_g * \frac{\rho_{soil}}{\rho_{water}} \quad \text{.....(2.36)}$$

$\rho_{water} \approx 1$

ρ_{soil} is termed soil bulk density (ρ_{bulk})

2.7.5 Measurement of Water Content in the Soil

Measurement of soil water content is of significance in many studies and it is applicable in soil mechanics, agriculture, hydrology, hydraulic engineering, and meteorology. Soil water content plays a fundamental role in plant growth as a result of its ability to dissolve the solid nutrient into solution. Direct and indirect approaches have been used in determining soil water content.

Direct method

This is destructive in nature by removing the soil sample from the sample location and estimating the quantity of water present in it. The gravimetric method is the most widely used because it is not complicated, precise and the equipment for the evaluation is not expensive. The disturbed or undisturbed soil samples can be taken from the appropriate depth, weighed, and sealed to prevent evaporation or gain of moisture before the conduct of laboratory analysis. The soil sample is placed in a can and taken

into the oven and dried at 105^0 to 110^0C for 24 hours, the weight of the oven-dried soil sample is measured, pending no further weight loss.

The demerit of the gravimetric method

1) An error may be introduced at the time of sampling

2) Soil cores may include roots, stones, and voids may mask the determination of soil volumetric water content.

3) Soil sampling and laboratory analysis are laborious and time-consuming.

Indirect methods

This is a non-destructive method and the measurement may be repeated at the same sample location. The indirect method engages the use of physical or physico-chemical properties of soil which are highly related to the water content in the soil. These methods include time-domain reflectometry (TDR), electrical resistance, gamma attenuation, neutron thermalization, nuclear magnetic resonance imaging, and remote sensing (Brocca *et al*., 2017). Neutron method is based on high energy neutrons colliding with the hydrogen atom and it is responsible for the energy loss of the fast-moving neutrons resulting in slow neutron pulses and it exhibits a linear relationship with soil water content. Time-domain reflectometry (TDR) measures the velocity of the EM wave, it measures the dielectric permittivity of soil. This is achieved by monitoring the time of travel of an EM field to propagate the soil at a specified depth. It is the dielectric property of the medium which makes its constituent molecules become polarized, thus describing the relative dielectric permittivity (ε) of the medium.

A dielectric material is an electrical insulator that does not conduct electric charge but becomes polarized. The ability to store the polarized charges depends on the nature of the constituent material in the soil unit. The total dielectric of soil is the sum of the dielectric of each of the individual soil components.

$$\varepsilon_t^b = \varepsilon_m^b V_m + \varepsilon_a^b V_a + \varepsilon_w^b \theta + \varepsilon_{om}^b V_{om} \quad \text{.....(2.37).}$$

$$\theta = \frac{1}{\varepsilon_w^b} * \varepsilon_t^b - \frac{(\varepsilon_m^b V_m + \varepsilon_a^b V_a + \varepsilon_{om}^b V_{om})}{\varepsilon_w^b} \quad \text{.....(2.38)}$$

Where b = constant

θ = volumetric water content

t = total

m = mineral soil

a = air

om = organic matter

w = water

V = volume fraction

2.8 Theory of Soil Textural Analysis

The particle size distribution of minerals in the soil is crucial in defining the nutrient and water retention capability of the soil. The larger the surface area per unit volume (clay and silt), the better the nutrient and water retention than those of the smaller surface area (sand). The fertility status, water infiltration, and retention are based on the content of soil fine particles. Separation of particles size of soil can be achieved via mechanical sieving and sedimentation methods. The soil particles are disaggregated using hexametaphosphate to remove the binding or cementing materials such as organic matter, iron oxide, calcium, and magnesium. Separation by sedimentation operates based on Stoke's law.

Stoke's law is used to describe the pendulums' motion in the viscous fluid. He examined the influence of internal friction of fluid (viscosity) resisting the motion of a moving body in it. The frictional resistance is dependent on the radius (r) and velocity (v) of the particle coupled with the viscosity of the medium (η).

$$F_r = 6\pi\eta r v \quad \text{.....(2.39)}$$

F_r = Frictional force.

Another force that opposes the downward movement of the particle is the buoyant force (F_b), this is equal to the weight of the liquid displaced by the particles, and this is calculated as the mass of the particle. It is the product of volume ($\frac{4\pi r^3}{3}$) and density (ρ_l) with the gravitational constant (g).

$$\text{Force (F)} = \text{Mass(m)} * \text{Acceleration (a)} \quad \text{.....(2.40)}$$

$$\text{Density} = \frac{\text{Mass (m)}}{\text{volume (v)}} \quad \text{.....(2.41)}$$

$$F_b = \frac{4\pi r^3}{3} * \rho_l g \quad \text{.....(2.42)}$$

The gravitational force (F_g) accelerating the body downward is given as;

$$F_g = \frac{4\pi r^3}{3} * \rho_s g \quad \text{.....(2.43)}$$

ρ_s = Density of the particle.

A particle accelerates rapidly as it begins to fall through a liquid medium, this is due to greater gravitational force (F_g) of the body than the buoyant force (F_b) which has a higher solid density (ρ_s) than the liquid density (ρ_s).

The particle attains constant velocity as a result of balance in the opposing forces.

$$F_g = F_b + F_r \text{.....(2.44)}$$

$$V = \frac{2r^2 g(\rho_s - \rho_l)}{9\eta} \text{.....(2.45)}$$

Where V = velocity of fall of the particle

g= gravity acceleration

ρ_s = density of solid particle

ρ_l = density of liquid

r = radius of the particle

η = viscosity of the fluid

Basic assumptions supporting the application of Stoke's law;

1) Once the particles settling begin, then terminal velocity is attained.

2) The settling rate and resistance are solely dependent on fluid viscosity.

3) It assumes that the particles are smooth and spherical in shape.

4) It is based on the fact that there is no interaction between the individual particle within the solution.

5) Water temperature is expected to be constant during sedimentation.

2.9 The Flow of Heat in the Soil

The source of heat at the soil surface is solar. Soil temperature varies in time and space which is propagated into the soil profile resulting in a temperature gradient. This is responsible for the transfer of kinetic energy causing the collision of moving molecules from hotter regions to colder areas. Heat is transported via three primary means; conduction, convection, and radiation. Transport of heat through soil profile involves accumulation and discharge; soil thermal properties are used in engineering, soil science, and agronomy. Conduction is the transmission of heat energy within a body through internal molecular motion. Convection is the heat energy flow in the body of fluid by the actual motion of matter. Radiation is the transfer of heat energy in the form of electromagnetic waves with the source of emission from bodies having temperatures above 0^0K.

The rate of heat flow through a rod in the steady-state is directly proportional to the area (A) and temperature difference (T_1-T_2), and inversely proportional to the rod thickness (L).

$$H \propto A \quad \text{.....(2.46)}$$

$$H \propto (T_1\text{-}T_2) \quad \text{.....(2.47)}$$

$$H \propto \frac{1}{L} \quad \text{.....(2.48)}$$

$$H = K\frac{A(T_1\text{-}T_2)}{L} \quad \text{.....(2.49)}$$

H = Heat convent (quantity of heat flowing through a rod per unit time).

K = Thermal conductivity.

Thermal conductivity (λ) of soil is the rate at which heat energy is transferred by thermal conduction across a unit area of soil subjected to a unit temperature gradient. Considering the heat flow in a thin layered material, which has a thickness (X) of the layer and cross-sectional area (A). The negative connotes that the temperature decreases in the direction of increasing X, that is, from region of high temperature to region of low temperature.

$$H = -K\frac{A\Delta T}{\Delta X} \quad \text{.....(2.50)}$$

$$\therefore K = -\frac{H\Delta X}{A\Delta T} \quad \text{.....(2.51)}$$

$$K = \frac{\left({}^{1J}/_{s}\right)(1m)}{(1m)^2(1K)} \quad \text{.....(2.52)}$$

$$= JS^{-1}m^{-1}K^{-1} \quad \text{.....(2.53)}$$

$$= Wm^{-1}K^{-1} \quad \text{.....(2.54)}$$

Soil volumetric heat capacity (C) is the energy required to raise the soil temperature of 1 cm^3 by 1^0C, it is also the product of specific heat capacity (J/gK) and density (g/m^3). Volumetric heat capacity of soil is the computation of the heat capacities of the individual components of soil such as mineral grains, water, air, ice, and organic matter multiplied by their volume fraction.

$$C_v = C_aV_a + C_wV_w + C_sV_s + C_{om}V_{om} + C_iV_i \quad \text{.....(2.55)}$$

C_v = Volumetric heat capacity

C_a, C_w, C_s, C_{om} and C_i = Heat capacity of air, water, solid particles, organic matter and ice.

V_a, V_w, V_s, V_{om} and V_i = Volume fraction of air, water, solid particles, organic matter and ice.

$$= \text{mJ/m}^3\text{K} \quad \text{.....(2.56)}$$

Thermal diffusivity is the proportion of thermal conductivity to the volumetric heat capacity.

$$\text{Thermal diffusivity} = \frac{\text{Thermal conductivity}}{\text{Volumetric heat capacity}} \quad \text{.....(2.57)}$$

$$= \text{mm}^2/\text{s} \quad \text{.....(2.58)}$$

2.10 Principle of Geochemical Investigation

The distribution from magma to weathered horizons follows two suites of dispersion, the primary and secondary dispersions. Primary dispersion is the migration of elements by magmatic, hydrothermal, and metamorphic processes below the surface of the earth, which is responsible for the formation of igneous and metamorphic rocks (crystalline rocks). Secondary dispersion is associated with the weathering episodes of bedrock under the different climatic system. It avails the weathering history to be recorded in the landform and the regolith covering the bedrock. The imprint of the geochemical and mineralogical characteristics is preserved in the soil profile.

Weathering is dominated by the physical and chemical changes required to bring into equilibrium the rocks and the new conditions at the earth's surface, in order words, minerals that are stable at the subsurface environment are added up to form new stable minerals in the surface environment. In mapping, chemical analysis of soils brings out the spatial distribution of minerals for easy identification of anomalous areas.

2.10.1 Principle of Soil pH

It gives information on the nature of soil; acidic, basic, and neutral, and this is measured regarding the activity of the hydrogen ions in the soil water system. pH is the term used for the negative logarithm of the hydrogen ion activity. pH of a soil is not the amount of acid in the soil but a measure of the strength of hydrogen (H) ion activity (H).

$$\text{pH is } \log\frac{1}{\text{H}} = -\log\text{H}^+ \quad \text{.....(2.59)}$$

2.10.2 Principle of Soil Electrical Conductivity (EC)

It is the specific conductivity at 25^0C of soil solution extracted from the mixture of soil and water in a distinct ratio. This is a measurement of dissolved salt in soil solution and it obeys Ohm's law. It was based on the migration of ions in soil solution when an

electric field is applied. The strength of the EC is a function of ions quantity in the solution.

$$V \propto I \quad \text{.....(2.60)}$$

$$V = IR \quad \text{.....(2.61)}$$

V = Voltage

I = Current

R = Resistance

2.10.3 Principle of Organic Carbon and Organic Matter Evaluation

Walkey-Black chromic acid wet oxidation technique was used in determining the organic carbon in the soil, 1N $K_2Cr_2O_7$ aids in oxidising the oxidisable matter in the soil. Heat is generated from the addition of one volume of potassium dichromate with two volumes of sulphuric acid. It is titrated with the ferrous sulphate and the titre value is related to the quantity of carbon present in the soil. A conversion factor of 1.724 multiply with total organic carbon quantifies the content of total organic matter.

2.10.4 Principle of Total Nitrogen Determination

Determination of total nitrogen passes through three stages; digestion, distillation, and titration.

Digestion converts organic nitrogen into ammonium ions (NH_4^+). Organic carbon is acidified with sulphuric acid to form CO_2 and water. This is done in the presence of a catalyst at a temperature between 350^0 and 380^0C to fasten the digestion.

$$\text{Protein (N)} + H_2SO_4 \xrightarrow{\text{Catalyst}} (NH_4)_2SO_4 + CO_2 + H_2O \quad \text{.....(2.62)}$$

The digest is cooled at room temperature, diluted with distilled water.

Distillation is engaged to convert ammonium ions (NH_4^+) to ammonia (NH_3) by adding NaOH.

$$(NH_4)_2\,SO_4 + 2NaOH \rightleftharpoons 2NH_3 + Na_2SO_4 + 2H_2O \quad \text{.....(2.63)}$$

Then, boric acid is added ($B(OH)_3$) in order to capture the ammonia and forming ammonium ions.

$$B(OH)_3 + NH_3 + H_2O \rightleftharpoons NH_4^+ + B(OH)_4^- \quad \text{.....(2.64)}$$

Direct titration is used to capture ammonium ions with hydrochloric acid.

$$B(OH)_4^- + HCl \rightleftharpoons Cl^- + B(OH)_3 + H_2O \quad \text{.....(2.65)}$$

2.10.5 Principle of Exchangeable Acidity

1N potassium chloride (KCl) solution is added to the soil, and exchangeable hydrogen and aluminum ions are taken into solution. Phenolphthalein is added to the filtrate, the solution is titrated with a standard solution of alkali until the solution is permanently pink. The content of hydrogen and aluminum ions is equivalent to the amount of alkali used.

$$H^+ + OH^- \rightarrow H_2O \quad \text{.....(2.66)}$$

$$Al^{3+} + 3OH^- \rightarrow Al(OH)_3 \quad \text{.....(2.67)}$$

2.10.6 Principle of Available Phosphorus Evaluation

Bray and Kurtz-P1 method was developed by R.H. Bray and T. Kurtz in 1945; it is the portion of total phosphorus in the soil that can be consumed by the plant. Ammonium fluoride (NH_4F) solution will remove phosphate ions from insoluble iron phosphate and aluminum. The concentration of the fluoride ions must be kept constant in tests and standards because it has a slightly depressant effect on the development of blue colour. The spectrophotometer measures the colour intensity of the monochromatic beam.

2.10.7 Principle of Sodium and Potassium Determination in Flame Photometry

1N ammonium acetate is added to the soil, the content undergoes shaking to ensure the extraction of the exchangeable potassium and sodium. The solution containing Na and K ions are fed as a spray into the flame. The valence electrons of the Na and K atomized into a flame become excited to a higher energy level. The electrons emit photons of light energy as they return to the ground state energy level. Each of the elements has a light of a characteristic wavelength in which its intensity is proportional to its concentration in the sample being examined. K is excited in a flame giving a lilac colour at a wavelength of 767 millimicrons and intense yellow colour is produced from the excitation of sodium in a flame at approximately 590 millimicrons wavelength.

2.10.8 Principle of Magnesium and Calcium Determination in Atomic Absorption Spectrometry (AAS)

Exchangeable calcium and magnesium are determined in neutral 0.1N ammonium acetate, the extraction is executed by shaking the content, and this is followed by

titration and AAS is used to determine the concentration of Mg and Ca in the sample. The filtrate is analysed by atomic absorption spectrometry, and it measures the quantity of energy absorbed by the sample in form of photon.

The wavelength of the transmitted light is measured by the detector and the concentration of the analyte is directly proportional to the absorbance, which is determined from the calibration curve using a standard of known concentration.

2.11 Physics of X-Ray Diffraction (XRD) Technique

A crystal consists of the ordered internal arrangement of cells into a lattice. Crystals have atomic planes that are spaced at a distance (d) apart and different d-spacing can be obtained when the atomic planes are resolved. Crystal has specified lengths a, b, and c with angles (α, β, and γ) between a, b, and c which can be determined by analysis. XRD studies are useful in determining XRD pattern, measuring the d-spacing, and intensities of the wave. All these parameters aid the analysis of the crystal structures.

Electrons are produced from hot filament with high accelerating voltage between the cathode and anode which collide with a metal target, such as Co, Al, Mo, and Mg, thereby generating x-rays. The incident beam of x-rays travels through the crystal along its atomic plane and becomes diffracted as they leave the crystal. This is known as x-ray diffraction (Fig. 2.8). For diffraction to occur, there must be constructive interference of x-ray 1 and 2 from planes with d-spacing so that Bragg's law is satisfied (Fig. 2.9). Constructive interference connotes that the intensities of the wave add-up while destructive interference is responsible for the canceling of the intensities.

Bragg's law used to explain x-ray scattering in crystals, x-ray beams set at an angle of incidence (theta, θ) is reflected by the cleavage face of the crystal.

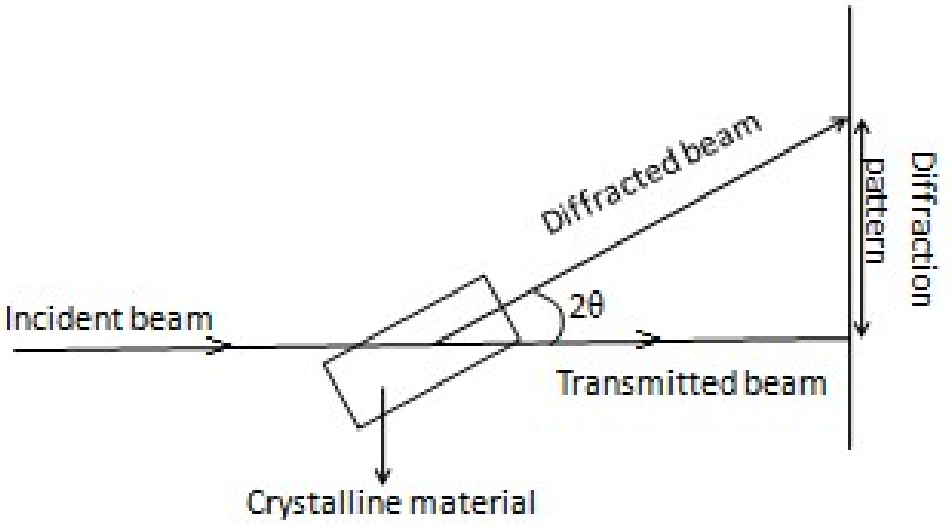

Figure 2.8: Schematic of X-ray diffractions.

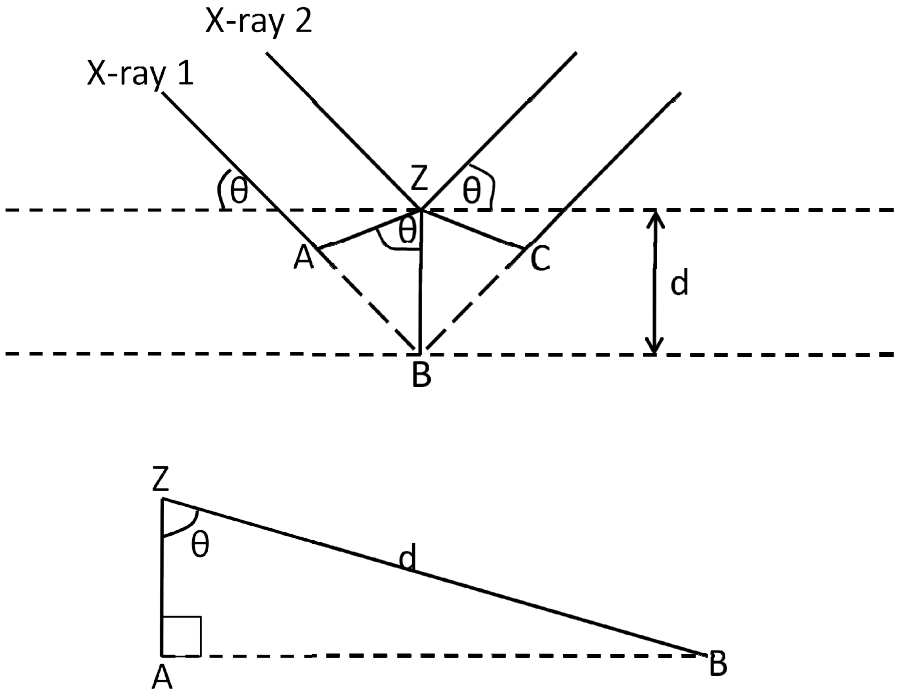

Figure 2.9: Diffraction of X-rays from a set of planes.

$$n\lambda = AB + BC \quad \text{.....(2.68)}$$

$$AB = BC \quad \text{.....(2.69)}$$

$$n\lambda = 2AB \quad \text{.....(2.70)}$$

$$\text{Sin}\,\theta = AB/d \quad \text{.....(2.71)}$$

$$AB = d\,\text{Sin}\theta \quad \text{.....(2.72)}$$

$$n\lambda = 2d\,\text{Sin}\theta \quad \text{.....(2.73)}$$

Where n = Integer

λ = Wavelength of incident x-ray

d = Interplanar spacing

θ = Angle of incidence

Parameters measured in XRD

1) It measures the spacing between layers of atoms.

2) It establishes the orientation of a crystal.

3) It establishes the size, shape, and internal stress of crystalline areas.

4) It aids in determining the crystal structure.

CHAPTER THREE

METHODOLOGY

3.1 Field Inspection of Cacao and Kola Fields

This research stemmed from observations made on both kola and cacao plants at Cocoa Research Institute of Nigeria (CRIN). It was discovered that some of the kola trees were characterized with stunted growth with respect to other kola trees planted or cultivated at the same period. More so, some of the cacao trees produced fewer cocoa pods compared with other having higher number of pods, the cacao trees within the farm were planted at the same season or time. Visual observation of the cacao trees carried out during the peak of dry season showed that some of the trees withered while others exhibited healthy growth.

3.1.1 Geological Mapping and Laboratory Analysis

The studied outcrops were situated between Latitudes 7˚13′10.2″N and 7˚14′04.6″N, and Longitudes 3˚51′34.8″Eand 3˚51′55.6″E. The geological mapping was conducted around the study area using global positioning system (GPS), geological hammer, compass-clinometer, measuring tape, field note, camera and sample bag. Sectioning of the rock samples into slides was carried out at the Department of Earth Sciences, Ajayi Crowther University, Oyo using Hillquist thin section machine and the petrographic studies were conducted via Brunel petrographic microscope.

Laboratory preparation of rock into thin section

(1) The rock samples obtained from the field were cut into small size of about 8 mm thick using Hillquist trim saw.

(2) One of the surfaces of the cut rock section was polished using 400 grade carborundum on the glass plate.

(3) The polished surface was then mounted on the glass slide using aradite epoxy resin.

(4) The mounted slide was allowed to set for 30 minutes and it was then cut into a sheet of about 90 microns size.

(5) The sample was then grinded on the grinding plate using four grades of carborundum, that is, 90, 400, 600 and 800. The rock sample was grinded to 30 micron size.

(6) Excess aradite was removed from the surrounding of the sample and the slide was then covered using aradite epoxy resin on the hot plate.

Thin section analysis

(1) The rock thin section was viewed under the Brunel petrographic microscope using both the cross and plane polarised light.

(2) The mineral constituents of the rock were identified under plane polarised light and cross polar by observing all the necessary mineral properties, and the modal analysis of the minerals composition were counted per grid to determine the relative composition of minerals in the rock sample.

3.1.2 Field Data Acquisition Pattern

Seasonal assessment of spatial variability of soils in cacao and kola farms were carried out in August 2016 and March 2017 to check variations during the peak of wet and dry seasons. Rhoades *et al.* (1989) suggested that EC_a measurement should be carried out when the soil moisture content is near its field capacity, this is to ensure homogeneous distribution of soil moisture content such that apparent electrical conductivity is near the electrical conductivity of soil saturation extract. This was taken into cognizance, which has guided the time of field data acquisition to be during the peak of rainy season (August 2016), although it was taken when there was no rainfall (August rainfall break) as change in soil moisture content would affect field measurement (Figs. 3.1 and 3.2) and subsequent measurement were carried out during dry season (March 2017). Cacao root distribution is characterized as a thick mat with a tap root for anchoring onto the soil (Fig. 3.3) and water uptake in a soil layer is proportional to the root hairs area in that layer.

Figure 3.1: Electrical earth resistance measurement taken with resistivity meter using electrodes mounted in a fixed configuration at kola farm

Figure 3.2: Electrical earth resistance measurement taken with allied Ohmega resistivity meter.

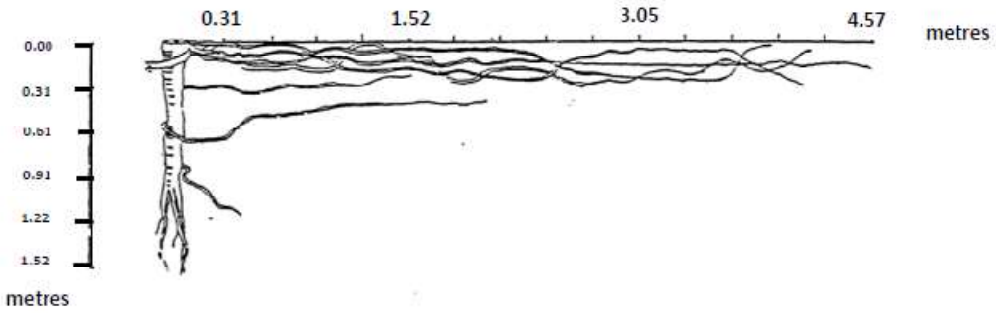

Figure 3.3: The root system of cacao plant (Modified after Mommer, 1999).

3.1.3 Depth of Investigation

Mommer (1999) stated that 90% of cacaos' root hairs are situated within the 30 cm of soil while remaining 10 % is found at deeper depth. Kola nitida has both the buttress and taproot, as at the time of study, the lateral roots have their concentration between 0.28 m and 0.32 m; and the kola nitida plot was cultivated in 2010. While the hybrid cacao is hybrid farm was established in the year 2000. The investigation was carried out at both farms at a depth of 0.30 m.

3.1.4 Geo-Electric Instrumentation

Equipment used in the course of geo-electric measurement are frame model with fixed electrodes, allied earth resistivity meter, set of cable reels, global positioning system (GPS) and measuring tapes.

(i) GPS Instrument: Garmin GPS is used in taking the geographical coordinates and precise elevation in the field.

(ii) Resistivity meter: Allied Ohmega resistivity earth meter was engaged for the field survey. It measures the resistance of soil horizon and takes the resistance readings of subsurface layer automatically and the result was averaged continually to obtain a precise value. Resistance readings are computed to resistivity value (in Ωm) as a product of the resistance in Ohms (Ω) and the geometric factor (K); which was later converted into conductivity by taking its reciprocal.

(iii) Electrodes: Electrodes are fixed on a wooden frame at constant spacing of 40 cm for ease of mobility with a target of ensuring equal depth of penetration in a similar version with Corwin and Lesch (2003). The electrode is a steel rod with sharp pointed mouth driven into the ground for good contact. It comprises four set, two set are used as current electrodes while the other two are used as potential electrodes.

(iv) Cable reels: They contain connecting wires that were insulated with light weight plastic material and wound around the cylindrical plastic reels. It comprises four set, which was used to complete the electrical circuit between the electrodes and the earth resistivity meter.

(v) Measuring tapes: they are used to measure station points at which the resistances are taken on the field.

3.2 Apparent Soil Electrical Conductivity Measurements and Sampling Scheme

The soil's apparent electrical conductivity (EC_a) was measured using allied ohmega geophysical earth resistivity meter, and Wenner configuration was adopted for the resistivity measurement (Bozkurt *et al.*, 2009 and Costa *et al.*, 2014) at a constant inter-electrode spacing of 0.4 m (40 cm). The electrodes were fixed on a mobile handy wooden frame to ensure constant spacing, equal depth of penetration and ease of data acquisition (Fig. 3.4). A total of twenty-seven profiles consisting of 912 and 906 data points were established at the cacao field during wet and dry seasons respectively while twenty-one lines were instituted in the kola plot comprising 700 and 699 data locations during rainy and dry seasons respectively.

EC_a measurement at the root zone using a mobile handy electrical resistivity frame is quick, reliable and cost effective, the frame model adopted is similar to Corwin and Lesch (2003) and Peralta et al. (2013), a calculated attempt was made to take the resistivity measurement at 30 cm soil horizon (the root zone). Edward (1977) proposed the effective depth of penetration (Z_e) of electric current using Wenner array to be;

$$Z_e = 0.519 * a \quad \text{..... (3.1)}$$

$a = 40$ cm

$$Z_e = 40 * 0.519 = 20.76 \text{ cm} \quad \text{..... (3.2)}$$

Ejection of electric current from the electrode to the ground takes place at the point source, considering additional length of 10 cm from the electrode that has extended into the substrate, thus, the depth of measurement is 30.76 cm. Soil apparent electrical resistivity was taken at the mentioned depth (30.76 cm) for all the sample points. The direction of data acquisition was established in N-S. The cacao field was divided into 27 lines while 21 lines were established for the kola plot. Resistivity data were taken at every 3 m, that is, at interval of 0 m, 3 m, 6 m …99 m along a profile for the cacao and up to 105 m for kola fields while inter-line spacing was 3 m apart (Table 3.1).

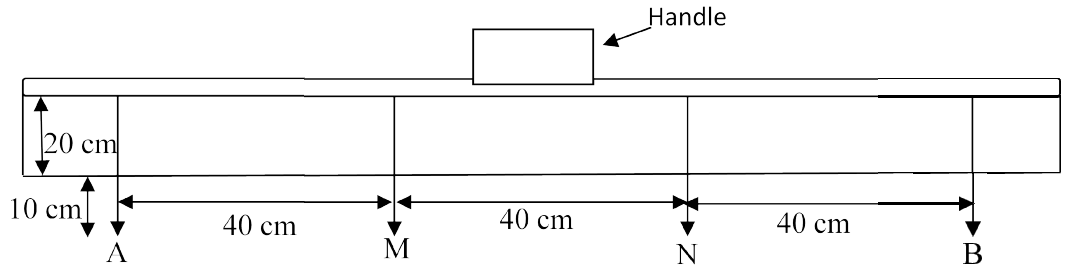

Figure 3.4: Schematic arrangement of electrodes mounted on a fixed wooden frame

Table 3.1: Data acquisition layout showing intra-data point and inter-line spacing.

Line 1	Line 2	-	-	Line 27
0 ← 3 m →	0	-	-	0
3	3	-	-	3
6	6	-	-	6
9	9	-	-	9
-	-	-	-	-
-	-	-	-	-
-	-	-	-	-
99	99	-	-	99
102	102	-	-	102
105	105	-	-	105

The data points were geo-referenced with the aid of Garmin global positioning system (GPS) to provide spatial pattern of soil properties influencing crop growth and its yield. EC_a map was generated using ARCGIS 10.2 software to classify the soil into zones of low, medium and high EC_a.

3.3 Volumetric Water Content (VWC) of Soil

Digital VG-Meter-200 soil moisture meter was used in this study to sense the volumetric water content through the measurement of dielectric constant of soil solution. Dielectric constant measures the ability of a substance to store electrical energy in an electric field. It is a modification of VH400 which has been reported to have provided accurate results (Smarsly, 2013). The probe is a slender waterproof 5 inches long which could easily be used in potted plants and ground. It is not sensitive to soil salinity, never corrodes and uses a capacitive based VH400 probe. The length of cable connecting the probe with the digital meter is 1 m long. Smarsly (2013) examined the soil moisture at depth of 30 cm representing a typical root zone of crop by inserting the sensors at this depth.

Volumetric water content (Θv) is the volume of water per volume of soil. Volume is the ratio of mass to density (ρ) given as;

$$\theta_v = \frac{\text{Volume of water}}{\text{Volume of soil}} = \frac{\frac{\text{Mass of water}}{\text{Density of water}}}{\frac{\text{Mass of soil}}{\text{Density of soil}}} \quad \text{..... (3.3)}$$

$$\theta_v = \frac{\text{Mass of water}}{\text{Mass of soil}} * \frac{\text{Density of soil}}{\text{Density of water}} = \theta_g * \frac{\text{Density of soil}}{\text{Density of water}} \quad \text{.....(3.4)}$$

$$\theta_v = \theta_g * \text{Specific Gravity} \quad \text{.....(3.5)}$$

Where, Θg is the gravimetric water content

The Θv data were acquired at same spot where EC_a data were collected; this indicates that same numbers of data points were generated at each of the fields.

3.4 Procedure of Thermal Assessment

Thermal properties of soils at root zone were determined with the aid of hand held portable KD2Pro thermal analyzer; it makes use of transient line heat source to determine the thermal conductivity, volumetric heat capacity, thermal diffusivity and soil temperature. SH-1 (a small twin needle) sensor was used to measure the stated properties. In order to determine the thermal regime at the root zone, pits of 30 cm depth were dug and the sensor was carefully positioned in the soil at 30 cm depth after being connected with KD2Pro. Then, KD2Pro was turned on to take the measurement and allowed to rest for ten minutes before next reading is taken.

Thermal properties at the root zone were analyzed at 90 and 89 locations within the cacao farm using KD2Pro along ten lines (1, 4, 7, 10, 13, 16, 19, 22, 25 and 27) during wet and dry seasons respectively. Along a profile, measurement were taken at 0 m, 12 m, 24 m, 36 m, 48 m, 60 m, 72 m, 84 m and 96 m; and inter-line spacing of 9 m was adopted except 6 m between lines 25 and 27. A total of 67 stations were occupied at the kola section during the wet and dry seasons. Readings were obtained at eight lines (1, 4, 7, 10, 13, 16, 19 and 21), intra-line data point spacing of 0 m, 12 m, 24 m, 36 m, 48 m, 60 m, 72 m, 84 m and 96 m depending on the length of each of the traverse lines while a distance of 9 m was maintained between lines, except a spacing of 6 m between lines 19 and 21.

3.5 Determination of Soil Permeability

Permeability is defined as the measure of ease with which water flows through soil pores without damage to the fabric of the soil. The test was conducted using both falling head permeameter produced by ELE International and modified Wageningen constant head permeameter.

3.5.1 Falling Head Techniques

The experiment was carried out at the Department of Petroleum Engineering, University of Ibadan. It consists of the following components:

(1) Compaction Permeameter (falling head): It is a metallic cylindrical mould clamped between a top and base cap in which the soil sample to be analyzed was place.

(2) Standpipe Panel: It consists of three glass tube; the length is 1.4 m with varying diameters (1.5 mm, 3.0 mm and 4.5 mm).

(3) De-airing Tank: It is a transparent plastic tank with de-airing jet inlet and a flow outlet connection with flexible tubing mounted on the wall.

(4) Soaking Tank: It is used for containing permeability cell during analysis.

(5) Stop watch: it is a hand held device for measuring start time and stop during test.

Procedure

Twenty undisturbed soil samples were collected at 0.3 m depth from regions of high, medium and low conductivity/VWC from cacao and kola farms in order to establish the rate at which water flows through these earth materials. Each of the soil samples was confined within a metallic cylinder (cell) and connected to a glass tube of de-aired water. This permeameter cell consists of a porous base plate, three tie rods and a top plate machined to allow fixing of small diameter rubber tube. Undisturbed soil samples were completely saturated as presence of air will restrict water flow and false values of permeability will be obtained. Flow of water through the sample was observed by monitoring the rate at which water falls in the standpipe after the water supply from de-aired tank has been disconnected with the aid of stop watch. The measurement was repeated thrice and the average reading was computed.

The approach involves measuring the drop in water level in a standpipe. Assuming the time taken by water to fall from the starting head "H_1" to final head "H_2" is "t", let "H" represents the head at any intermediate time, and "Q" is the volume of water. Let "–*d*H" be the change in head in time interval "*d*t" with cross-sectional area "*a"* in the stand pipe, Darcy's law can be used to establish the rate of flow of water and is given as;

$$Q = \frac{-d\ .a}{dt} = KA\frac{\Delta H}{L} \quad \text{..... (3.6)}$$

Let "L" be the length of soil column while "A" is the cross-section of the soil in the permeameter

Hydraulic gradient $= \Delta\frac{H}{L}$

$$\left(\frac{KA}{a.L}\right)dt = \frac{-dH}{H} \quad \text{..... (3.7)}$$

Integrating both the two component of equation 3.1

$$\frac{K.A.}{a.L}\int_0^t dt = -\int_{H1}^{H2}\frac{dH}{H} \quad \text{..... (3.8)}$$

$$\frac{K.A}{a.L}.\ t = \ln\frac{H1}{H2} \quad \text{……...……...…} \quad (3.9)$$

$$K = \left(\frac{a.L}{A.t} ln \frac{H1}{H2}\right) \text{ or } \left(2.303\left[\frac{a.L}{A.t}\right].\log_{10}\frac{H1}{H2}\right) \text{……...} \quad (3.10)$$

Parameters to be calculated and formulae

Length of sample = L (cm)

Diameter of the sample = D (cm)

Diameter of the standpipe = d (cm)

Area of the standpipe = a (cm^2) = $\pi d^2/4$

Cross-sectional area of the sample= A (cm^2) = $\pi D^2/4$

Initial Hydraulic Head = H_1 (cm)

Final Hydraulic Head = H_2 (cm)

Time taken for water flow from H_1 to H_2 (change in head) = Δt (second)

Hydraulic conductivity, $k = \left(2.303\left(\frac{a.L}{A.\Delta t}\right)\log_{10}\frac{H1}{H2}\right)$ cm s^{-1}…… (3.11)

3.5.2 Constant Head Techniques

This analysis was conducted at soil laboratory, Department of Agronomy, University of Ibadan using modified Wageningen constant head permeameter. It consists of cylindrical metallic core cutter, tripod stand, funnel, beaker and stop watch.

Procedure

A total of twenty undisturbed soil samples were taken at the root zone (0.3 m) with the aid of cylindrical metallic core cutters of 7 cm diameter and height of 7 cm from cacao and kola farms. Soil samples in their respective metallic cores were saturated in water for 24 hours prior to the analysis in order to ensure water rises through the capillary fringes. In an attempt to establish the pressure head difference, another empty metallic core cutter was clamped tightly on top of the core with soil sample and filled with water. The water was made to flow through the soil sample and it was collected at the down flow end of the metallic core through outlet tubing onto a funnel seated on a

beaker. Volume of water that passed through the soil unit was quantified using measuring cylinder while time taken for the water to pass through the sample was measured with stop watch.

Darcy's law was used in ascertaining the hydraulic conductivity, parameters measured include; volume of the water (Q) that flows through the soil column (cm^3), the cross-sectional area (A) of flow (soil core) through the soil column (cm^2); time interval (t), length of soil (L) column (cm) and the hydraulic head difference (ΔH) in cm. Saturated hydraulic conductivity was determined using eq. (3.12) as described by Hillel (2004).

$$K_{sat} = \frac{QL}{At\Delta H} \quad \ldots\ldots\ldots\ldots\ldots\ldots\ldots\ldots\ldots \text{(3.12)}$$

3.6 Determination of Soil Particle Sizes

Soil samples were taken at the root zone (30 cm) with the aid of hand auger. A total of fifty-four and forty-two soil samples were collected from cacao and kola plots respectively. They were placed in polythene bags and labeled to avoid mix-up of samples. Samples were taken at every 18 m along a profile and inter-line spacing of 9 m was adopted; six sampling spots were established per line with subsequent inter-line spacing of 9 m from the initial spot, that is, line 1, 4, 7…25 depending on the area extent of study location and Garmin global position system (GPS) was used in taking the coordinates of the sample locations.

The soil samples were air dried at room temperature, each of the air dried sample was subjected to coning in order to ensure uniform distribution of soil fraction, followed by quartering and opposite quarters were mixed together before measuring 500 grams of soil required for mechanical sieve analysis. Soil particles larger than 2mm in diameter were eliminated via 2 mm sieve aperture using mechanical sieve device set to agitate the sample for fifteen minutes. Sample fractions with less than or equal to 2 mm were also subjected to coning and quartering to ensure that a representative sample was taken for hydrometer test.

Stokes' law is the basis for hydrometer analysis; it relates velocity of fall & diameter of particles sphere in a fluid together with specific gravity of the sphere and that of the fluid, and the fluid viscosity. The equation is given as;

$$V = \frac{2}{9} * \frac{(Gs - Gf)}{\eta} * \left(\frac{D}{2}\right)^2 \ldots\ldots\ldots\ldots\ldots\ldots\ldots\ldots \text{(3.13)}$$

Where,

v = velocity of fall of particle sphere in cm/s

G_s = specific gravity of sphere

G_f = specific gravity of fluid which varies with temperature

η = viscosity of the fluid (g/(cm*s))

D = the diameter of particle sphere in cm

Substituting G_f for G_w which is the specific gravity of water, D can be determined by the equation below,

$$D = \sqrt{\frac{18\eta V}{(Gs - Gw)}} \quad \text{..... (3.14)}$$

Where, $v = \frac{L}{T}$

L= effective length in cm, T= time taken in s

$$\text{Therefore, } D = \sqrt{\frac{18\eta L}{(Gs - \quad)T}} \quad \text{..... (3.15)}$$

Procedure for Particle Size Analysis

50 g of soil particles that passed through the 2 mm sieve aperture was taken for particle size analysis to determine the percentage of clay, silt and sand using Bouyoucos hydrometer method. United State Department of Agriculture (USDA) soil texture triangle was used in classifying the textural class of the soils from the farms. It comprises twelve textural classes (Fig. 3.5).

The sample was put in a 500 ml dispersing cup, 20 ml of dispersing solution (sodium hexametaphosphate) was added and distilled water was added to almost the top mark of the cup. It was allowed to soak for fifteen minutes and baffle stirrer blade was used in stirring the content for ten minutes. After this, it was transferred into 1000 ml sedimentation flask and makes it up to 1000 ml mark with distilled water. The mouth of cylinder was covered by a stopper, palm was placed on it and the content is shaken vigorously by turning upside down and upright (inverting up and down) for several times.

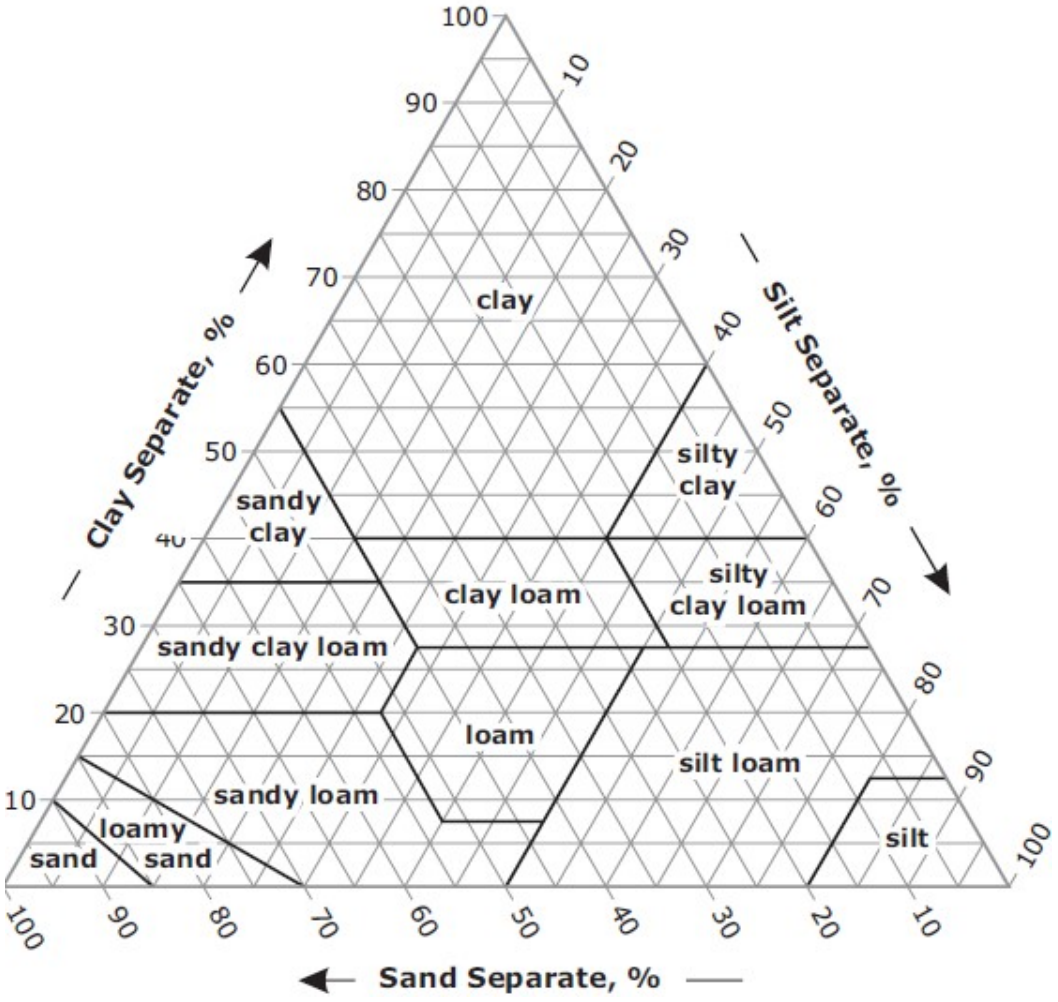

Figure 3.5: Soil textural triangle (Adapted from Schoeneberger *et al.,* 2012)

Cylinder was gently placed on the working bench, after thirty seconds, the hydrometer was placed in the suspension slowly, it was allowed to stay for one minute and hydrometer reading was taken at the top of the meniscus of water and hydrometer. Hydrometer was then removed and cleaned in distilled water while the temperature of the suspension was measured with thermometer. The hydrometer was gently returned into the suspension again after two hours and another reading was taken, it was then removed and the thermometer was inserted and its reading was noted. Correct hydrometer readings are determined by adding 0.3 for every degree centigrade above the calibration temperature (20^0C) and 0.3 was subtracted for every degree below calibration temperature (20^0C).

Hydrometer reading at one minute = (silt + clay) fractions

$$\% \text{ (silt + clay)} = \frac{\text{Corrected hydrometer reading}}{\text{Weight of the sample (50g)}} * 100 \quad \ldots\ldots\ldots \quad (3.16)$$

Hydrometer reading after two hours = clay content

$$\% \text{ clay} = \frac{Corrected\ hydrometer\ reading}{Weig \quad of\ the\ sample\ (50g)} * 100 \quad \ldots\ldots\ldots\ldots\ldots \quad (3.17)$$

$$\text{Therefore, } \%\text{silt} = \%(\text{silt} + \text{clay}) - \%\text{clay} \quad \ldots\ldots\ldots\ldots\ldots\ldots\ldots \quad (3.18)$$

$$\%sand = 100 - \%(silt + clay) \quad \ldots\ldots\ldots\ldots\ldots\ldots\ldots \quad (3.19)$$

3.7 Procedures of Chemical Assessment of Agricultural Soils

3.7.1 pH/EC in Soil

(1) 10 grams of fine soil particle (<75 μm) was weighed into an extraction cup.

(2) Then 10 millilitres of distilled water was added and shaken for 10 minutes using mechanical shaker.

(3) After the shaking was completed, the pH reading was read using Hanna electrical pH meter with aid of its probe.

(4) The reading was allowed to stablise before it was taken and the probe is rinsed with distilled water before the next reading.

Similar procedure was engaged for the electrical conductivity (EC) such that 10 grams of fine soil particle was weighed, 10 millilitres of distilled was added onto it and shaking for 10 minutes. The Hanna EC meter was used to measure electrical conductivity of soil sample.

3.7.2 Percentage Organic Carbon in Soil

The method employed was Walkey-Black and the procedure is stated below:

(1) 0.5 gram of the prepared soil sample that has passed through 0.5 millimetre sieve size was weighed into a 250 millilitres conical flask

(2) 10 millilitres of 1N potassium dichromate ($K_2Cr_2O_7$) solution and 20 millilitres concentrated sulphric acid (hydrogen tetraoxosulphate) (H_2SO_4) were added onto the sample in the conical flask.

(3) The content was mixed thoroughly and the reaction was allowed to complete for about an hour for oxidation to take place.

(4) After an hour, the reaction was diluted with 100 millilitres of distilled water and it was then allowed to stand for another one hour for the temperature to come down.

(5) 3 drops of ferroine indicator (1-10 phenanthroline monohydrate) was added.

(6) The solution was titrated with 2.5M Fe_2SO_4 (ferrous sulphate) solution to give a maroon brown colour, and then the titre value was recorded.

(7) A blank was run or repeated without soil for this analysis.

The calculated percentage of organic carbon is given by:

$$\%OC = \frac{R}{S} * (S - T) * 0.003 * 1.33 * \frac{100}{\text{Weight of soil sample}} \quad \ldots\ldots (3.20)$$

Where,

R= volume of $K_2Cr_2O_7$

S= volume of blank

T= titre value

Milliequivalent weight of carbon in gram = 0.003

OC= organic carbon

3.7.3 Percentage of Total Nitrogen

Micro Kjeldahl digestion method was used and the procedure is stated as follow:

(1) 0.5 gram of soil sample that has passed through 0.5 millimetre sieve size was weighed and placed in a digestion tube.

(2) 5 millilitres of concentrated H_2SO_4 together with 1 tablet of selenium was added and the tube was placed in the digestion block.

(3) The content was heated to digest at 360^0C for about 3 hours until a light yellow solution was obtained.

(4) The tube was removed and the digest was allowed to cool, the digest was taken into 400 millilitres volume beaker and 50 millilitres of distilled water was added.

(5) 5 millilitres of digest was measured into the distillation chamber.

(6) 5 millilitres of forty-percent NaOH was added and distilled into 100 millilitres conical flask which contained 5 millilitres boric acid indicator until 50 millilitres of distillate (greenish colour solution) was obtained.

(7) The distillate was titrated against 0.01N HCL in a burette until a faint pink colour wass obtained and the titre value was recorded.

(8) A blank was run without soil for this analysis.

Then calculate the percentage of total nitrogen using the formula below:

$$\%\mathrm{TN} = [\mathrm{T} - \mathrm{B}] * \mathrm{N} * \mathrm{R} * 14.01 * \frac{100}{\text{Sample weight} * 1000} \quad \ldots\ldots\ldots (3.21)$$

Where,

B= Blank

T= Titre value

N= Normality of titrating acid, that is, 0.01N

R= Distillation ratio, that is, $\frac{50}{5} = 10$

14.01= Molar mass of nitrogen

3.7.4 Available Phosphorus in Soil

Procedure;

(1) 2 grams of soil sample that has passed through 2 millimetre sieve size was weighed into an extraction cup.

(2) 20 millilitres of Bray P solution was added and it was shaked on a shaker for 15 minutes.

(3) The content passed through 90 mm whatmann filter paper and drained through it.

(4) 5 millilitres of the filtrate was measured into a 50 millilitres volume beaker, 5 millilitres of colour reagent (Murphy and Riley solution) was added and it was diluted to about 25 millilitres with distilled water.

(5) It was then allowed to stand for about 10 minutes for the colour to develop in which a bluish colour was obtained.

(6) Spectrophotometer was used to read the bluish colour at 882 nm wavelength, the absorbance of each solution was determined and a standard curve was prepared for this

analysis which was used to produce a slope from which the value of P was computed in mg/kg for each of the samples.

Then calculate the available phosphorus (mg/kg) using the formula below:

$$\text{Available Phosphorus } \left(\frac{\text{mg}}{\text{kg}}\right) = \text{x} * \text{DF} * \text{EF} \quad \ldots\ldots\ldots\ldots\ldots\ldots \quad (3.22)$$

Where,

X is determined from the standard curve

DF is the dilution factor

EF is the extraction factor.

3.7.5 Acidity in Soil

Procedure;

(1) 2 grams of soil sample that has passed through 2 millimetre sieve size was weighed into an extraction cup.

(2) 20 millilitres of 1 N KCL solution was added; it was then shaked on a mechanical shaker for about 15 minutes.

(3) The content was passed through 90mm whatmann filter paper and the solution was allowed to drain through it.

(4) 3 drops phenolphthalein indicator was added to the filtrate.

(5) The filtrate was titrated against 0.01N NaOH in the burette until pink colour is obtained and the titre value was recorded.

The acidity is given by:

$$\text{Acidity} = \text{N} * \text{V} * \frac{\text{T}}{\text{Sample weight}} \quad \ldots\ldots\ldots\ldots\ldots\ldots\ldots\ldots \quad (3.23)$$

Where;

N = Normality of titrating solution

V = Volume of extractant

T = Titre value

3.7.6 Determination of Exchangeable Cations in Soil (Na, Mg, K and Ca)

Procedure;

(1) 2 grams of soil sample that has passed through 2 millimetre sieve size was weighed into an extraction cup.

(2) 20 millilitres of 0.1N ammonium acetate extractant (NH_4OAc) was added to the soil content in the extraction cup.

(3) The content was shaked for about 10 minutes using mechanical shaker.

(4) The content was made to pass through 90 mm whatmann filter paper and the filtrate was made to drain completely.

(5) The potassium and sodium in the filtrate was determined with flame photometer while calcium and magnesium in the filtrate was determined using atomic absorption spectrophotometer.

Buck scientific atomic absorption spectrophotometer (AAS) 210/211 model was used for elemental composition of soil matrix in the department of Agronomy, University of Ibadan. The AAS was connected to a standard electrical outlet via a connecting plug, the compressed air and acetylene gas buttons are pressed, they combined at the nebulizer and ignited to give flame. The cathode lamp of the element to be analysed was inserted into the hollow cathode lamp socket. Then set the wavelength depending on the element under study. The spectrometer was calibrated with the standard solution of the element to get a curve, the standard solution was aspirated by the tube onto the monochromator, then to the nebulizer, it is finally displayed on the screen. It was used in determining the concentration of calcium and magnesium element in soil.

Jenway flame photometer FP640 was used in analysing the sodium and potassium elements in soil at department of Agronomy, University of Ibadan. It makes use of methane gas and compressed air, and ignited by the spark button. The standard was set between the highest and lowest value. Distill water was used to clean the component of the photometer which is aspirated or injected through the tube in the distill water can. It serves as the lowest standard while standard solution is the highest standard. Over range error results when the concentration of element is higher than the set standard, the solution needs to be diluted further and dilution factor comes to play in order to determine the final concentration of the element. The photometer is capable of determining the concentration of sodium and potassium simultaneously and digital reading is displayed on the LCD screen.

3.7.7 Cation Exchange Capacity (CEC)

This is computed from the addition of all cations plus the acidity.

$$\text{CEC} = \text{Ca} + \text{Mg} + \text{Na} + \text{K} + \text{Exchangeable acidity} \ldots\ldots\ldots \quad (3.24)$$

3.8 XRD Analysis

Procedure;

Soil samples were sieved at the Departmental of Earth Sciences, Ajayi Crowther University; XRD analysis was carried out on twelve representative samples, six samples from each of the farms (cacao and kola) cutting across the low EC_a, moderate EC_a and high EC_a zones, that is, two soil samples from each of the sections. Samples were sent to XRD laboratory for mineralogical examination at College of Petroleum Engineering and Geosciences, King Fahd University of Petroleum and Minerals, Kingdom of Saudi Arabia. Malvern PaNalytical empyrean XRD system was used for the analysis of the fine fraction obtained from the soil samples. It is an automated multipurpose research x-ray diffractometer which is equipped with alpha (Kα), β radiation, Cu x-ray tubes and it consists of four major components; x-ray source, goniometer, sample stages and radiation enclosure. The diffractometer has capability to measure the mineral composition in varying sample types such as powder form, solid, thin films and nanomaterials. It measures the intensity of scattered beam against 2-theta angle of the diffractometer. Minerals identification was carried out by comparing calculated d-spacing with a library of standard d-spacing. Fine fraction (< 45 μm) of soil was packed into a hollow-cavity sample mount and the quantitative XRD analysis is achieved by means of a whole-pattern fitting method utilizing measured and calculated XRD scan.

3.9 Coding of Soil Samples

Soil samples were collected from region of low, moderate and high EC_a from both farms (cacao and kola), Tables 3.2 and 3.3 showed the coding engaged in the conduct of the x-ray diffraction and chemical analyses.

Table 3.2: Cacao soil sample identity code and region of EC_a selection

Analytical Method	EC_a Section	Label
XRD		
CL1@72 m	XRD1 HIGH	A1
CL13@90 m	XRD2 LOW	A2
CL25@0 m	XRD3 HIGH	AA8
CL19@36m	XRD4 MEDIUM	AA7
CL25@36m	XRD5 LOW	A3
CL19@90m	XRD6 MEDIUM	AA9
Chemical analysis		
CL1@0 m	LOW	MP1
CL1@36 m	LOW	MP2
CL1@54 m	HIGH	MP3
CL1@72 m	HIGH	MP4
CL7@0 m	LOW	MP5
CL7@36 m	LOW	MP6
CL7@54 m	HIGH	MP7
CL7@90 m	MEDIUM	MP8
CL13@0 m	MEDIUM	MP9
CL13@54 m	LOW	MP10
CL13@72 m	LOW	MP11
CL13@90 m	LOW	MP12
CL19@0 m	HIGH	MP13
CL19@36 m	MEDIUM	MP14
CL19@54 m	HIGH	MP15
CL19@90 m	MEDIUM	MP16
CL25@0 m	HIGH	MP17
CL25@36 m	LOW	MP18
CL25@72 m	LOW	MP19
CL25@90 m	MEDIUM	MP20

Table 3.3: Kola soil sample identity code and region of EC_a selection

Analytical Method	EC_a Section	Label
XRD		
KL1@18 m	XRD1 LOW	A4
KL19@72 m	XRD3 HIGH	A5
KL21@18 m	XRD2 HIGH	A6
KL7@90m	XRD4 LOW	AA10
KL13@0m	XRD5 MEDIUM	AA11
KL13@90m	XRD6 MEDIUM	AA12
Chemical analysis		
KL1@0 m	LOW	MP21
KL1@18 m	LOW	MP22
KL1@54 m	LOW	MP23
KL1@90 m	LOW	MP24
KL4@18 m	LOW	MP25
KL7@18 m	LOW	MP26
KL7@54 m	LOW	MP27
KL7@90 m	LOW	MP28
KL13@0 m	MEDIUM	MP29
KL13@18 m	LOW	MP30
KL13@54 m	LOW	MP31
KL13@90 m	MEDIUM	MP32
KL19@0 m	HIGH	MP33
KL19@18m	HIGH	MP34
KL19@54 m	HIGH	MP35
KL19@72 m	HIGH	MP36
KL21@0 m	HIGH	MP37
KL21@18 m	HIGH	MP38
KL21@54 m	HIGH	MP39
KL21@72 m	HIGH	MP40

CHAPTER FOUR

RESULTS AND DISCUSSION

4.1 Geological Assessment of Basement Rock

Field observation revealed that rock outcrops were strongly foliated, as noticed from the alternating or banding of mafic (dark) and felsic (light) mineral constituents (Fig. 4.1a). The colour is grey, it trends in the North-South direction (N-S); striking between 354^0 and 14^0 with elevation 115 m to 144 m above the sea level (Fig. 4.1b). The rock unit dips towards the east (36^0-80^0E) indicating a gentle to steep dip. The joints were trending between 254^0 and 90^0, signifying the direction of brittle deformation experienced by the outcrop, they orientate in N-S and East-West (E-W) directions and the dominant azimuth is E-W (Fig. 4.2a). The quartzo-feldspathic segregations are concordant with the host rock (Fig 4.2b), striking between 359^0 and 6^0, and a maximum length of 4 m. Biological weathering was the dominant agent of denudation noticed on the outcrops (Fig. 4.3). The area extents of the outcrops vary from 20 m^2 to 300 m^2. The outcrops have medium grained texture, the major minerals include quartz, feldspar, mica (biotite-abundant and muscovite-less abundant) while the mafic components dominate the felsic counterpart and gneissic in appearance.

Figure 4.1a: Banding of mafic and felsic mineral components

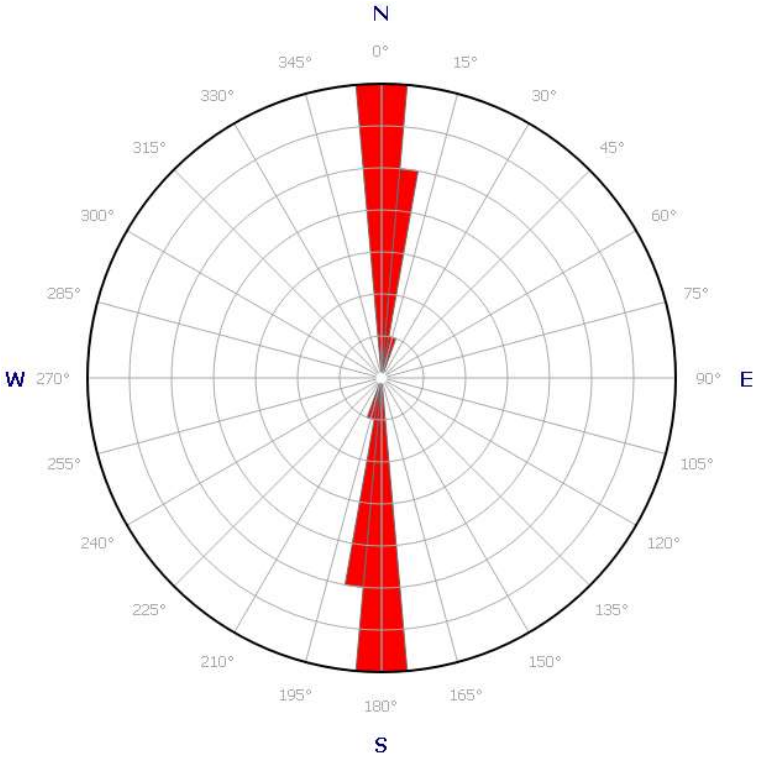

Figure 4.1b: Orientation of the strike direction of the foliated rock unit

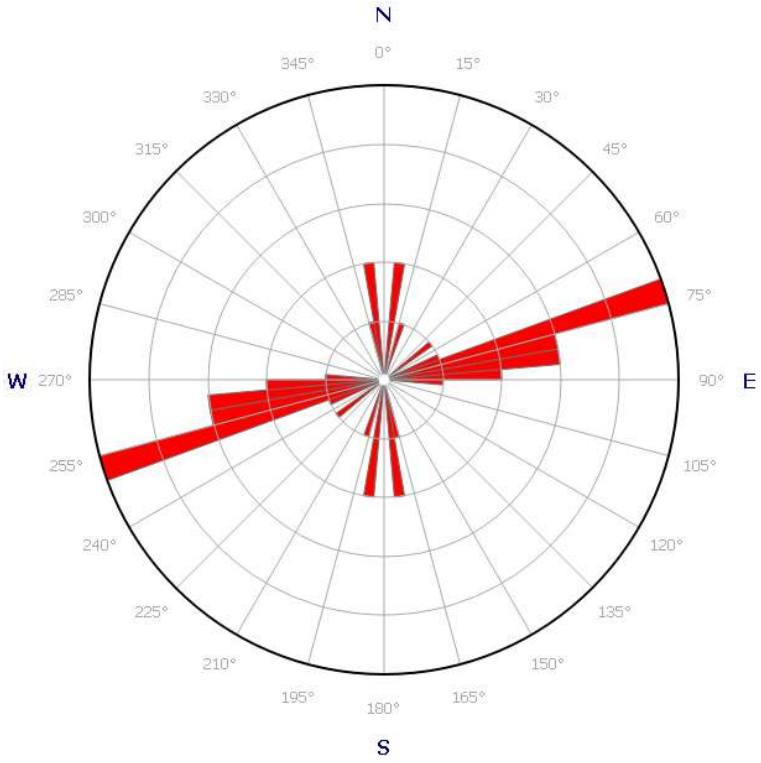

Figure 4.2a: Orientation of joint noticed on the rock unit

Figure 4.2b: Outcrop intruded with quartzo-felspathic vein

Figure 4.3: Biological weathering noticed on the outcrop

The Petrographic Study of Rock Samples

The study of the thin sectioned rock showed that the interlocking mosaic of mineral contains feldspars (plagioclase, microcline and orthoclase), mica (biotite and phlogopite), quartz and accessory mineral zircon. The petrographic study under cross and plane polarised light showed that the quartz crystals are elongated and they have preferred alignment along with the biotite minerals present (Figs 4.4a and 4.4b). The quartz crystals are characterised with wavy extinction, the feldspars (plagioclase, microcline and orthoclase), biotite and quartz are elongated along line of orientation. Some of the feldspars occurred as porphyroclast within the ground mass of the deformed mineral grains (locations 1 and 2). The thin section of sample from location 1 revealed the inclusion of zircon as an accessory mineral in the groundmass (Figs 4.5a and 4.5b). The plagioclase feldspars in locations 3 and 4 have undergone selective sericitization (Figs 4.6a and 4.6b). The modal analysis showed the percentage composition of the mineral contents from each of the locations (Table 4.1).

Based on the modal analysis and a comparison with established works (Parsons and Zwanzig (2003); Ibrahim *et al.* (2015) and Egesi (2019)), the rock outcrops (Figs. 4.4a-4.4.8b) in the study location are biotite granite gneisses. The rock constituents will weathered into soil when subjected to temperature and pressure varying from that of their formation. The plagioclase, microcline, orthoclase and biotite weather into kaolinite; plagioclase and biotite weathered rapidly than microcline and orthoclase while quartz is more resistant to weathering (White *et al.* 2001 and Wilson 2004).

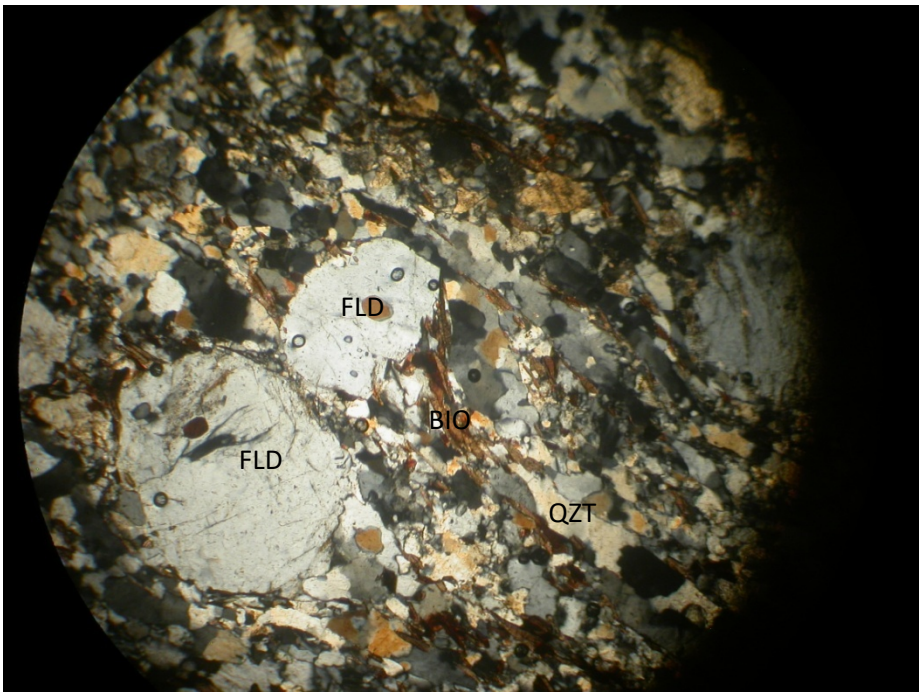

Figure 4.4a: Photomicrograph showing the porphyroclast of feldspar grains in the matrix of biotite quart and medium grain feldspar minerals (cross polar) at location 1. Mag. x100.

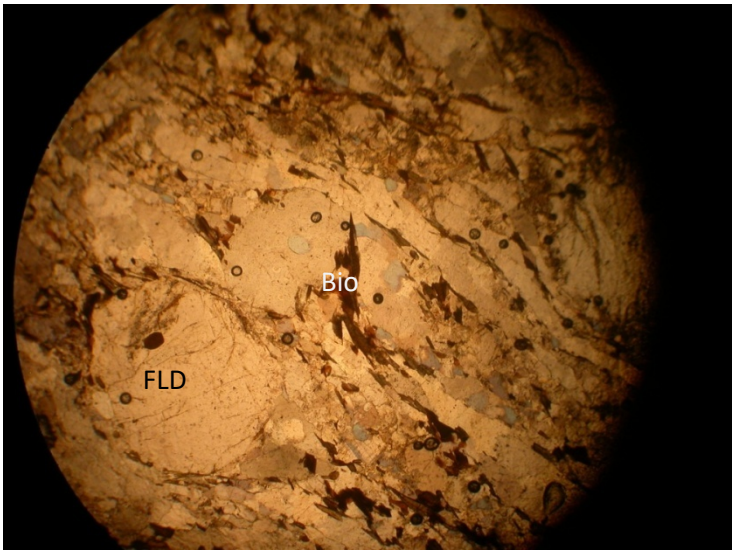

Figure 4.4b: Photomicrograph showing the biotite (Bio), porphyroclast of feldspar (FLD) grains in the matrix of others minerals (plane polar) at location 1. Mag. x100.

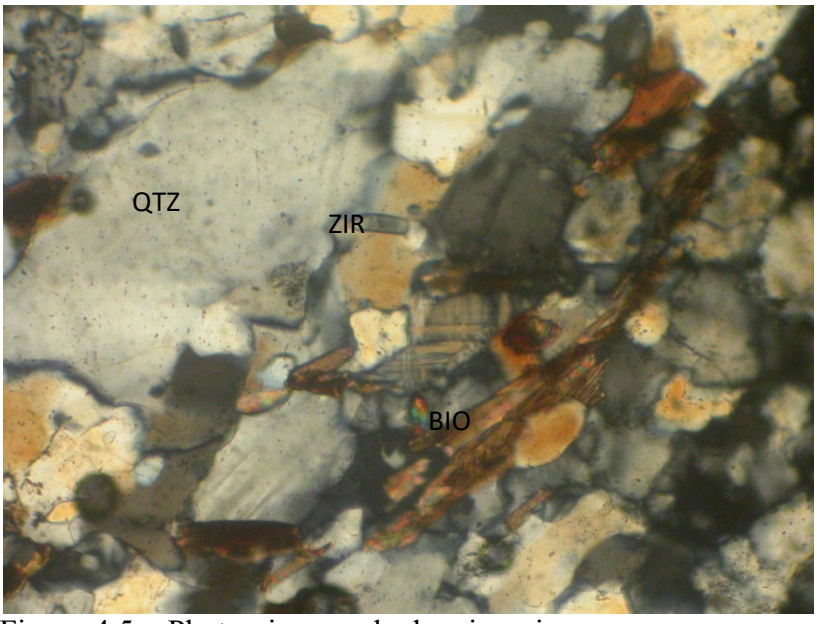

Figure 4.5a: Photomicrograph showing zircon as an accessory mineral, biotite, quart and feldspar under cross polar at location 1. Mag. x100

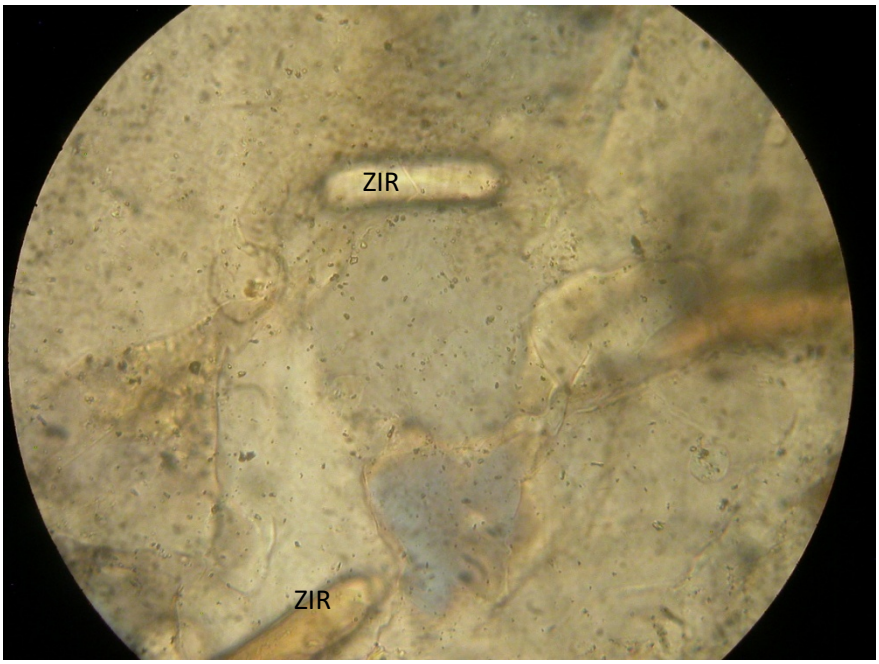

Figure 4.5b: Photomicrograph showing zircon as an accessory mineral under plane polar at location 1. Mag. x600

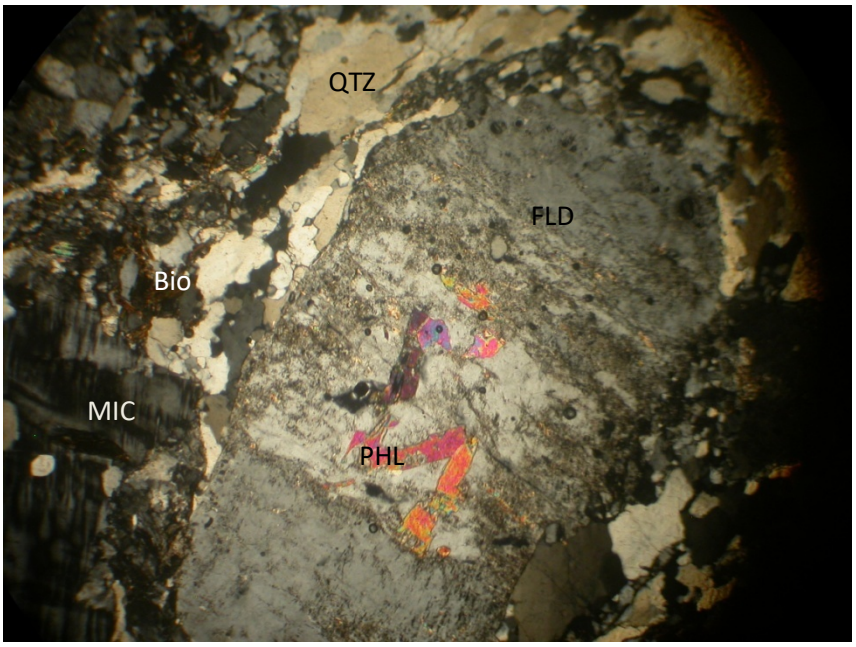

Figure 4.6a: Photomicrograph showing the inclusion of phlogopite in selective sericite feldspar porphyroclast (cross polar) at location 4. Mag. x100

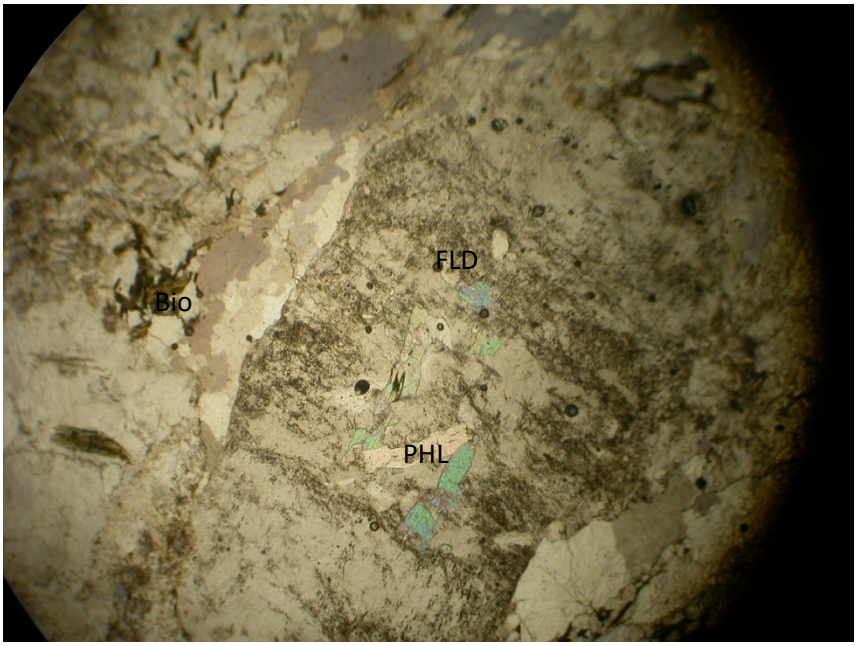

Figure 4.6b: Photomicrograph showing the inclusion of phlogopite in a feldspar porphyroclast (plane polar) at location 4. Mag. x100

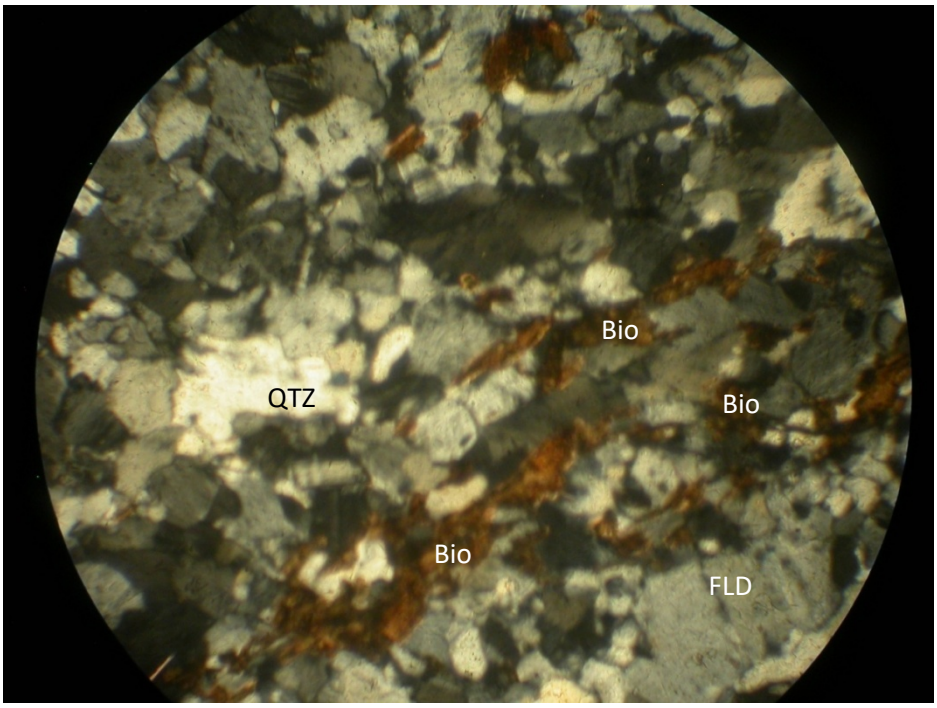

Figure 4.7: Photomicrograph showing the biotite (Bio), quartz, porphyroclast of feldspar (FLD) grains in the matrix of others minerals (plane polar) at location 2. Mag. x100

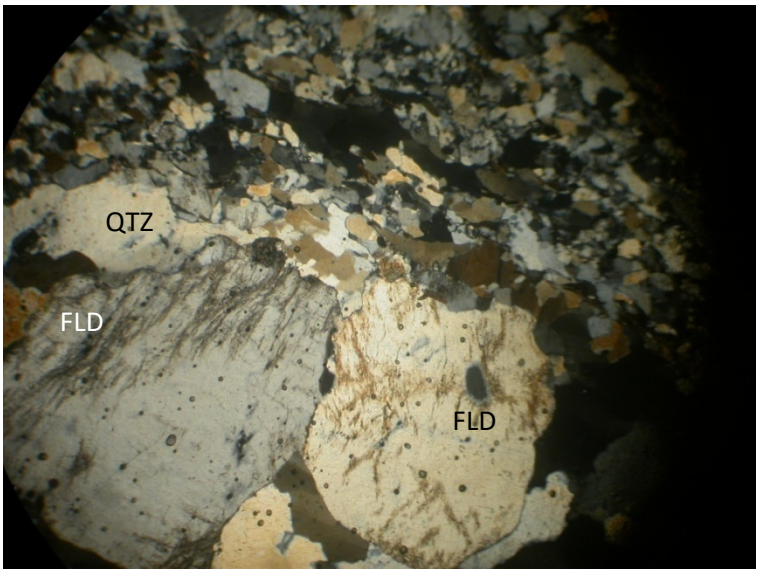

Figure 4.8a: Photomicrograph showing coarse grain plagioclase feldspar and quartz grain band, alongside the medium grains band of biotite, quartz and feldspar matrix at location 3. (Cross polar) Mag. x100

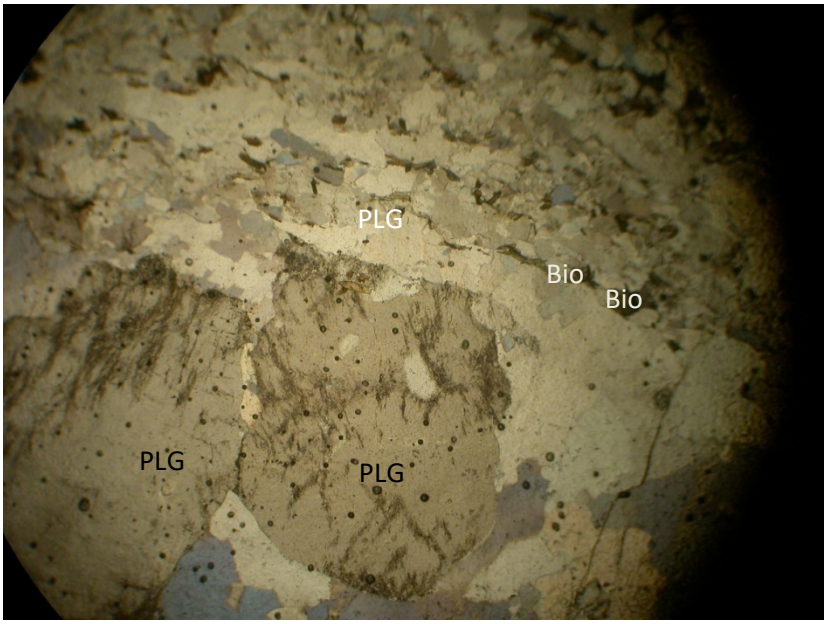

Figure 4.8b: Photomicrograph plagioclase feldspar and quartz grain band, alongside the medium grains band of biotite, quartz and feldspar matrix at location 3. (Plane polar) Mag. x100

Table 4.1: Modal analysis of analysed rock samples in the study area

	This study						Referenced Authors			
	L1	L2	L3	L4						
Mineral (%)	3°51'55.6" 7°13'12.8"	3°51'53.3" 7°13'10.2"	3°51'48.5" 7°13'54.5"	3°51'34.8" 7°14'04.6"	Range	Average	Parsons and Zwanzig (2003) Composition of Granite Gneiss	Egesi (2019) Average Composition of Granite Gneiss	Ibrahim *et al.* 2015 Hornblende Granite Gneiss	Yusof & Zabidi (2016) Granitic Compositional Range
Plagioclase	25.2	23.6	18.0	19.3	18.0-25.2	21.5	35	20	35	40.0-70.0
Microcline	28.1	27.0	21.3	20.8	20.8-28.1	24.3	21	30	-	
Orthoclase	3.4	4.0	-	-	3.4-4.0	3.7			-	
Quartz	23.3	23.7	26.0	27.5	23.3-27.5	25.1	24	27	30	5.0-30.0
Biotite	14.0	14.2	33.2	31.4	14.0-33.2	23.2	7	7	5	20.0-40.0
Zircon	5.3	6.5	-	-	5.3-6.5	5.9	-	-	-	
Hornblende Cummingtonite	-	-	-	-	-	-	0-24	6	15	
Muscovite	-	-	-	-	-	-	-	5	-	
Opaque Mineral	-	-	-	-	-	-	-	2	10	
Total	99.3	99.0	98.5	99.0						

*L1-Location 1

4.2 Electrical Conductivity of Soils

Soils apparent electrical conductivity (EC_a) data were subjected to statistical analyses and the following features were computed using SPSS software: minimum value, maximum value, mean value, standard deviation (SD) and coefficient of variation (CV) of data set. These were used for the data analyses in order to determine the data behaviour. Coefficient of variation was employed in establishing the variability of data acquired from the fields. Table 4.2 showed the breakdown of statistical parameters generated from the field data. The coefficient of variation model proposed by Warrick and Nielsen (1980) was used to ascertain the degree of variability (Table 4.3).

EC_a data of Cacao field showed moderate variability (60.97 %) during rainy period while high variation (64.11 %) occurred during the dry period. High variability of 82.83 % was computed for the EC_a in the wet period whereas moderate class was generated from EC_a data during dry season at the kola field. Molin and Faulin (2013) considered the CV as the first indicator in determining spatial variability of the measured parameter. Thus, EC_a may serve as soil quality evaluator from which subsequent investigation sites could be established.

There is need to ascertain the level of salinity within cacao and kola farms because this could impede the growth and productivity of the crops, therefore, the range of EC_a values was compared with the established USDA (2011) salinity classes (Table 4.4). The salinity level in the cacao and kola fields during wet and dry seasons falls within the non-saline class, suggesting that concentration of soluble ions in the field is not high and the crops have the ability to absorb water when present. Mean ECa values recorded in the dry season is lesser than that of wet season which is consistent with the work of Doerge (1999).

Table 4.2: Exploratory statistics for soil apparent electrical conductivity (ECa) of cacao and kola fields.

Variable		Number of points	Minimum	Maximum	Mean	Standard Deviation	Coefficient of Variation (%)
Cacao	**Wet**						
Field	**Season**						
	EC_a (µS/cm)	912	13	344	68.04	41.48	60.97
	Dry						
	Season						
	EC_a (µS/cm)	906	10	267	45.11	28.92	64.11
Kola	**Wet**						
Field	**Season**						
	EC_a (µS/cm)	700	12	545	92.72	76.80	82.83
	Dry						
	Season						
	EC_a (µS/cm)	699	13	188	47.64	25.83	59.35

Table 4.3: Coefficient of variation, its range and classification (After Warrick and Nielsen 1980)

S/N	Coefficient of Variation (CV)	Class
1	CV < 12 %	Low
2	12 <CV< 62 %	Moderate
3	CV>62 %	High

Table 4.4: Ranges of EC value and their corresponding salinity classes (After USDA 2011)

S/N	EC (μS/cm)	Class
1	0-2000	Non-saline
2	2000 – 4000	Very slightly saline
3	4000 – 8000	Slightly saline
4	8000 – 16000	Moderately saline
5	≥ 16000	Strongly saline

Marshall (1987) noted that water has an inherent property in which electrical conductivity of water in the absence of dissolved ions is 0.055 μS/cm. Lide (2007) also indicated that electrical conductivity increases linearly with an increase in the concentration of electrolytes. This suggests that the measured electrical conductivity values in the farms were above the threshold of absence of soluble ions, thus indicating presence of dissolved soil nutrients made available for plant uptake.

4.3 Volumetric Water Content (VWC) of Soils

The raw data were analyzed using SPSS software (Table 4.5) and the degrees of their variability were established by comparing with the variation model (Table 4.3) generated by Warrick and Nielsen (1980). Variation of volumetric water content during wet season in the cacao field was moderate (53.84 %) and its variation in dry period was also moderate but there was significant reduction in its numerical value compared with the value obtained in the wet season. Numerical analysis showed that the distribution of volumetric water content in the kola section falls within moderate category, its variation is higher in the wet season (59.35 %) than dry season (34.91 %). Variations in VWC at both fields were moderate; this suggests that data quality is within the acceptable range which can be used for further soil spatial assessment analyses.

Variability of VWC recorded in the cacao field was moderate but higher variation was observed in wet season (53.84 %) with respect to the dry period (33.40 %). The mean VWC was ~26 % in wet season while it was ~10 % at the peak of dry season; this showed that approximately a quarter of soil volume was filled with water at the peak of wet period whereas less soil water was made available for plant up take during the dry season. This invariably contributes to the crop yield as fewer nutrients were supplied to the plant as a result of reduction in soil moisture content and its sparse distribution (Ryšan and Šařec 2008).

Variation in VWC around kola farm was moderate at both seasons. Numerically its variability was very high (59.35 %) in the wet season compared with the obtained value (34.91 %) in the dry season. It is worthy to note that the average amount of VWC in soil was slightly above a quarter of the entire soil volume, while in the dry season an average of less than 8 % VWC was present in soil. The statistical analysis (Table 4.5) showed that there was significant reduction in soil moisture content in the dry season.

Table 4.5: Statistical analyses of volumetric water content (VWC) in cacao and kola fields

Variable		Number of points	Minimum	Maximum	Mean	Standard Deviation	Coefficient of ariation (%)
Cacao	**Wet**						
Field	**Season**						
	VWC (%)	912	3.00	69.00	25.52	13.95	53.84
	Dry						
	Season						
	VWC (%)	906	2.00	26.00	9.70	3.24	33.40
Kola	**Wet**						
Field	**Season**						
	VWC (%)	700	3.00	65.00	28.59	16.97	59.35
	Dry						
	Season						
	VWC (%)	699	3.00	15.00	7.82	2.73	34.91

Water has been the medium of nutrients transport in soil and this would affect nutrient uptake for the crops during said season.

4.3.1 Correlation Analysis between Volumetric Water Content and Electrical Conductivity

Regression analysis has been the norm in evaluating the relationship between soil water content and apparent electrical conductivity (EC_a) values in precision agriculture in order to establish the influence of soil moisture on electrical conductivity (Brevik *et al.,* 2006; Ali *et al*., 2009; Ekwue and Bartholomew, 2011 and Hossain *et al.*, 2010).

The scattered plot between VWC and EC_a (Fig. 4.9a) showed that as the VWC increases, ECa also rises with it and coefficient of correlation (r) is 0.972 (strong correlation), a small change in moisture content leads to greater change in conductivity. Pedrera-Parrilla *et al.* (2016) and Samouëlian *et al.* (2005) also made known that such fit exists between electrical conductivity and soil water content. Apparent electrical conductivity (EC_a) increases as the moisture content increases due to the fact that salt constituent (ions) extracted from soils increases with a rise in soil moisture content, in other word, total ion constituents increase with increase in moisture content at extraction and capability of soil solution to conduct electrical current depends on the concentration of ions in the solution (Ryšan and Šařec 2008; Corwin and Yemoto, 2017). Also the air occupying the voids is replaced with water invariably increasing the electrical conductivity of the medium. The contact of water with soil material promotes the transfer of ions from it into water, thus forming a circle around the particles, and it contributes to electrical conduction. It returns to particles from which it was dislodged once the water is removed (Chenhui *et al.*, 2013).

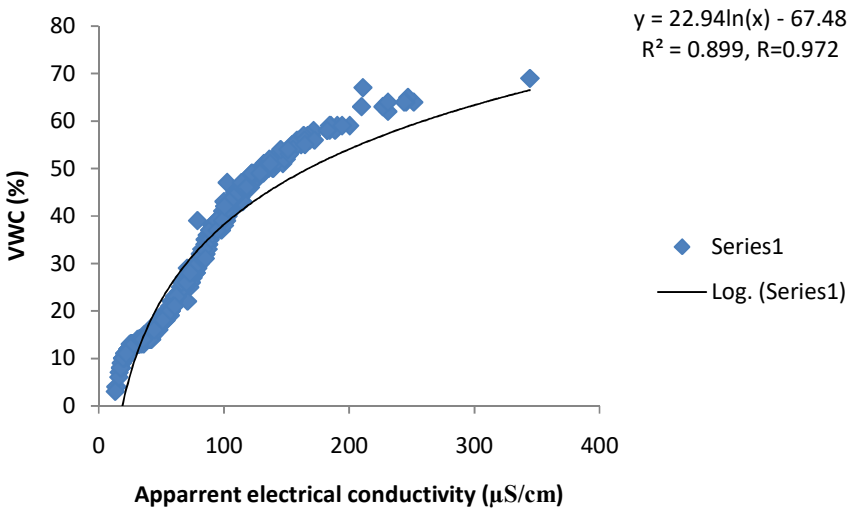

Figure 4.9a: Variation of volumetric water content with the apparent electrical conductivity in the cacao farm during wet season

Relationship between volumetric water content and apparent electrical conductivity was geometric, and a strong correlation existed between them with a coefficient of 0.807 (Fig. 4.9b), this showed that the EC_a increase as the VWC increases during dry period and a non-linear relationship was observed between EC_a and VWC (McCutcheon *et al.*, 2006; Asif *et al.,* 2016; Sudhir and Pradeep, 2014). Presence of soil moisture content controls the extent to which the void spaces are filled with water. Soil moisture aids the mobility of ions in solution, as the pore spaces are filled with increasing water content, therefore there is an increase in the movement of free ions that are associated with the soil resulting in the rise of soil electrical conductivity (Ekwue and Bartholomew, 2011). As the soil moisture reduces, decrease in EC_a values were noted and this is consistent with the works of Doerge (1999); McCutcheon *et al*., 2006; Kizito *et al.* (2008) and Costa *et al.* (2014) and Wang *et al.,* (2017) in which they reported similar relationship between the stated parameters.

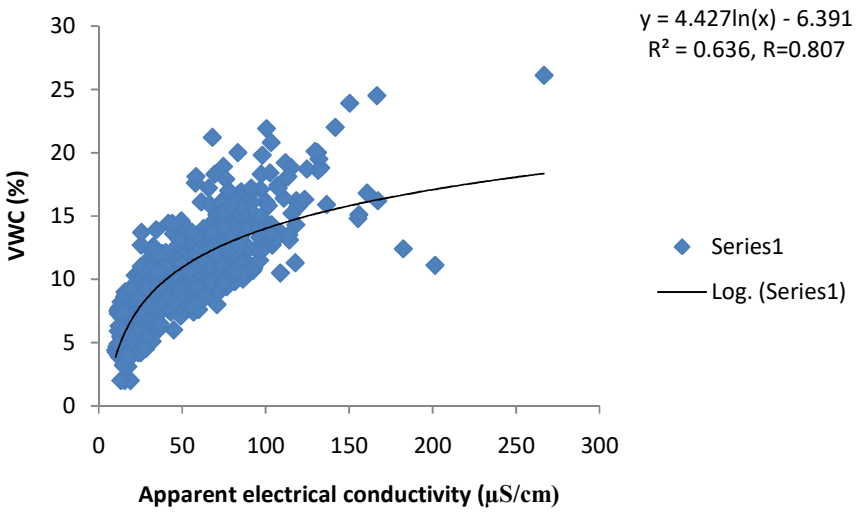

Figure 4.9b: Variation of volumetric water content with apparent electrical conductivity in the cacao farm during dry season

The relationship between volumetric water content and electrical conductivity in the kola farm was positive with a strong coefficient (0.852) during the wet season as noted in Figure 4.10a and it increases non-linearly. A non-linear curve was obtained from the interaction of EC_a with water content, suggesting that electrical conductivity observed at higher water content was due to further compaction of the soil (Ekwue and Bartholomew, 2011), thereby expelling the air in pore spaces, increasing grains contact and resulting in density increase which leads to increase in electrical conductivity.

Electrical conductivity in soils is a function of the amount of water in the pores and on its quality (Samouëlian *et al.,* 2005) and evapotranspiration (Siqueira *et al*., 2016). As VWC increases across the kola farm, the EC_a also increased due to the fact that more pore spaces were filled with soil moist leading to an increase in dissolution of soluble salt associated with the soil particles (Peralta and Costa 2013). It could also be inferred that reduction in volume of water content across the field leads to decrease in EC_a. This indicates that electrical conductivity was significantly influenced by water content.

Figure 4.10b showed a strong correlation coefficient (0.874) between the VWC and EC_a in kola farm during dry season, increase VWC leads to rise in EC_a and at a point rise in VWC tends to be almost constant whereas EC_a continues to increase logarithmetically. Similar relationship was noticed between electrical conductivity and water content in earlier works of Friedman (2005); Ozcep *et al.* (2010) and Shin and Son (2015). The greater the quantity of dissolved ions in the pore-water, the higher will be the conductivity of these ions in soil solution (Samouëlian *et al.*, 2005; Ryšan and Šařec 2008). Conductivity recorded could be attributed to the presence of dissolved ions responsible for greater mobility of these ions in soil water. Distribution of soil moisture content in kola plot implies that region of low EC_a has low capacity to retain water for plant uptake while zones with high EC_a have the capability to hold water.

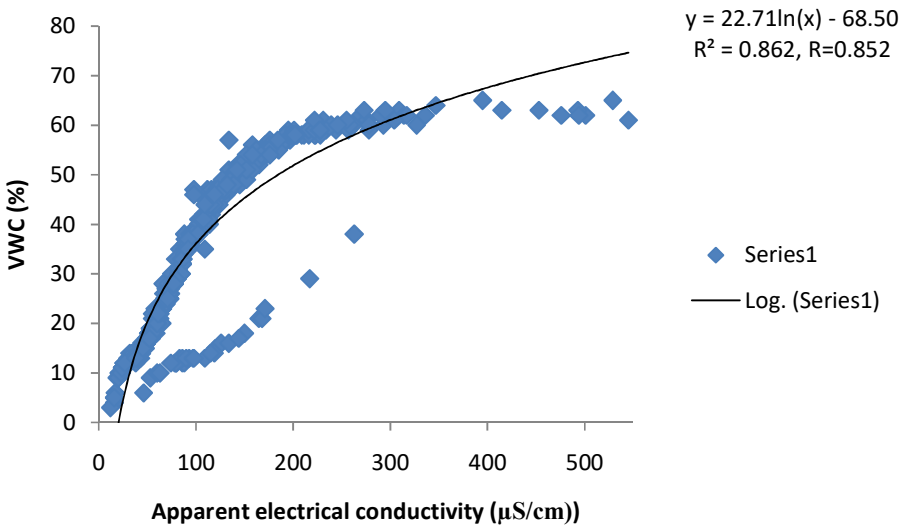

Figure 4.10a: Variation of volumetric water content with the apparent electrical conductivity in kola farm during wet season

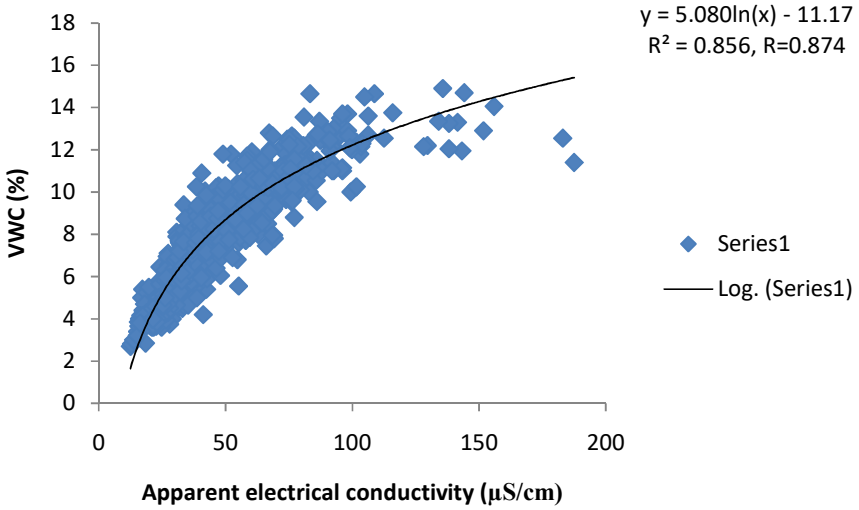

Figure 4.10b: Variation of volumetric water content with the apparent electrical conductivity in kola farm during dry season

Spatial distribution of electrical conductivity in the coca farm was done using ArcGIS 10.2 software and exponential function was engaged in kriging the data points. During the wet season (Fig. 4.11), the farm was classified into three categories based on its electrical conductivity, low EC_a ranging from 0-49 µS/cm, moderate EC_a (50-99 µS/cm) while high EC_a has conductivity greater than 100 µS/cm; subsequent investigations were based on this classification. The most conductive section (red colour) occurred mainly at three spots namely; north/northeast, southwestern and almost central portion of the map. Moderate EC_a zone was coloured light brown, it stretches from the high EC_a area grading into low EC_a area notably at the southeastern, central and some part of the northern portion of the map. Low EC_a terrain was denoted with blue colouration, it was conspicuously observed in the southeast, southern section, central and northwest/northnorthwest (NNW) of the map.

Extremely reddish and bluish segments are the productive and non-productive sections respectively while the light brown was regarded to be fairly productive. VWC map generated for the cacao farm during the wet period (Fig. 4.12) showed that the percentage of water content varied from one section to another, high VWC vicinity was denoted with red colour (> 45%), yellow colour was used for the moderate VWC (15-44%) and green colour for low VWC (< 15%). Abundant soil moisture was observed in the south western, north/north eastern and almost central portion of the map, there is gradual reduction in water content from high VWC to moderate VWC and the yellow colour grades into the green portion. Moderate VWC was noted in the south western, south eastern and scattered in the northern segment of the map.

Similar colour codes were used for the distribution of electrical conductivity in the cacao plot during the dry season (Fig. 4.13) as that of the wet season. Fractions with red colour connote high EC_a (> 60 µS/cm) and it occurs around the north/north eastern and western segment of the map. Region of moderate EC_a (40-59 µS/cm) extends from the most conductive stretching into low conductive medium whereas the low conductive section (< 40 µS/cm) was coloured blue (Fig. 4.14). Also similar colour notations were used for VWC map in the dry season such that red colour signifies region of high VWC (> 15%), moderate VWC area (10-15%) was coloured yellow while low VWC is green (< 10%).

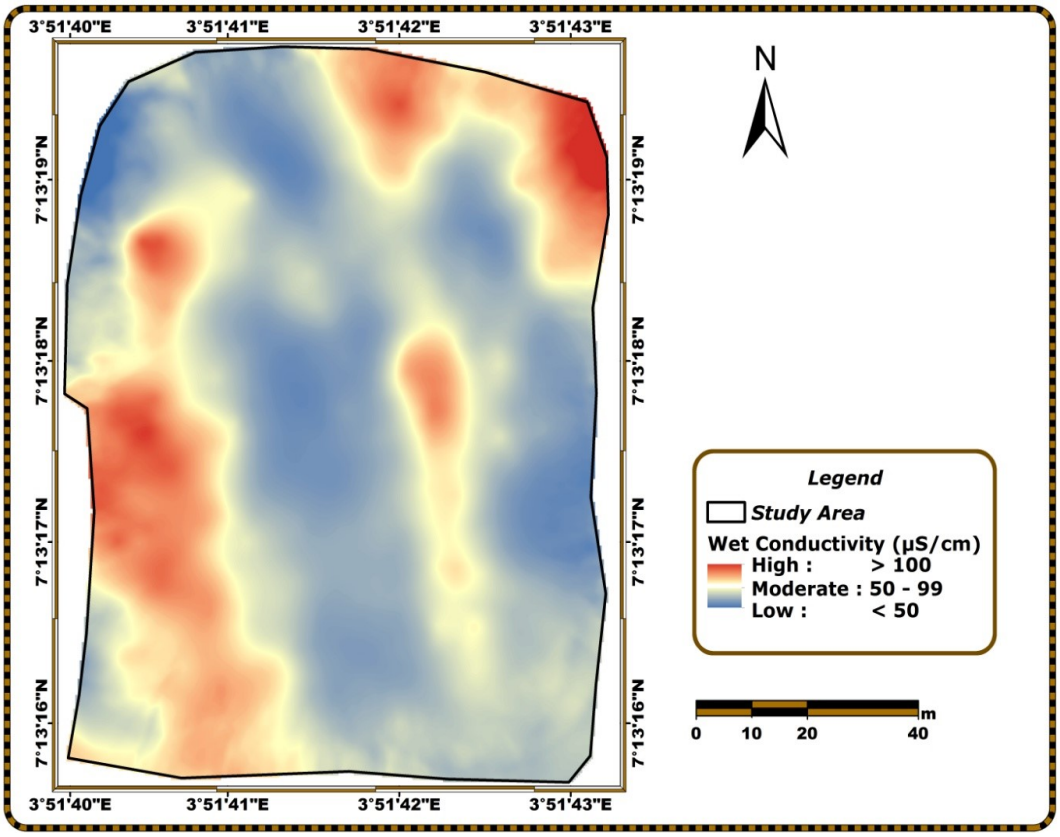

Figure 4.11: Apparent electrical conductivity distributions within the cacao field during wet season

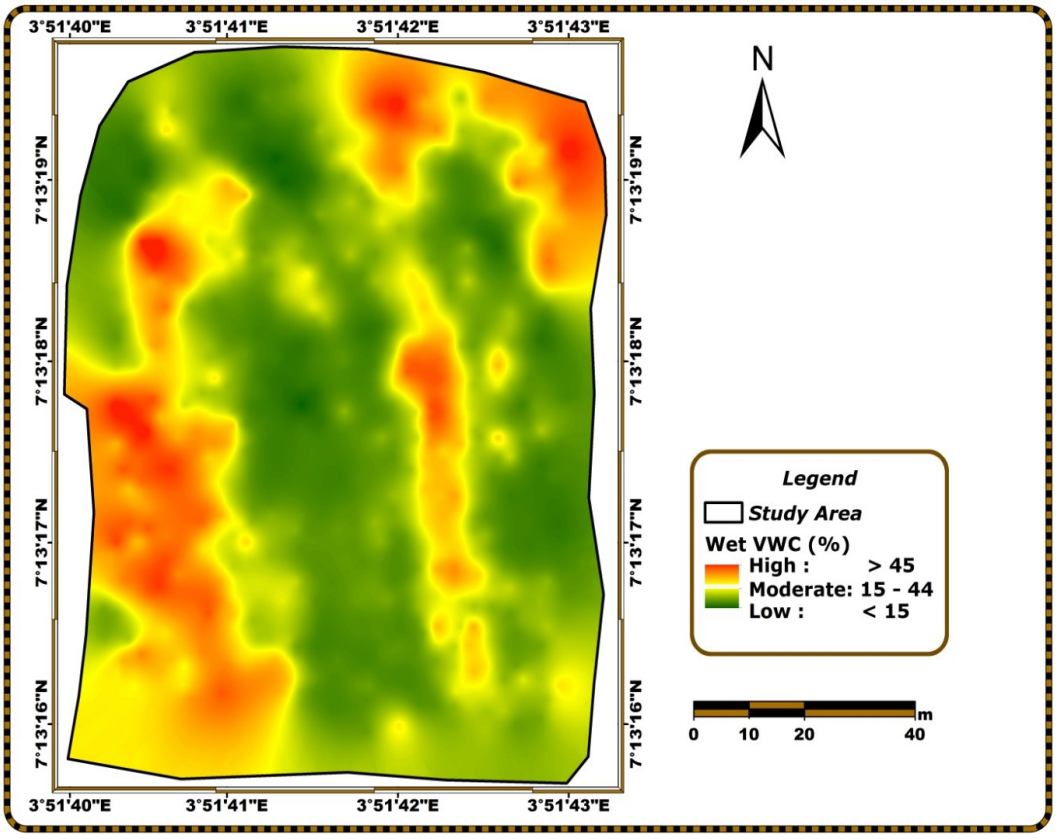

Figure 4.12: Volumetric water content distributions within the cacao field during wet season

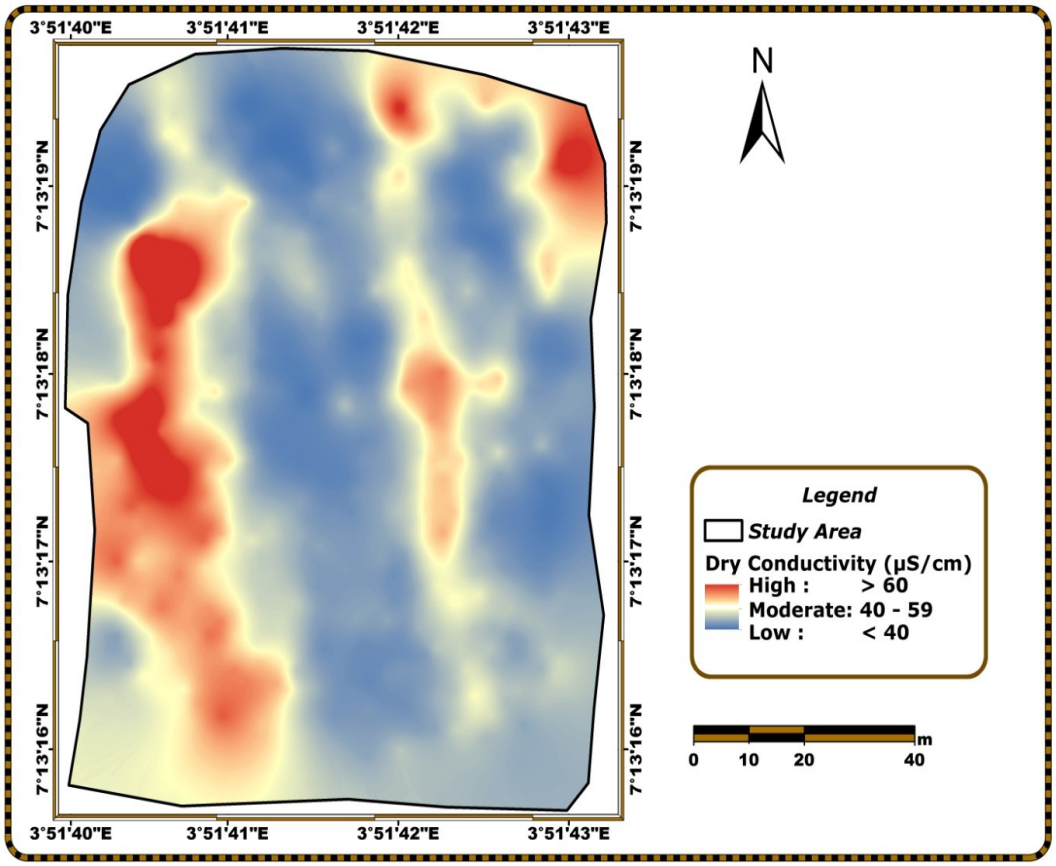

Figure 4.13: Apparent electrical conductivity distributions within the cacao field during dry season

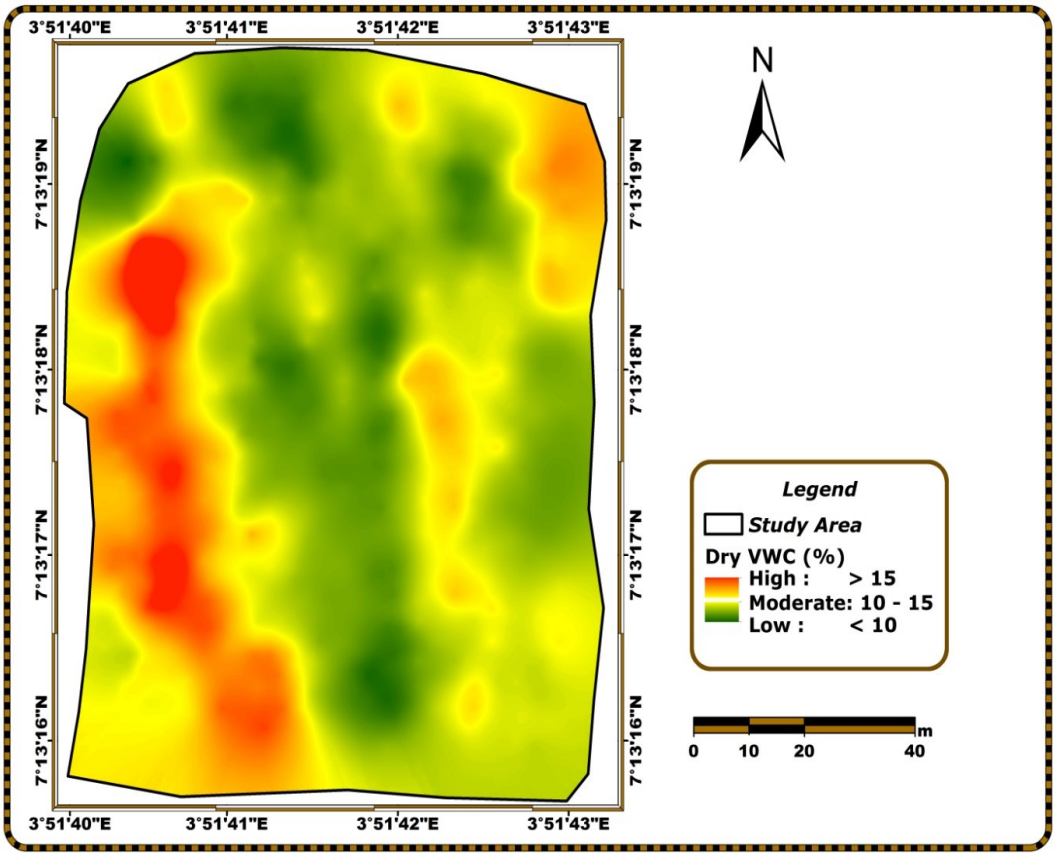

Figure 4.14: Volumetric water content distributions within the cacao field during dry season

Observations from the maps show that regions of high EC_a, moderate EC_a and low EC_a corresponds to high VWC, moderate VWC and low VWC respectively. The difference spotted between the two seasons is that there is wide spread/coverage of EC_a and VWC during the wet season whereas low EC_a/VWC segments are distinctly pronounced in the dry season with reduction in the area extent of high and moderate EC_a. It can be inferred that zones with high water content usually have more fine soil fractions than region of low moisture content (Mzuku *et al.,* 2005; Rodríguez-Pérez *et al.*, 2011 and Gholizadeh *et al.*, 2012), region with low EC_a loses water faster than other regions resulting in variability of water content (Costa *et al.,* 2014) as the water drains through it.

ArcGis 10.2 software was used in the production of EC_a and VWC maps from the kola farm because of its ability to relate one point of measurement with another. Soil EC map from kola field during the rainy season was delineated into three zones; low, moderate and high (Fig. 4.15). The dominant EC_a pattern is the low proportion (< 50 µS/cm) with largest coverage of about two-third of the entire field; also there are enclosures of moderate conductivity in it. Central and south eastern parts are extremely dominated with least conductivity (light yellow). Moderate EC_a (50-99 µS/cm) region was situated along the western portion of the map (orange colour) stretching from top (north) to bottom (south) with pockets of high and low conductivity sandwiched in it. Most conductive (high) district was coloured blue/pink/red and its conductivity value is above 100 µS/cm.

In the dry spell, the farm was also classified into three EC_a regions and maintain similar pattern as obtained during wet season (Fig. 4.16). Zone of high conductivity (> 60 µS/cm) with the highest conductivity coloured blue and moderate EC_a section encloses the highly conductive district. Moderate EC_a (40-59 µS/cm) section (orange) spreads outward from the most conductive area while the remaining zone is low (< 40 µS/cm). Area of low conductivity (light yellow) was situated in the SE and central portion of the map.

Region of high VWC was coloured red (> 45%), moderate VWC area (15-44%) was shaded light brown while low VWC section (< 15%) was coloured blue (Fig. 4.17). High VWC zone covers nearly one-third of the map with inclusions of low and moderate VWC. This shows that abundant soil moisture was located on the western

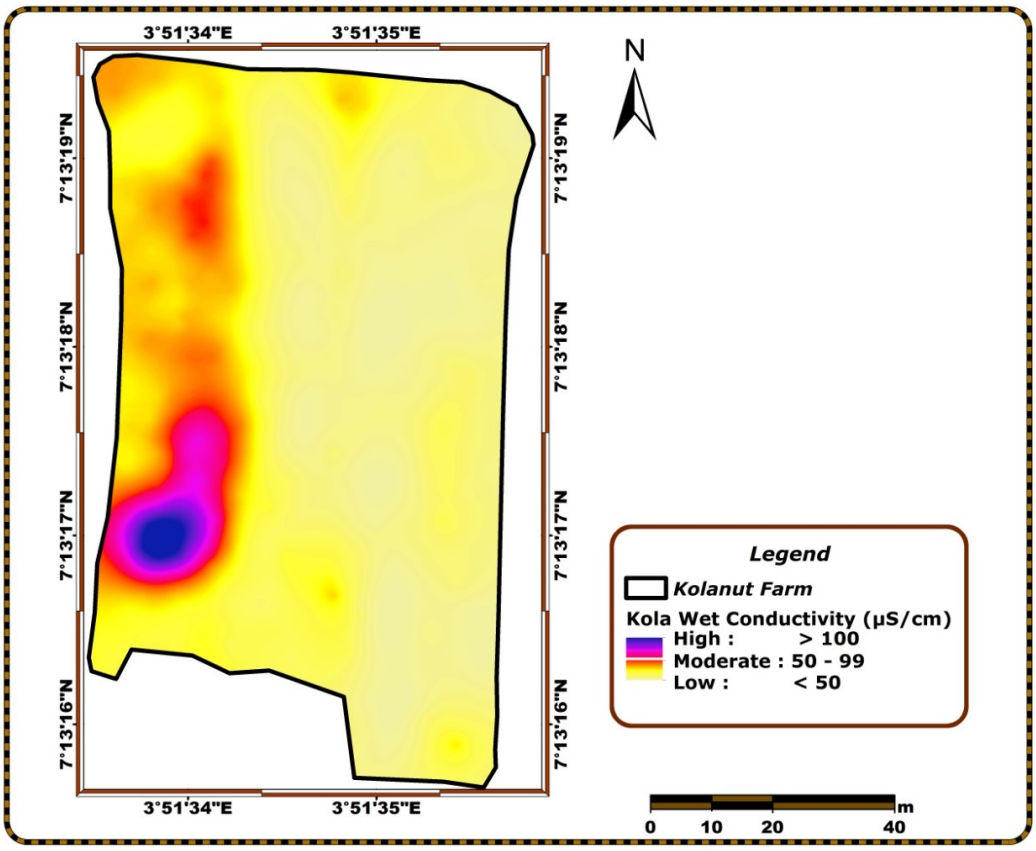

Figure 4.15: Apparent electrical conductivity distributions within the kola field during wet season

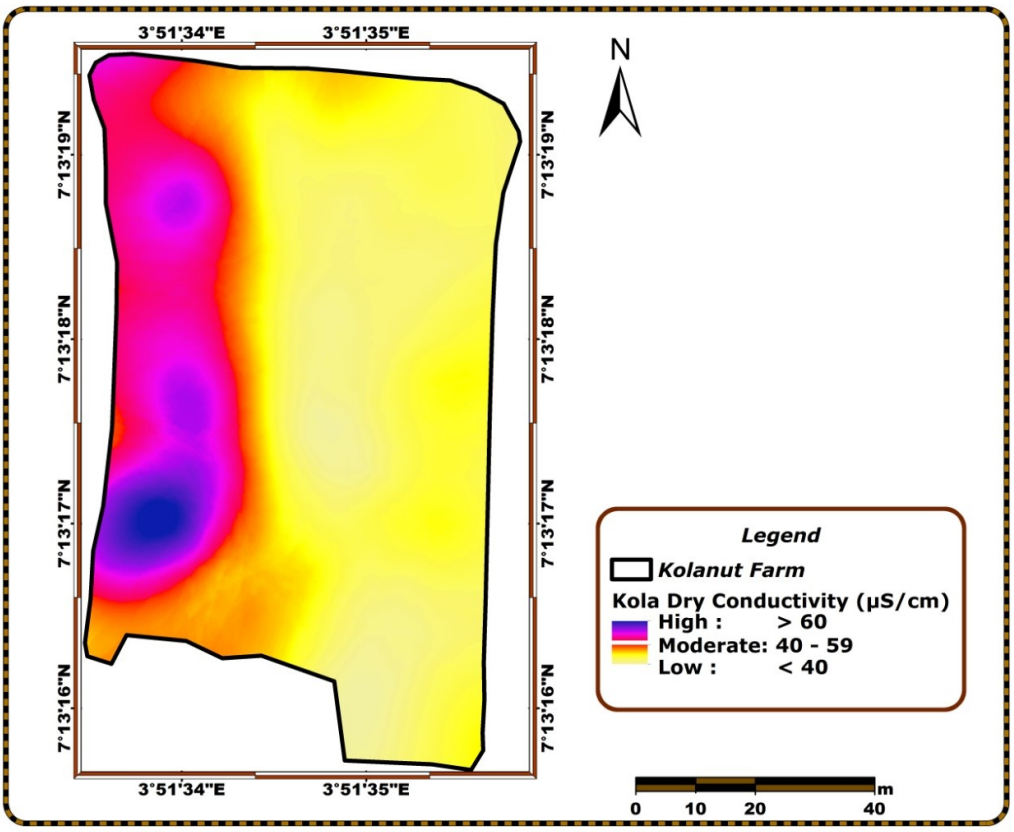

Figure 4.16: Apparent electrical conductivity distributions within the kola field during dry season

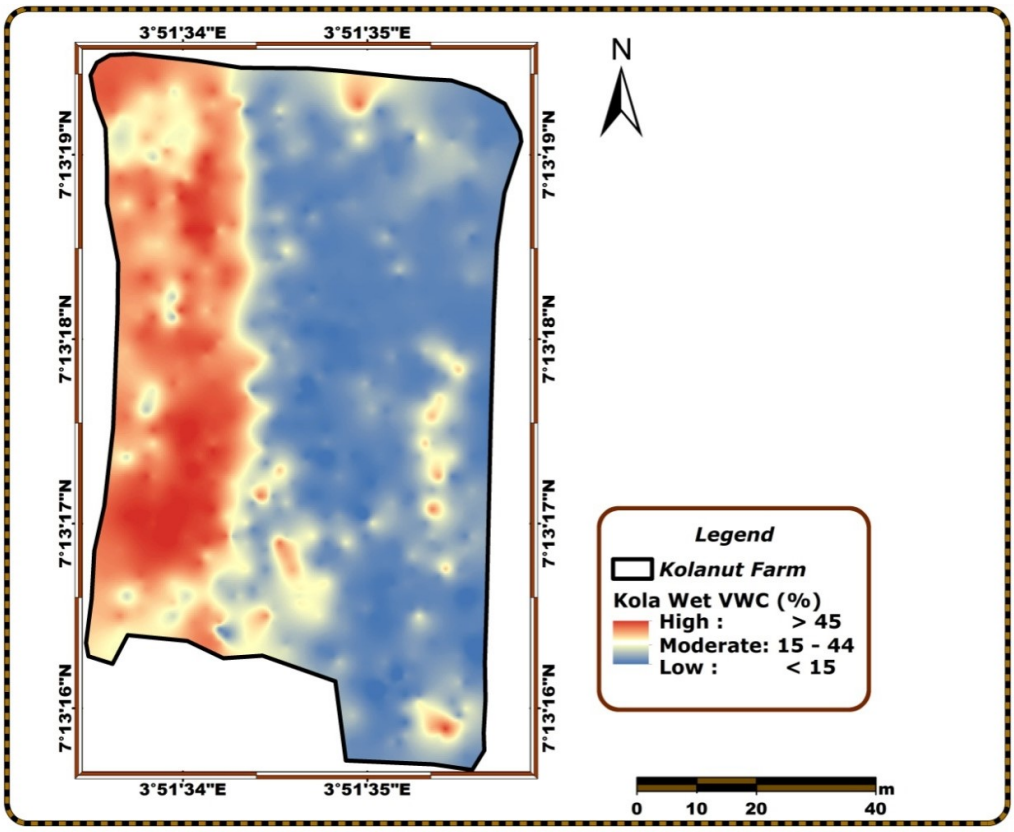

Figure 4.17: Volumetric water content distributions within the kola field during wet season

part of the field while the remaining segment has low moisture content with varying portion of high and moderate soil moisture.

During the dry season, water content distribution follows similar pattern (Fig. 4.18) as that of the wet period. Precinct of high VWC (red colour) was characterised water content above 15%, moderate VWC section (light brown) has its percentage distribution ranging between 10% and 15% whereas water content less than 10% is peculiar to the low VWC (blue) segment. Field distribution of water in the kola soil is alike in both seasons but the quantity of soil moisture in the dry period has reduced, compared to the wet season. Spatial variability of water is due to inhomogeneous nature of the root zone.

Possible deduction from the EC_a and VWC maps at both seasons indicates that areas of high EC_a, moderate EC_a and low EC_a are known for high, moderate and low soil moisture respectively. Brevik *et al.* (2006) reported that soil EC_a is influenced by soil water content, accounting for 50 to 70% EC_a variability. This provides an insight on the soil texture varying from one region to another (Rodríguez-Pérez *et al.,* 2011), therefore healthy growth of kola nut trees was noticed in the region of high VWC but stunted growth is peculiar to low EC_a/VWC and aiding the identification of areas with contrasting soil texture.

District with high moisture content has higher clay content than others (Molin and Faulin, 2013), making EC_a a qualitative indicator in regions with high spatial variability. Presence of water supports the mobility of ions in soil solution within the pore spaces, thereby resulting in high electrical conductivity as the ions move freely (Ekwue and Bartholomew, 2011). Water holding capacity of the soil could be one of the major factors affecting the growth of the kola trees. The kriged EC_a map provides useful information on soil properties which helps in segregating the field into management zones. There is direct relationship between soil apparent electrical conductivity and soil water contet (Clay *et al.,* 2001 and El-Naggar *et al.,* 2017).

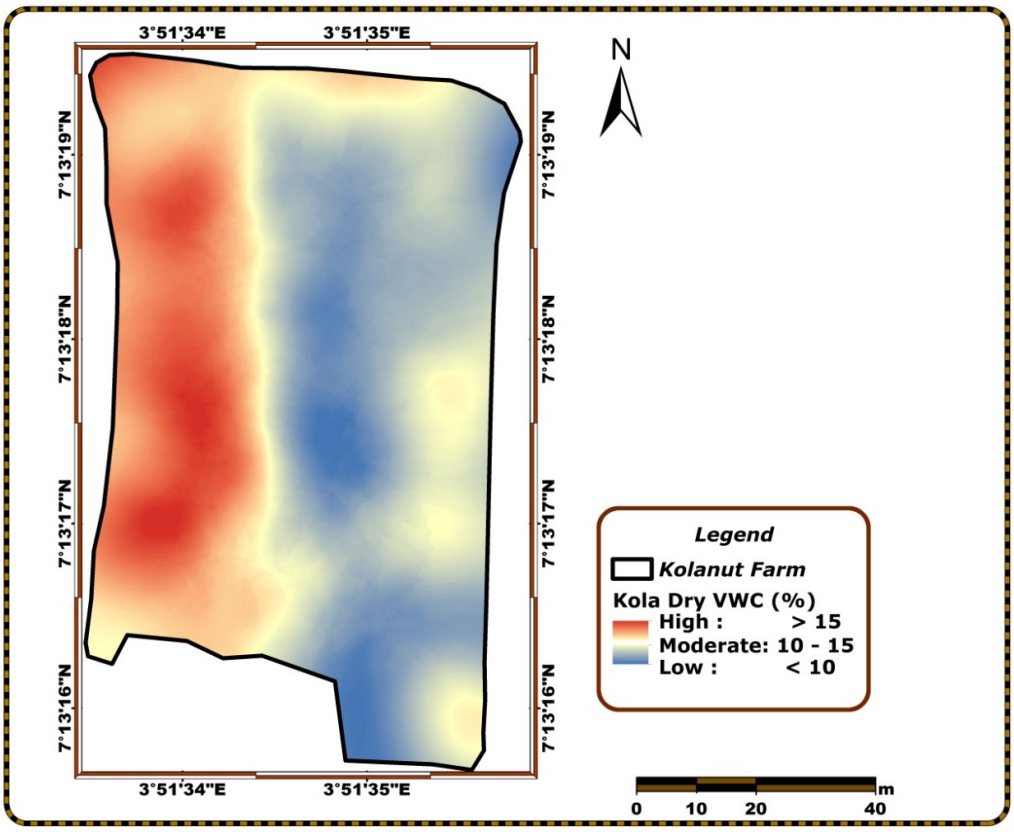

Figure 4.18: Volumetric water content distributions within the kola field during dry season

4.4 Thermal Assessment of Soils

It has been reported by various authors (Brevik *et al*., 2004; Amidu and Dunbar, 2007; Kizito *et al*., 2008; USDA, 2011; Bai *et al*., 2013) that electrical conductivity fluctuates with respect to changes in temperature of earth materials. Then, there is need to examine the thermal properties influencing the electrical conductivity and the effect of volumetric water content on thermal regime.

4.4.1 Thermal Assessment of Soils in the Farms

(i) **Cacao Farm**

The acquired data were subjected to statistical analysis using SPSS software to determine their variability; coefficient of variation (CV) was used in establishing the variability and a comparison with Warrick and Nielsen (1980) to classify the degree of variability (Table 4.3). Data collected from all the sampling points were analyzed to determine their degree of variability.

Assessment of thermal data (Table 4.6) during the wet season showed that soil thermal conductivity ranged from 1.342 to 2.715 W/mk with an average value of 2.101 W/mk and its variability is moderate (13%). Volumetric heat capacity varied from 1.167 to 4.578 mJ/m^3k while its mean value is 2.333 mJ/m^3k, it exhibited a moderate variation (23 %). Soil thermal diffusivity has its minimum value to be 0.502 mm^2/s and 1.994 mm^2/s as the highest, also exhibiting moderate variation (23 %). The apparent electrical conductivity values obtained from the selected thermal sampling points ranged from 15 to 252 µS/cm and its mean value is 68 µS/cm with the highest coefficient of variation (71 %). The volumetric water contents at the thermal sampling points vary from 4 to 64 % and its mean value is 25 %; its data variability was classified as high. Temperature pattern across the farm is uniformly distributed as suggested by its low variability (3%)

In the dry period, soil thermal conductivity indicates a moderate variation (24 %) with a mean value of 1.411 W/mk, the values of volumetric heat capacity varied between 0.876 and 4.233 mJ/m^3k and its data varies moderately (30 %); with a reduction in its average value in comparison with the wet season. Thermal diffusivity data also varied moderately (31 %) and its value ranged from 0.351 to 1.959 mm^2/s. Temperature variability within farm was regarded as low (5%). High data variation (69 %) was observed in apparent electrical conductivity, it ranged between 11 and 161 µS/cm while its average value was 45 µS/cm. The measured volumetric water content

Table 4.6: Thermal properties of soil in the cacao field during wet and dry seasons

	Thermal onductivity (W/mk)	Volumetric Heat Capacity (mJ/m^3k)	Thermal Diffusivity (mm^2/s)	Electrical Conductivity (µS/cm)	Volumetric Water Content (%)	Soil Temperature (ºC)
Wet Season						
Minimum	1.342	1.167	0.502	15	4	25
Maximum	2.715	4.578	1.994	252	64	28
Mean	2.101	2.333	0.937	68	25	26
Standard Deviation	0.277	0.539	0.218	47.95	15.28	0.70
% Coefficient of Variation	13	23	23	71	62	3
Dry Season						
Minimum	0.7	0.876	0.351	11	4	26
Maximum	2.251	4.233	1.959	161	19	34
Mean	1.411	2.027	0.746	45	10	28
Standard Deviation	0.343	0.605	0.232	31.14	3.192	1.284
% Coefficient of Variation	24	30	31	69	33	5

exhibited moderate variation (33 %) and its mean value was 10 % and a summary of data analysis is presented in Table 4.6.

Comparison of data acquired during wet and dry seasons showed that moderate variation occurred in soil thermal properties (conductivty, volumetric heat capacity and diffusivity), apparent electrical conductivity maintained high data variation at both seasons while volumetric water content data variation was high in wet season and moderate during dry season. Soil moisture content tends to influence data variation, the mean values of thermal properties got reduced during dry period with an increase in its numerical strenght of variation coefficient. Reduction in the mean value of EC_a and water content in the dry season tend to lower the coefficient of variation.

(ii) **Kola Farm**

An overview of thermal values measured during the wet and dry seasons showed that the average volumetric water content recorded in the wet period was 27% while 8% was recorded during dry season, and there was a significant drop in soil moisture content accounting for 70% with respect to the wet season (Table 4.7). It was also noted that the electrical conductivity value obtained reduced by 43.5 % considering the fall in its value from 85µS/cm during wet season to 48µS/cm in dry period; this could be as a result of decrease in moisture content and less heat energy stored responsible for reduction in mobility of ions. The mean temperature during rainy weather was 27 ºC while an increase of 3 ºC was observed in dry season.

Record of thermal conductivity values ranged from 1.074 to 2.230 W/mk with an average value of 1.633 W/mk during the wet season, while a mean value of 1.392 W/mk was computed during the dry season, an increase in moisture content is synonymous with an increase in thermal conductivity while drop in moisture content resulted in reduction of thermal conductivity during the dry season.

The numerical values of volumetric heat capacity showed higher values (1.397-3.473 mJ/m^3k) in wet period but lesser values (0.760-3.279 mJ/m^3k) were recorded in dry period. The amount of heat energy required to raise the temperature of a unit volume of soil increases with an increase in moisture content, thus establishing a reduction in moisture content and less heat energy stored in the dry season.

Table 4.7: Thermal properties of soil in the kola field during wet and dry seasons

	Thermal Conductivity (W/mk)	Volumetric Heat Capacity (mJ/m^3k)	Thermal Diffusivity (mm^2/s)	Electrical Conductivity (µS/cm)	Volumetric Water Content (%)	Soil Temperature (ºC)
Wet Season						
Minimum	1.074	1.397	0.424	16	5	25
Maximum	2.230	3.473	1.329	476	63	29
Mean	1.633	2.329	0.726	85	27	27
Standard Deviation	0.291	0.521	0.170	75.212	16.81	0.625
% Coefficient of Variation	18	22	23	88	61	2
Dry Season						
Minimum	0.758	0.760	0.453	12	3	27
Maximum	2.039	3.279	1.605	144	15	34
Mean	1.392	2.041	0.728	48	8	30
Standard Deviation	0.257	0.540	0.233	26.16	2.84	1.682
% Coefficient of Variation	19	27	32	55	36	6

Diffusion of heat energy passing through a unit area of soil in kola farm over a unit time also showed a negligible variation. The average thermal diffusivity in wet period was 0.726 mm^2/s whereas it was 0.728 mm^2/s during dry season indicating a negligible fractional increase of 2/1000.

Degree of data variability for the thermal properties was moderate in both seasons with higher numerical values in the dry season. Volumetric water content and electrical conductivity exhibited moderate and high data variability during wet season respectively while the data varied moderately in the dry season with a reduction in its numerical values. The mean values for all the stated parameters were reduced in the dry season compared to the wet period, suggesting an influence by soil moisture content.

4.4.2 Variation of thermal properties according to EC_a segments in the farms

(i) **Cacao Farm**

Thermal studies were carried out on low EC_a (46 stations), moderate EC_a (26 data points) and high EC_a (18 spots) segments. During the wet season, all the soils in the farm exhibit almost similar temperature ranging from 25.67^0C to 25.84^0C (Table 4.8). Thermal conductivity of the soil in low EC_a area varies between 1.342 W/mk and 2.479 W/mk with an average of 2.009 W/mk, in the moderate EC_a area the prevailing thermal conductivity is 2.196 w/mk and varies from 1.645 W/mk to 2.715 W/mk whereas the mean thermal conductivity in the high EC_a division is 2.148 W/mk and ranges from 1.821 W/mk to 2.515 W/mk.

The volumetric heat capacities of the soil in low EC_a region range from 1.167 mJ/m^3k to 2.903 mJ/m^3k and has a mean of 2.121 mJ/m^3k, region of moderate EC_a was characterised with the quantity of heat energy ranging from 1.809 mJ/m^3k to 4.578 mJ/m^3k with a peculiar value of 2.521 mJ/m^3k whereas it varies from 2.011 to 3.456 mJ/m^3k and an average of 2.604 mJ/m^3k in the high EC_a segment.

The average diffusion of thermal energy in the low EC_a soil is 0.996 mm^2/s and ranges between 0.543 mm^2/s and 1.994 mm^2/s. Soil in the moderate EC_a section has its thermal diffusivity between 0.542 and 1.229 mm^2/s with an average of 0.903 mm^2/s whereas the mean value recorded for soil in high EC_a is 0.835 mm^2/s and it varies from 0.527 mm^2/s to 1.006 mm^2/s.

Table 4.8: Distribution of thermal properties in the cacao farm

Wet Season			Dry Season	
	Range	Mean	Range	Mean
Low EC_a segment				
Thermal conductivity	1.342-2.479 W/mk	2.029 W/mk	0.700-2.075 W/mk	1.300 W/mk
Volumetric heat capacity	1.167-2.903 mJ/m^3k	2.121 mJ/m^3k	0.876-3.662 mJ/m^3k	1.898 mJ/m^3k
Thermal diffusivity	0.543-1.994 mm^2/s	0.996 mm^2/s	0.352-1.959 mm^2/s	0.755 mm^2/s
Soil temperature	24.59-27.29^{0}C	25.67^{0}C	26.05-33.71^{0}C	28.04^{0}C
Moderate EC_a segment				
Thermal conductivity	1.645-2.715 W/mk	2.196 W/mk	1.039-2.251 W/mk	1.529 W/mk
Volumetric heat capacity	1.809-4.578 mJ/m^3k	2.521 mJ/m^3k	1.004-3.234 mJ/m^3k	2.068 mJ/m^3k
Thermal diffusivity	0.502-1.229 mm^2/s	0.903 mm^2/s	0.351-1.329 mm^2/s	0.767 mm^2/s
Soil temperature	24.60-27.63^{0}C	25.84^{0}C	26.24-31.55^{0}C	28.49^{0}C
High EC_a segment				
Thermal conductivity	1.821-2.515 W/mk	2.148 W/mk	0.714-2.213 W/mk	1.523 W/mk
Volumetric heat capacity	2.011-3.456 mJ/m^3k	2.604 mJ/m^3k	1.472-4.233 mJ/m^3k	2.300 mJ/m^3k
Thermal diffusivity	0.527-1.006 mm^2/s	0.835 mm^2/s	0.386-1.064 mm^2/s	0.691 mm^2/s
Soil temperature	24.89-27.46^{0}C	25.75^{0}C	26.59-29.54^{0}C	28.17^{0}C

Thermal conductivity of soil in the moderate EC_a section (2.196 W/mk) is higher than the high EC_a division (2.148 W/mk) and low EC_a segment (2.029 W/mk). Soils in high EC_a require greater heat energy (2.604 mJ/m^3k) to raise its temperature than the moderate EC_a (2.521 mJ/m^3k) and low EC_a (2.121 mJ/m^3k) suggesting that the quantity of soil water present is higher than those in other segments. Soils in the low EC_a (0.996 mm^2/s) and moderate EC_a (0.903 mm^2/s) quickly attain thermal equilibrium than high EC_a (0.835 mm^2/s) which retain heat energy over a longer period. The heat retained is vital for plant growth, microbial activity and root development (Gardner *et al*., 1999).

During the dry period, the soil temperature (28.04^0C-28.49^0C) is nearly the same throughout the segments. The average thermal conductivity in the low EC_a (0.7-2.075 W/mk) is 1.30 W/mk, the mean thermal conductivity in the moderate EC_a is 1.529 W/mk and ranged between 1.039 W/mk and 2.251 W/mk while the high EC_a area varies from 0.714 W/mk to 2.213 W/mk with an average of 1.523 W/mk.

Volumetric heat capacity ranges from 1.167 mJ/m^3k to 2.903 mJ/m^3k with a mean of 1.899 mJ/m^3k in the soils of low EC_a, the equitable heat capacity in the moderate EC_a is 2.068 mJ/m^3k, and it varies between 1.004 mJ/m^3k and 3.234 mJ/m^3k. Region of high EC_a has its average volumetric heat capacity of 2.30 mJ/m^3k, and varies from 1.472 mJ/m^3k to 4.233 mJ/m^3k. Heat energy diffusion in soil of low EC_a is between 0.352 mm^2/s and 1.959 mm^2/s and the mean thermal diffusivity is 0.755 mm^2/s, soils in the moderate EC_a has peculiar thermal diffusivity of 0.767 mm^2/s, varying from 0.351 mm^2/s to 1.329 mm^2/s. Thermal diffusion in soils of high EC_a ranges from 0.386 mm^2/s to 1.064 mm^2/s with mean distribution of 0.691 mm^2/s.

The average thermal conductivity of soil in the moderate EC_a (1.529 W/mk) and high EC_a (1.523 W/mk) is nearly uniform whereas low thermal conductivity is recorded for soils in low EC_a (1.300 W/mk) area. Greater heat energy is needed by the soils of high EC_a (2.300 mJ/m^3k) than soils situated in the moderate EC_a (2.068 mJ/m^3k) and low EC_a (1.898 mJ/m^3k) indicating larger amount of soil moisture in this region. Heat diffusion rate is high in soils of moderate EC_a (0767 mm^2/s) and low EC_a (0.755 mm^2/s) whereas it is low in soils of high EC_a (0.691 mm^2/s). Soils in high EC_a have the ability to retain the heat energy as it diffuses slowly than other EC_a segments. Ionic mobility varies with temperature (Moore et al., 2008) and this is responsible for the greater movement of ions in less viscous solution as the temperature rises.

(ii) **Kola Farm**

The thermal regime in the kola farm was analysed at 67 stations in such a way that 25 stations were situated in the low EC_a area, 22 data points in the moderate EC_a segment while high EC_a division has 20 thermal stations.

During the wet period, the average soil temperature across all the EC_a segments ranged between 26.43^0C and 26.92^0C indicating a near-uniform distribution (Table 4.9). The thermal conductivity in the soil of low EC_a segment varies from 1.074 W/mk to 2.160 W/mk and have average value of 1.529 W/mk. Soils in the moderate ECa area have thermal conductivity ranging from 1.123 W/mk to 2.230 W/mk and a mean of 1.720 W/mk whereas the prevailing thermal conductivity in the soils of high EC_a was 1.668 W/mk and has a spread of 1.280 W/mk to 2.111 W/mk.

The soil volumetric heat capacity in the low EC_a area stretches from 1.397 mJ/m^3k to 3.431 mJ/m^3k and the common heat capacity in this region was 2.150 mJ/m^3k. Moderate EC_a section was characterised with capacity of heat energy varying from 1.447 mJ/m^3k to 3.205 mJ/m^3k and a mean of 2.176 mJ/m^3k. The high EC_a part has its volumetric heat capacity spanning from 2.064 mJ/m^3k to 3.473 mJ/m^3k and the equitable capacity of 2.721 mJ/m^3k was computed for this section.

The thermal diffusivity of soils in the low EC_a portion extends from 0.424 mm^2/s to 1.002 mm^2/s with a prevailing diffusion rate of 0.728 mm^2/s, it varies from 0.425 mm^2/s to 1.329 mm^2/s in the moderate EC_a district and the average thermal diffusion rate was 0.819 mm^2/s. Soils of high EC_a have diffusion of heat energy stretching from 0.459 mm^2/s to 0.770 mm^2/s and the common rate of heat diffusion in this segment was 0.622 mm^2/s.

The mean conductivity of heat energy through the soils in the moderate EC_a area (1.720 W/mk) was higher than the mean values of the high EC_a (1.668 W/mk) and low EC_a (1.529 W/mk). The volumetric heat capacity of soils in the high EC_a (2.721 mJ/m^3k) was greater than the capacities of moderate EC_a (2.176 mJ/m^3k) and low EC_a (2.150 mJ/m^3k). The rate of diffusion of thermal energy to return to a balance state is low in high EC_a district (0.622 mm^2/s) whereas soils in the low EC_a (0.728 mm^2/s) and moderate EC_a (0.819 mm^2/s) attain thermal equilibrium faster than soils in high EC_a.

Table 4.9: Distribution of thermal properties in the kola farm

Wet Season			Dry Season	
	Range	Mean	Range	Mean
Low EC_a segment				
Thermal conductivity	1.074-2.160 W/mk	1.529 W/mk	1.002-1.674 W/mk	1.320 W/mk
Volumetric heat capacity	1.397-3.431 mJ/m^3k	2.150 mJ/m^3k	0.863-2.755 mJ/m^3k	2.005 mJ/m^3k
Thermal diffusivity	0.424-1.002 mm^2/s	0.728 mm^2/s	0.466-1.161 mm^2/s	0.692 mm^2/s
Soil temperature	25.42-29.04^{0}C	26.50^{0}C	27.65-34.48^{0}C	30.42^{0}C
Moderate EC_a segment				
Thermal conductivity	1.123-2.230 W/mk	1.720 W/mk	0.758-1.869 W/mk	1.399 W/mk
Volumetric heat capacity	1.447-3.205 mJ/m^3k	2.176 mJ/m^3k	0.954-3.232 mJ/m^3k	2.065 mJ/m^3k
Thermal diffusivity	0.425-1.329 mm^2/s	0.819 mm^2/s	0.453-1.341 mm^2/s	0.733 mm^2/s
Soil temperature	25.60-27.55^{0}C	26.43^{0}C	27.15-33.08^{0}C	29.74^{0}C
High EC_a segment				
Thermal conductivity	1.28-2.111 W/mk	1.668 W/mk	0.888-2.039 W/mk	1.474 W/mk
Volumetric heat capacity	2.064-3.473 mJ/m^3k	2.721 mJ/m^3k	0.760-3.279 mJ/m^3k	2.059 mJ/m^3k
Thermal diffusivity	0.459-0.770 mm^2/s	0.622 mm^2/s	0.506-1.605 mm^2/s	0.767 mm^2/s
Soil temperature	26.11-28.17^{0}C	26.92^{0}C	27.27-31.68^{0}C	29.04^{0}C

Comparing the thermal properties in the low and high EC_a divisions, soils in the high EC_a were characterised with higher heat conductivity, better heat capacity and release the stored energy at a slower rate than the soils in the low EC_a segment, helping the mobility of the dissolved ions and creates a habitable environment (microbial activity) for plant survival (Haskell *et al*., 2010).

During the dry season, the mean soil temperature at all the segments stretches from 29.04^0C to 30.42^0C. The thermal conductivity in the low EC_a segment increases from 1.002 W/mk to 1.674 W/mk and a mean of 1.320 W/mk was noted in this region. The moderate EC_a section has its thermal conductivity varying from 0.758 W/mk to 1.869 W/mk with an equitable conductivity of 1.399 W/mk whereas a value of 1.474 W/mk was common to the high EC_a division and its distribution varies from 0.888 W/mk to 2.039 W/mk.

The volumetric heat capacity lies between 0.863 mJ/m^3k and 2.755 mJ/m^3k for soils in the low EC_a zone and has an average of 2.005 mJ/m^3k. It varies from 0.954 mJ/m^3k to 3.232 mJ/m^3k in the moderate EC_a segment with a mean of 2.065 mJ/m^3k. Soils in the high EC_a section have an average of 2.059 mJ/m^3k, extending from 0.760 mJ/m^3k to 3.279 mJ/m^3k.

The thermal diffusion rate in the low EC_a segment varies from 0.466 mm^2/s to 1.161 mm^2/s and a mean of 0.692 mm^2/s was computed. The moderate EC_a has the diffusion of heat energy varying from 0.453 mm^2/s to 1.341 mm^2/s and the average value of 0.733 mm^2/s is peculiar to this division. The thermal diffusivity in the high EC_a area was situated between 0.506 mm^2/s and 1.605 mm^2/s and its overall mean value amounts to 0.767 mm^2/s.

High thermal conductivity was noted in the soils of high EC_a (1.474 W/mk) but soils in the low EC_a have low thermal conductivity (1.320 W/mk). Soils in the high EC_a division have larger heat capacity (2.059 mJ/m^3k) to set up a degree rise in temperature than those in the low EC_a district (2.005 mJ/m^3k). Low thermal diffusivity was recorded in the soils of low EC_a (0.692 mm^2/s) while diffusion rates in the moderate EC_a (0.733 mm^2/s) and high EC_a (0.767 mm^2/s) are high. Omer and Omer (2014) reported that in a damp situation when the moisture content is low, the thermal diffusivity of fine grain is higher than coarse grain. The lowest mean water content (8%) was noticed in the kola farm compared to the cacao farm (10%) in the dry season,

the moisture variation could be responsible for observed contrast in thermal diffusivity across these regions. Numerically, the computed thermal diffusivities for all the segments are near-uniform. Despite this variation, the soils in the high EC_a have greater ability to conduct and store heat energy, thus, supporting the activities of micro-organism and flow dynamic of dissolved ions (Dec *et al*., 2009).

4.4.3 Correlation Analysis of Thermal Properties with Electrical Conductivity and Volumetric Water Content in the Farms

(i) **Cacao Farm**

A plot of the thermal conductivity data and electrical conductivity of soil at their corresponding sample points showed a correlation cofficient (r) to be 0.210 (Fig. 4.19a) and this consider to be a weak positve relationship. The positive linear correlation indicates that there is direct relationship between these parameters, that is, an increase in thermal conductivity also favours increase in electrical conductivity (Wang *et al.,* 2017), it could be inferred that distribution of thermal conductivity across the cacao farm aided the electrical conductivity of ions in solution. As the heat energy rises across the medium, the ions in solution become more agitated with increasing mobility and electric current in solutions is transferred by ions. Ekwue and Bartholomew (2011) and Bai *et al.* (2013) reported that temperature tends to increase electrical conductivity of soil solution by about 2 % and 2.02 % per ºC respectively.

Transmission of heat energy increases with increase in volumetric water content within the cacao field as noted in Figure 4.19b; a weak correlation coefficient (0.239) was generated between these variables. It has also been established that thermal conductivity increases as soil moisture increases (Ghuman and Lal, 1985; Oladunjoye *et al.*, 2013; Dong *et al.,* 2015; Shein and Mady, 2016: Bertermann and Schwarz 2017) because water tends to be a good conductor of heat energy. Water has thermal conductivity greater than the air and pores space fully saturated with water tend to have higher thermal conductivity than a combination of air and water. Coarse grains fraction tends to have low thermal conductivity than the fine grains content when they are equally saturated with water (Wang *et. al*., 2017). It could be inferred that zones of higher soil moisture are associated with high thermal conductivity, having higher fraction of fines and conversely.

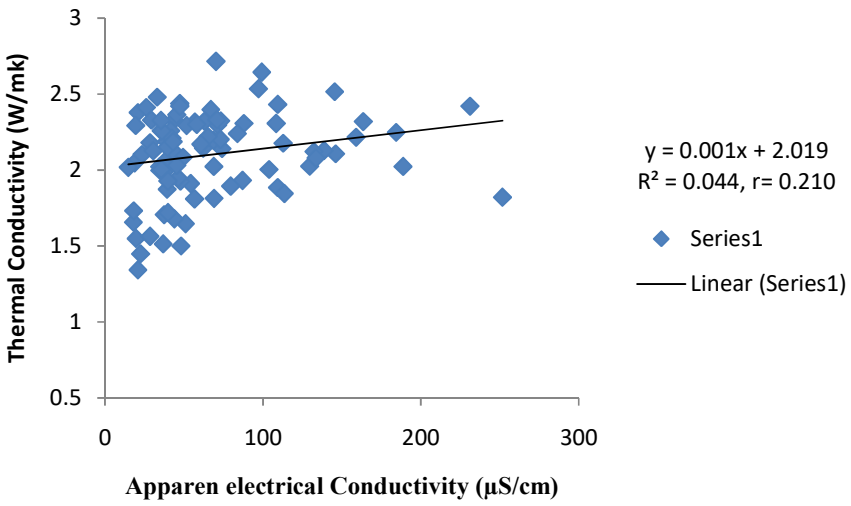

Figure 4.19a: Variation of thermal conductivity with apparent electrical conductivity in the cacao farm during wet season

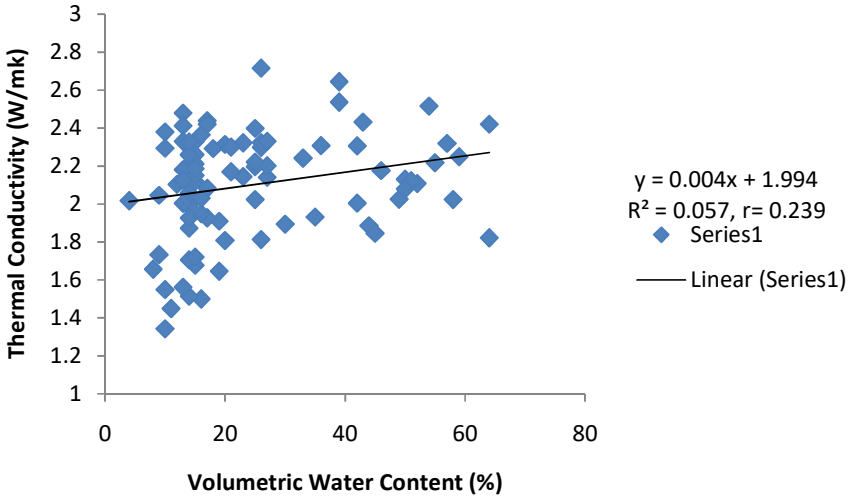

Figure 4.19b: Variation of thermal conductivity with volumetric water content in the cacao farm during wet season

The thermal conductivity varied from 0.700 to 2.251 W/mk and its mean conductivity is 1.411 W/mk during the dry season, comparing the thermal conductivity between the two seasons there is significant drop in value with respect to wet period and this could be attributed to variation in moisture content. Figure 4.20a shows that a weak positive correlation (0.286) exists between thermal conductivity and electrical conductivity indicating that the conductivity of ions in solution increases as heat energy is conducted through the soil in cacao field and vice versa.

There is a moderate positive relationship (0.314) between the thermal conductivity and the volumetric water content during the dry season (Fig. 4.20b). This result also agrees with the findings of previous workers (Cosenza *et al.,* 2003; Hamdham and Clarke, 2010; Barry-Macaulay *et al.*, 2014) suggesting that conduction of heat energy increases with an increases in moisture content.

The measured volumetric heat capacity values in the cacao field ranged from 1.167 to 4.578 J/m^3k with an average value of 2.333 J/m^3k during wet season. Also, the volumetric water content at these points varied between 4 and 64 %. Moderate correlation coefficient (0.40) was deduced from the plot of volumetric heat capacity with electrical conductivity (Fig. 4.21a), this suggests that locations of high volumetric heat capacity are characterized with high electrical conductivity due to the fact that rise in temperature aids the mobility of electrolytes in it. Samouëlian *et al.* (2005) reported that temperature rise tends to decrease the viscosity of fluid and thereby increasing the agitation of ions; rise in temperature led to an increase in electrical conductivity (Othaman *et al.,* 2020)

Plot of volumetric heat capacity against volumetric water content in Figure 4.21b indicates a moderate positive correlation coefficient (0.377) between them. The amount of heat energy required to change the unit temperarue in the medium depends on the quantity of soil water present. The greater the water quantity; the higher the volumetric heat capacity and vice versa. Similar results were reported by previous workers (Oladunjoye *et al.,* 2013; Barry-Macaulay *et al.*, 2014; Shein and Mady, 2016). This shows that the volumetric heat capacity of soils in the cacao field was influenced by volumetric water content.

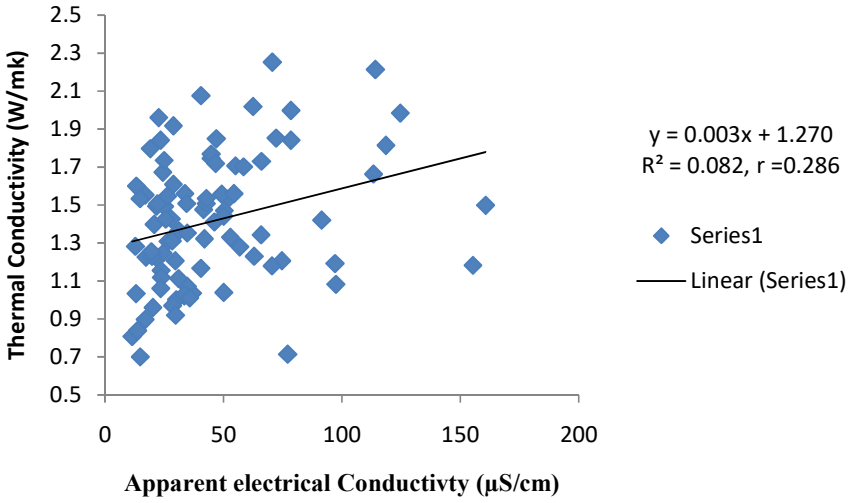

Figure 4.20a: Variation of thermal conductivity with apparent electrical conductivity in the cacao farm during dry season.

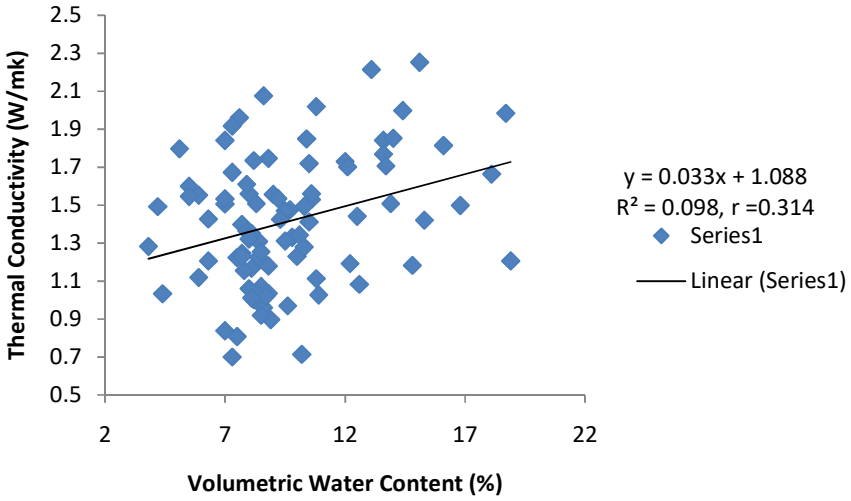

Figure 4.20b: Variation of thermal conductivity with volumetric water content in the cacao farm during dry season

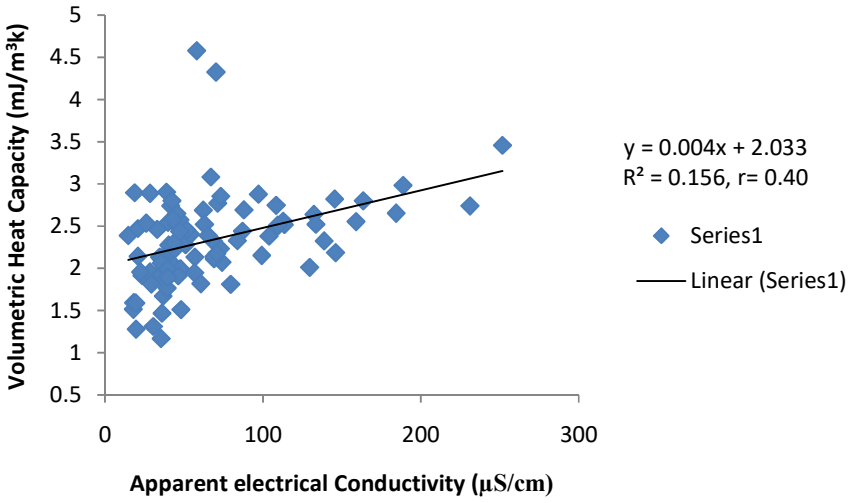

Figure 4.21a: Variation of volumetric heat capacity with apparent electrical conductivity in the cacao farm during wet season

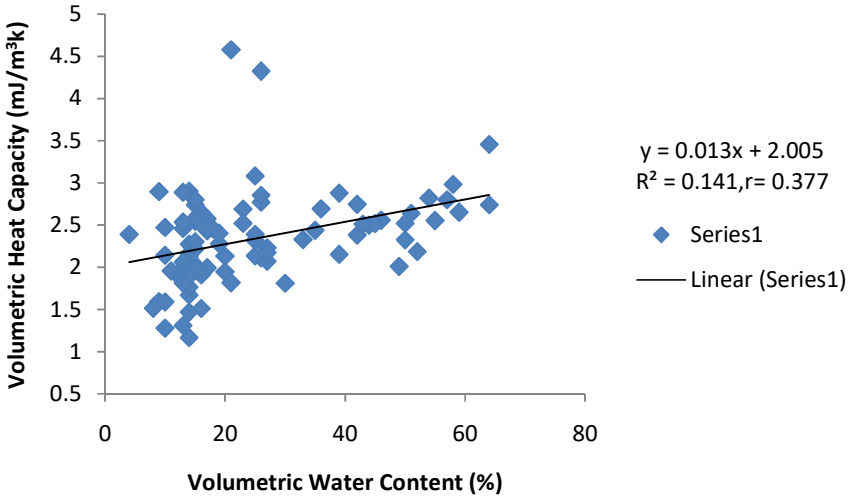

Figure 4.21b: Variation of volumetric heat capacity with volumetric water content in the cacao farm during wet season

It was observed that the recorded volumetric heat capacity during dry season decreases in comparison with the wet period, such that the minimum value was 0.876 J/m^3k and the highest value during this period was 4.233 J/m^3k while the average value noted was 2.027 J/m^3k. Moderate correlation of 0.311 was generated from the plot of volumetric heat capacity against electrical conductivity (Fig. 4.22a). The heat energy needed in raising the soil temperature could be regarded as the likely source of ions agitation in solution, thus contributing to electrolytic conduction.

It has been established that the volumetric heat capacity increases with increase in soil moisture content (Oladunjoye *et al.*, 2013; Barry-Macaulay *et al*., 2014; Shein and Mady, 2016). Figure 4.22b shows similar agreement with previous findings in which the volumetric heat capacity increases as volumetric water content rises across the farm with a weak positive correlation coefficient of 0.286. The soil's void space is either filled with air or water or a combination, Barry-Macaulay *et al.* (2014) confirmed that a fully saturated soil has high volumetric heat capacity and decreases as volume of air increases. The variation in volumetric heat capacity across the cacao farm during the wet season showed that regions of high capacity are synonymous with regions of high electrical conductivity and high volumetric water content and vice versa.

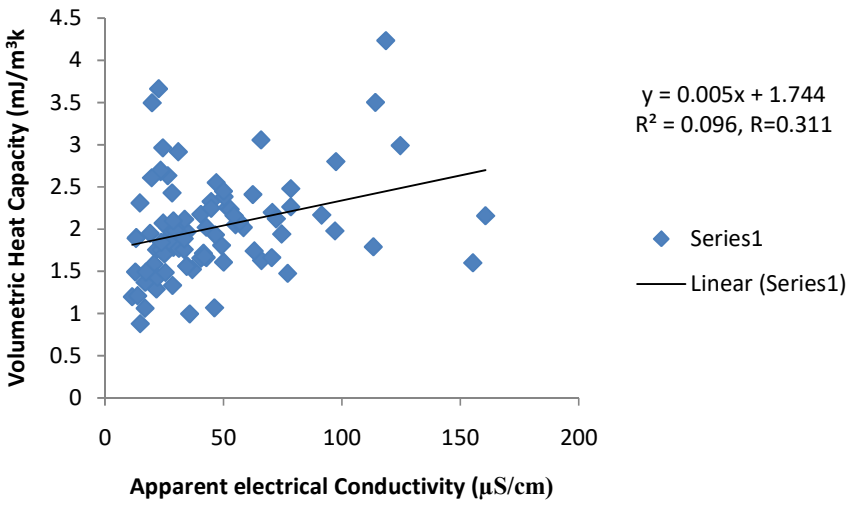

Figure 4.22a: Variation of volumetric heat capacity with apparent electrical conductivity in the cacao farm during dry season

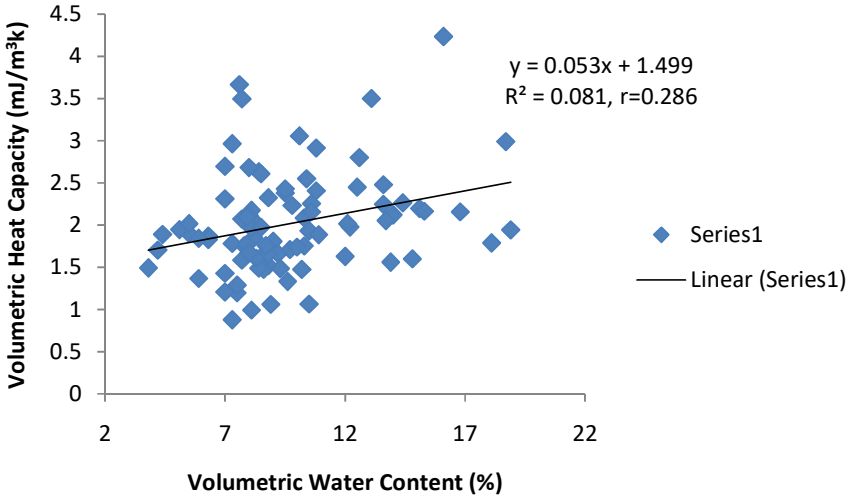

Figure 4.22b: Variation of volumetric heat capacity with volumetric water content during dry season

It has been reported by various authors (Brevik *et al.,* 2004; Amidu and Dunbar, 2007; USDA 2011; Bai *et al.,* 2013) that electrical conductivity fluctuates with respect to changes in temperature of earth materials. There is need to examine the thermal properties influencing the electrical conductivity and the effect of volumetric water content on thermal regime.

The range of thermal diffusivity during wet period was 0.502 to 1.994 mm^2/s with a mean of 0.937 mm^2/s. Correlation coefficient generated from the plot of thermal diffusivity and electrical conductivity was a weak negative value (-0.295), indicating an inverse relationship between them (Fig. 4.23a). As the thermal diffusivity of soil increases, the electrical conductivity decreases suggeting that heat energy within this soil diffuses rapidly to attain thermal equilibrium such that the electrolytes present in soil received less agitation and vice versa.

The thermal diffusivity showed an inverse relationship with volumetric water content, a weak correlation coefficient (-0.275) was generated. This shows that soils of low volumetric water content attain thermal equilibrium rapid than those of high volumetric water content (Fig. 4.23b). It agreed with the findings of past workers (Farouki, 1986; Adeniyi *et al.,* 2012; Barry-Macaulay *et al.*, 2014; Shein and Mady, 2016), the degree of water saturation influence thermal diffusivity of a soil unit. A fully moistened soil exhibits low thermal diffusivity suggesting higher heat energy retention than the partially saturated soil with high thermal diffusivity. The thermal diffusivity of fine grain soil particles is lower than that of coarse grain when saturated with water (Omer and Omer, 2014).

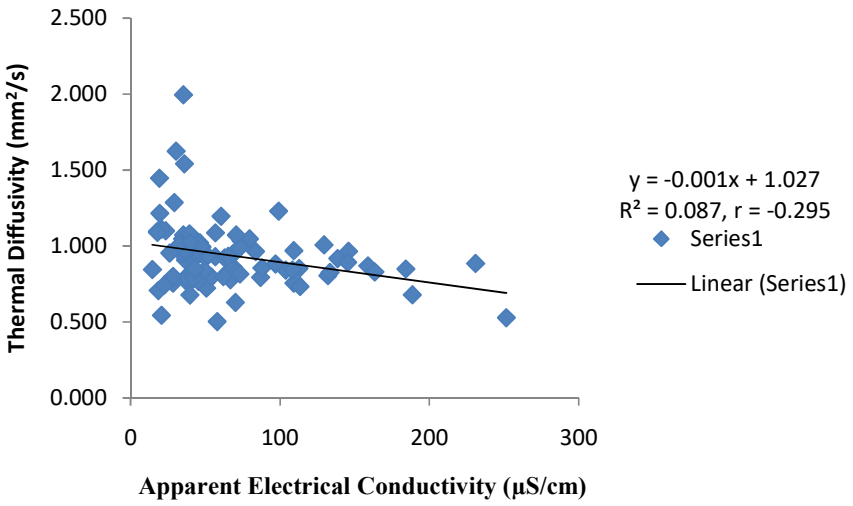

Figure 4.23a: Variation of thermal diffusivity with apparent electrical conductivity in cacao farm during wet season

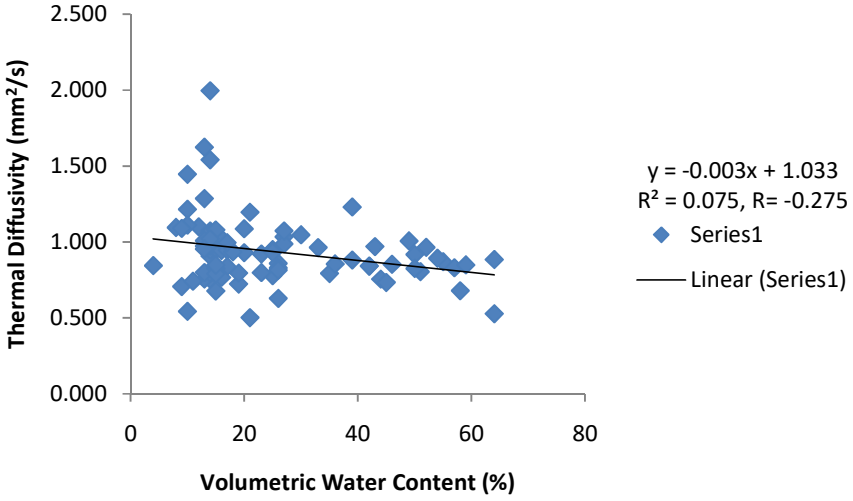

Figure 4.23b: Variation of thermal diffusivity with volumetric water content in cacao farm during wet season

Thermal diffusivity data ranged between 0.351 and 1.959 mm^2/s while the computed mean value was 0.746 mm^2/s. Figure 4.24a shows a weak negative correlation coefficient (-0.122), as electrical conductivity rises, the thermal diffusivity reduces but it reduces as thermal diffusivity increased. The heat energy retained over time by soils of low thermal diffusivity aided the mobility of ions in solution, therefore, contributing to its electrolytic conduction.

A weak negative correlation was generated with -0.07 coefficient (Fig. 4.24b), indicating that as the volumetric water content increases, thermal diffusivity decreases. Farouki (1986), Adeniyi *et al.* (2012), Barry-Macaulay *et al.* (2014) and, Shein and Mady (2016) noted similar deduction that thermal diffusivity of soil was influenced by the degree of water saturation. At low water content, thermal energy diffuses rapidly and vice versa. Increase temperature of a medium corresponds to an increase in electrical conductivity (Bai *et al.*, 2013).

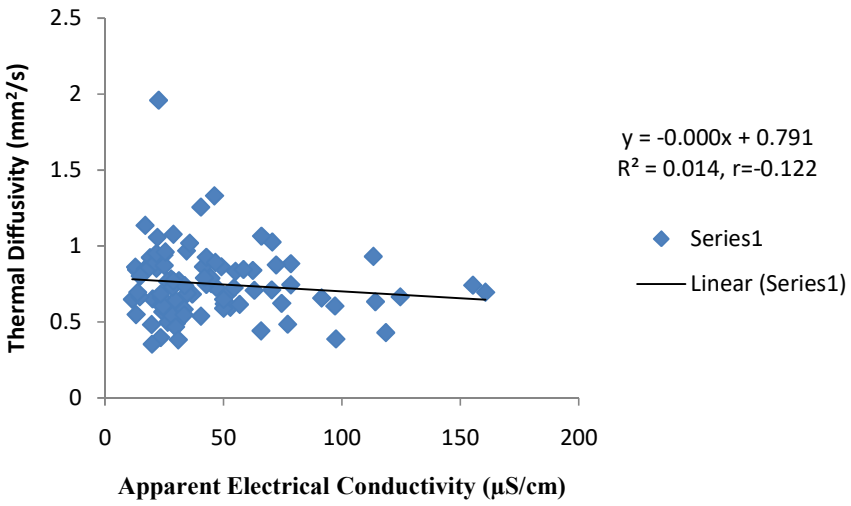

Figure 4.24a: Variation of thermal diffusivity with apparent electrical conductivity in the cacao farm during dry season

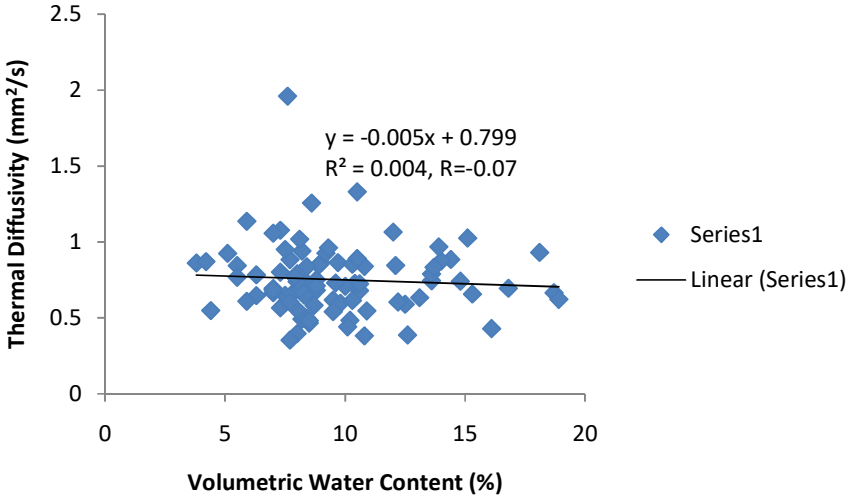

Figure 4.24b: Variation of thermal diffusivity with volumetric water content in the cacao farm during dry season

(ii) **Kola Farm**

Transmission of heat energy across the soil unit showed a weak positive relation (0.179) with apparent electrical conductivity (Fig. 4.25a), as the heat energy conducted through the soil increases, the electrical conductivity of the electrolyte increases due to the increase in kinetic energy of molecules of water (Curado et al., 2013). This suggests that regions of less water content are characterized with less heat energy, thereby restraining the agitation of ions in soil. It has been reported that electrical conductivity increases by 2% for every degree rise in temperature (Friedman, 2005) and Corwin and Yemoto (2017) stated that electrical conductivity rises by 1.9% per degree centigrade.

A weak positive linear relation (0.153) existed between thermal conductivity and volumetric water content (Fig. 4.25b), this interaction agrees with the findings of previous worker (Brandon and Mitchell, 1989; van Lier and Durigon, 2012; Curado *et al.*, 2013; Rubio, 2015; Wardani and Purqon, 2016). Thermal conductivity increases with an increase in soil moisture because the pores space within the soil structure are filled with water which has higher thermal conductivity than the air. Barry-Macaulay *et al.* (2014) reported that the thermal conductivity of air was about 25 times lower than water and 100 times lower than soil minerals.

It was observed that the electrical conductivity of electrolyte in the soil unit increases with an increase in heat energy raising the temperature of the soil unit and a strong correlation coefficient of 0.538 was generated. Bai *et al.* (2013) examined the effect of temperature on electrical conductivity and reported that electrical conductivity increases as the temperature rises. Figure 4.26a showed direct relationship between volumetric heat capacity and the electrical conductivity, it could be extrapolated that rise in temperature tends to aid the agitation of ions within water body and a flow of electric current is generated. A strong positive correlation (0.513) exists between volumetric water content and volumetric heat capacity (Fig. 4.26b), indicating that as the moisture content increases, the heat energy required to achieve a degree rise in temperature also increases. This is consistent with the results of Oladunjoye *et al.* (2013), Abu-Hamdeh (2001) and, Shein and Mady (2016). Barry-Macaulay *et al.* (2014) stated the heat capacity of air, soil solid particles and water was 0.0012 mJ/m^3k, 2-2.5 mJ/m^3k, and 4.18 mJ/m^3k respectively. This implies that water saturated soil unit tends to have higher magnitude of heat capacity than the partially saturated soil body.

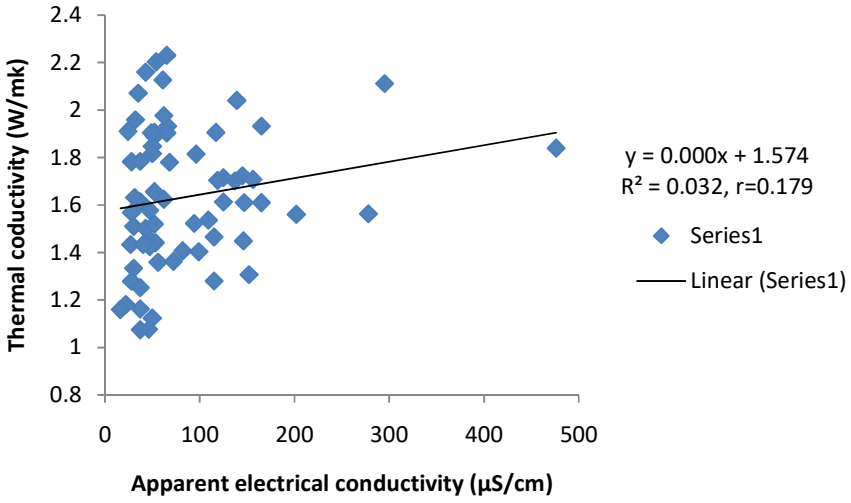

Figure 4.25a: Variation of thermal conductivity with apparent electrical conductivity in the kola farm during wet season

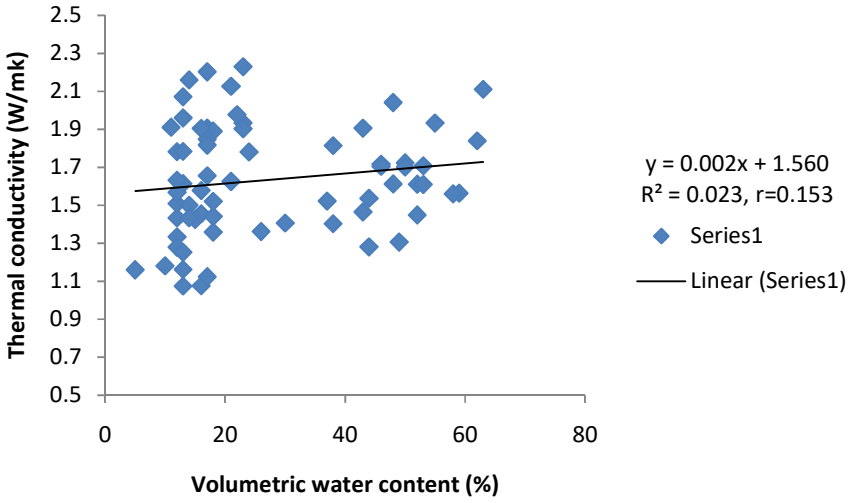

Figure 4.25b: Variation of thermal conductivity with volumetric water content in the kola farm during wet season

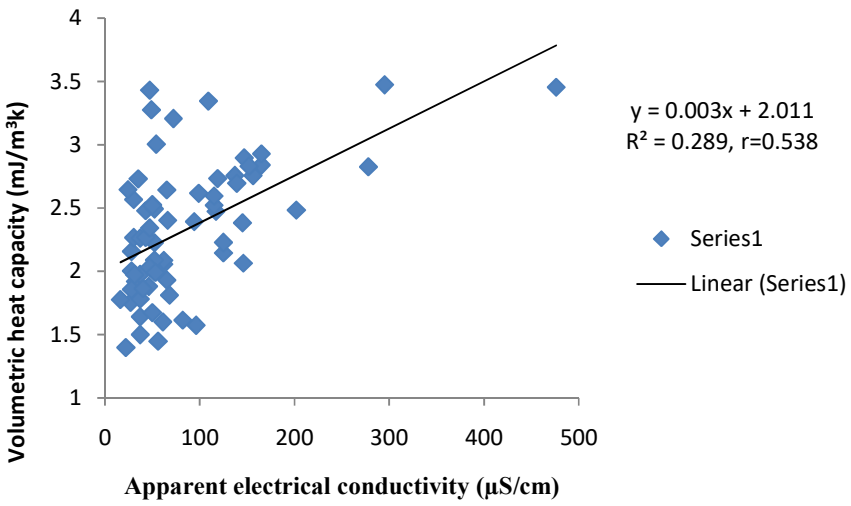

Figure 4.26a: Variation of volumetric heat capacity with apparent electrical conductivity in the kola farm during wet season

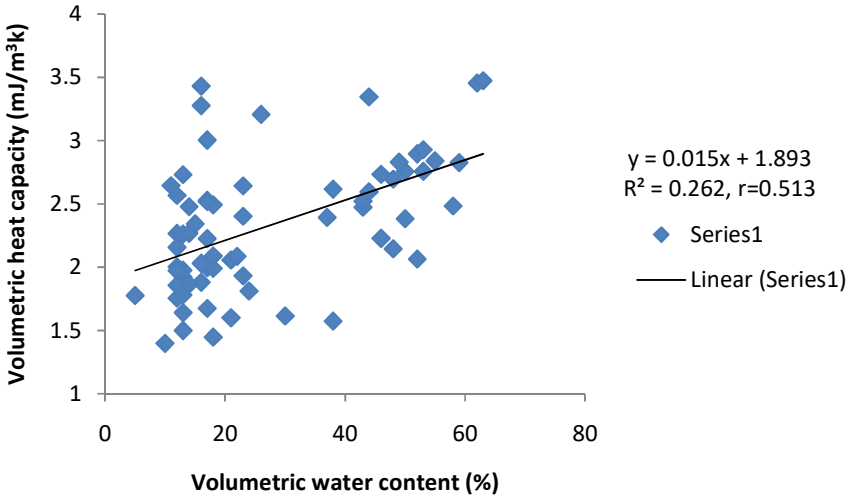

Figure 4.26b: Variation of volumetric heat capacity with volumetric water content in the kola farm during wet season

Thermal diffusivity recorded during wet season showed an inverse relationship with the electrical conductivity with a moderate coefficient of 0.328 (Fig. 4.27a). Regions of low thermal diffusion favoured electrical conductivity of the electrolyte within the soil unit due to a slower rate of attaining thermal equilibrium while heat energy is retained for longer period. Areas of high thermal diffusivity rapidly attain thermal equilibrium thus; it was characterized with less mobility of ions. Low thermal diffusivity occurs in the zones of abundant water saturation; Figure 4.27b showed that a moderate relationship (0.336) existed between diffusion rates of thermal energy with volumetric water content. This result is consistent with the deductions of Adeniyi *et al.* (2012) and van Lier and Durigon (2012) in which the higher the thermal diffusivity, the lower the moisture content.

Flow of heat energy across the soil in the kola farm during the dry season exhibited a positive correlation coefficient (0.172) with the electrical conductivity (Fig. 4.28a). Increase in thermal conductivity corresponds to an increase in electrical conductivity. Ionic mobility and EC vary with temperature as a result of effect of temperature on the viscosity of water (Moore *et al.,* 2008). A moderate positive (0.315) relationship occurred between thermal conductivity and volumetric water content in the dry period (Fig. 4.28b). As the soil moisture content increases the thermal conductivity also increase which is in agreement with the findings of Brandon and Mitchell (1989), Curado *et al.* (2013) and Rubio (2015) due to the fact that water has greater thermal conductivity than air. This suggests that the proportion of water to air in the voids space is higher in the region of high thermal conductivity and vice versa.

Thermal conductivity can be indirectly used to infer the soil particle size such that region of higher thermal conductivity has more of fine content than the low thermal conductivity section (Wang *et al.,* 2017).

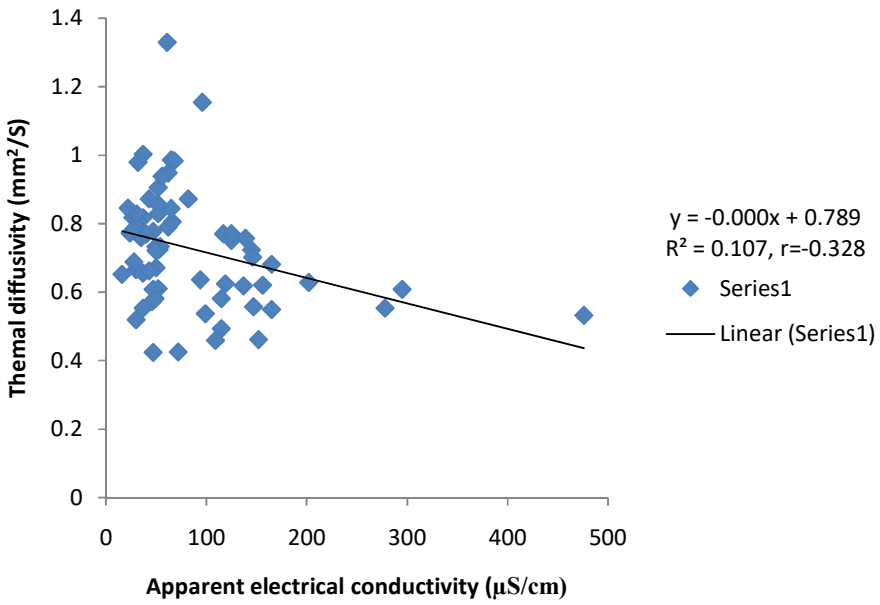

Figure 4.27a: Variation of thermal diffusivity with apparent electrical conductivity in the kola farm during wet season

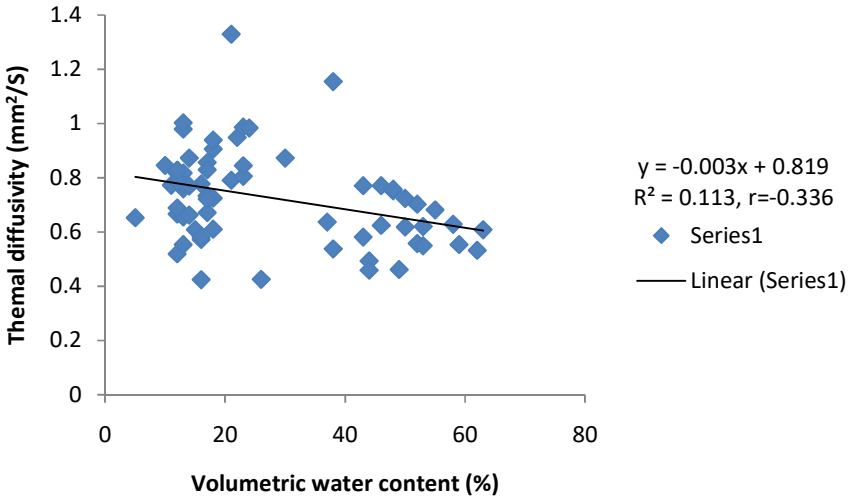

Figure 4.27b: Variation of thermal diffusivity with volumetric water content in the kola farm during wet season

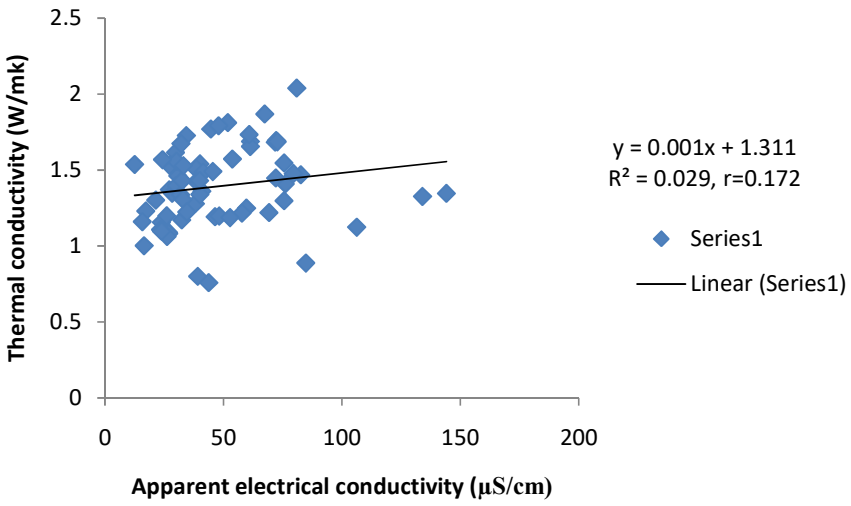

Figure 4.28a: Variation of thermal conductivity with apparent electrical conductivity in the kola farm during dry season

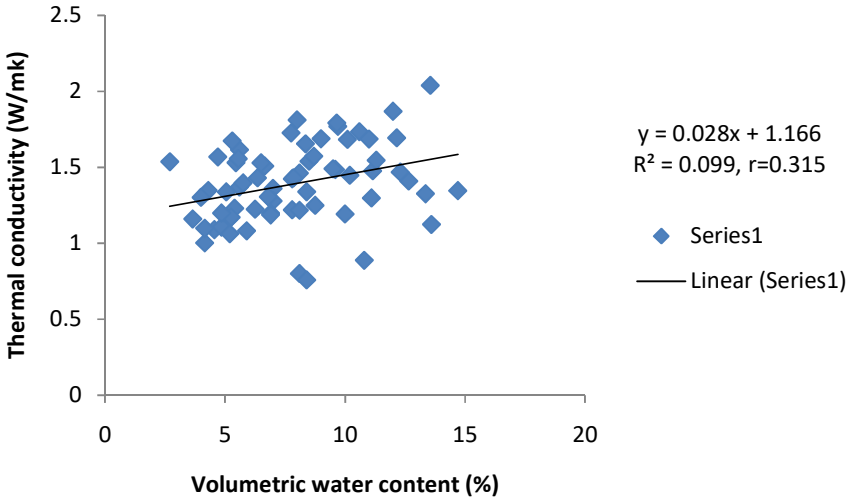

Figure 4.28b: Variation of thermal conductivity with volumetric water content in the kola during dry season

A weak positive correlation coefficient (0.127) was generated from the relationship between volumetric heat capacity and electrical conductivity (Fig. 4.29a). As the amount of heat energy required in raising the unit temperature increases, the electrical conductivity also increases, indicating that heat energy was made available to increase the mobility of ions in solution. Electrolytes conduct an electric current as a result of migration of ions under the influence of an electric field (Mäntynen, 2001).

Plot of volumetric heat capacity against the volumetric water content (Fig. 4.29b) indicates a weak positive correlation (0.228), this is consistent with the results of Kodesova *et al.,* (2013), Abu-Hamdeh (2001), Barry-Macaulay *et al.* (2014), Shein and Mady (2016) and Di Sipio and Bertermann (2018), in which the volumetric heat capacity increases with an increase in soil moisture content. Heat capacity of water is greater than that of the solid particles and air, thus water saturated soil tends to display higher volumetric heat capacity.

A very weak negative correlation (-0.015) existed between electrical conductivity and thermal diffusivity during the dry period, although the relationship was inverse suggesting that at low thermal diffusivity, there is an increase in the mobility of electrolytes (Fig. 4.30a). Relationship between thermal diffusivity and volumetric water content is a weak negative correlation (-0.056), the diffusion rate is higher at locations with low moisture content (Fig 4.30b). This agrees with the findings of previous workers (Adeniyi *et al.*, 2012; van Lier and Durigon, 2012) in which soil thermal diffusivity decreased with soil moisture content but increases with soil air content.

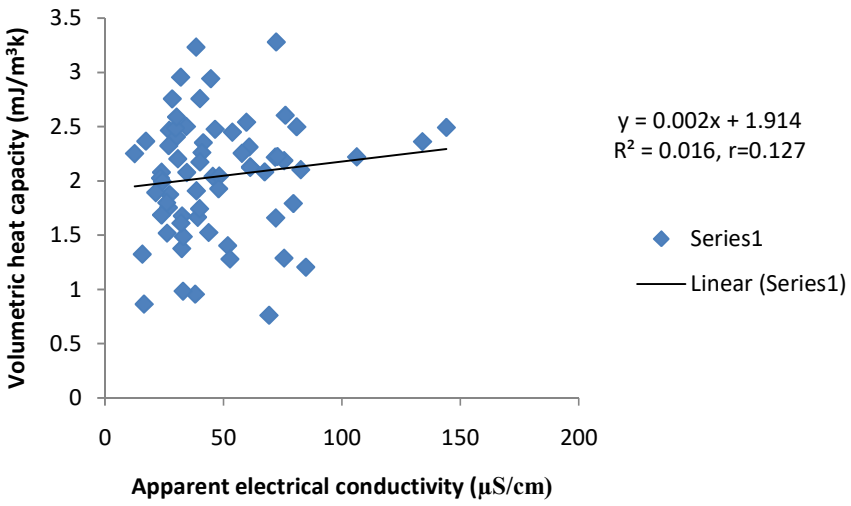

Figure 4.29a: Variation of volumetric heat capacity with apparent electrical conductivity in the kola farm during dry season

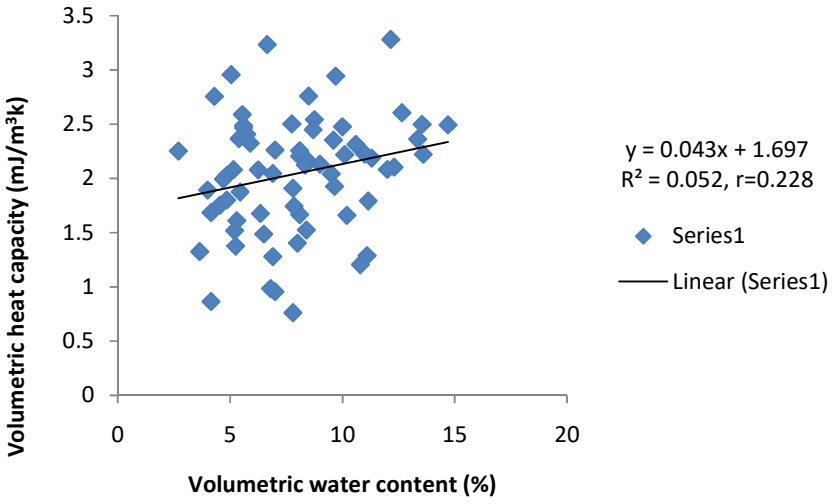

Figure 4.29b: Variation of volumetric heat capacity with volumetric water content in the kola farm during dry season

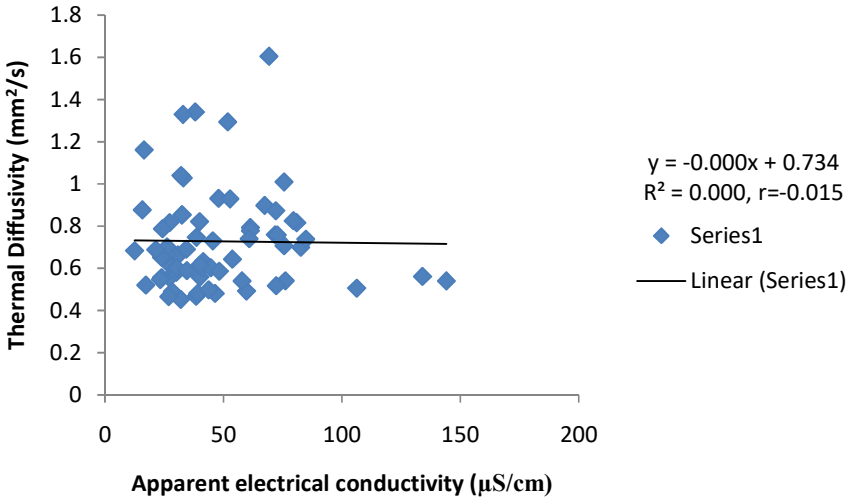

Figure 4.30a: Variation of thermal diffusivity with apparent electrical conductivity in the kola farm during dry season

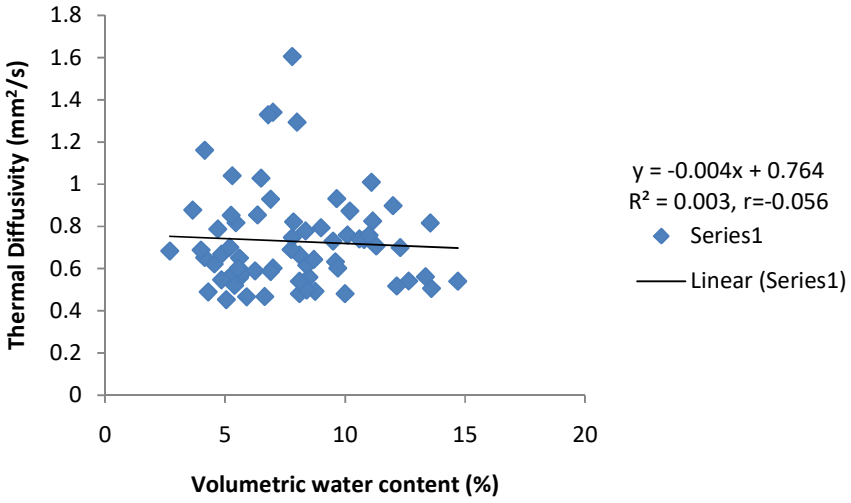

Figure 4.30b: Variation of thermal diffusivity with volumetric water content in the kola farm during dry season

The thermal measurement together with EC_a and VWC values from their respective thermal stations were used in the production thermal, EC_a and VWC maps in order to establish a comparison between them. EC_a was used in the comparison assessment due to the fact that regions of high EC_a correspond to high VWC and vice-versa. The maps (Fig. 4.31a-d) showed that zones with high EC_a are characterised with rising thermal conductivity, high volumetric heat capacity and low thermal diffusivity, although poor pictorial representation was noticed in thermal conductivity when placed side by side with EC_a map but better assessment was observed with the volumetric heat capacity and thermal diffusivity in cacao farm during rainy season.

A better juxtaposition was figured out between EC_a map and all thermal maps (Fig. 4.32a-d) but thermal conductivity map displayed better disposition with EC_a map in the cacao field during dry season. Therefore, krigged maps of the soil thermal properties showed the generalized distribution of flow of heat energy within the root zone, suggesting possible regions of high/low volumetric water contents together with areas of high/low electrical activities.

An effort was also made to relate the thermal maps with the EC_a map to view the pictorial variation. Thermal properties measured in the kola farm and their corresponding EC_a data were produced as maps in order to identify best-fit map with the EC_a map. During the rainy season, out of the three thermal maps (Fig. 4.33a-d), similar variation was noticed when comparing EC_a map with volumetric heat capacity and thermal diffusivity maps suggesting that areas of high EC_a are typified with high thermal energy required to heat up the unit volume of soil by a degree rise in temperature coupled with low diffusion rate of the stored energy. There was reduced variation when thermal conductivity was compared with the EC_a map as previously indicated by its correlation coefficient. Inverse appearance was noticed with respect to wet season during the dry period such that thermal conductivity map and EC_a map exhibit similar variation while volumetric heat capacity and thermal diffusivity maps were at variance (Fig. 4.34a-d).

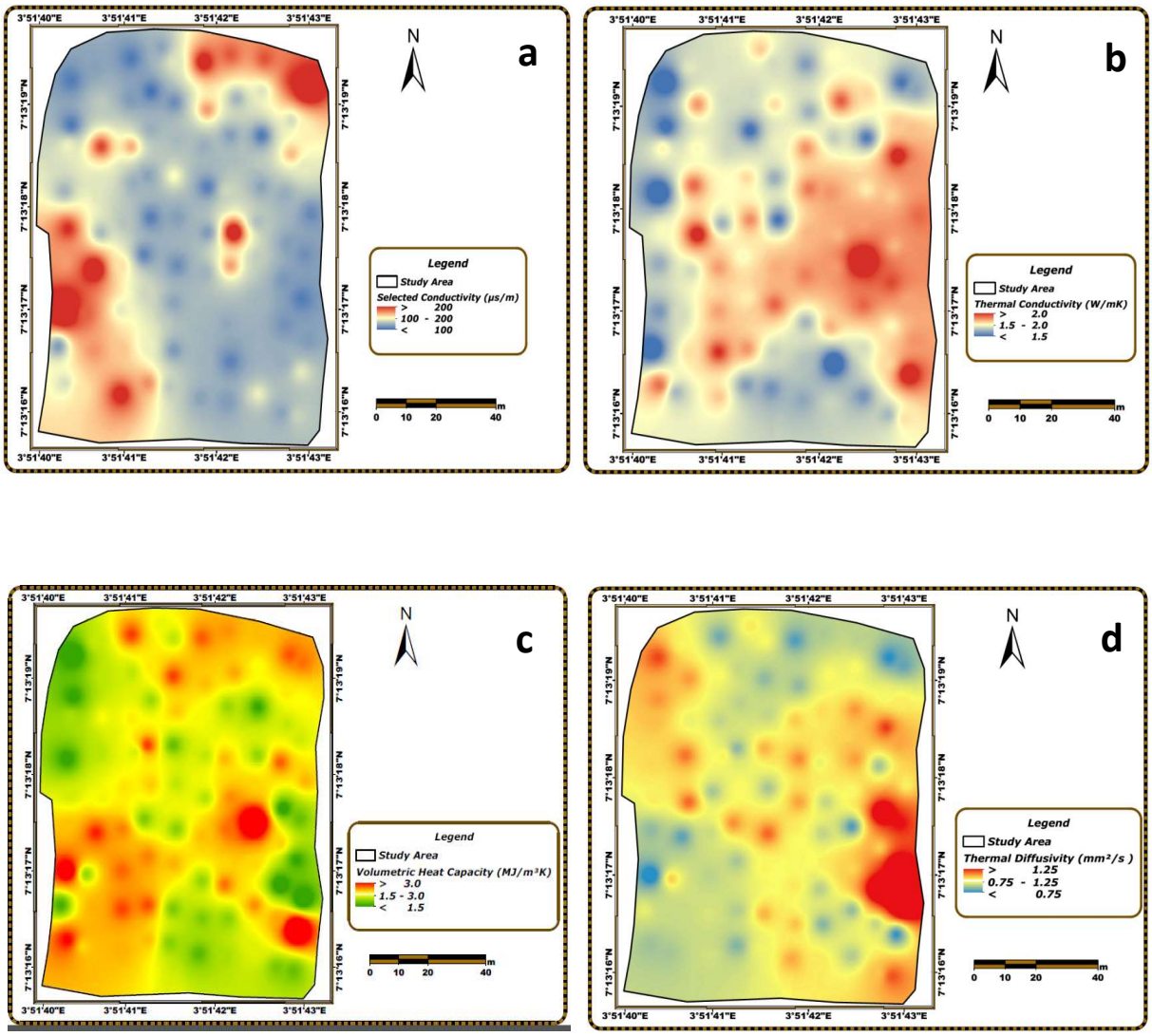

Figure 4.31: Krigged maps of thermal properties with their corresponding EC_a measured in the cacao field during wet season; **a**-EC_a map, **b**-thermal conductivity map, **c**-volumetric heat capacity map and **d**-thermal diffusivity map.

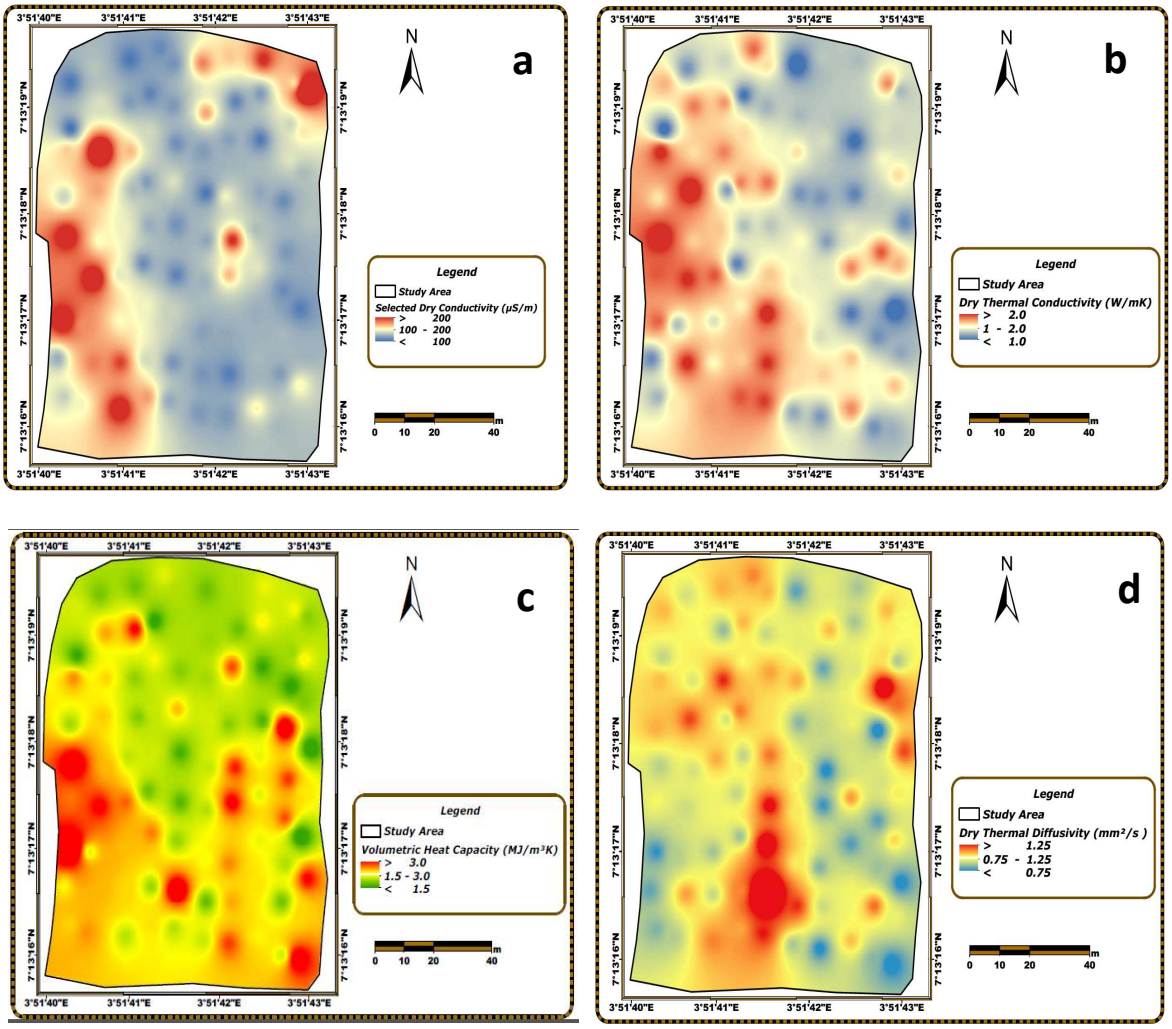

Figure 4.32: Krigged maps of thermal properties with their corresponding EC_a measured in the cacao field during dry season; **a**-EC_a map, **b**-thermal conductivity map, **c**-volumetric heat capacity map and **d**-thermal diffusivity map.

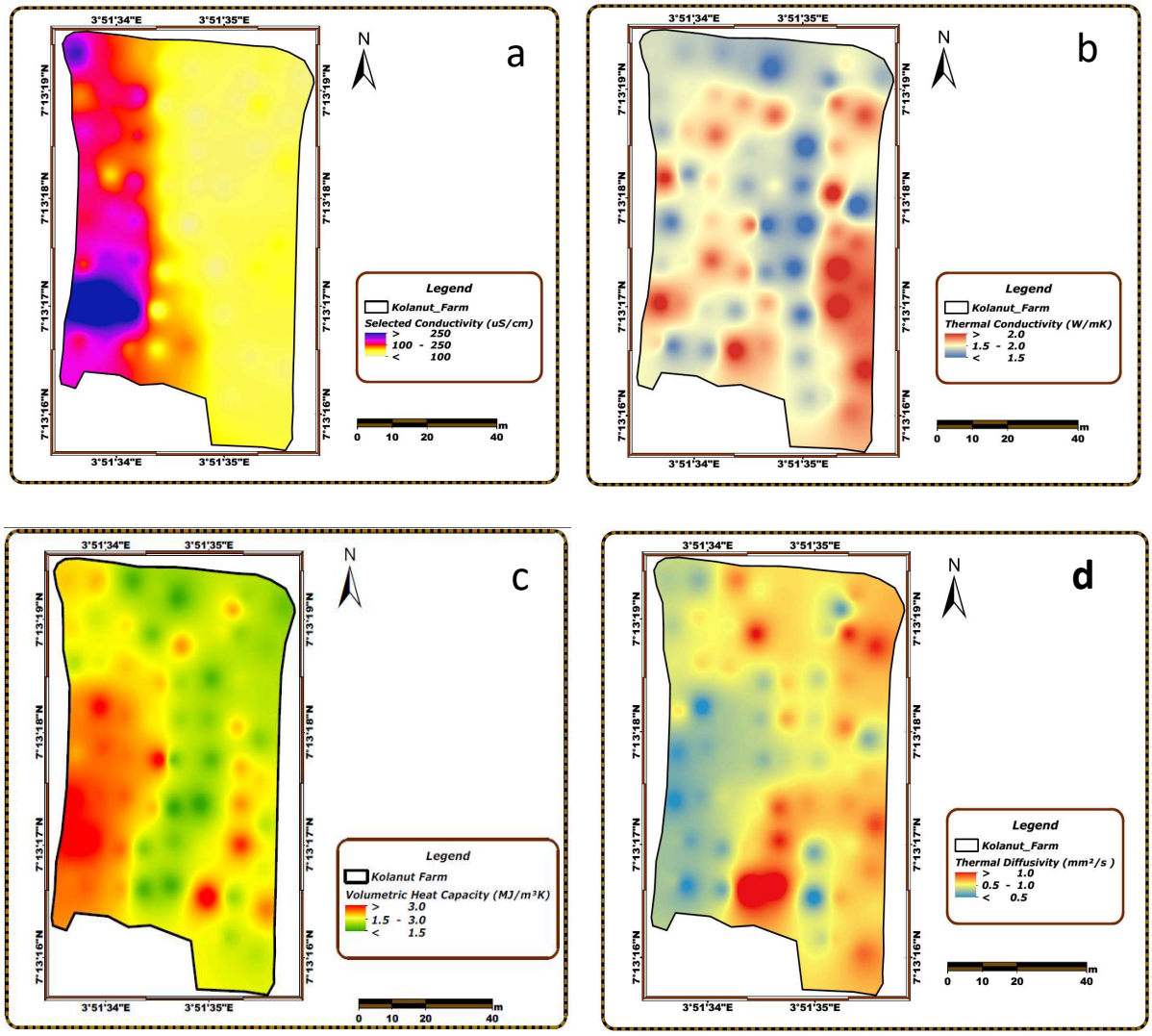

Figure 4.33: Kriged maps of thermal properties with their corresponding EC_a measured in kola field during wet season; **a**-EC_a map, **b**-thermal conductivity map, **c**- volumetric heat capacity map and **d**-thermal diffusivity map.

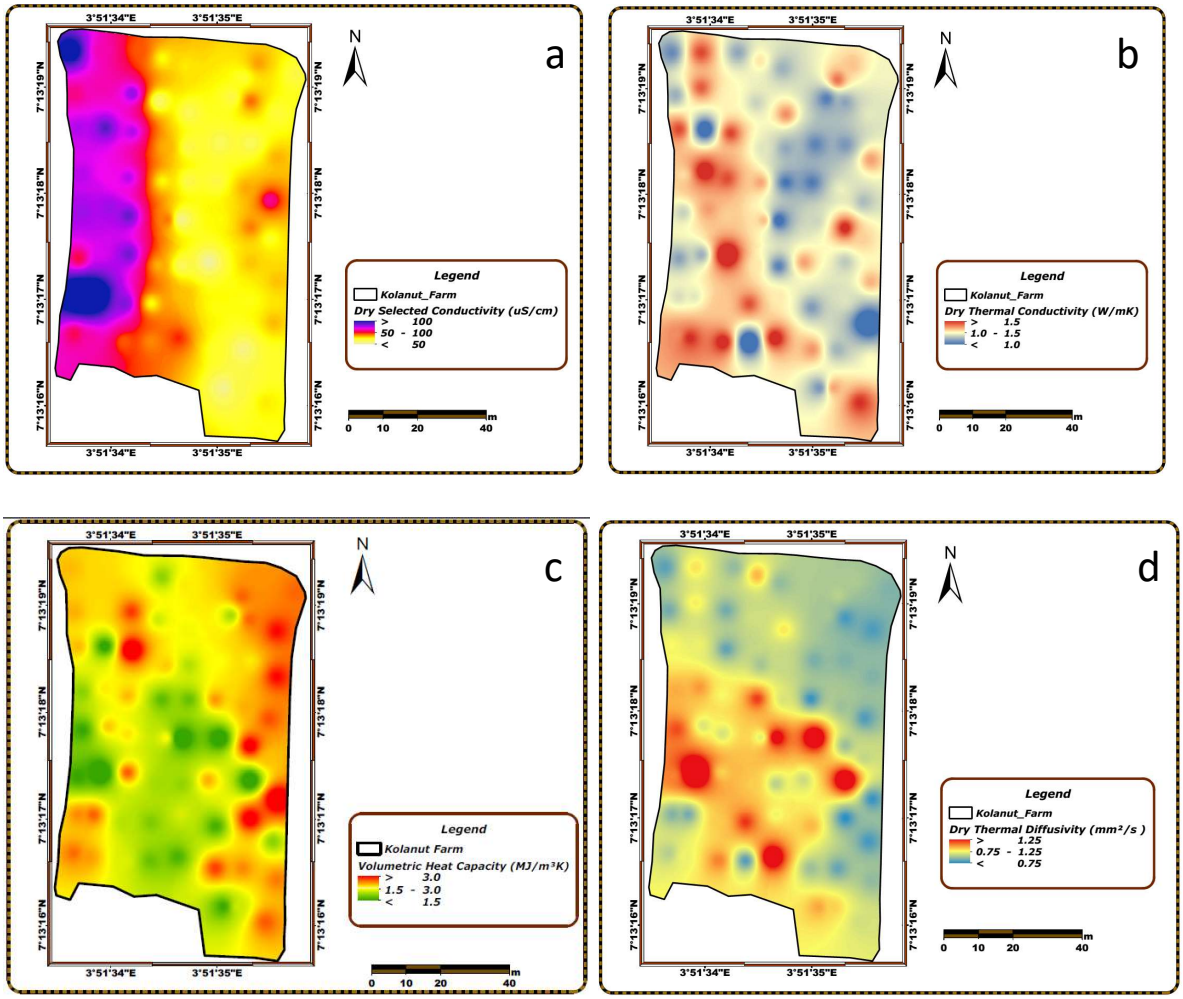

Figure 4.34: Krigged maps of thermal properties with their corresponding EC_a measured in kola field during dry season; **a**-EC_a map, **b**-thermal conductivity map, **c**-volumetric heat capacity map and **d**-thermal diffusivity map.

4.5 Permeability Assessment of Soils

There is need to assess the ease of flow of water in soils, so that water retention and its availability for plant uptake can be established. This view prompted selection of ten undisturbed soil samples taken at depth of 0.3 m in duplicates from the region of high, medium and low electrical conductivity at both farms, through the aid of ARCGIS generated electrical conductivity map.

4.5.1 Permeability Assessment of Soils in the Farms

It has been observed that electrical conductivity is not uniformly distributed within the cacao farm, some of the cacao trees in the region of high electrical conductivity yielded more cocoa pods than those situated within the medium while least pods were obtained from the trees around low conductive section. Two approaches were engaged involving falling head and constant head permeability techniques.

(i) **Cacao Farms**

Falling Head Permeability Assessment of Soils in the Cacao Farm

Table 4.10 showed the computations of falling head hydraulic conductivity performed on selected soil samples in cacao farm. Regions of high electrical conductivity exhibited low permeability ranging from 0.0000411 to 0.000657 cm/sec (sample number 1-3, 8 and 10). Section characterised with medium range electrical conductivity has its permeability to be 0.000654 cm/sec while segments of low electrical conductivity showed high permeability (0.000187-0.00397 cm/sec).

Table 4.11 showed a typical breakdown of hydraulic conductivity of already established soils, soils from high electrical conductivity section are characterized with permeability coefficient ranging between 0.0000411 cm/sec and 0.000657 cm/sec; and it was classified to be silty sand to silt (Terzaghi and Peck, 1967) with relative permeability signifying low hydraulic conductivity. For soil with 0.000654 cm/sec coefficient of permeability, it can be categorized to be silty sand and its relative permeability of this material was low. Soils of high permeability (0.000187-0.00397 cm/sec) have their permeability class varying between low and medium and soils within this category can be regarded to be fine sand/silty sand.

Table 4.10: Falling head permeability (k) coefficients of some selected soil samples from cacao farm

S/N	Coordinate	EC_a region	a (cm^2)	L (cm)	A (cm^2)	Δt (sec)	H_1 (cm)	H_2 (cm)	k (cm/sec)
1	$7^0$13′18.5″N $3^0$51′40.6″E	High	0.159	7	38.49	176	143	26	0.00028
2	$7^0$13′16.8″N $3^0$51′40.6″E	High	0.159	7	38.49	1200	143	26	$4.11x10^{-5}$
3	$7^0$13′16.2″N $3^0$51′41.1″E	High	0.159	7	38.49	384	143	26	0.000128
4	$7^0$13′17.7″N $3^0$51′41.6″E	Low	0.159	7	38.49	74	143	26	0.000666
5	$7^0$13′19.3″N $3^0$51′41.4″E	Low	0.159	7	38.49	263	143	26	0.000187
6	$7^0$13′16.4″N $3^0$51′41.9″E	Low	0.159	6.2	38.49	11	143	26	0.00397
7	$7^0$13′16.6″N $3^0$51′42.9″E	Medium	0.159	6.5	38.49	70	143	26	0.000654
8	$7^0$13′17.8″N $3^0$51′42.3″E	High	0.159	7	38.49	75	143	26	0.000657
9	$7^0$13′17.9″N $3^0$51′41.9″E	Low	0.159	6.8	38.49	112	143	26	0.000428
10	$7^0$13′19.0″N $3^0$51′43.0″E	High	0.159	7	38.49	450	143	26	0.00011

Table 4.11: Classification of soils according to their coefficients of permeability (After Terzaghi and Peck, 1967)

S/N	Relative Permeability	Typical Soil	Value of k (cm/s)
1	High	Coarse gravel	$> 10^{-1}$
2	Medium	Sand, fine sand	10^{-1} to 10^{-3}
3	Low	Silty sand, dirty sand	10^{-3} to 10^{-5}
4	Very Low	Silt, fine sandstone	10^{-5} to 10^{-7}
5	Practically impermeable	Clay	$<10^{-7}$

Constant Head Permeability Assessment of Soils in the Cacao Farm

The constant head permeability test (Table 4.12) performed on soils from the section of high EC_a showed that low permeability was observed within this section and it ranges from $5.56x10^{-5}$ to $1.67x10^{-4}$ cm/sec. Soil of moderate EC_a has its permeability to be 0.00128 cm/sec whereas the permeability ranges from $6.67x10^{-4}$ to $2.86x10^{-3}$ cm/sec in the low EC_a section.

An attempt was made to deduce the soil type from its permeability; Terzaghi and Peck (1967) classification (Table 4.11) was adopted for this purpose. Soils of high EC_a are characterized with low relative permeability ($5.56x10^{-5}$ to $1.67x10^{-4}$ cm/sec) are classified to be silty sand. Soil in the moderate EC_a segment was categorized to be sand/fine sand ($1.28x10^{-3}$ cm/sec) with a medium range relative permeability. Region of low EC_a has its soil types ranging from sand/fine sand to silty sand with a low to medium range relative permeability.

Soil Permeability and Infiltration Rate in the Cacao Plot

Scherer *et al*. (2013) established the infiltration rate of soil as the amount of rain or irrigation water that is absorbed by the soil over a given time. The authors classified the soil permeability based on its infiltration rate (Table 4.13).

Falling head permeability test was performed on soils from region of high, medium and low EC; in high EC_a section the permeability ranges from 0.0000411 cm/sec to 0.000657 cm/sec which can be categorized as very slow/slow/moderately slow/moderate (very slow – moderately slow). Permeability of 0.000654 cm/sec obtained from soil in medium class electrical conductivity was suggestive of moderate infiltration rate while soils (0.000187-0.00397 cm/sec) in electrically less conductive section were classified to range from moderate slow to moderately rapid infiltration.

Table 4.12: Constant head permeability (k) coefficients of some selected soil samples from cacao farm

S/N	Coordinates		EC_a of sample selection point	k_{sat} (cm/sec)
	Northing	Easting		
1	$7^0$13′18.5″N	$3^0$51′40.6″E	High	$8.33x10^{-5}$
2	$7^0$13′16.8″N	$3^0$51′40.6″E	High	$8.33x10^{-5}$
3	$7^0$13′16.2″N	$3^0$51′41.1″E	High	$5.56x10^{-5}$
4	$7^0$13′17.7″N	$3^0$51′41.6″E	Low	$6.67x10^{-4}$
5	$7^0$13′19.3″N	$3^0$51′41.4″E	Low	$1.61x10^{-3}$
6	$7^0$13′16.4″N	$3^0$51′41.9″E	Low	$2.86x10^{-3}$
7	$7^0$13′16.6″N	$3^0$51′42.9″E	Medium	$1.28x10^{-3}$
8	$7^0$13′17.8″N	$3^0$51′42.3″E	High	$1.11x10^{-4}$
9	$7^0$13′17.9″N	$3^0$51′41.9″E	Low	$7.50x10^{-4}$
10	$7^0$13′19.0″N	$3^0$51′43.0″E	High	$1.67x10^{-4}$

Table 4.13: Classification of soil moisture infiltration rate (Modified after Scherer *et al*., 2013)

S/N	Classification	Infiltration Rate (inches/hour)	Infiltration Rate (cm/s)
1	Very slow	less than 0.06	$< 4.233 \times 10^{-5}$
2	Slow	0.06 to 0.2	4.233×10^{-5} to 1.411×10^{-4}
3	Moderately slow	0.2 to 0.6	1.411×10^{-4} to 4.233×10^{-4}
4	Moderate	0.6 to 2.0	4.233×10^{-4} to 1.411×10^{-3}
5	Moderately rapid	2.0 to 6.0	1.411×10^{-3} to 4.233×10^{-3}
6	Rapid	6.0 to 20.0	4.233×10^{-3} to 1.411×10^{-2}
7	Very rapid	greater than 20.0	$> 1.411 \times 10^{-2}$

The numerical value of the constant head permeability test conducted on soils in the region of high EC suggests that rate at which water moves through soil unit ranges from moderately slow to slow ($5.56x10^{-5}$ to $1.67x10^{-4}$ cm/sec) whereas the rate of water movement in the region of moderate EC indicates moderate infiltration (1.28 $x10^{-3}$ cm/sec). Soil materials in the low EC segment suggest moderate to moderately rapid infiltration rate ($6.67x10^{-4}$ to $2.86x10^{-3}$ cm/sec). Strong correlation (0.819) exists between the permeability values obtained from the two approaches engaged in the conduct of the permeability test (Fig. 4.35). On the basis of the permeability data calculated from the two approaches engaged in the analysis, both approaches suggest similar textural content in seven out of the ten samples analyzed.

The techniques classified soils of high EC_a section to be silty sand except sample in s/n 2 in which was reported as silt (falling head) and silty sand (constant head), while in the medium EC_a segment, they suggest varying texture; sand/fine sand (constant head) and silty sand (falling head). Values obtained from soils in low EC_a section indicate textural composition of fine sand to silty sand content by both techniques, although similar textures were recorded by both technique on each of the samples but a varying composition was recorded in sample with s/n 5 in which was reported as sand/fine sand (constant head) and as silty sand (falling head).

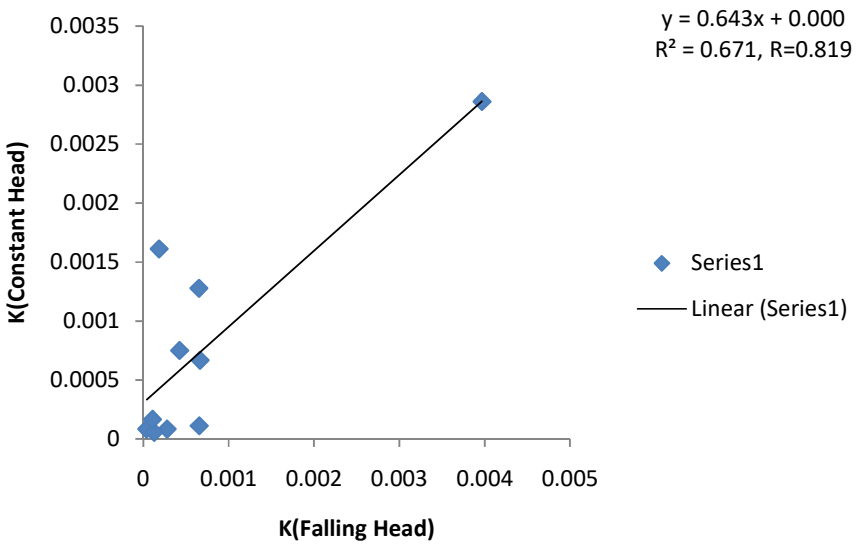

Figure 4.35: Degree of relationship between the falling and constant head permeability data on some soil samples in the cacao farm.

(ii) **Kola Farm**

Permeability Assessment of Soils in the Kola Farm

It has been observed that some of the kola trees were characterized with stunted growth while some were flourishing within the plot. Electrical conductivity map aided in classifying the plot into zones/regions of high, medium and low electrical conductivity. Areas of high electrical conductivity are characterized with high volumetric water content (VWC), also regions of medium and low EC_a have medium and low VWC respectively. Kola nut crops planted on high conductivity section exhibited steady/rapid growth; plant growth is gradual in the medium section while stunted/redundant growth was associated with kola trees in low conductivity segment. Water is an essential fluid that aid plants growth and it is not uniformly distributed within this farm. There is need to conduct permeability on some soil materials to ascertain the capacity of the soils to retain moist.

Falling Head Permeability Assessment of Soils in the Kola Farm

A total of ten soil samples were taken at root zone (0.3 m) from sections of high, medium and low EC_a (Table 4.14). The result of the permeability coefficients of soils shows that those soil samples from region of high EC_a are characterized with low permeability ($6.2x10^{-6}$ to $6.66x10^{-4}$ cm/sec), soil in medium range EC_a has 0.000398 cm/sec while those from low EC_a section exhibited high permeability and it ranges from 0.00034 to 0.000836 cm/sec in this segment.

In an attempt to deduce its soil types, Terzaghi and Peck (1967) permeability classification (Table 4.11) was adopted to delineate the possible soil type. Soils of low permeability (0.0000062 to 0.000666 cm/sec) are classified to be silty sand to silty whereas it is silty sand in the moderate EC region (0.000398 cm/sec). Highly permeable soils (0.00034 to 0.000836 cm/sec) in kola farm are regarded to have textural feature of silty sand.

Table 4.14: Falling head permeability (k) coefficients of some selected soil samples from kola plot

S/N	Coordinate	ECa region	a (cm^2)	L (cm)	A (cm^2)	Δt (sec)	H_1 (cm)	H_2 (cm)	k (cm/sec)
1	$7^0$13′15.9″N $3^0$51′35.4″E	High	0.159	7	38.49	488	143	26	0.000101
2	$7^0$13′16.6″N $3^0$51′35.1″E	Low	0.159	7	38.49	59	143	26	0.000836
3	$7^0$13′17.6″N $3^0$51′35.4″E	High	0.159	7	38.49	74	143	26	0.000666
4	$7^0$13′18.4″N $3^0$51′35.3″E	Low	0.159	7	38.49	145	143	26	0.00034
5	$7^0$13′19.0″N $3^0$51′35.4″E	Medium	0.159	7	38.49	124	143	26	0.000398
6	$7^0$13′18.1″N $3^0$51′34.7″E	Low	0.159	7	38.49	126	143	26	0.000391
7	$7^0$13′16.4″N $3^0$51′34.2″E	High	0.159	6.8	38.49	3540	143	26	$1.35x10^{-5}$
8	$7^0$13′17.0″N $3^0$51′33.8″E	High	0.159	7	38.49	7950	143	26	$6.2x10^{-6}$
9	$7^0$13′17.9″N $3^0$51′34.0″E	High	0.159	7	38.49	4356	143	26	$1.13x10^{-5}$
10	$7^0$13′19.3″N $3^0$51′33.6″E	High	0.159	6.8	38.49	2420	143	26	$1.98x10^{-5}$

These soils have varying rate at which recharge (rain water) percolates, Scherer *et al.* (2013) classified permeability with respect to infiltration rate (Table 4.13). Infiltration rate in soils of low permeability could be ranked as moderate to very slow; soil of medium permeability (0.000398 cm/sec) is suggestive of moderately slow rate of infiltration while rate of infiltration for soils of 0.00034 to 0.000836 cm/sec is moderate to moderately slow. Thus, it safe to adduce that the soils from kola plot have varying water retention capability and soils of moderate to moderately slow infiltration rate has lesser water and nutrient retention capacity than low permeable soils (Nyugen and Marschner, 2013 and Scherer *et al.*, 2013). Kola trees planted in soil section characterized with moderate to moderately slow infiltration rate are known with stunted growth whereas steady growth was observed at zones of moderate to very slow infiltration rate.

Constant Head Permeability Assessment of Soils in the Kola Farm

The permeability coefficients were segregated according to regions of high, medium and low EC_a; it ranges from $8.33x10^{-5}$ cm/sec to $8.06x10^{-4}$ cm/sec in high EC_a section, region of medium range EC_a has its permeability to be $3.06x10^{-4}$ cm/sec while a range of $8.89x10^{-4}$ cm/sec to $9.44x10^{-4}$ cm/sec was noticed in the low EC_a segment (Table 4.15). Terzaghi and Peck (1967) permeability soil's classification scheme (Table 4.11) was used in predicting the likely soil material the kola farm is composed. Relatively low permeability observed in the region of high EC_a ($8.33x10^{-5}$ cm/sec to $8.06x10^{-4}$ cm/sec) was suggestive of silty sand materials. Similar textural compositions (silty sand) were also deduced in the moderate and low EC_a sections.

Based on its soil type, nearly a uniform soil material has been established from the permeability coefficients of soils in the kola farm using but there is need to determine the rate at which the water percolates through these media. Scherer *et al.* (2013) infiltration rate classification was adopted in establishing the rate of water percolation. Soils of low permeability ($8.33x10^{-5}$ cm/sec to $8.06x10^{-4}$ cm/sec) are classified to have moderate to very slow infiltration rate; soil in the moderate EC_a section has moderately slow infiltration rate ($3.06x10^{-4}$ cm/sec) while low EC_a segment has soils with moderate rate of infiltration.

Table 4.15: Constant head permeability (k) coefficients of some selected soil samples from kola farm

S/N	Coordinate		EC_a of sample selection point	k_{sat} (cm/sec)
	Northing	Easting		
1	$7^0$13′15.9″N	$3^0$51′35.4″E	High	$2.78x10^{-5}$
2	$7^0$13′16.6″N	$3^0$51′35.1″E	Low	0.000889
3	$7^0$13′17.6″N	$3^0$51′35.4″E	High	0.000806
4	$7^0$13′18.4″N	$3^0$51′35.3″E	Low	0.000917
5	$7^0$13′19.0″N	$3^0$51′35.4″E	Medium	0.000306
6	$7^0$13′18.1″N	$3^0$51′34.7″E	Low	0.000944
7	$7^0$13′16.4″N	$3^0$51′34.2″E	High	0.000111
8	$7^0$13′17.0″N	$3^0$51′33.8″E	High	$2.78x10^{-5}$
9	$7^0$13′17.9″N	$3^0$51′34.0″E	High	0.000139
10	$7^0$13′19.3″N	$3^0$51′33.6″E	High	$8.33x10^{-5}$

Comparing the rate at which water percolates through the soils in the various EC_a segments, it could be established that soils of low permeability have tendency to retain soil moisture over time than those from medium and low EC_a section. Soil nutrients are made available for plant consumption in solution, soils of low permeability have the affinity to retain moist and also prevent leaching of nutrients in it (Nyugen and Marschner, 2013 and Scherer *et al.*, 2013). Since soils of high permeability are characterized with moderate infiltration, then there is tendency for them to be susceptible to nutrient leaching and less water retention relative to those of high and medium EC_a in which its infiltration rate ranges from moderately slow to very slow. Therefore, kola nut trees grown on this plot were subjected to varying water content and nutrient availability which was responsible for non-uniform rate of development noticed on this farm.

Strong correlation (0.83) occurred between the permeability coefficients calculated from both techniques (Fig. 4.36) with 68.2 % of these variables could be represented linearly. The techniques classified eight out of the ten samples analysed to be silty sand while the most electrically conductive unit (545 μS/cm) was categorized to be either silty sand (constant head permeability) or silty sand to silt (falling head permeability) horizon.

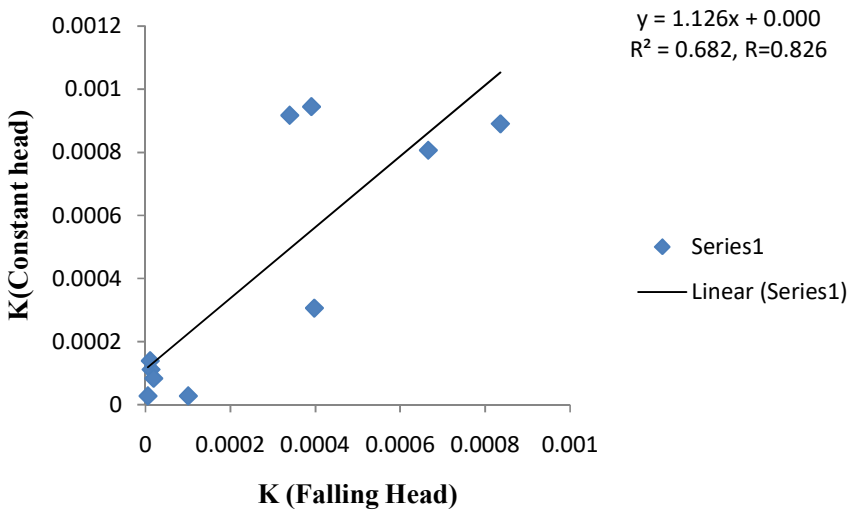

Figure 4.36: Degree of relationship between the falling and constant head permeability data on some soil samples in the kola farm.

4.5.2 Correlation Analysis between Permeability (k) Coefficients and EC_a/VWC of Soils in the Farms

(i) **Cacao Farm**

The data used in analyzing coefficient of determination (R^2) and correlation coefficient are presented in table 4.16.

Falling head permeability: Coefficient of determination (R^2) of permeability versus electrical conductivity in the wet season (Fig. 4.37a) was 0.139 which suggests 13.9 % of permeability (k) and electrical conductivity (EC_a) variables correlate, negative correlation indicates that as permeability increases, the electrical conductivity decreases. Figure 4.37b shows that the coefficient of determination R^2 is 0.148 indicating 14.8 % of the total variation in k can be expressed by the linear relationship between k and VWC. Relationship between these two parameters shows that as VWC increases, permeability decreases.

Similar trend was also displayed during the dry season (Fig. 4.38a), 14.3 % (R^2) in variation of k can be expressed by direct relationship between k and EC_a, negative correlation exists between these variables. Coefficient of determination (R^2) was 13.2 % (Fig. 4.38b) and negative correlation also exists between k and VWC in the dry period. It can be concluded that the coefficient of determination (R^2) obtained from these variables in the wet and dry season has close numerical values and correlation coefficients (r) ranged from 0.363 to 0.385 (moderate). It can be deduced from the correlation analyses that soils of high electrical conductivity and high VWC have low permeability and vice versa.

Constant head permeability: A plot of permeability coefficients with electrical conductivity (Fig. 4.39a) shows that its determination coefficient is 0.460 in which 46.0% of the variables can be related linearly and also exhibits a strong negative correlation coefficient (0.68) in the wet season. Relationship between permeability and VWC (Fig. 4.39b) in the wet season reveals that 51.2 % of these variables have linear representation from its coefficient of determination; it's also characterized with a strong negative correlation coefficient (-0.72).

Degree of interaction between the EC and permeability coefficient (k) data in the dry period (Fig. 4.40a) indicates 50.1 % of these variables have linear dependence as suggested by the determination coefficient while a negatively strong correlation

Table 4.16: Soil permeability and seasonal variation in electrical conductivity and VWC of the cacao plot

S/N	Permeability 'k' (cm/sec)		Wet Season		Dry Season	
	Falling Head	Constant Head	EC_a (µS/cm)	VWC (%)	EC_a (µS/cm)	VWC (%)
1	0.00028	$8.33x10^{-5}$	133	50	112	19
2	$4.11x10^{-5}$	$8.33x10^{-5}$	159	55	89	17
3	0.000128	$5.56x10^{-5}$	118	46	81	13
4	0.000666	0.000667	23	11	20	9
5	0.000187	0.001611	40	14	15	5
6	0.00397	0.002861	49	18	30	8
7	0.000654	0.001278	51	18	36	10
8	0.000657	0.000111	114	46	85	11
9	0.000428	0.00075	48	17	26	9
10	0.00011	0.000167	136	52	103	14

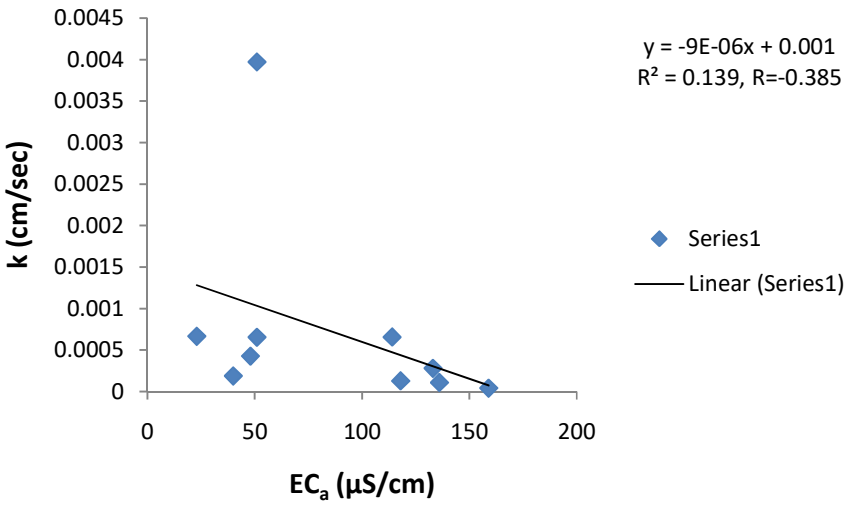

Figure 4.37a: Plot of permeability (FHP) versus apparent electrical conductivity in the cacao farm during the wet season.

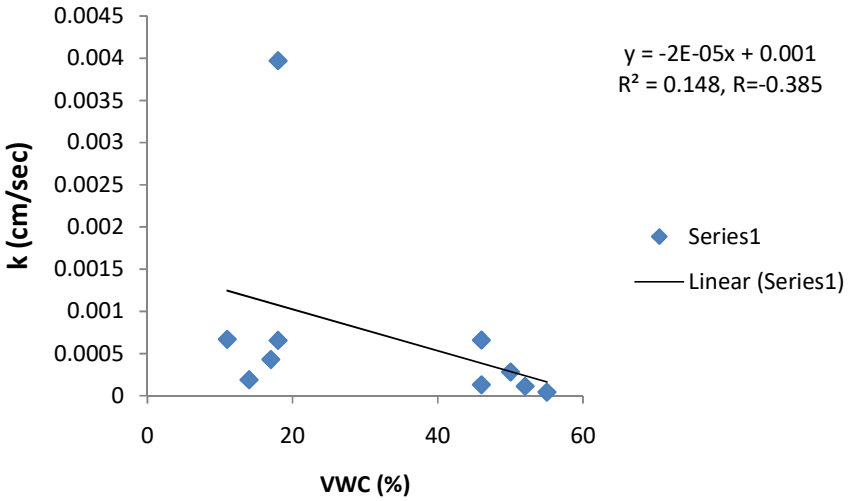

Figure 4.37b: Plot of permeability (FHP) versus VWC in the cacao farm during the wet season.

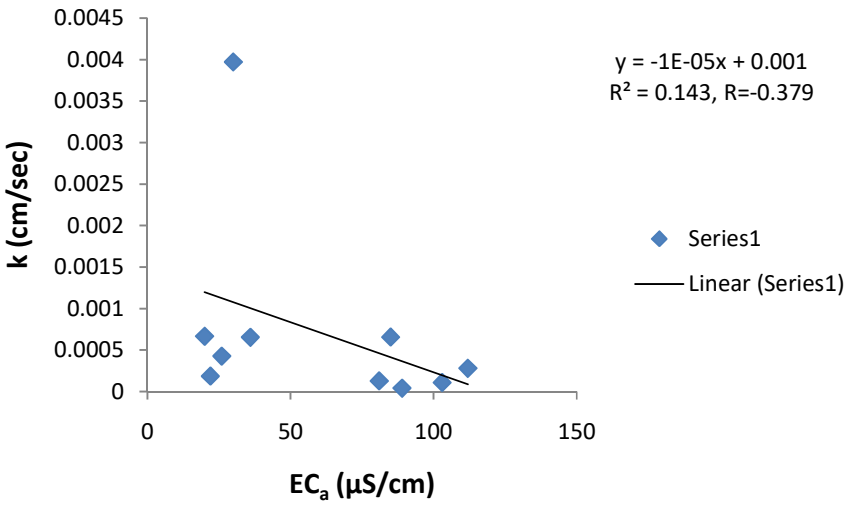

Figure 4.38a: Plot of permeability (FHP) versus apparent electrical conductivity in the cacao farm during the dry season.

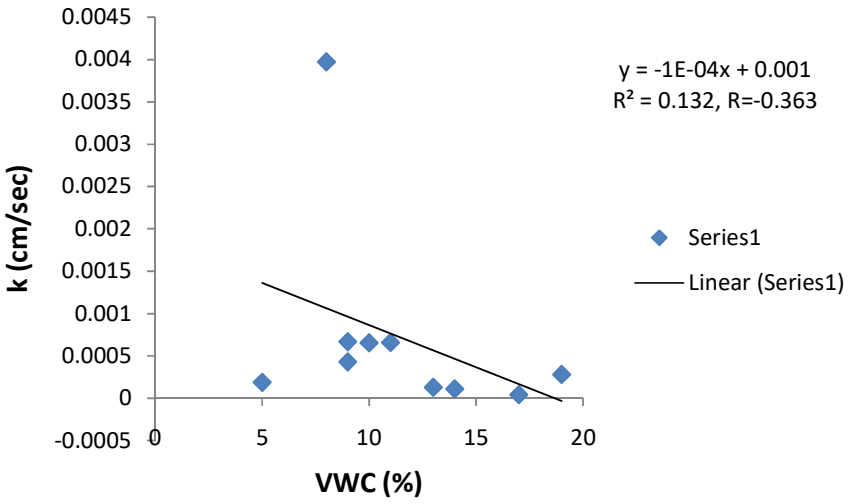

Figure 4.38b: Plot of permeability (FHP) versus VWC in the cacao farm during the dry season

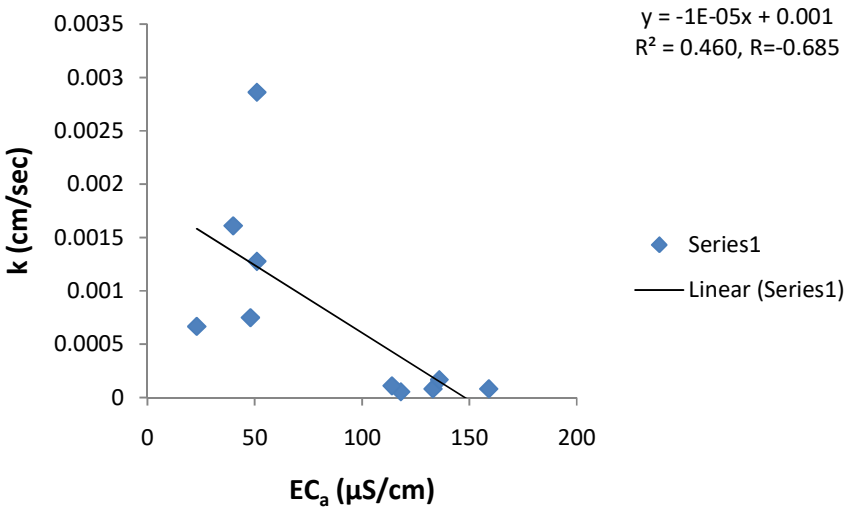

Figure 4.39a: Plot of permeability (CHP) versus EC_a in the cacao farm during the wet season

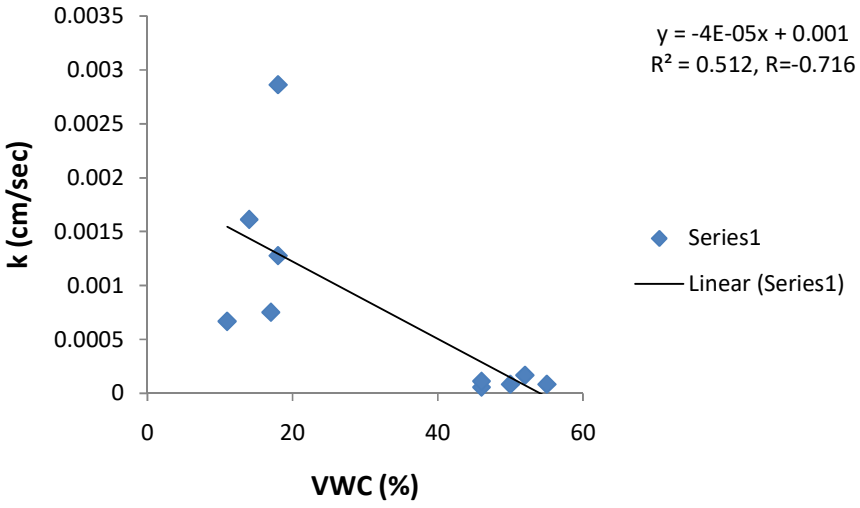

Figure 4.39b: Plot of permeability (CHP) versus VWC in the cacao farm during the wet season

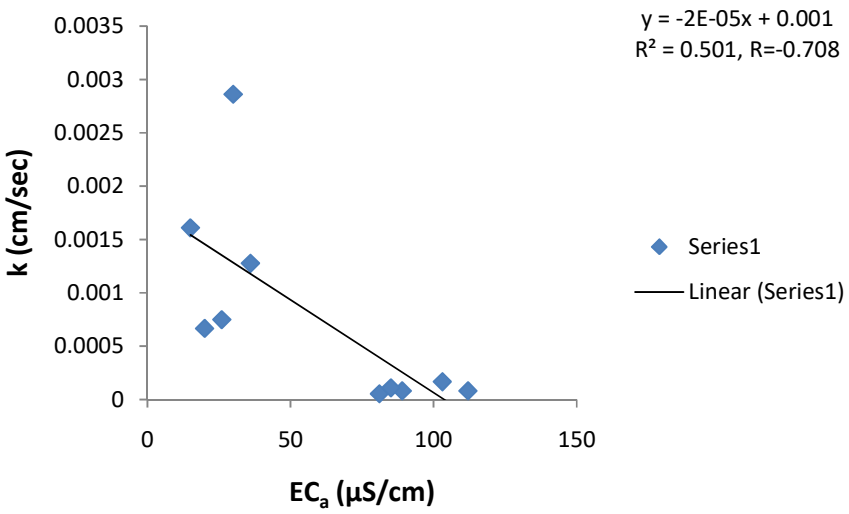

Figure 4.40a: Plot of permeability (CHP) versus EC_a in the cacao farm during the dry season

coefficient (-0.71) was observed. Examining the relationship between the permeability coefficients with the VWC data (Fig. 4.40b) in the dry period, it reveals that a strong negative correlation coefficient (-0.69) exists between these variables and 47.6 % of these variables are linearly related.

It was observed that a better precision was obtained from the permeability coefficients extracted from constant head permeability than falling head permeability technique due to higher values of determination coefficient (0.460 to 0.512) and a strong correlation coefficients (-0.68 to -0.72) compare to a moderate correlation coefficients (-0.36 to -0.39) and less relationship between the variables (0.132 to 0.148) in the falling head permeability with the electrical conductivity and volumetric water content. Fagbenro and Woma (2013) reported positive correlation from the plot of electrical resistivity with hydraulic conductivity. Although the two techniques used in evaluating the soils permeability agreed clearly that area of high EC/VWC are characterized with low permeability at both seasons and vice versa.

(ii) **Kola Farm**

In order to establish the relationship between permeability and electrical conductivity/volumetric water content (EC_a/VWC) at kola farm, data presented in Table 4.17 was used in the conduct of the analysis.

Falling head technique

Relationship between electrical conductivity and permeability is a moderate negative correlation (-0.63) which implies that increase in EC_a of soil was associated with decreasing k (Fig. 4.41a). Coefficient of determination (R^2) is 0.393 suggesting 39.3 % of k is predictable from variation in EC_a. As VWC increases, the permeability 'k' reduces (Fig. 4.41b) and a strong negative correlation (-0.721) was observed between these variables. Determination coefficient (R^2) indicated that 52.0 % of k correlates with VWC. A strong negative correlation (-0.733) was noticed between k and EC_a in the dry season (Fig. 4.42a). Coefficient of determination showed that 53.7 % of the entire variation in k is predictable by the linear relationship between k and EC_a. Correlation between k and VWC (Fig. 4.42b) showed that R^2 is 54.0 % and a strong negative coefficient (-0.735) existed between these variables. The deduction is that electrically conductive soil is less permeable while less conductive soil unit has higher permeability and soils of low permeability have more water retention than those of high permeability within the kola plot.

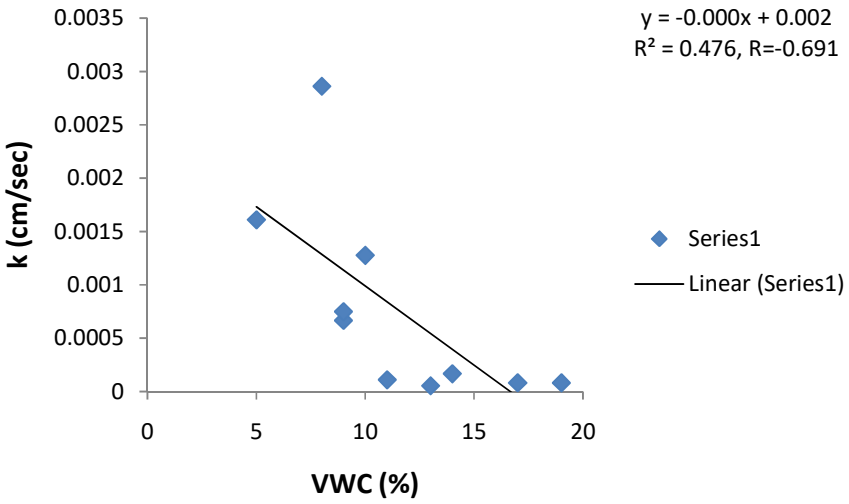

Figure 4.40b: Plot of permeability (CHP) versus VWC in the cacao farm during the dry season

Table 4.17: Soil permeability and seasonal variation in electrical conductivity and VWC of the kola plot

S/N	Permeability 'k' (cm/sec)		Wet Season		Dry Season	
	Falling Head	Constant Head	EC_a (µS/cm)	VWC (%)	EC_a (µS/cm)	VWC (%)
1	0.000101	$2.78x10^{-5}$	269	62	60	11
2	0.000836	0.000889	23	10	19	4
3	0.000666	0.000806	123	45	69	10
4	0.00034	0.000917	32	13	23	6
5	0.000398	0.000306	71	25	52	9
6	0.000391	0.000944	20	9	15	3
7	$1.35x10^{-5}$	0.000111	145	50	103	12
8	$6.2x10^{-6}$	$2.78x10^{-5}$	545	61	99	13
9	$1.13x10^{-5}$	0.000139	209	58	102	12
10	$1.98x10^{-5}$	$8.33x10^{-5}$	202	58	106	14

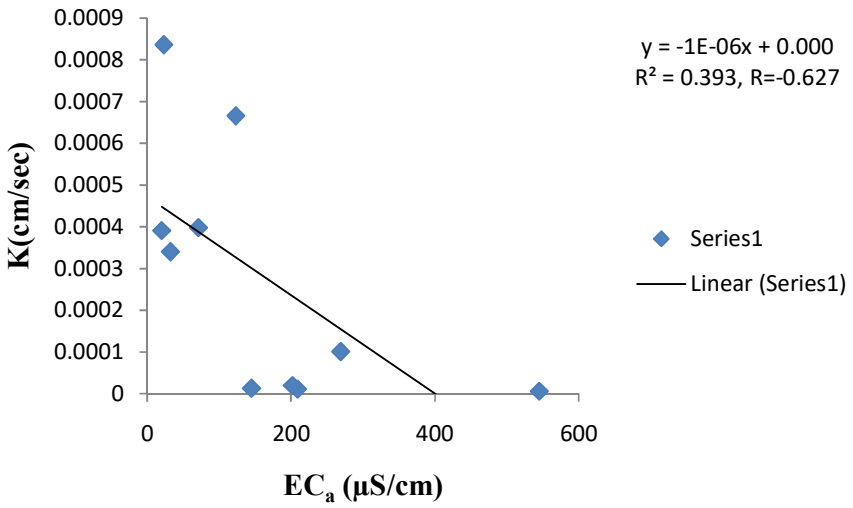

Figure 4.41a: Plot of permeability (FHP) versus EC_a in the kola farm during the wet season

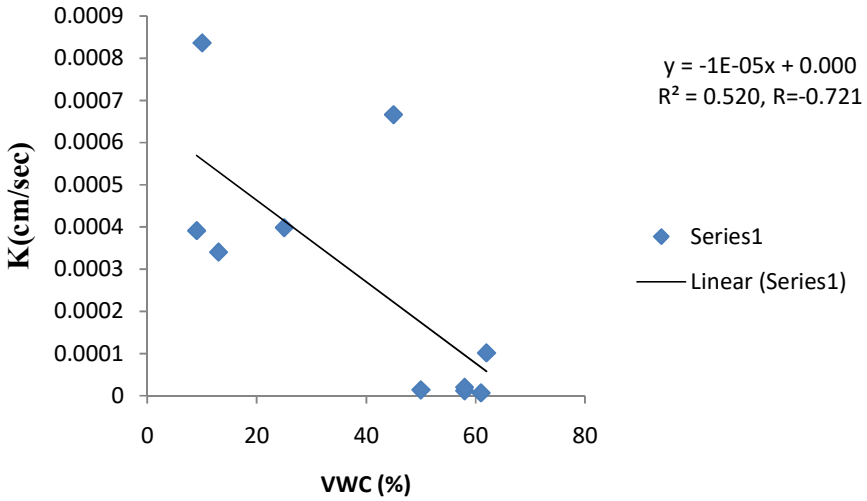

Figure 4.41b: Plot of permeability (FHP) versus VWC in the kola farm during the wet season

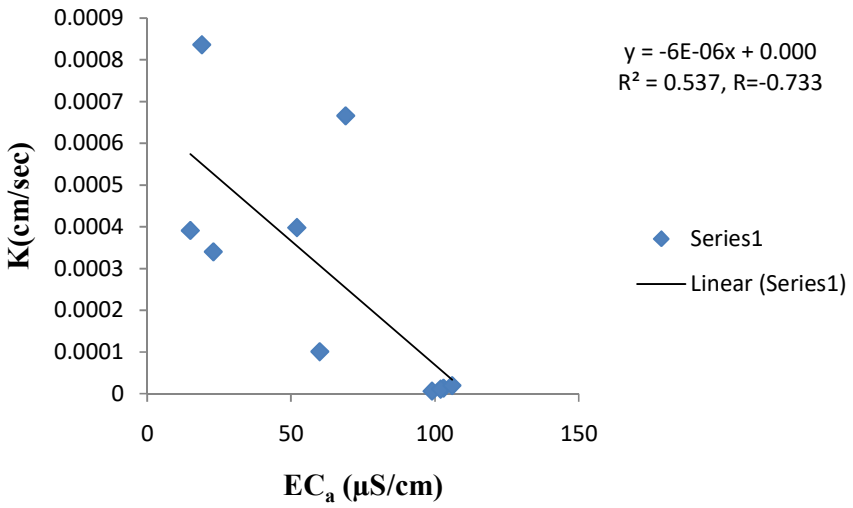

Figure 4.42a: Plot of permeability (FHP) versus EC_a in the kola farm during the dry season

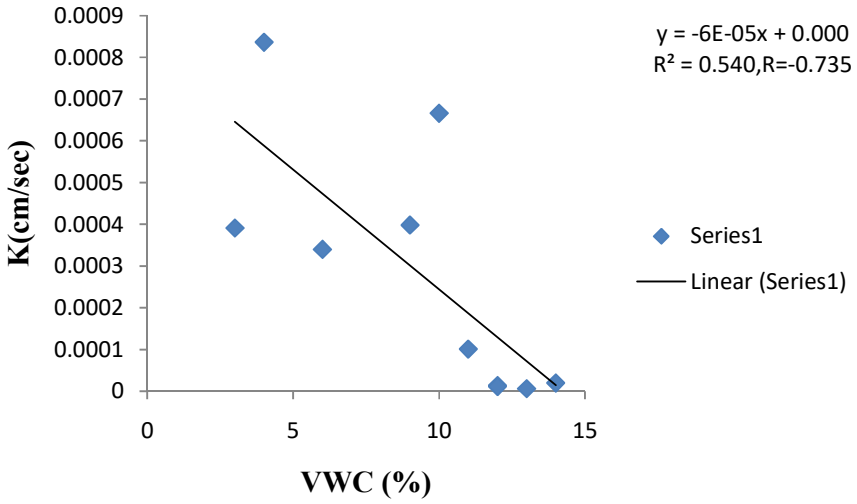

Figure 4.42b: Plot of permeability (FHP) versus VWC in the kola farm during the dry season

Constant head permeability

Correlating the permeability coefficients determined via constant head technique with apparent electrical conductivity and volumetric water content of the soil is to ascertain the relationship between these variables. Figure 4.43a shows that a strong negative correlation exists between the K and EC_a while the determination coefficient indicates 52.1 % of these parameters has linear relationship. Rise in the apparent electrical conductivity of the soils was noted with decrease in the permeability of the medium. A strong negative correlation coefficient (-0.866) was observed in Figure 4.43b when the permeability and the VWC data were systematically related and 74.9 % of the data engaged were linearly related. In the dry season, it was also observed that 69.5 % of the related parameters (EC_a & K) are linearly associated with a strong negative correlation (Fig. 4.44a). The magnitude of the relationship between K and VWC was -0.882 while 77.7% of these data are related (Fig. 4.44b).

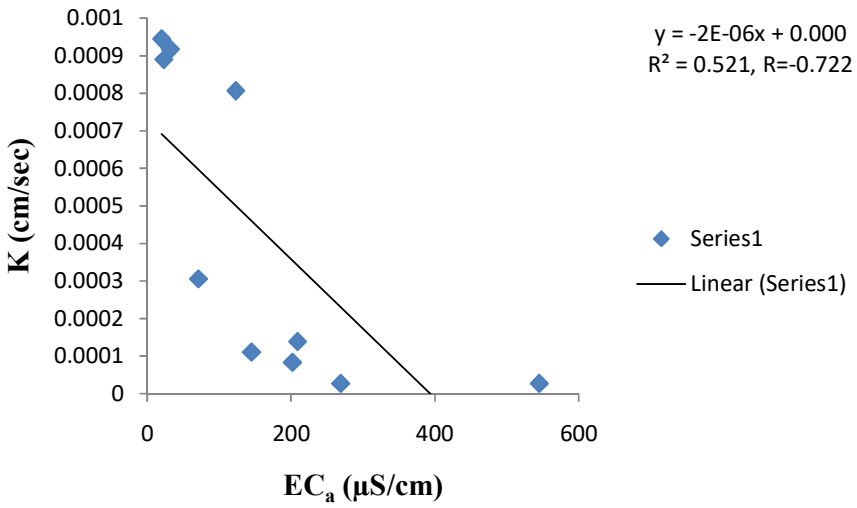

Figure 4.43a: Plot of permeability (CHP) versus EC_a in the kola farm during the wet season

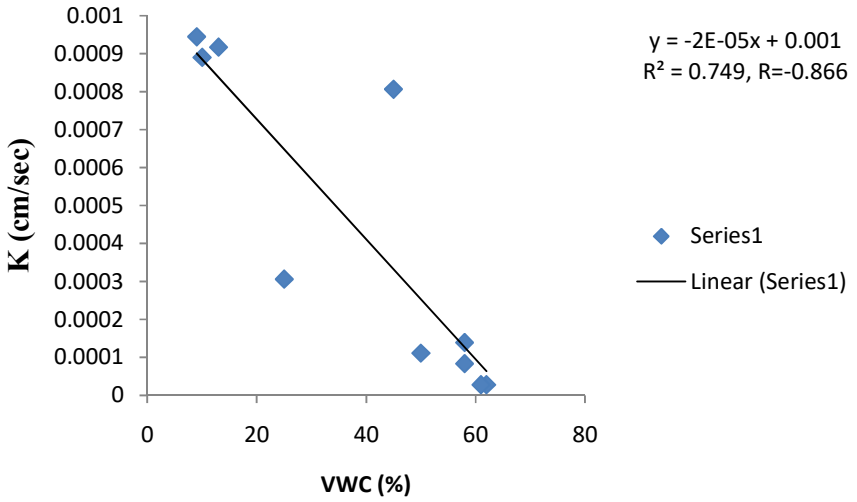

Figure 4.43b: Plot of permeability (CHP) versus VWC in the kola farm during the wet season

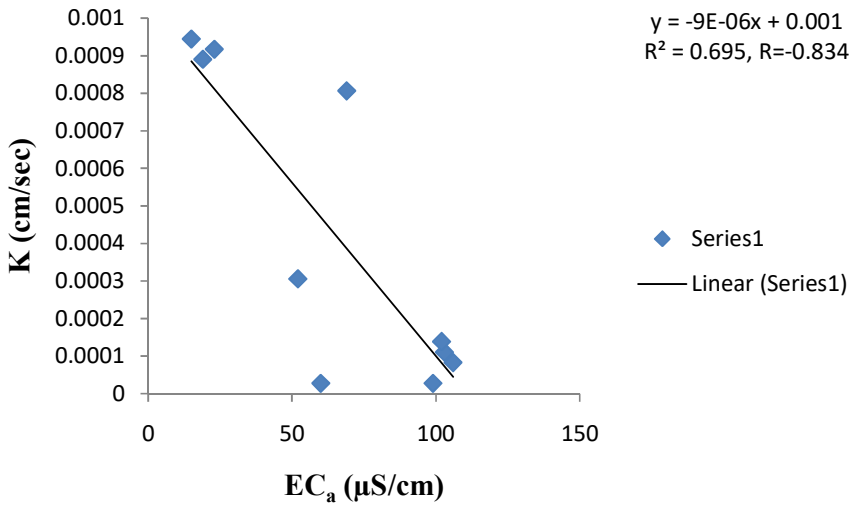

Figure 4.44a: Plot of permeability (CHP) versus EC_a in the kola farm during the dry season

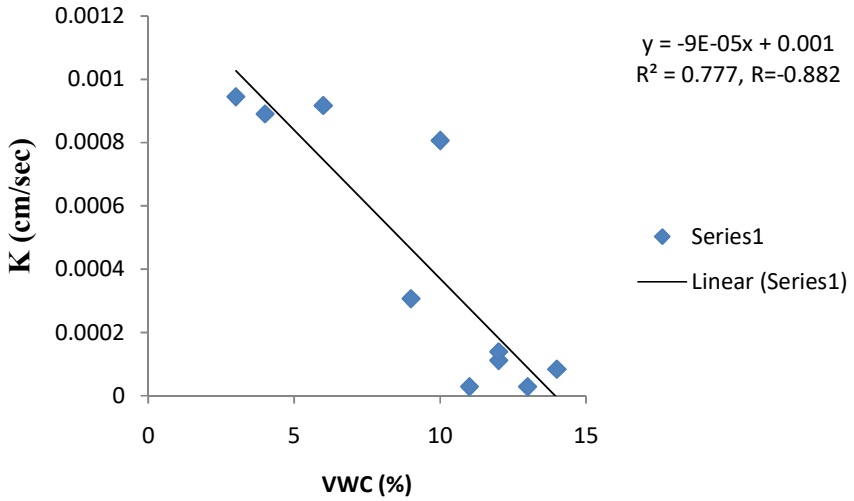

Figure 4.44b: Plot of permeability (CHP) versus VWC in the kola farm during the dry season

4.6 Textural Assessment of Soils

The essence of soil textural analysis is to determine the varying class present in the farms, its influence on the electrical properties of sub-soil material coupled with the inconsistent soil moisture content and also to deduce the proportion of the particle grains in each of the electrically conductive zones.

4.6.1 Soil Textural Assessment of the Farms

(i) **Cacao Farm**

Clay particles range from 4.8g/kg to 26.8 g/kg with a mean distribution of 12g/kg; proportion of silt fractions range from 4.8 g/kg to 24.8 g/kg and its average composition was 15g/kg; the amount of sand material in soil varies from 57.8g/kg to 89.8g/kg (Table 4.18). Particle size data were subjected to variability test using Warrick and Nielsen (1980) classification (Table 4.3), the distribution of clay particle is within the moderate class (35%), also silt fraction is in the class of moderate proportion (27%) while the proportion of sand size has low variability (9%) suggesting nearly uniform distribution in the cacao farm.

Plots of particle size distribution for soil samples taken at the various sample location (Table 4.18) were executed using soil textural triangle by the United State Department of Agriculture (USDA), three soil textures classes were established from grain size distribution and these include sandy loam (42), loamy sand (11) and sandy clayey loam (1) with percentage distribution of 78%, 20% and 2% respectively, thus sandy loam is the dominant class (Fig 4.45). Region of high EC_a has soil classes ranging from sandy loam to sandy clayey loam whereas loamy sand to sandy loam class was inherent in the moderate and low EC_a segments. Khadka *et al.* (2018) reported that soil with sandy loam texture is satisfactory for most of agricultural purposes. There is need to critically look at the varying size distribution at the low, moderate and high EC_a sections due to presence of nearly uniform soil texture, that is, occurrence of sandy loam texture in all the segments.

Table 4.18: Particle size distribution with EC_a values for soils in cacao farm

S/N	I.D	Clay	Silt	Sand	ECa (Wet)	ECa (Dry)
		g/kg	g/kg	g/kg	µS/cm	µS/cm
1	CL 1 at 0m	7.4	20.8	71.8	20	13
2	CL 1 at 18m	7.4	10.8	81.8	36	21
3	CL 1 at 36m	9.4	16.8	73.8	48	42
4	CL 1 at 54m	11.4	14.8	73.8	155	84
5	CL 1 at 72m	17.4	24.8	57.8	252	119
6	CL 1 at 90m	16.4	11.8	71.8	52	34
7	CL 4 at 0m	7.4	10.8	81.8	38	37
8	CL 4 at 18m	11.4	14.8	73.8	71	63
9	CL 4 at 36m	7.4	12.8	79.8	69	71
11	CL 4 at 54m	5.4	12.8	81.8	91	84
11	CL 4 at 72m	13.4	12.8	73.8	130	75
12	CL 4 at 90m	15.4	18.8	65.8	103	61
13	CL 7 at 0m	17.4	16.8	65.8	19	13
14	CL 7 at 18m	5.4	4.8	89.8	58	44
15	CL 7 at 36m	9.4	10.8	79.8	44	35
16	CL 7 at 54m	17.4	20.8	61.8	160	54
17	CL 7 at 72m	13.4	14.8	71.8	71	53
18	CL 7 at 90m	15.4	14.8	69.8	96	96
19	CL 10 at 0m	10	15.4	74.6	40	19
20	CL 10 at 18m	12	13.4	74.6	37	32
21	CL 10 at 36m	12	13.4	74.6	39	25
22	CL 10 at 54m	10	15.4	74.6	28	19
23	CL 10 at 72m	18	19.4	62.6	62	50
24	CL 10 at 90m	10	17.4	72.6	59	66
25	CL 13 at 0m	8	21.4	70.6	69	22
26	CL 13 at 18m	18	15.4	66.6	69	17
27	CL 13 at 36m	12	13.4	74.6	80	45
28	CL 13 at 54m	8	23.4	68.6	23	20
29	CL 13 at 72m	10	15.4	74.6	40	40
30	CL 13 at 90m	6	13.4	80.6	21	31
31	CL 16 at 0m	10	17.4	72.6	164	77
32	CL 16 at 18m	12	17.4	70.6	89	49
33	CL 16 at 36m	8	13.4	78.6	21	13
34	CL 16 at 54m	18	17.4	64.6	72	30
35	CL 16 at 72m	12	13.4	74.6	48	26

Table 4.18 cont'd

S/N	I.D	Clay	Silt	Sand	ECa (Wet)	ECa (Dry)
		g/kg	g/kg	g/kg	µS/cm	µS/cm
36	CL 16 at 90m	8	13.4	78.6	23	17
37	CL 19 at 0m	10	23.4	66.6	132	63
38	CL 19 at 18m	10	19.4	70.6	75	31
39	CL 19 at 36m	10	15.4	74.6	63	50
40	CL 19 at 54m	18	17.4	64.6	147	67
41	CL 19 at 72m	18	15.4	66.6	41	28
42	CL 19 at 90m	14	13.4	72.6	51	26
43	CL 22 at 0m	12	19.4	68.6	134	97
44	CL 22 at 18m	10	15.4	74.6	42	20
45	CL 22 at 36m	10	13.4	76.6	40	28
46	CL 22 at 54m	10.8	9.4	79.8	54	40
47	CL 22 at 72m	12.8	17.4	69.8	47	30
48	CL 22 at 90m	26.8	13.4	59.8	110	63
49	CL 25 at 0m	9.8	19.4	70.8	145	58
50	CL 25 at 18m	12.8	13.4	73.8	72	47
51	CL 25 at 36m	6.8	5.4	87.8	42	20
52	CL 25 at 54m	8.8	11.4	79.8	35	21
53	CL 25 at 72m	14.8	9.4	75.8	31	33
54	CL 25 at 90m	14.8	11.4	73.8	94	35
	Mean	12	15	73	71	44
	Std. Dev.	4	4	6	47	24
	CV%	35	27	9	66	56

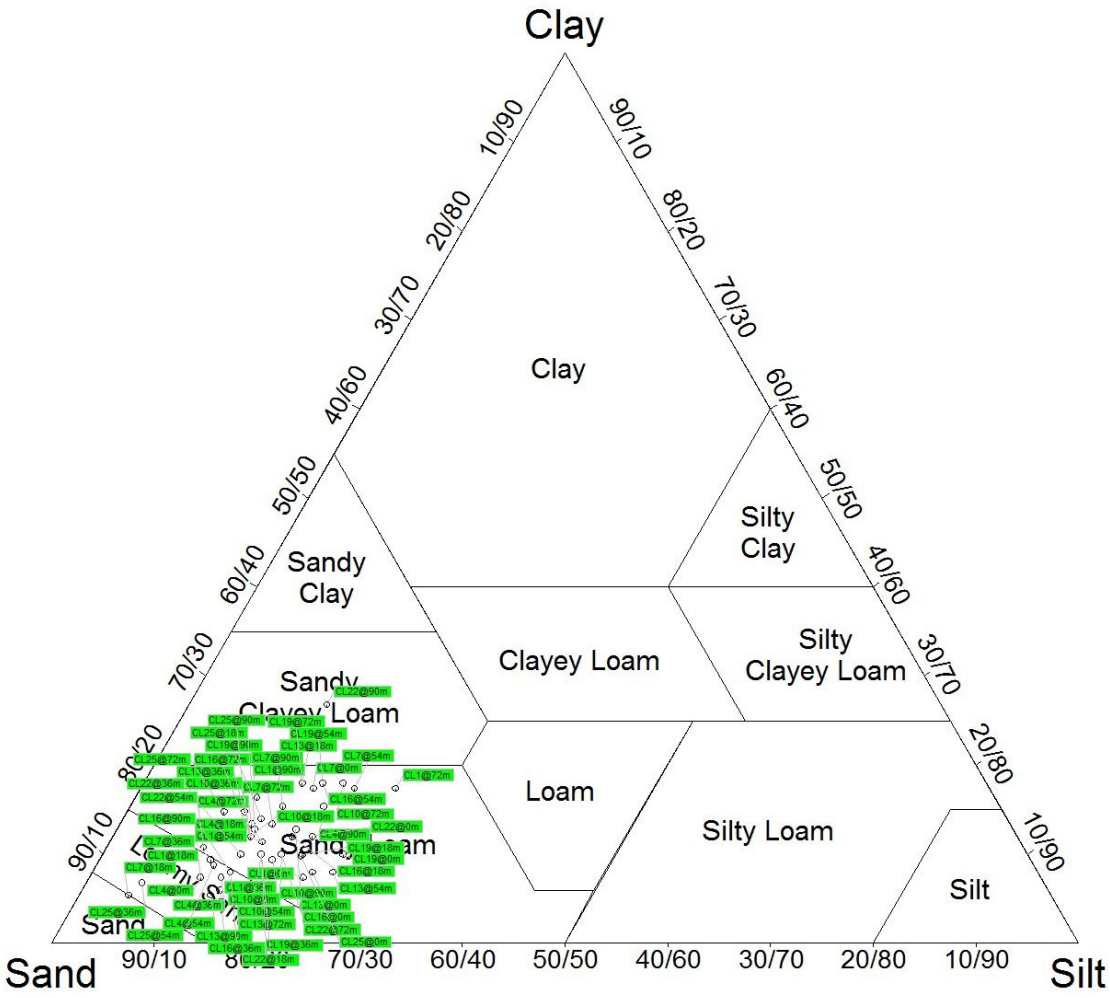

Figure 4.45: Soil textural classes of soils in cacao farm

(ii) **Kola Farm**

A total of forty-two soil samples were collected from the regions of low EC_a, moderate EC_a and high EC_a in the kola plot to classify their soil texture. Twenty-two samples were within the low EC_a section, while eleven and nine soil samples were taken from moderate and high EC_a sections respectively.

An overview of the particle size distribution within the farm (Table 4.19) shows that the clay fraction ranges from 6.8 g/kg to 19.4 g/kg and its mean proportion is 13 g/kg. The silty particles are in the range of 11.4 g/kg to 25.4 g/kg; its net average is 19 while proportion of sand is between 55.2 g/kg and 79.8 g/kg with a mean of 68 g/kg. It can be inferred that the net proportion of sand fraction (Fig. 4.46) outweigh the silt and clay size (sand>silt>clay). The data were subjected to variation coefficient analysis to determine its degree of variability using Warrick and Nielsen (1980) classification (Table 4.2). Variation analysis revealed that both the clay (%CV-25) and silt (%CV-19) size fractions are within the moderate class but the sand fraction has low variation coefficient (8%). This suggests that the distribution of clay and silt particles varies from one section to another whereas sand fraction with low variation was distributed across the soil unit in nearly uniform order. Figure 4.47 showed that the textural analysis was conducted using USDA texture triangle, forty-one out of the forty-two soil samples was classified to be sandy loam with percentage of 98 while a sample was regarded as loamy sand (2%).

Table 4.19: Particle size distribution with EC_a values for soils in the kola farm

S/N	I.D	Clay	Silt	Sand	ECa (Wet)	ECa (Dry)
		g/kg	g/kg	g/kg	µS/cm	µS/cm
1	KL 1 at 0m	10.8	15.4	73.8	27	27
2	KL 1 at 18m	14.8	11.4	73.8	24	26
3	KL 1 at 36m	14.8	17.4	67.8	46	60
4	KL 1 at 54m	10.8	19.4	69.8	31	23
5	KL 1 at 72m	16.8	17.4	65.8	52	39
6	KL 1 at 90m	14.8	15.4	69.8	33	32
7	KL 4 at 0m	14.8	17.4	67.8	52	41
8	KL 4 at 18m	14.8	17.4	67.8	39	29
9	KL 4 at 36m	14.8	19.4	65.8	43	41
10	KL 4at 54m	18.8	21.4	59.8	62	34
11	KL 4 at 72m	14.8	11.4	73.8	54	32
12	KL 4 at 90m	18.8	19.4	61.8	48	30
13	KL 7 at 0m	14.8	13.4	71.8	30	30
14	KL 7 at 18m	8.8	17.4	73.8	46	28
15	KL 7 at 36m	14.8	19.4	65.8	28	27
16	KL 7 at 54m	6.8	13.4	79.8	46	24
17	KL 7 at 72m	8.8	19.4	71.8	37	32
18	KL 7at 90m	8.8	15.4	75.8	26	27
19	KL 10 at 0m	6.8	17.4	75.8	37	34
20	KL 10 at 18m	8.8	17.4	73.8	34	28
21	KL 10 at 36m	8.8	15.4	75.8	31	26
22	KL 10 at 54m	17.8	15.4	66.8	33	21
23	KL 10 at 72m	12.8	15.4	71.8	68	39
24	KL 10 at 90m	12.8	23.4	63.8	88	39
25	KL 13 at 0m	10.8	19.4	69.8	54	33
26	KL 13 at 18m	9.4	21.4	69.2	47	39
27	KL 13 at 36m	9.4	19.4	71.2	47	33
28	KL 13 at 54m	11.4	21.4	67.2	39	34
29	KL 13 at 72m	11.4	13.4	75.2	40	32
30	KL 13 at 90m	11.4	21.4	67.2	71	56
31	KL 16 at 0m	11.4	17.4	71.2	82	48
32	KL 16 at 18m	15.4	23.4	61.2	153	74
33	KL 16 at 36m	13.4	21.4	65.2	137	72
34	KL 16 at 54m	15.4	23.4	61.2	200	89
35	KL 16 at 72m	15.4	21.4	63.2	278	80

Table 4.19 cont'd

S/N	I.D	Clay	Silt	Sand	ECa (Wet)	ECa (Dry)
		g/kg	g/kg	g/kg	µS/cm	µS/cm
36	KL 16 at 90m	13.4	21.4	65.2	151	50
37	KL 19 at 0m	15.4	19.4	65.2	115	61
38	KL 19 at 18m	15.4	19.4	65.2	117	98
39	KL 19 at 36m	9.4	21.4	69.2	72	67
40	KL 19 at 54m	17.4	25.4	57.2	234	79
41	KL 19 at 72m	19.4	25.4	55.2	476	144
42	KL 19 at 90m	13.4	19.4	67.2	98	56
	Std Deviation	3.32	3.45	5.37	85	25
	% CV	25	19	8	104	55

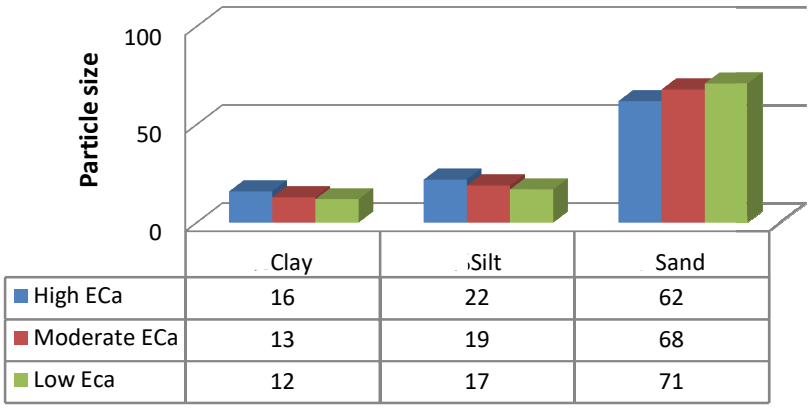

Figure 4.46: Mean size distribution of soil particles at different EC_a sections in the kola farm

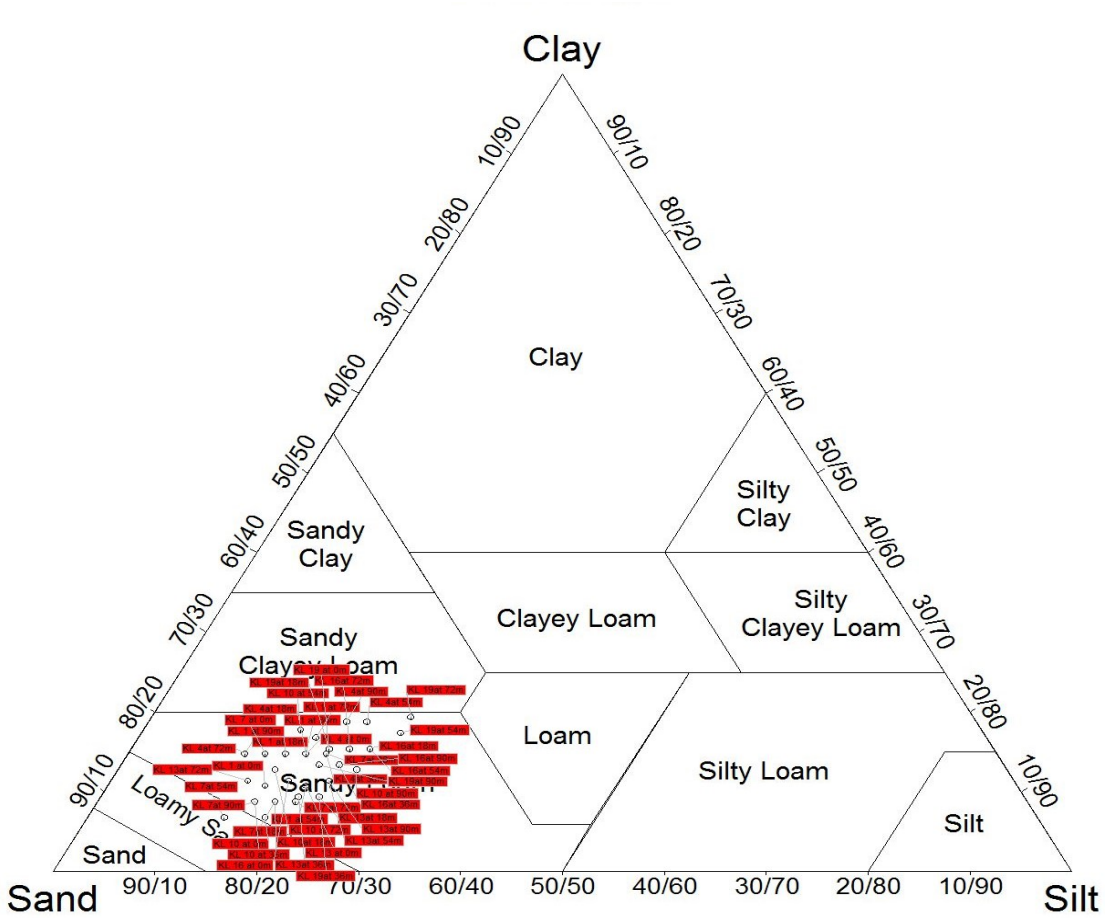

Figure 4.47: Soil textural classes of soils in kola farm

4.6.2 Particle Size Variation at EC_a Sections in the Farms

(i) **Cacao Farm**

At low EC_a section clay distribution ranged from 6.0 g/kg to 17.4 g/kg and its average proportion is 10 g/kg; the silt component in the soil varied from 5.4 g/kg to 23.4 g/kg with a mean distribution of 14g/kg while its sand proportion varied between 65.8 g/kg and 87.8 g/kg with a mean of 76 g/kg. Particle size computation for the soil samples taken at the moderate EC_a section shows that the clay size is between 5.4 g/kg and 18.0 g/kg and has an average proportion of 12 g/kg. Silt fraction varies from 4.8 g/kg to 21.4 g/kg with an average composition of 15 g/kg. The sand fraction in soils from this segment ranges from 62.6 g/kg to 89.8 g/kg and its mean contribution is 73 g/kg. In the region of high EC_a, the clay size has an average distribution of 15 g/kg and this size varies between 9.8 g/kg and 26.8 g/kg. The silt fraction has its content ranging from 12.8 g/kg to 24.8 g/kg and its mean proportion is 18 g/kg. Sand particle size ranges from 57.8 g/kg to 73.8 g/kg, its average proportion in these soils is 67 g/kg.

Considering the mean distribution of the soil particles (Fig. 4.48), it can be observed that the clay content increases from low (10 g/kg) through moderate (12 g/kg) to high (15 g/kg) EC_a sections. Also there is an increase in proportion of silt across the region of low ECa (14 g/kg) to moderate EC_a (15 g/kg) and finally to high EC_a (18 g/kg). More so, the sand particles decrease from low (76 g/kg) via moderate (73 g/kg) to high (67 g/kg) EC_a sections. This reveals that areas of low EC_a are characterised with less finer soil textures than the moderate and high EC_a zones, it tends to be more porous, permit faster water infiltration into lower soil horizons, therefore, it is prone to low water holding capacity and less retention of soil nutrients as a result of low clay content leading to low soil fertility (Ritchey *et al.,* 2015; Jaja, 2016 and Mukungurutse *et al*., 2018).

Soils in the low EC_a section have sandier textures than the moderate EC_a and high EC_a sections; they hold less water and less nutrients because they are prone to nutrients' leaching (Botta, 2015). High clay content was observed in the moderate (12 g/kg) and high EC_a (15 g/kg) sections, these soil particles retain more water than the low EC_a portion due to the presence of small pores with capacity to hold more soil nutrient (Botta, 2015).

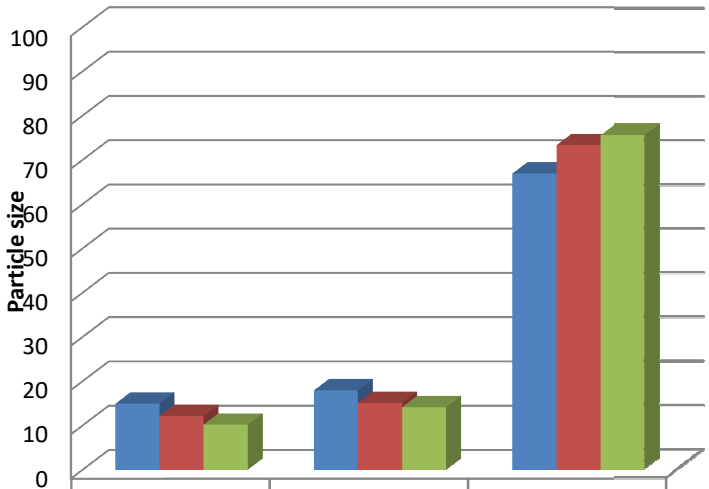

	Clay	Silt	Sand
High EC Section	15	18	67
Moderate EC Section	12	15	73
Low EC Section	10	14	76

Figure 4.48: Mean distribution of soil particles at different EC_a sections in the cacao farm

(ii) **Kola Farm**

In the low EC_a portion, soil particle distribution shows that clay fraction ranged from 6.8 g/kg to 18.8 g/kg with an average content of 12 g/kg; silt component varied between 11.4 g/kg and 21.4 g/kg, and has a mean value of 17 g/kg. Sand proportion has an average fraction of 71 g/kg while it ranged from 61.8 g/kg to 79.8 g/kg. Soil particle size in the moderate EC_a section shows that the sand proportion is the dominant size, ranging from 59.8 g/kg to 73.8 g/kg and has an average composition of 68 g/kg. Average distribution of silt in this segment is 19 g/kg and has its size distribution varying from 11.4 g/kg to 23.4 g/kg. The finer particle (clay) distribution varies from 9.4 g/kg to 18.8 g/kg; its mean proportion is 13 g/kg. Particle size variation in high EC_a section also follows similar pattern of distribution noted in low and moderate EC_a sections, sand fraction occupied greater proportion of the soil unit ranging from 55.2 g/kg to 65.2 g/kg with an average composition of 62 g/kg. Computational assessment of the silt fraction was between 19.4 g/kg and 25.4 g/kg, and its mean distribution is 22 g/kg while the mean proportion of clay size particle is 16 g/kg with its size distribution varying from 13.4 g/kg to 19.4 g/kg.

The mean distributions of the soil particles were used in evaluating its productivity across the kola plot; the clay division in kola farm increases slightly from low EC_a (12 g/kg) section to moderate EC_a (13 g/kg) and a conspicuous rise in quantity is noted in high EC_a (16 g/kg) region. Distribution of silt content also follows similar trend with that of the clay in which it has 22 g/kg in high EC_a area, 19 g/kg and 17 g/kg were computed for its variation in the moderate and low EC_a portions respectively.

There is an inverse distribution of sand fraction with the spread of apparent electrical conductivity; region of high EC_a has the least content of sand (62 g/kg) in it, it increases across the moderate EC_a section (68 g/kg) while highest proportion of sand (71 g/kg) was situated in the low EC_a. Soil productivity could be established from its textural characteristics, soils with high clay content tend to retain soil nutrients and have high water holding capacity than sandier unit (Moral and Rebollo, 2017).

It can be concluded that presence of relatively high proportion of clay size particle in high EC_a sections aided the retention of soil nutrients and greater water holding capacity than segments of fewer clay fraction. Tkaczyk *et al*. (2018) noted that crop yield in soils with sandy loam texture is higher than that obtained from loamy sand section while silty soil has the highest yield. Therefore, the average proportion of fine

fraction (clay and silt content) in high EC_a parts is 38 g/kg, moderate EC_a has a mean fine portion of 32 g/kg while 29 g/kg was deduced in the low EC_a areas, abundance of siliceous sand content with less fraction of fine resulted in their poor nutrient holding capability (Ho *et al*., 2019). Soils with greater proprotion of fine (38 g/kg) in high EC_a section have larger available surface area to hold water and nutrient effectively than those with less proportion of fine in moderate (32 g/kg) and low (29 g/kg) EC_a because of the particle sizes are small and fit in properly thereby reducing the pore spaces than grains of sand having larger pore space (Crouse, 2018)

4.6.3 Relationship between Soil Particle Size and Apparent Electrical Conductivity (EC_a) in the Farms

(i) **Cacao Farm**

An attempt was made to examine the soil particle influencing the apparent electrical conductivity of soil measured during the wet and dry seasons. The measured parameters (clay, silt, sand) were related with EC_a to determine soil component contributing to the rise or decrease in measured EC_a values across the cacao plot.

During the wet period, a moderate positive correlation coefficient (0.358) was observed between clay content and apparent electrical conductivity (EC_a), suggesting that as the clay fraction increases the EC_a also rises (Fig. 4.49a) and agrees with the results of Gholizadeh *et al.,* (2012). Rise in EC_a values was also noted as the proportion of silt particle size increases across the soil unit (Fig. 4.49b), and a moderate correlation coefficient of 0.435 was generated from their relationship (Chaudhari *et al.,* 2014). Figure 4.49c shows the interaction between EC_a and sand particle size fraction to be a moderate negative coefficient (-0.508), it can be inferred that EC_a values tend to be reduced across soil unit with abundant sand proportion compared to portion of fewer sand quantity (Chaudhari *et al.,* 2014) . Interaction between fine fraction (clay+silt) and EC_a indicates a moderate positive coefficient (0.508) occurring between these parameters (Fig. 4.49d).

EC_a data acquired during the dry season were also related with the soil particle size to access their relationship. Relating EC_a with the clay content (Fig. 4.50a), a weak positive correlation coefficient (0.213) was generated, indicating that an increase in clay content leads to rise in EC_a value measured on cacao plot (Heil and Schmidhalter, 2017). A weak positive coefficient (0.264) is noted from the interaction of EC_a with silt

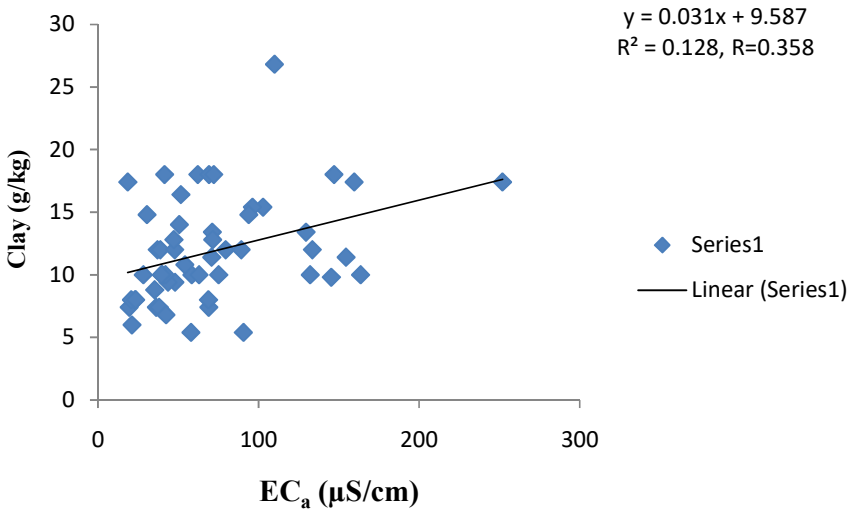

Figure 4.49a: Plot of EC_a versus clay fraction in the cacao farm during the wet season

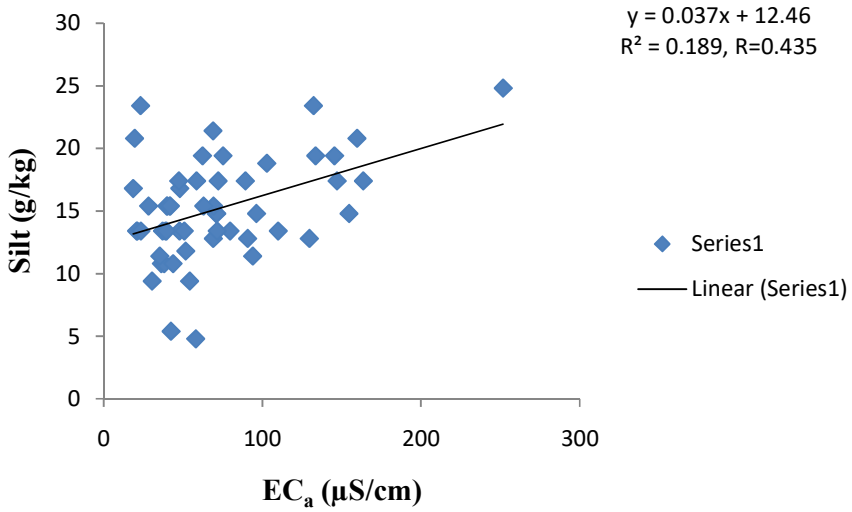

Figure 4.49b: Plot of EC_a versus silt fraction in the cacao farm during the wet season

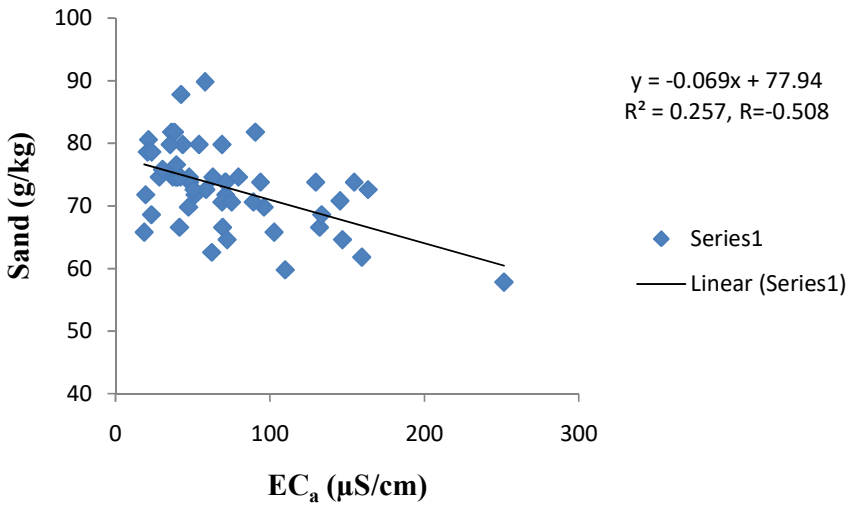

Figure 4.49c: Plot of EC_a versus sand fraction in the cacao farm during the wet season

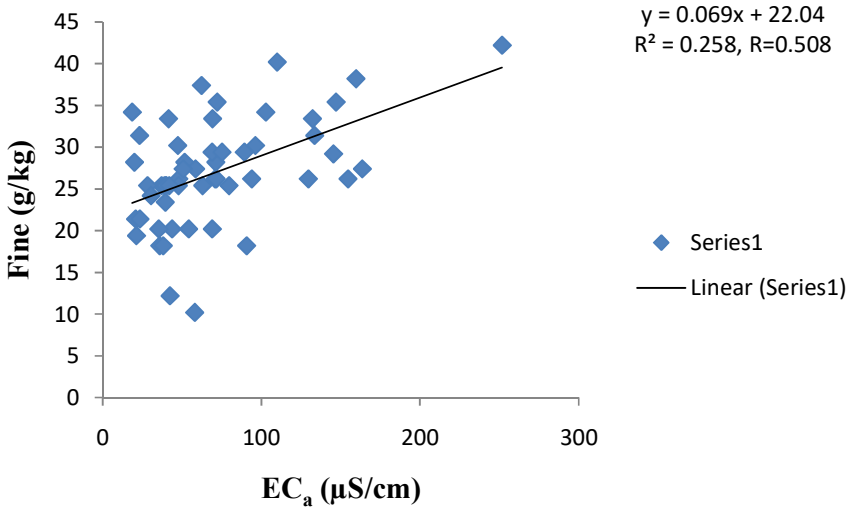

Figure 4.49d: Plot of EC_a versus fine fraction in the cacao farm during the wet season

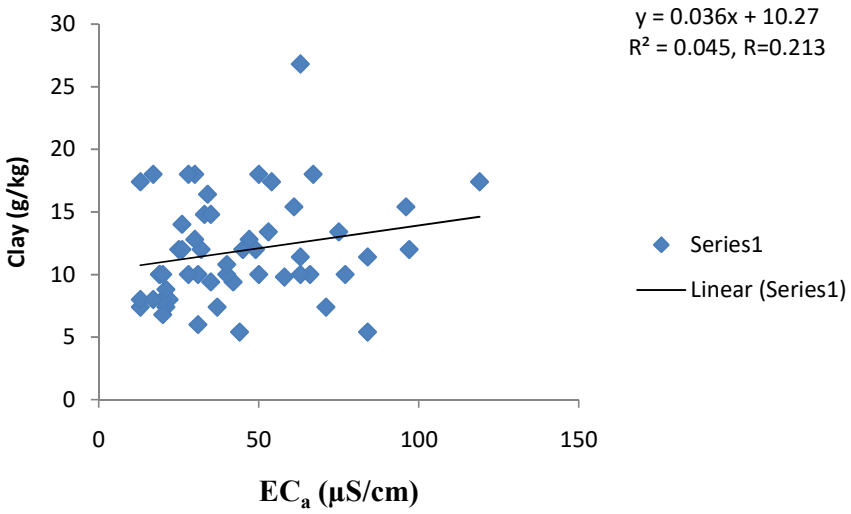

Figure 4.50a: Plot of EC_a versus clay fraction in the cacao farm during the dry season

content in figure 4.50b, suggesting that soils with increasing silt fractions tend to have high EC_a value. Evaluating the relationship between EC_a and sand fraction in figure 4.50c, increase in sand fraction is noted with decrease in EC_a value measured in the farm and its correlation coefficient is -0.305 (Korsaeth, 2005). Coefficient of correlation determined from the interaction of EC_a with the fine fraction (Fig. 4.50d) was a moderate positive correlation (+0.305). Relating the EC_a with the soil particles has shown that a better correlation was established with these variables in the wet season than in the dry season.

Evaluating soil's fertility from its textural classes in the regions of low, moderate and high EC_a with respect to the result of the electrical conductivity assessment of the soil has helped to delineate sections classified to be productive, partly productive and non-productive. EC_a analysis was corroborated with the soil textural variation within the cacao plot. The dominant soil texture class across the entire farm is sandy loam as determined from USDA soil texture triangle.

Close examination of the soil particle size has aided in ascertaining between non productive and productive segments. Region of low EC_a was characterised with fewer proportion of clay and silt contents and high proportion of sand fraction whereas the moderate EC_a segment has more content of clay and silt, and less of sand particles than the low EC_a portion. High EC_a areas are noted with a greater proportion of clay & silt and far less of sand compare to the low and moderate EC_a regions. Soils in high EC_a region have high proportion of fine (clay and silt) than other regions; they have the ability to retain more water, soil nutrient and less prone to nutrient leaching due to the presence of small pores (Sharu *et al.*, 2013; Amos-Tautua *et al*., 2014). Relationship between the EC_a data measured in wet and dry seasons and soil particle has shown that EC_a values increase in soil with high proportion of clay and silt and less of sand fraction and vice versa.

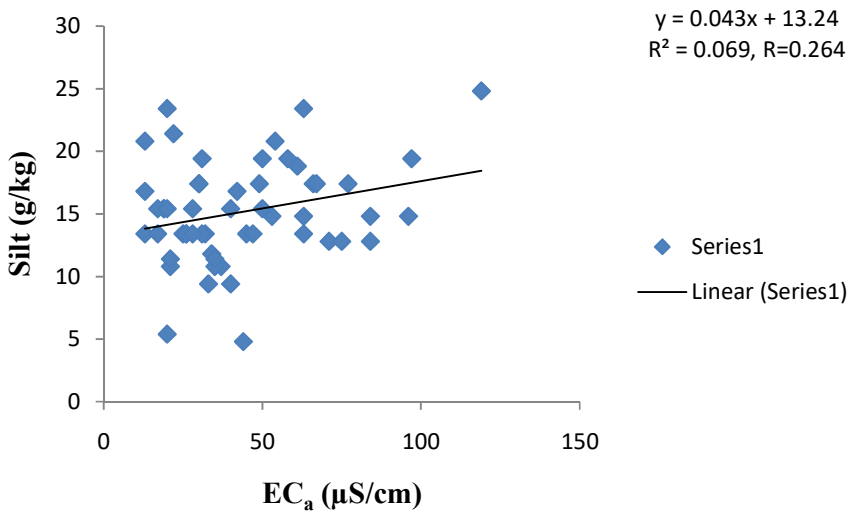

Figure 4.50b: Plot of EC_a versus silt fraction in the cacao farm during the dry season

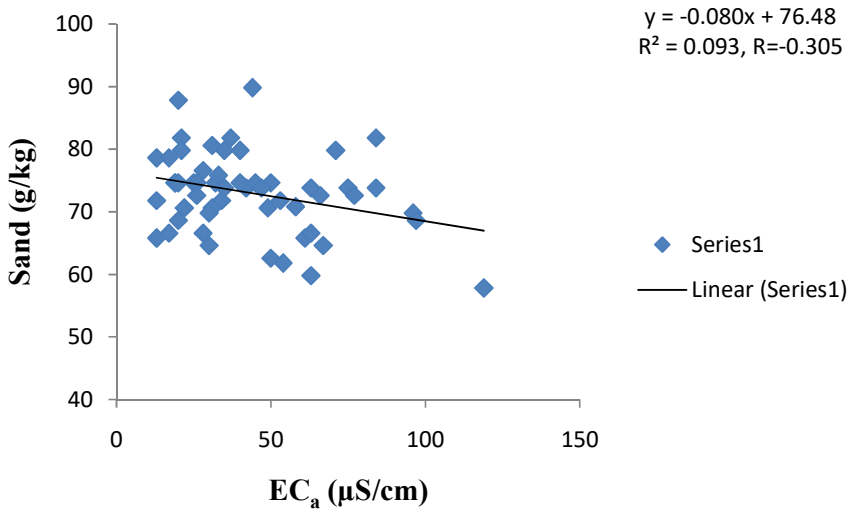

Figure 4.50c: Plot of EC_a versus sand fraction in the cacao farm during the dry season

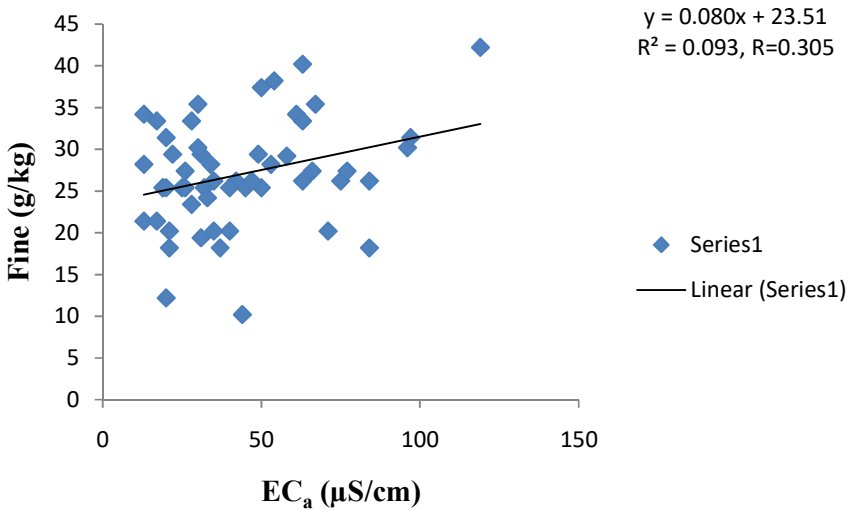

Figure 4.50d: Plot of EC_a versus fine fraction in the cacao farm during the dry season

(ii) **Kola Farm**

Relating the clay contained in the soil with the EC_a (Fig. 4.51a) in the wet season, resulted in a correlation coefficient of 0.449 signifying a moderate positive coefficient and it is consistent with the findings of McCutcheon *et al.,* (2006). Moderate positive correlation coefficient was deduced from the interaction of EC_a with silt content (0.627) as shown in Figure 4.51b, exhibiting similar relationship as observed by Chaudhari *et al.,* 2014. The quantity of sand was related with the EC_a and moderate negative coefficient (-0.681) was determined from their interaction (Fig. 4.51c), related response was observed by Rodríguez-Pérez *et al.,* (2011). The fine content was related with the EC_a and a resultant 0.681 positive correlation coefficient was generated (Fig. 4.51d).

Similar inferences were also made while relating EC_a with soil particle sizes in the dry season. The relationship between EC_a and clay fragment is a moderate positive factor with numerical value of 0.425 (Fig. 4.52a), Korsaeth (2005) and Heil and Schmidhalter (2017) also noticed similar trend. Moderate positive coefficient (0.643) occurred when quantity of silt was compared with the EC_a, this implied that the greater the fraction of this particle, the higher the measured EC_a value (Fig. 4.52b). A moderate negative coefficient (-0.676) was generated from the relationship of EC_a with the relative sand size (Fig. 4.52c) present in the soil (Korsaeth (2005)). The fine division (clay and silt) that constituted part of the soil reveals positive interaction between it and the EC_a value (Fig. 4.52d).

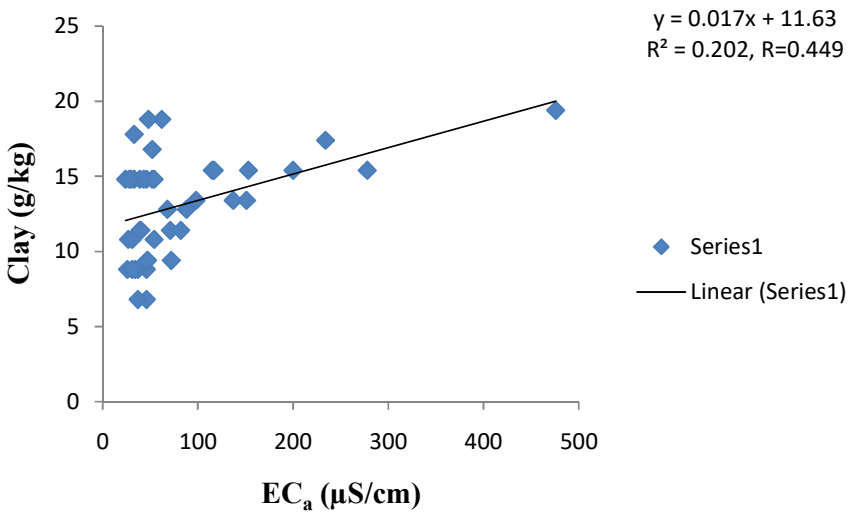

Figure 4.51a: Plot of EC_a versus clay in the kola farm during the wet season

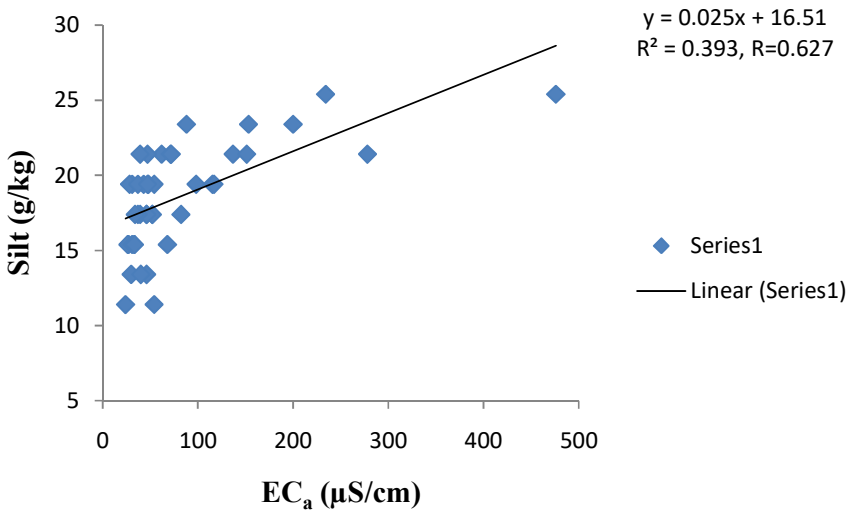

Figure 4.51b: Plot of EC_a versus silt in the kola farm during the wet season

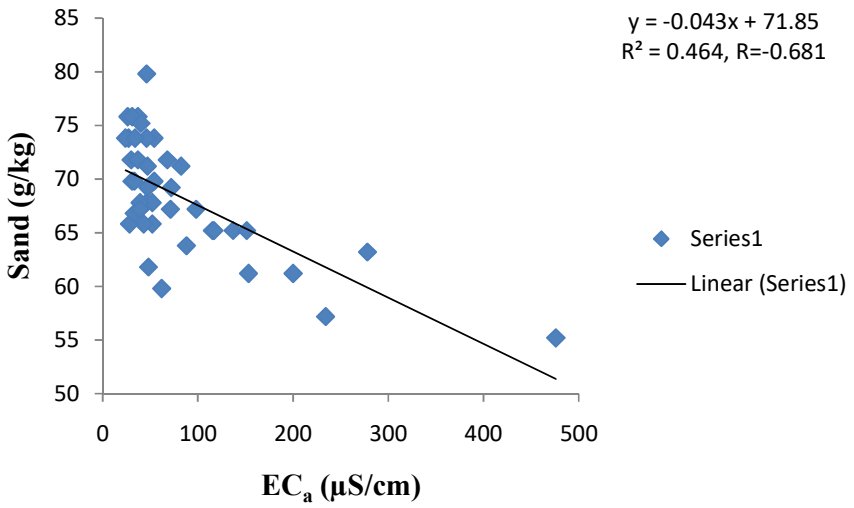

Figure 4.51c: Plot of EC_a versus sand in the kola farm during the wet season

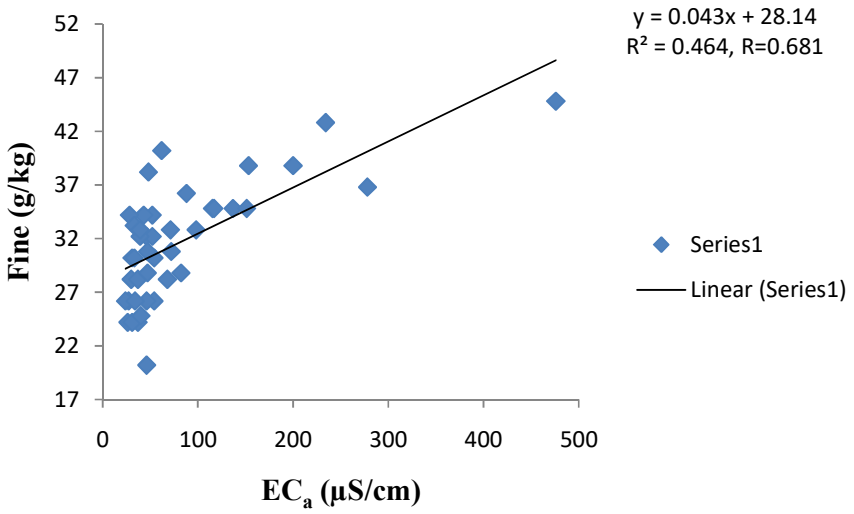

Figure 4.51d: Plot of EC_a versus fine in the kola farm during the wet season

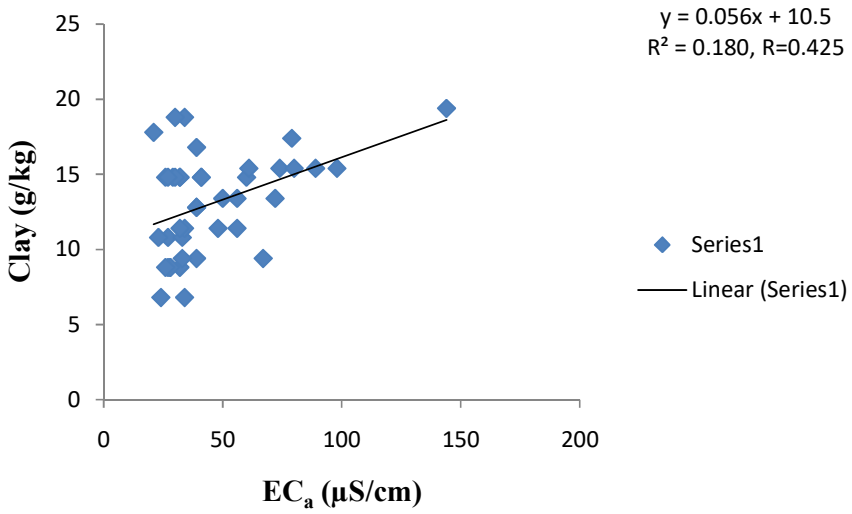

Figure 4.52a: Plot of EC_a versus clay in the kola farm during the dry season

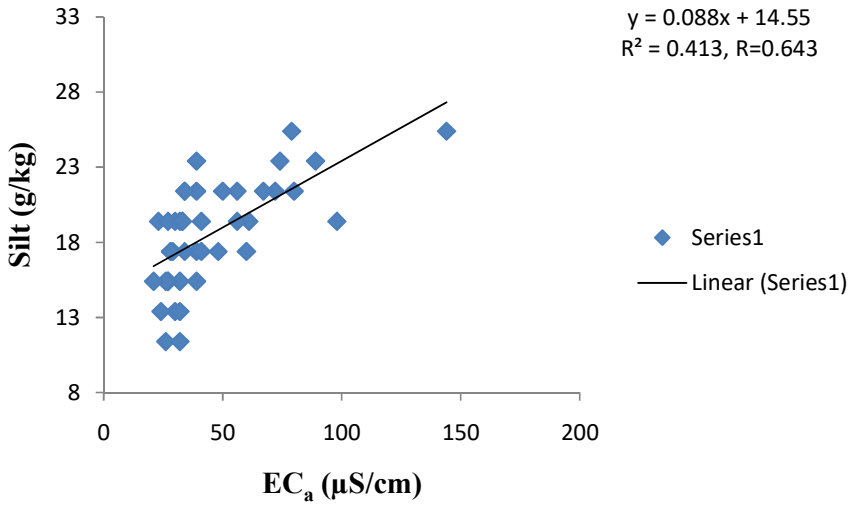

Figure 4.52b: Plot of EC_a versus silt in the kola farm during the dry season

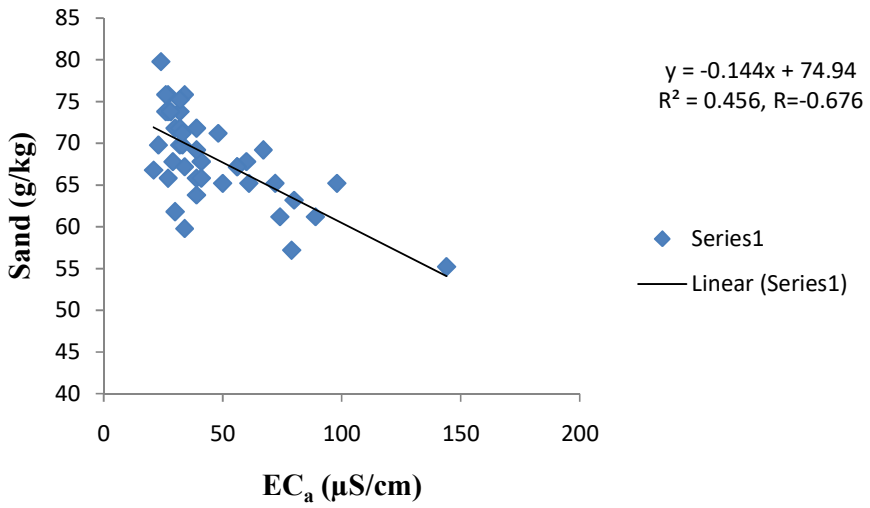

Figure 4.52c: Plot of EC_a versus sand in the kola farm during the dry season

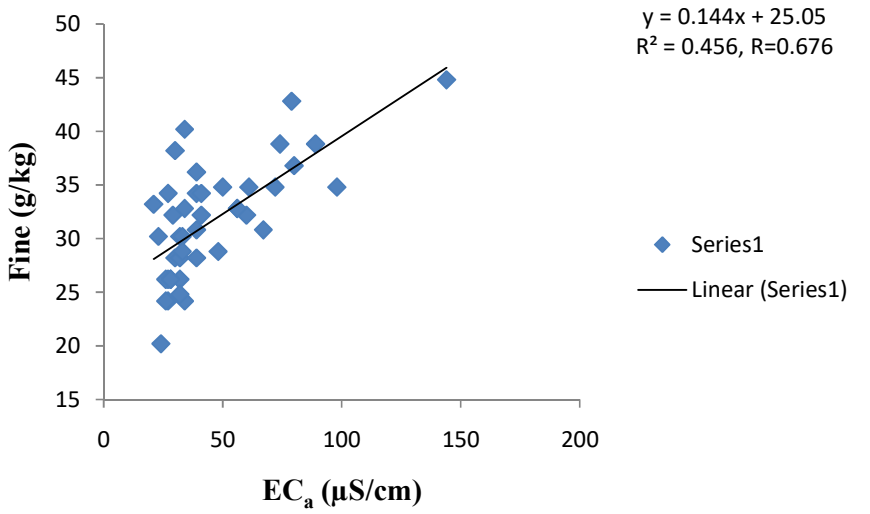

Figure 4.52d: Plot of EC_a versus fine in the kola farm during the dry season

Deduction made from the interaction of ECa with the various soil particle sizes proves that the EC_a was being influenced by the clay, silt or a combination (fine), as the proportion of these particle increases so also the rise in value of EC_a measured in such vicinity. Rise in quantity of sand across the farm contributed to decrease in measured EC_a values. Regions of high EC_a tends to have high proportion of clay, silt or a combination which favours the nutrients and soil moisture being held in this section. Segment characterised with moderate EC_a has larger quantity of clay, silt or fine than the low EC_a portion. Low EC_a division was characterised with high fraction of sand and less content of clay, silt or fine. Soils having more quantity of clay, silt or fine have better water and nutrient retention capability than those of less fine fraction. Soil with high quantity of sand and low content of clay has greater leaching potential while clay texture has low permeability (Amos-Tautua *et al.*, 2014). Clay was characterised with good water and nutrient retention capability as a result of its large surface area while high sand fraction has low water and poor nutrient holding capacity due to its predominant larger particle size which allows water to drain quickly leading to low fertility (Oyeyiola and Agbaje, 2013; Sharu *et al.*, 2013 and Musa *et al.*, 2016).

4.7 Soil Chemical Assessment

4.7.1 Assessment of Physical and Chemical Properties of Soil in the Farms

(i) Cacao Farm

Results of the elemental composition were subjected to statistical analysis in order to draw inferences from the coefficient of variation (Table 4.20). There is need to evaluate the varying distribution of the elemental components within the soil unit. Warrick and Nielsen (1980) classification was adopted (Table 4.3). Variant analysis was done to determine whether the elements are spatially or uniformly distributed within the soil in the farm.

pH has low variability (3) indicating nearly uniform distribution of hydrogen ions concentration in the farm. Parameters that fall within the moderate class include EC (54%), %OC (41%), %OM (41%), %TN (39%), acidic cation (18%), available P (16%), Ca (58%), K (37%), Na (16%), CEC (39%). Their concentrations suggest moderate dispersion of these elements in the cacao field, that is, it is not excessively distributed at a section. Magnesium (Mg) has its coefficient of variation to be high (62%) suggesting that it is highly variable within the cacao plot.

Soil pH

Overall pH values range from 6.1 to 7.1 and has a mean concentration of 6.71, average hydrogen ion concentration in the low EC_a horizon is 6.62 and it varies from 6.1 to 6.8; moderate EC_a section (pH: 6.6-6.8) has a mean value of 6.70 while the high EC_a segment has the pH level ranging between 6.4 and 7.1, and its mean concentration is 6.80.

All the mean pH recorded from soil samples falls in the neutral (6.6-7.3) category (Horneck *et al.*, 2011) in Table 4.21. The measured pH at all the zones is within the required concentration (6.0 – 7.5) which favours availability of soil nutrients for most crops (Moral and Rebollo, 2017, and Khadka *et al.*, 2018). All the analysed elements or soil nutrients would be available for the consumption of cacao plant since pH values are close to either side of neutrality and they are not prone to the presence of excessive amount of soluble salt because its pH values is not above 8.0 -8.5 (FAO, 2008). These cacao plants are not likely subjected to Al^{3+} toxicity which can limit root growth, restraining access to soil water and nutrient due to the fact that the pH is considerably above 5.5 (Ribeiro *et al.,* 2013 and Botta, 2015).

Table 4.20: Concentration of elements in the root zone at the cacao farm

Sample ID	pH	E.C (µS/cm)	%O.C	%O.M	%T.N	Avail P (mg/kg)	Acidity	Ca	Mg	K
								cmol/kg		
MP1	6.5	70	0.72	1.23	0.08	9.20	0.72	1.25	0.61	0.28
MP2	6.8	50	0.91	1.56	0.10	8.32	0.80	1.28	1.97	0.21
MP3	7.0	80	1.29	2.22	0.13	7.59	0.96	2.4	1.29	0.31
MP4	6.8	180	1.53	2.63	0.15	8.54	1.20	3.72	2.65	0.44
MP5	6.6	30	0.85	1.46	0.08	10.29	0.96	0.46	0.50	0.14
MP6	6.7	40	0.51	0.88	0.06	9.49	0.96	0.88	0.53	0.21
MP7	6.4	100	0.27	0.47	0.03	6.00	0.88	2.25	0.84	0.36
MP8	6.6	70	0.75	1.29	0.08	7.23	0.96	1.25	1.38	0.31
MP9	6.8	80	0.81	1.40	0.09	10.51	0.72	1.34	1.35	0.26
MP10	6.1	60	0.70	1.21	0.08	9.56	0.72	0.55	0.25	0.19
MP11	6.6	30	0.45	0.77	0.05	8.69	0.64	0.68	0.26	0.17
MP12	7.0	40	0.67	1.15	0.06	8.47	0.72	0.90	0.79	0.41
MP13	6.8	50	0.89	1.54	0.10	8.76	0.8	1.32	1.64	0.28
MP14	7.0	30	0.56	0.96	0.06	7.59	1.04	0.87	0.83	0.16
MP15	6.7	70	0.65	1.12	0.07	8.32	0.72	1.27	1.23	0.21
MP16	6.7	40	0.75	1.29	0.08	8.91	0.88	0.77	0.37	0.22
MP17	7.1	60	0.68	1.18	0.07	10.15	0.64	1.31	0.58	0.18
MP18	6.6	60	1.62	2.80	0.17	12.71	0.72	1.35	1.38	0.36
MP19	6.7	50	1.11	1.92	0.12	8.98	0.80	1.02	0.59	0.51
MP20	6.7	50	0.81	1.40	0.09	8.39	0.64	0.88	0.78	0.25
L EC	6.62	48	0.84	1.44	0.09	9.52	0.78	0.93	0.76	0.28
M EC	6.76	54	0.73	1.27	0.08	8.53	0.85	1.02	0.94	0.24
H EC	6.80	90	0.89	1.53	0.09	8.23	0.87	2.05	1.37	0.30
Mean	6.71	62	0.83	1.42	0.09	8.89	0.82	1.29	0.99	0.27
St Dev	0.23	34	0.34	0.58	0.03	1.40	0.15	0.75	0.62	0.10
CV%	3	54	41	41	39	16	18	58	62.3	37

*L EC-Low EC, M EC-Moderate EC, H EC-High EC, St. Dev-Standard Deviation

Table 4.20 cont'd

Sample ID	Na	C.E.C	% BS	Ca:Mg Disp	%Exch for Ca	%Exch for Mg	%Exch for K	Exch Na%
	cmol/kg							
MP1	0.22	3.08	76.62	2.0	40.58	19.81	9.09	7.14
MP2	0.27	4.53	82.34	0.6	28.26	43.49	4.64	5.96
MP3	0.3	5.26	81.75	1.9	45.63	24.52	5.89	5.70
MP4	0.27	8.28	85.51	1.4	44.93	32.00	5.31	3.26
MP5	0.20	2.26	57.52	0.9	20.35	22.12	6.19	8.85
MP6	0.22	2.80	65.71	1.7	31.43	18.93	7.50	7.86
MP7	0.27	4.60	80.87	2.7	48.91	18.26	7.83	5.87
MP8	0.23	4.13	76.76	0.9	30.27	33.41	7.51	5.57
MP9	0.34	4.01	82.04	1.0	33.42	33.67	6.48	8.48
MP10	0.21	1.92	62.50	2.2	28.65	13.02	9.90	10.94
MP11	0.22	1.97	67.51	2.6	34.52	13.20	8.63	11.17
MP12	0.33	3.15	77.14	1.1	28.57	25.08	13.02	10.48
MP13	0.28	4.32	81.48	0.8	30.56	37.96	6.48	6.48
MP14	0.23	3.13	66.77	1.0	27.80	26.52	5.11	7.35
MP15	0.25	3.68	80.43	1.0	34.51	33.42	5.71	6.79
MP16	0.21	2.45	64.08	2.1	31.43	15.10	8.98	8.57
MP17	0.23	2.94	78.23	2.3	44.56	19.73	6.12	7.82
MP18	0.2	4.01	82.04	1.0	33.67	34.41	8.98	4.99
MP19	0.25	3.17	74.76	1.7	32.18	18.61	16.09	7.89
MP20	0.24	2.79	77.06	1.1	31.54	27.96	8.96	8.60
L EC	0.24	2.99	71.80	1.5	30.91	23.19	9.34	8.36
M EC	0.25	3.30	73.34	1.2	30.89	27.33	7.41	7.71
H EC	0.27	4.85	81.38	1.7	41.52	27.65	6.22	5.99
Mean	0.25	3.62	75.06	1.51	34.09	25.56	7.92	7.49
St Dev	0.04	1.43						
CV%	16	39						

*BS-Base Saturation, Disp-Dispersion, Exch- Exchangeable

Table 4.21: Soil pH ranges (Adapted from Horneck *et al.*, 2011)

pH	Description
<5.1	Strongly acidic
5.2-6.0	Moderately acidic
6.1-6.5	Slightly acidic
6.6-7.3	Neutral
7.4-8.4	Moderately alkaline
>8.5	Strongly alkaline

Soil EC

Soil electrical conductivity values ranged from 30µS/cm to 180 µS/cm throughout the farm, with mean concentration of 62 µSc/m. Soils in the farm has been sectionalized into three; the low EC_a section has its values ranging from 30 -70 µS/cm with an average conductivity of 48 µS/cm, those in the moderate class vary from 30-80 µS/cm and has an average value of 54 µS/cm. The most conductive section has an average conductivity of 90 µS/cm and it ranges from 50 – 180 µS/cm.

On the basis of EC value, there is presence of more conductive ions (soluble salts) in the high EC_a region than the other sections. EC values measured in soil samples were below the ideal level (<0.5 dS/m), indicating that the soil is regarded as a non-saline soil (Botta, 2015). Horneck *et al.* (2011) estimated the range of EC values determining the performance of crops grown on soil from its saturated paste, the measured EC values from cacao soil were in the low category (Table 4.22) suitable for the optimum plant growth, in essence, the cacao trees can uptake the soil solution without resulting in water stress.

Organic carbon / organic matter

The percentage organic carbon (%OC) in the soils of cacao farm varies from 0.27 to 1.62 and its mean percentage was 0.83. Low EC_a region has an average %OC to be 0.84, it ranges from 0.45 to 1.62, in the moderate EC_a area the percentage distribution ranges from 0.56 to 0.81 with a mean of 0.73%, percentage organic carbon in high EC_a section was between 0.27 and 1.53, and has a mean of 0.89%.

Percentage distribution of organic carbon in the cacao soil falls within the low class (<1.8) reported in table 4.23 by Botta (2015). Despite low content of organic carbon in the soil, the highly conductive section has the highest percentage of OC than other sections, though it is slightly higher than the organic carbon in least conductive zone. Textural classes of soils used for chemical assessment were categorised to be sandy loam (85%) and loamy sand (15%), the percentage proportion of organic matter was classified in Table 4.24 to be moderately distributed (1.27-1.53%) in these soils (Proffitt, 2014). Rate of decomposition of cacao leaf litter is relatively slow (Ogeh and Ipinmoroti, 2015), which may be responsible for nearly uniform distribution of organic at this depth. The conversion factor is a multiple of 1.724 with percentage organic carbon and large amount of plant available nutrients are released during decomposition of organic matter.

Table 4.22: Soil EC determined from its saturated paste (Adapted from Horneck *et al.,* 2011)

Class	EC (mmhos/cm or dS/cm)	ppm salt	Siutability for crop production
Low	<1.0	<640	Suitable
Moderate	1.0-2.5	640-1,600	Marginal
High	>2.5	>1,600	Poor, unsuitable for many crop

Table 4.23: Organic carbon percentages (%) (Adapted from Botta, 2015)

Organic carbon levels	Pastures -low rainfall (<400 mm)	Pastures -high rainfall (>400 mm)
Low	<1.8	<3.0
Normal	1.8-2.7	3.0-5.0
High	>2.7	>5.0

Table 4.24: Level of organic matter (%) for different soil texture (Adapted from Proffitt, 2014)

Organic matter rating	Sand	Sandy loam	Loam	Clay loam/Clay
Low	<0.9	<1.2	<1.6	2.1
Moderate	0.9-1.7	1.2-2.4	1.6-3.1	2.1-3.4
High	>1.7	>2.4	>3.1	>3.4

Percentage total nitrogen (%TN)

General outlook of the percentage total nitrogen concentration in soils shows that it ranges from 0.05% to 0.17% with a mean percent of 0.09; 0.09% TN is equivalent to 1800 kg/ha which is below the required proportion (0.12% TN that is 2400 kg/ha) for effective cacao production (Ibiremo *et al*., 2011and Okoffo *et al*., 2016). Low EC_a has its %TN between 0.05 and 0.17, and has an average percentage nitrogen of 0.09 indicating a presence of 1800 kg/ha across the less conductive soil. Moderate EC_a has its percentage total nitrogen varying from 0.06 to 0.09 but has the least mean %TN value of 0.08 suggesting abundance of 1600 kg/ha. Region of high EC_a has its %TN concentration in the range of 0.07 to 0.15 and its average %TN is 0.09 signifying an occurrence of 1800 kg/ha. This justifies the results obtained from organic carbon in which there is nearly equal percentage at both the high and the low EC_a regions as the source of nitrogen is organic matter (Botta, 2015 and van Vliet *et al*., 2015).

Available phosphorus

Concentrations of available phosphorus across all the investigated sections in the cacao farm ranged from 6.0 mg/kg to 12.71 mg/kg with an average concentration of 8.89 mg/kg. Region of low EC_a has the highest mean concentration of available P (9.52 mg/kg) and its concentration across this section is between 8.32 mg/kg and 12.71 mg/kg. Its proportion in the moderate EC_a areas varied between 7.32 mg/kg and 10.51 mg/kg, and 8.32 mg/kg is the mean concentration. Least available P concentration was noticed in the high EC_a region, such that its availability ranges from 6.0 mg/kg to 10.51 mg/kg and its mean value is computed to be 8.23 mg/kg. The strength of available P in the entire farm declines from low EC_a segment to moderate area, and finally to the high EC_a terrain. Mean concentration of available P (8.89 mg/kg) across the whole farm was below the critical limit (12 mg/kg) needed to maximize crop productivity (van Vliet *et al*., 2015) and it can be classified (Table 4.25) within the low category (Horneck *et al*., 2011).

Table 4.25: Phosphorus (P) soil test categories (Adapted from Horneck et. al. 2011)

Category	Bray P1 test P (ppm)
Low	<20
Medium	20-40
High	40-100
Excessive	>100

Acidity of soil

Soils in cacao farm have their acidic cation ranging from 0.64 cmol/kg to 1.20 cmol/kg across the whole farm with an average concentration of 0.82 cmol/kg. Zone of low EC_a has a mean concentration of 0.78 cmol/kg with concentration varying between 0.64 cmol/kg and 0.96 cmol/kg. Moderate EC_a segment was characterised with a common concentration of 0.85 cmol/kg and it extended from 0.64 cmol/kg to 1.04 cmol/kg. The concentration stretched from 0.64 cmol/kg to 1.20 cmol/kg with an equal strength of 0.87 cmol/kg in high EC_a portion. Mean concentration in low EC_a (0.78 cmol/kg) was close to the overall average concentration (0.82 cmol/kg) in the entire farm whereas the prevailing concentrations in the moderate and high EC_a regions were above it.

Soil acidification in the high EC_a was ranked highest due to preferential consumption of base cations by cacao tree and organic acid being derived from decomposition of litters (Watanabe *et al*., 2015), it is not a useful nutrient for plant survival but it could be toxic to plant once the pH is below 5.5 (Botta, 2015). pH value in the cacao soils across the entire farm is within the neutral level (Horneck *et al*., 2011), therefore acidic cation content in cacao soils is not harmful to the growth of the cacao plant.

Soil Calcium Content

Quantity of Ca concentration across the cacao field ranges from 0.46 cmol/kg to 3.72 cmol/kg and its average concentration was 1.29 cmol/kg. Concentration of Ca is evaluated in the three distinct areas. The distribution in the low EC_a varies from 0.46 cmol/kg to 1.28 cmol/kg with a mean proportion of 0.93 cmol/kg. It also varies from 0.77 cmol/kg to1.34 cmol/kg in the moderate EC_a zone, and its average concentration was 1.02 cmol/kg. Proportion of Ca in the high EC_a segment was between 1.27 cmol/kg and 3.72 cmol/kg and the specific distribution peculiar to this region was estimated to be 2.05 cmol/kg.

There is no significant difference in the concentration of Ca in the low EC_a field (0.93 cmol/kg) and moderate EC_a section (1.02 cmol/kg) but the concentration of Ca was doubled in the high EC_a segment (2.05 cmol/kg) and these mean values fall within the low category (Proffitt, 2014) in Table 4.26. Botta (2015), and White and Broadley (2003) reported that the deficiency of Ca is not a common phenomenon but its excessive can restrict adequate growth. Its deficiency is noted in soils having low base

Table 4.26: Interpreting exchangeable cation results (Adapted from Proffitt, 2014)

Cation	Low cmol/kg	Moderate cmol/kg	High cmol/kg
Ca	<5.0	5.0-10.0	>10.0
Mg	<1.0	1.0-5.0	>5.0
Na	<0.3	0.3-1.0	>1.0

saturation and high acidic content (White and Broadley, 2003and Horneck *et al*., 2011).

Magnesium Content

Magnesium concentration in the cacao field has been spatially distributed such that its quantity in the low EC_a varies between 0.25 cmol/kg and 1.97 cmol/kg, on the average it is 0.76 cmol/kg. Mean distribution in the moderate EC_a zone was 0.94 cmol/kg while its concentration ranges from 0.37 cmol/kg to 1.38 cmol/kg. The most electrically conductive zone has its mean concentration to be 1.37 cmol/kg, determined from its various concentrations ranging between 0.58 cmol/kg and 2.65 cmol/kg.

Mg distribution in this farm increases across the three designated zones, from low EC_a segment to moderate EC_a and finally in the high EC_a soils which has the largest proportion. Considering the concentration at a glance, shows that the average concentration computed from the cacao soils was 0.99 cmol/kg. It ranges from 0.25 cmol/kg and 2.65 cmol/kg cutting across low (<1.0 cmol/kg) and moderate (1-5 cmol/kg) categories (Proffitt, 2014) in Table 4.26. Classifying the mean proportion of exchangeable Mg in all soils analysed, proportion of Mg in low EC_a and moderate EC_a regions was within the low class (<1.0 cmol/kg), although Mg concentration in the high EC_a is moderate (1-5 cmol/kg) category (Proffitt, 2014) in Table 4.26 and it was approximately twice the content in the low EC_a while it was approximately one and half the content in the moderate EC_a section. Thus, it can be concluded that the quantity of Mg content in high EC_a region plays a greater role in the photosynthesis because it was an essential element for chlorophyll pigment (Botta, 2015).

Potassium Content

This is the third most important soil nutrient along with phosphorus and nitrogen. Potassium content analysed in all soil samples ranges from 0.14 cmol/kg to 0.44 cmol/kg indicating that its distribution was categorized between low (<0.4 cmol/kg) and medium (0.4-0.6 cmol/kg). Its mean value is 0.27 cmol/kg was classified to be low by Horneck *et al.* (2011) as stated in Table 4.27. Region of low EC_a has its potassium concentration varying between 0.14 cmol/kg and 0.44 cmol/kg with an average potassium content of 0.28 cmol/kg which falls within the low category. Similar trend was observed in the moderate EC_a section in which its concentration ranges from

Table 4.27: Interpreting exchangeable potassium cation results (Adapted from Horneck *et al*., 2011)

Category	Concentration in cmol/kg
Low	<0.4
Medium	0.4-0.6
High	0.6-2.0
Excessive	>2.0

0.16 cmol/kg to 0.31 cmol/kg with an average distribution of 0.24 cmol/kg (low potassium category). High EC_a segment has potassium concentration in the range of 0.18 cmol/kg to 0.44 cmol/kg, and a mean concentration of 0.30 cmol/kg which was classified as low.

There is slight difference in the mean potassium concentration at the high and low EC_a segments. Despite the low category, cacao plants in the high EC_a zone are at an advantage over the moderate and low EC_a sections. The quantity of potassium available in high EC_a for plant's consumption was greater than those from other regions. Thus aiding a better regulation of nutrient uptake, water, flowering and seed bearing, and ensuring resistance to stress (Wodaje and Abebaw, 2014 and Botta, 2015) invariably contributing to the productivity in that section.

Sodium Content

Proportion of exchangeable sodium content in soil of low EC_a segment ranges from 0.2 cmol/kg to 0.27 cmol/kg with a representative quantity of 0.24 cmol/kg. In soils of moderate EC_a, its concentration varies from 0.21 cmol/kg to 0.34 cmol/kg and the concentration was averaged to be 0.25 cmol/kg . Concentration of sodium in the highly conductive segment extends from 0.23 cmol/kg to 0.30 cmol/kg with mean fraction of 0.27 cmol/kg.

These mean concentrations were classified as low in low EC_a and, moderate in moderate EC_a sections and high EC_a portion as stated in Table 4.26. Mean concentration computed from the geochemical data in the entire farm was 0.25 cmol/kg. There is no significant difference in its distribution across the three zones, which was also confirmed by its percentage variation coefficient (16). It has been reported that sodium is not considered as an essential soil nutrient for plants (Horneck *et al*., 2011, and Botta, 2015). Sections classified with low proportion of sodium have its productivity being affected as a result of low content but high EC_a section has the highest sodium content contributing to the cacao productivity than the other two segments (Proffitt, 2014).

Cation Exchangeable Capacity of soils

This is the property of soil that expresses its nutrient catchment/adsorption capacity and its release. Region of low ECa was characterised with low cation exchangeable capacity (CEC) such that its mean value was 2.99 cmol/kg recorded from soil CEC ranging from 1.92 cmol/kg to 4.53 cmol/kg. CEC values recorded from soils of moderate EC_a region vary from 2.45 cmol/kg to 4.13 cmol/kg and its average capacity was 3.30 cmol/kg. High EC_a section has CEC varying between 2.94 cmol/kg and 8.28 cmol/kg with a representative value of 4.85 cmol/kg.

CEC in the low EC_a segment was classified to be low (<3.0 cmol/kg) while the mean capacity in the moderate and high EC_a sections is between 3.30 & 4.85 cmol/kg and considered as moderate (3.0-10.0 cmol/kg) in Table 4.28 according to Proffitt (2014). An attempt was also made to determine the clay type present in the soil fraction (Table 4.29), the clay type in all the analysed soils falls within the kaolinite (Sonon *et al*., 2014). Soils in the high EC_a area have greater capacity to hold soil cations in soil solution for cacao plant uptake within the root zone (Sonon *et al*., 2014). Thus, soils in the high EC_a areas are more fertile than those of the other sections (Arévalo-Gardini *et al*., 2015). Region of high EC_a has high CEC indicating the presence of more cations being held by the soil against leaching and lessen the effect of pH change (Wood end research laboratory, 1996). In other words, soils having high CEC retain more soil nutrients than low CEC soils.

Table 4.28: Interpreting cation exchangeable capacity results (Adapted from Proffitt, 2014)

CEC rating	CEC cmol[+]/kg
Low	<3.0
Moderate	3.0-10.0
High	>10.0

Table 4.29: Cation exchange capacities for some clay types (Adapted from Sonon *et al*., 2014)

CEC rating	CEC_{bases} cmol/kg
Kaolinite	3.0-15.0
Illite	15.0-40.0
Montmorillonite	80.0-100.0

Percentage Base Saturation

This is the percentage proportion of basic cations in overall CEC. Percentage concentration of base cation with respect to CEC in the soils of low EC_a ranges from 57.52 to 82.34% with a mean saturation of 71.80%. Section of moderate EC_a was characterised with base saturation in the range of 64.08% to 82.04% but a rise in mean saturation percent (73.34) when compared with result obtained from low EC_a zone. Percentage base saturation in the high EC_a was ranked highest with mean saturation (81.38%) while its saturation varies from 78.23% to 85.51%.

This gives an indication that proportion of exchangeable base cation in soils of high EC_a exceeded those from the moderate and low EC_a sections. As base saturation increases, soil cations in solution are available for plant uptake. High percentage base saturation signifies more fertile soil with little or no acidic cation that will hinder crop growth, buffered against acidic cation and greater amount of basic cation for plant consumption (Sonon *et al*., 2014).

Ca:Mg Dispersion

Ratio of calcium to magnesium in low EC_a region stretches from 0.6 to 2.6 and the average ratio peculiar to this section was 1.5. Its ratio stretches from 0.9 to 2.1 in the moderate EC_a zone, with an equitable ratio of 1.2. Ca:Mg dispersion ratio in the high EC_a section extends from 0.8 to 2.7 with a mean ratio of 1.7.

Soils in this farm have their Ca:Mg ratio to be less than 2 indicating that the soils are not well structured (Botta, 2015). Closest ratio to this value was 1.7 in the high EC_a soil suggesting that it is fairly structured than other segments. Concentration of Mg was relatively high compare to Ca concentration; Mg can have a negative effect in soil physical properties thereby sealing the soil surface leading to infiltration decrease, increase in run-off resulting in erosion during rainfall (Dontsova and Norton, 2001). Specific effect of Mg on soil is that hydration energy is greater than that of Ca, thus resulting into larger hydration radius/shell which in turn causes a higher distance of separation between clay layers with less surface attraction makes it flocculate (Dontsova and Norton, 2001). Swelling and dispersion of soil lead to reduction in water infiltrating it, thereby increasing run-off water and soil erosion. Mg-dominated

soils have greater proportion of exchangeable Na accumulating on its surface than those of the Ca-dominated soils (He *et al*., 2013).

Exchangeable calcium percentage

Percentage content of Ca in the CEC within low EC_a area extends from 20.35 to 40.58% and the percentage assigned to this zone was 30.91%. Calcium exchangeable percentage in the moderate EC_a region lies between 27.80 and 33.42% with a prevailing percentage of 30.89%. Mean value for percentage exchangeable Ca in high EC_a area was 41.52% which extends from 30.56% to 48.91%.

The percentage exchangeable calcium computed for the three zones falls below the desirable range of 65% to 80% (Botta, 2015). It is worthy to note that the closest % exchange Ca to the desirable range was that from the high EC_a (41.52%). This signifies that the proportion of Ca in relation to other base cation was low/not adequate.

Exchangeable Magnesium Percentage

Arithmetic mean computed from the percentage contribution of Mg in CEC was 23.19% in low EC_a portion and its percentage varies from 13.02 to 43.49%. Exchangeable Mg percentage in the moderate EC_a area spanned between 15.10% and 33.67% with an average value of 27.33%. The content of Mg in the high EC_a division with respect to CEC showed values of 18.26% to 37.96% and the common value attributed to this portion was 27.65%. All the stated mean percentage of the exchangeable Mg in the three EC_a categories was above the desirable range (10%-20%) suggesting an excess in relation to other cations and it will be deleterious for cacao productivity (Botta, 2015).

Exchangeable Potassium Percentage

The content of exchangeable potassium in relation to the cation exchangeable capacity as expressed in percentage in the soils of low EC_a portion showed that its distribution lies between 4.64% and 16.09%, and the prevailing percentage is 9.34%. Percentage peculiar to the moderate EC_a division was 7.41% and it stretches from 5.11% to 8.98%. Percentage exchangeable potassium in the soils of high EC_a section varies between 5.31 and 7.83%, and its average percentage was 6.22%.

Relating the mean percentages of the exchangeable potassium with the Botta's (2015) desirable range for optimum crop production, the contents of moderate (7.41%) and high (6.22%) EC_a divisions are within the desirable range (3-8%) while that of the low EC_a (9.34%) exceeded the limit. This will affect productivity in that area.

Exchangeable Sodium Percentage (ESP)

Soils in the region of low EC_a are characterised with exchangeable sodium percentage ranging from 4.99% to 11.17% and the mean percentage was 8.36%. Zone of moderate EC_a has ESP in soils varying from 5.57% to 8.60% with an equitable percentage distribution of 7.71%. The percentage exchangeable sodium in the soils of high EC_a starts from 3.26% to 7.82% and the average percentage computed for this zone was 5.99%.

Relating the mean percentages of the exchangeable sodium with the desirable range for the three zones, low EC_a and moderate EC_a areas were classified to be above 6% which is marginally sodic and its aggregate is susceptible to dispersion when wet (Proffitt, 2014 and Botta, 2015), therefore they tend to have poor drainage, aeration and susceptible to erosion. Soils in the high EC_a portion are categorized as non-sodic (<6%), they are generally stable, good aeration, drainage and not vulnerable to erosion.

(ii) **Kola Farm**

The classification scheme of Warrick and Nielsen (1980) (Table 4.3) was used in ascertaining the distribution of pH, EC, organic carbon (OC), organic matter (OM), total nitrogen (TN) available phosphorus, acidic cation, Ca, Mg, K, Na and cation exchange capacity (CEC) in the kola field (Table 4.30). Those that fall within the high class include Ca (82%) and K (90%), category in the moderate includes EC (43%), OC (36%), OM (36%), TN (30%), available P (36%), acidic cation (25%), Mg (59%), Na (28%) and CEC (59%) while pH is classified to be low (4%).

Highly variable parameters suggest enormous concentration of these elements at one section than the others, which varied widely; those in moderate class indicate medium distribution, that is, not too high concentration at a particular segment while low variation gives an indication of nearly uniform distribution of the element at all segments of the field.

Table 4.30: Concentration of elements in the root zone at the kola farm

Sample ID	pH	E.C (µS/cm)	%O.C	%O.M	%T.N	P Avail (mg/kg))	Acidity	Ca	Mg	K
							cmol/kg			
MP21	6.8	40	1.145	1.974	0.109	7.78	0.41	1.29	0.64	0.23
MP22	7.0	40	0.775	1.336	0.083	5.15	0.64	0.6	0.49	0.22
MP23	6.9	40	0.994	1.714	0.103	6.93	0.56	0.63	0.52	0.15
MP24	6.9	50	1.196	2.062	0.098	7.85	0.55	1.01	0.98	0.25
MP25	7.0	40	0.371	0.64	0.044	6.60	0.56	0.64	0.48	0.15
MP26	7.5	50	0.522	0.900	0.061	9.50	0.42	1.31	0.85	0.25
MP27	7.2	50	0.960	1.655	0.100	9.83	0.65	1.21	0.71	0.44
MP28	6.9	50	0.842	1.452	0.076	7.59	0.64	0.91	0.61	0.22
MP29	7.2	40	0.502	0.866	0.052	8.25	0.55	0.85	0.83	0.18
MP30	6.9	40	0.623	1.074	0.066	6.14	0.64	0.78	0.76	0.13
MP31	6.7	30	1.078	1.859	0.111	5.74	0.56	0.96	1.3	0.23
MP32	7.0	110	1.667	2.874	0.157	12.01	0.8	2.68	1.29	0.36
MP33	6.8	60	0.606	1.045	0.062	5.01	0.72	1.1	1.26	0.19
MP34	6.6	50	0.825	1.422	0.091	4.68	0.82	1.69	1.97	0.22
MP35	6.5	90	0.792	1.365	0.080	4.35	0.88	3.03	2.22	0.25
MP36	6.9	100	0.909	1.567	0.101	3.50	0.55	5.84	2.84	0.82
MP37	7.6	110	1.347	2.322	0.127	11.28	0.32	4.97	1.6	1.33
MP38	6.8	50	0.775	1.336	0.100	5.08	0.96	2.84	0.78	0.14
MP39	6.7	70	0.640	1.103	0.07	4.42	0.66	2.89	1.47	0.21
MP40	6.5	100	0.793	1.367	0.091	3.76	0.64	5.46	2.64	0.31
L EC	6.98	43	0.85	1.47	0.09	7.31	0.56	0.93	0.73	0.23
M EC	7.10	75	1.08	1.87	0.10	10.13	0.68	1.77	1.06	0.27
H EC	6.80	79	0.84	1.44	0.09	5.26	0.69	3.48	1.85	0.43
Mean	6.92	61	0.87	1.50	0.09	6.77	0.63	2.03	1.21	0.31
St Dev	0.29	26	0.31	0.54	0.03	2.46	0.16	1.67	0.71	0.28
CV%	4	43	36	36	30	36	25	82	59	90

*L EC-Low EC, M EC-Moderate EC, H EC-High EC, St. Dev-Standard Deviation

Table 4.30 cont'd

Sample ID	Na	C.E.C	% B S	Ca:Mg Disp	%Exch for Ca	%Exch for Mg	%Exch for K	Exch Na%
	cmol/kg							
MP21	0.17	2.74	85.04	2	47.1	23.4	8.4	6.2
MP22	0.2	2.15	70.23	1	27.9	22.8	10.2	9.3
MP23	0.15	2.01	72.14	1	31.3	25.9	7.5	7.5
MP24	0.17	2.96	81.42	1	34.1	33.1	8.4	5.7
MP25	0.18	2.01	72.14	1	31.8	23.9	7.5	9.0
MP26	0.21	3.04	86.18	2	43.1	28.0	8.2	6.9
MP27	0.2	3.21	79.75	2	37.7	22.1	13.7	6.2
MP28	0.16	2.54	74.80	1	35.8	24.0	8.7	6.3
MP29	0.15	2.56	78.52	1	33.2	32.4	7.0	5.9
MP30	0.17	2.48	74.19	1	31.5	30.6	5.2	6.9
MP31	0.2	3.25	82.77	1	29.5	40.0	7.1	6.2
MP32	0.25	5.38	85.13	2	49.8	24.0	6.7	4.6
MP33	0.23	3.5	79.43	1	31.4	36.0	5.4	6.6
MP34	0.22	4.92	83.33	1	34.3	40.0	4.5	4.5
MP35	0.23	6.61	86.69	1	45.8	33.6	3.8	3.5
MP36	0.28	10.33	94.68	2	56.5	27.5	7.9	2.7
MP37	0.42	8.64	96.30	3	57.5	18.5	15.4	4.9
MP38	0.19	4.91	80.45	4	57.8	15.9	2.9	3.9
MP39	0.22	5.45	87.89	2	53.0	27.0	3.9	4.0
MP40	0.24	9.29	93.11	2	58.8	28.4	3.3	2.6
L EC	0.18	2.64	77.87	1.3	35.0	27.4	8.5	7.0
M EC	0.20	3.97	81.82	1.6	41.5	28.2	6.9	5.3
H EC	0.25	6.71	87.73	2.0	49.4	28.4	5.9	4.1
Mean	0.21	4.40						
St Dev	0.06	2.53						
CV%	28	58						

* BS-Base Saturation, Disp-Dispersion, Exch- Exchangeable

Soil pH

Concentration of hydrogen ion in the region of low EC_a ranged from 6.7 to 7.5 with an average distribution of 7.0, in the moderate EC_a section the pH varied from 7.0 to 7.2 and its mean concentration was 7.1 while the highly conductive EC_a segment has the pH in the range of 6.5 to 7.6 and the prevailing pH in this region was 6.8. Considering the overall pH across the entire farm, it lies between 6.5 and 7.6, and the common pH attributed to this field was 6.9.

Mean hydrogen ion concentration across the kola field is within the level required for optimal growth of most plant (Khadka *et al*., 2018). Qing *et al*. (2018) reported that enzymes will only aid transformation of nutrient and formation of soil organic carbon in soil when the pH is not too high or low. Soil nutrient will be available for plant consumption or uptake when the pH is above 5.5 (Botta, 2015 and Crouse, 2018), invariably suggesting that the pH values within the kola field aid soil nutrient uptake by the kola plants. Belachew and Abera (2010), FAO (2008) and Moral and Rebollo (2017) stated that plants prefer soil whose hydrogen concentration is close to neutral level. The mean concentration across all the three segments falls within the desired neutral category (Table 4.21) which is the ideal soil pH (Horneck *et al*., 2011).

Soil electrical conductivity (EC)

EC measurement has been an indirect approach of evaluating the presence of soil's soluble nutrients (Qing *et al*., 2018). All the measured soil EC values in soil was in the desired range, which was classified to be salt free (0-2000 µS/cm) and its salinity is termed to be negligible with no incidence of salt (FAO, 2008). District of low EC_a has its EC value extending from 30 µS/cm to 50 µS/cm and the common EC value peculiar to this section was 43 µS/cm. The EC value was classified between 40 µS/cm and 110 µS/cm in the moderate EC_a area with an equitable EC distribution of 75 µS/cm. Region of high EC_a has the EC values stretching from 50 µS/cm to 110 µS/cm with an average concentration of 79 µS/cm.

The EC value in the high and moderate EC_a segments was approximately double the concentration of dissolved soluble salt in the low EC_a section, the higher the EC values the more the dissolved solid nutrient in solution whereas low EC suggests low nutrient concentration in soil solution; thus more soil nutrients are available for plant consumption in the high and moderate EC_a regions.

Organic Carbon/Organic Matter

Distribution of organic carbon in the kola farm stretched from 0.371% to 1.667% with an overall average of 0.87%. Based on the electrical conductivity zones, the least electrically conductive division has its percentages of organic carbon varying from 0.371 to 1.196 and its intermediate content was 0.85%. Organic carbon in the moderate EC_a segment lies between 0.502% and 1.667% with an arithmetical mean of 1.08%. The organic carbon in the most electrically conductive section was classified between 0.606% and 1.347%, and the common value attributed to this segment was 0.84%.

There was no significant difference in the mean organic carbon content in the low EC_a (0.85%) and high EC_a (0.84%) sections but a slight increase was observed in the moderate EC_a division (1.08%). Suarez and Gonzalez-Rubio (2017) reported organic matter may cause a decrease in infiltration rate leading to an increase in dispersion. Organic matter content in the kola soil was determined from multiplier effect of 1.742 with the organic carbon concentration. Majority of the soil texture was classified to be sandy loam (98%) while loamy sand covers 2% in the kola farm, the mean concentration of organic matter in the low, moderate and high EC_a areas are 1.47%, 1.87% and 1.44% respectively. The content of organic matter in kola soils falls within the intermediate class (Proffitt. 2014) in Table 4.24, suggesting that there is moderate distribution of organic matter in the kola farm. Clogging of pores space in soil with dissolved organic matter might reduce the infiltration leading to drainage reduction and aeration (Suarez and Gonzalez-Rubio, 2017).

Percentage Total Nitrogen (%TN)

Percentage total nitrogen across the kola farm varied from 0.09 to 0.10 and its mean value was 0.09%. In the region of low EC_a, the percentage total nitrogen ranged from 0.044 to 0.111 and the prevailing concentration was 0.09% which is equivalent to 1800 kg/ha. Section of moderate EC_a has its %TN extending from 0.052 to 0.157 and the peculiar nitrogen content in this zone was 0.10%, in other word it means 2000kg/ha in terms of its concentration. %TN distribution in the high EC_a division lies between 0.062% and 0.127% with an overall amount of 0.09% in this zone. The average content of %TN in the low EC_a and high EC_a portions are similar, that is, 0.09 indicating 1800 kg/ha. This distribution also follows similar trend in organic carbon and organic matter as the source of nitrogen is organic matter (Botta, 2015 and Khada *et al*., 2018).

Available Phosphorus

Available phosphorus in kola soils stretched from 3.5 mg/kg to 12.01 mg/kg with a mean content of 6.77 mg/kg. Portion of low EC_a was characterised with concentration ranging from 5.15 mg/kg to 9.83 mg/kg and the equivalent concentration in this segment was 7.31 mg/kg. Zone of moderate EC_a has its available phosphorus increasing from 8.25 mg/kg to 12.01 mg/kg and its mean content is 10.13 mg/kg. Relative content of available phosphorus in high EC_a section extends from 3.5 mg/kg to 11.28 mg/kg and its average content amounts to 5.26 mg/kg.

Out of the three designated zones, available P in the high EC_a is the least followed by its content in the low EC_a segment while the moderate EC_a district has the highest content. Evaluating the mean available P concentration across these zones, it signifies that the amount of available P is below the critical limit of 12 mg/kg recommended for adequacy of available P in soil for plant uptake according to van Vliet *et al*. (2015). The phosphorus content across the entire kola farm was regarded as low (Horneck *et al*., 2011) in Table 4.25.

Acidity of Soil

Overall concentrations of acidic cation in kola soils rank between 0.32 cmol/kg and 0.96 cmol/kg and the unifying concentration in this farm was 0.63 cmol/kg. Portion of low EC_a has acidic cation in the range of 0.41 cmol/kg to 0.65 cmol/kg with average content of 0.56 cmol/kg. Moderate EC_a segment was characterised wth acidic cation varying from 0.55 cmol/kg to 0.80 cmol/kg and the prevailing concentration in this zone was 0.68 cmol/kg. A stretch of 0.32 cmol/kg to 0.96 cmol/kg acidic cation concentration was noticed in soils of high EC_a section with a mean content of 0.69 cmol/kg.

Similar mean concentration was recorded in the high and moderate EC_a portion suggesting that kola nut plants consume base cation in these regions and decomposition of litters from the trees contribute to organic acid in the soil (Watanabe *et al*., 2015) because the zone was well nourished with soil nutrients, although it has been reported that acidic cations are not required for plant nutrient and they are toxic to plant when the pH was below 5.5 (Botta, 2015) but the measured pH in kola soils is above 5.5 which invariably suggest that the quantity of these cations could not inhibit the growth of the kola nut trees.

Calcium Content

Concentration of calcium in all the kola soils ranged from 0.6 cmol/kg to 5.84 cmol/kg with relative concentration of 2.03 cmol/kg. Region of low EC_a has calcium concentration varying from 0.60 cmol/kg to 1.31 cmol/kg and its average content was 0.93 cmol/kg in this zone. Its concentration was ranked between 0.85 cmol/kg and 2.68 cmol/kg in the moderate EC_a with a common concentration of 1.77 cmol/kg. Zone of high EC_a has mean concentration of 3.48 cmol/kg with its distribution varying from 1.1 cmol/kg to 5.84 cmol/kg.

Mean concentration in the moderate EC_a segment was approximately double the concentration in the low EC_a zone while concentration of calcium in high EC_a was approximately four fold the concentration in the low EC_a section. Proffitt (2014) classification scheme suggests that calcium concentration in kola soils can be considered as low (Table 4.26), despite its low content, area of high EC_a was well nourished with calcium content than other sections and Sharu *et al*. (2013) reported that calcium is one of the dominant cations in West African soils also affirming the dominance of calcium in kola soils.

Magnesium Content

Mean magnesium content across the entire kola farm was 1.21 cmol/kg in which its concentration extends from 0.48 cmol/kg to 2.84 cmol/kg. Concentration of magnesium in area of low ECa ranged from 0.48 cmol/kg to 1.3 cmol/kg while its prevailing content was 0.73 cmol/kg. Segment of moderate EC_a has its magnesium distribution varying from 0.83 cmol/kg to 1.29 cmol/kg with mean value of 1.06 cmol/kg. Content of magnesium in the high EC_a area lies between 0.78 cmol/kg and 2.84 cmol/kg with an average concentration of 1.85 cmol/kg.

The mean concentration of magnesium in the moderate EC_a area was about one and half the magnesium content in the low EC_a whereas the ratio increases in the high EC_a such that it is two and half the magnesium content in the low EC_a segment. Evaluating its proportion using Proffitt (2014) scheme in Table 4.26, magnesium content for plant consumption in the low EC_a was low (<1 cmol/kg) whereas the quantity of magnesium in the moderate and high EC_a was regarded as moderate (1-5 cmol/kg). Kola trees within the high EC_a area have access to substantial quantity of magnesium than the moderate while the least obtainable content was found in the low EC_a segment. It is

next to calcium in abundance and constitutes one of the dominant cations in West African soils (Sharu *et al*., 2013).

Potassium Content

Potassium concentration ranged from 0.13 cmol/kg to 1.33 cmol/kg with an average concentration of 0.31 cmol/kg across the entire kola soils. District of low EC_a has potassium content extending from 0.13 cmol/kg to 0.25 cmol/kg and the equitable concentration in this region was 0.23 cmol/kg. Portion of moderate EC_a has its potassium concentration varying from 0.18 cmol/kg to 0.36 cmol/kg and the computed average concentration was 0.27 cmol/kg. Potassium concentration in the high EC_a area stretched from from 0.14 cmol/kg to 1.33 cmol/kg and the relative strength peculiar to the region was 0.43 cmol/kg.

Relating the mean potassium concentration with the established classes according to Horneck *et al*. (2011) in Table 4.27, the mean potassium concentration in the low and moderate sections were regarded as low, that is, <0.4 cmol/kg whereas the mean potassium concentration of 0.43 cmol/kg was termed to be in medium class (0.4-0.6 cmol/kg). Based on this, kola nut trees within the high EC_a segment have access to moderate concentration of potassium than other segments.

Sodium Content

An overview of the sodium distribution in the kola field shows that it increased from 0.15 cmol/kg to 0.42 cmol/kg with a mean content of 0.21 cmol/kg. It ranged from 0.15 cmol/kg to 0.21 cmol/kg in the low EC_a segment while the prevailing concentration in this segment was 0.18 cmol/kg. Region of moderate EC_a has peculiar sodium concentration to be 0.20 cmol/kg determined from its concentration varying from 0.15 cmol/kg to 0.25 cmol/kg. Sodium concentration in high EC_a area extends from 0.19 cmol/kg to 0.42 cmol/kg with a common concentration of 0.25 cmol/kg.

Judging from its mean distribution across the three zones, their concentrations are classified as low (Proffitt 2014). Despite the fact that sodium content in the farm falls with the low category (Table 4.26), the ratio of sodium content in low, moderate and high ECa sections was given as 1:1.3:1.4, indicating that high EC_a is enriched with higher quantity of sodium nutrient than other segments.

Cation Exchange Capacity (CEC)

It is an indication of nutrient adsorption capacity of soil which is dependent on the clay mineral proportion and organic matter, the capacity varied from 2.01 cmol/kg to 10.33 cmol/kg with a common concentration of 4.40 cmol/kg in the entire kola soils. The CEC in the low EC_a zone increased from 2.01 cmol/kg to 3.25 cmol/kg with a prevailing CEC of 2.64 cmol/kg. Mean CEC in the moderate ECa section was 3.97 cmol/kg, with a spread from 2.56 cmol/kg to 5.38 cmol/kg. Region of high EC_a has its CEC extending from 3.50 cmol/kg to 10.33 cmol/kg and the average capacity was 6.71 cmol/kg.

Proffitt (2014) affirmed that capacity less than 3 cmol/kg was categorised as low, which invariably suggests that the CEC in the low EC_a falls within the low class (Table 4.28). CEC in the moderate EC_a (3.97 cmol/kg) and high EC_a (6.71 cmol/kg) regions was classified to be within the moderate class, once the exchange capacity varies between 3 cmol/kg and 10 cmol/kg. Sonon *et. al* (2014) also established the possible clay types from the CEC values, the mean CEC value determined from kola soil suggests that the clay material that is holding the cations is kaolinite (Table 4.29).

It can be concluded that soils in the region of high EC_a are enriched with soil nutrient solution with less leaching effect (Sonon *et al*., 2014), thus, the kola trees within this zone are not subjected to nutrient deficiency compared to those in low EC_a area which has resulted in stunted growth due to lack of nutrients viable for plant growth. Soils with high CEC values have high elemental retention capacity and less susceptible to nutrient leaching (Mukungurutse *et al*., 2018) due to high proportion of colloids in them (McCauley *et al*., 2005). Soils with high CEC number are better to buffer or do not allow rapid changes in the level of soil solution of the contained nutrient (Crouse, 2018).

Base Saturation of Exchangeable Cation

Base saturation is the percentage of desire cation components in the entire cation exchange capacity. Soils in low EC_a segment have their base saturation in proportion of 70.23% to 86.18% with an average percentage of 77.87. In the moderate EC_a zone, the base saturation varied from 78.52% to 85.13% and the equitable saturation in this region was 81.82%. Area of high EC_a has an average saturation of 87.78%, its content extends from 79.43% to 96.68%. Considering the percentage base saturation across the

three EC_a zones, soils in high EC_a portion are more saturated and retained basic cations than other divisions, this signifies that the zone was more enriched with soil nutrient less prone to leaching of basic cation necessary for healthy growth of kola nut trees (Sonon *et al*., 2014).

Ca:Mg Dispersion

Dispersion ratio of calcium to magnesium in kola soils extends from 1 to 4 and the common ratio peculiar to these soils is 1.65. In the region of low EC_a, this ratio varied from 1 to 2 with a mean dispersion ratio of 1.5. Ca:Mg ratio in the moderate EC_a zone ranged from 1 to 2 and the relative ratio was 1.5. The most electrical conductive district has an equal ratio of 2.0 extending from 1 to 4. At a glance, the soil in this farm has Ca:Mg ratio to be less than two (<2) indicating a poorly structured soil (Botta, 2015). Based on the EC_a conductivity regions, soils in zones of low and moderate EC_a are poorly structured (<2) suggesting poor infiltration of water, leaching of soil nutrient due to erosion whereas soils in the high EC_a section are well structured supporting good aeration, infiltration and less susceptible to nutrient leaching. Magnesium has higher hydrated radius than calcium, when the ratio is less than two (<2), this indicates that the proportion of Mg is higher than the Ca component; it gets easily leached off the clay surface and sealing the surface and increasing run-off (Dontsova and Norton, 2001). On the other hand, calcium aids infiltration and percolation of water through soil, and promotes good aeration (Sonon *et al*., 2014).

Exchangeable Calcium Percentage

Percentage of calcium content in the region of low EC_a relative to the entire acidic and basic cations concentration extends from 29% to 47% with an equi-percentage of 35%. Region of moderate EC_a has its exchangeable calcium percentage varied from 33 to 50 and the peculiar calcium percentage was 42%. Percentage distribution of calcium in the cation exchange capacity within the high EC_a segment stretched from 31% to 51% and the average percentage of exchangeable calcium in this zone is 49%. Botta (2015) reported that the desirable range of exchangeable calcium percentage adequate for plant growth is situated between 65% and 80%. Evaluating the mean exchangeable calcium percentage in the three divisions, their %exchangeable Ca is not within the

desirable range indicating that the proportion in these zones is deficient for plant growth, although region of high EC_a has a higher percentage than other zones.

Percentage of Exchangeable Magnesium

The range of exchangeable magnesium percentage in the low EC_a section is between 22% and 40% with a mean percent of 27%. It varied between 24% and 32% in the moderate district with an average percent of 28%. Segment of high EC_a was characterised with percent exchangeable magnesium ranging from 16% to 40% and the common percent in this zone is 28%. The required percent of exchangeable magnesium for adequate plant growth is situated between 10% and 20% (Botta, 2015). None of the mean percentages is within this desirable limit, indicating excessive proportion of exchangeable magnesium relative to other cations present in the soil.

Exchangeable Potassium Percentage

Soils of low EC_a have their percentages of exchangeable potassium ranging from 5% to 14% with an equi-percentage of 8.5. Percentage of exchangeable potassium in soils of moderate EC_a ranged between 6.7% and 7% with an average of 6.9%. These percentages of exchangeable potassium in soils of high EC_a stretched from 3% to 15% with a mean percent of 5.9%. Using Botta (2015) desirable range of exchangeable potassium percentage (3%-8%) for efficient crop productivity, the mean percent of exchangeable potassium in soils of low EC_a (8.5%) was not within the limit suggesting excessive proportion of potassium relative to other cations. The mean percentages of exchangeable potassium in soils of moderate EC_a (6.9%) and high EC_a (5.9%) are within the desirable range (3%-8%) which aids plant growth around these sections.

Exchangeable Sodium Percentage (ESP)

The purpose of evaluating the sodium percentage was to establish either the sodic or non sodic nature of soils. ESP in soils of low EC_a varied from 5.7% to 9.0% and the prevailing percentage in this zone was 7.0%. Section of moderate EC_a was characterised with ESP varying from 4.6% to 5.9% and the mean ESP was 5.3%. The mean percent of exchangeable sodium in soils of high EC_a was computed to be 4.0% and these percentages extends from 2.6 to 6.6.

Considering the mean ESP across the three divisions, mean ESP (7.0%) in the low EC_a segment was regarded to be sodic (>6%) indicating that the soils are characterised with poor aeration, poor water infiltration and they are susceptible to dispersion once wet (Botta, 2015). Soils in moderate EC_a and high EC_a with mean ESP of 5.3% and 4.0% respectively are considered to be non-sodic supporting kola trees' growth due to the presence of well aerated soil, good drainage and less susceptible to soil erosion via rainfall.

4.7.2 Soil Nutrients Influencing the Measured Field Electrical Conductivity in the Soils

(i) **Cacao Farm**

Reliability of the field measured EC_a was checked by correlating its data with that of the laboratory determined EC. Strong positive correlation (R) exists between the field EC_a data and laboratory determined EC (Figs. 4.53a and b), having coefficients of 0.8 and 0.7 in the wet and dry season respectively. Coefficient of determination (R^2) shows that 60.5% and 42.4% of the data were involved in the correlation during the wet and dry season respectively. Thus, it validates the effectiveness of the field EC_a data as a useful proxy of assessing soil productivity.

Relating the field EC_a data with the percentage organic carbon in soil (Figs. 4.54a and b), a weak positive correlation was established between the percentage organic carbon with the EC_a obtained in the wet and dry season with coefficients of 0.3 at both seasons. Determination coefficient indicates that 6.0% and 6.4% of the data correlate perfectly with one another. Positive correlation exists between EC_a and dissolved organic carbon (Monteiro *et al*., 2013) and it was concluded that EC_a is a useful proxy in estimating dissolved organic concentration which serves as a low cost alternative monitoring tool. Similar correlation was observed with percentage organic matter, 1.724 is the factor used in converting organic carbon to organic matter value by multiplying the factor with the values of organic carbon. Organic matter aids in modifying soil quality by stablising soil structure, decreases soil compaction and limiting soil erosion resulting in crop growth and its productivity (Ozlu and Kumar, 2018).

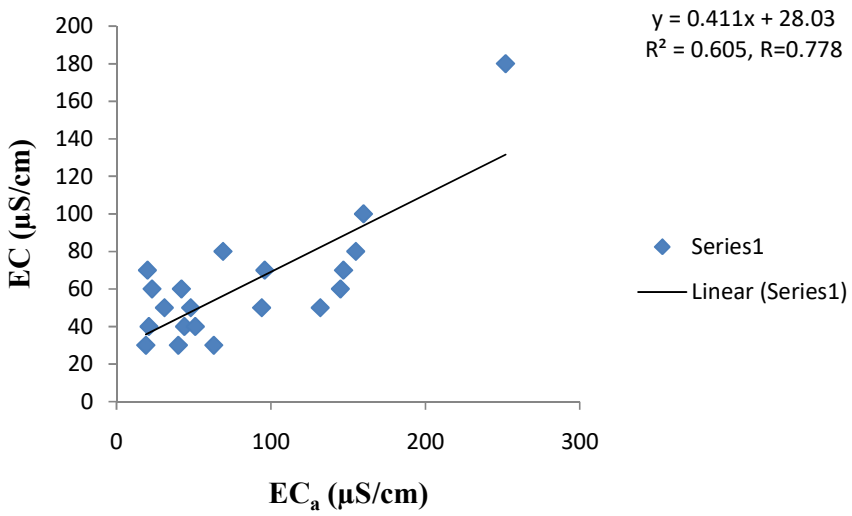

Figure 4.53a: Relationship between field EC_a and laboratory EC in the soils of cacao farm during the wet season

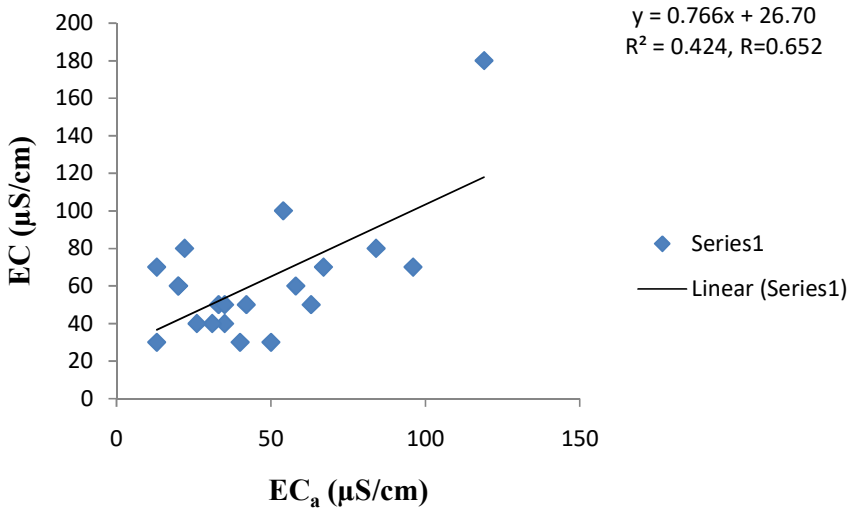

Figure 4.53b: Relationship between field EC_a and laboratory EC in the soils of cacao farm during the dry season

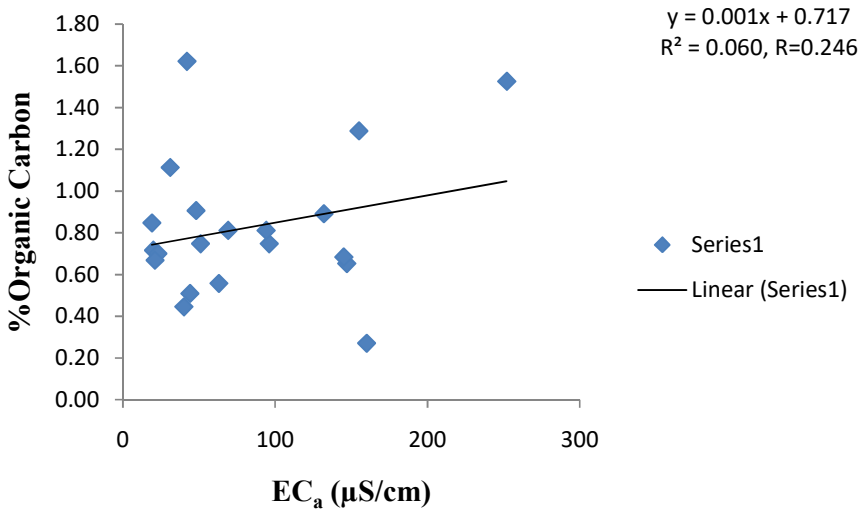

Figure 4.54a: Relationship between field EC_a and percentage organic carbon in the soils of cacao farm during the wet season

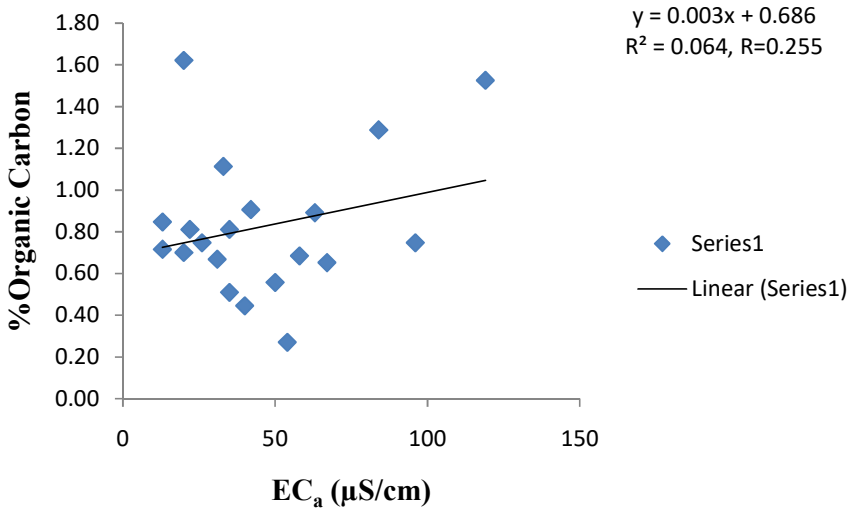

Figure 4.54b: Relationship between field EC_a and percentage organic carbon in the soils of cacao farm during the dry season

Weak interaction was observed between the % total nitrogen and EC_a, and its correlating coefficient was 0.2 at both seasons (Figs. 4.55a and b) while its coefficients of determination are 0.052 and 0.048 in wet and dry season respectively. Miyamoto *et al.,* (2015) concluded that there is reasonable agreement between soil nitrate-nitrogen (NO_3-N) concentrations with the EC measured with time domain reflectometry (TDR), that is, change in NO_3-N concentration influences EC measurement. Nitrogen-containing compounds are regarded as weak bases characterised with less conductivity (Nord, 2018) and exhibited positive correlation with apparent electrical conductivity (Heil and Schmidhalter, 2017).

Negative correlation was observed from the interaction of available phosphorus with EC_a, though a moderate coefficient was generated varying between -0.4 and -0.5 in the wet and dry season respectively (Figs. 4.56a and b). This is consistent with the findings of Mueller *et al*. (2003) in which negative correlation occurred between phosphorus and EC for soil assessment conducted at shallow depth (30 cm). Kim *et al*. (2007) observed that the concentration of phosphorus increases under anaerobic condition and for direct relationship to occur between phosphorus concentration and EC, denitrification must take place in advance before the release of phosphorus. Thus, negative correlation gives an indication that phosphorus is not contributing to the rise in EC_a value measured in the cacao farm.

Positive interaction was observed between the acidic cation and EC_a with moderate coefficients of 0.4 and 0.6 in the wet and dry periods respectively (Figs. 4.57a and b). Presence of acidic cations aids the conductivity of the media. Soil acidity tends to build-up hydrogen and aluminium cations in soil when the base cations are leached and replaced by aluminium or hydrogen ions (FAO & ITPS, 2015). These cations are not plant nutrient, soil with high level of acidic cations tends to lower the pH, thereby increasing the toxicity (Botta, 2015) but the measured soil pH in the farm is within tolerance range for plant growth.

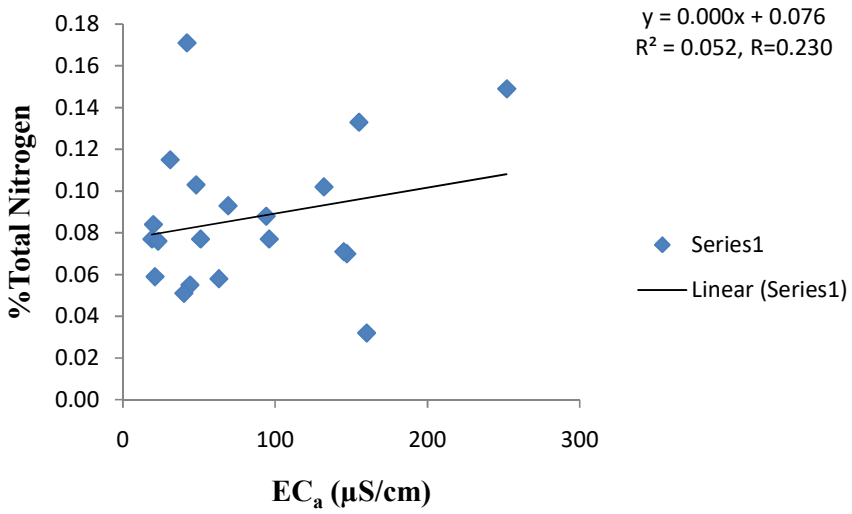

Figure 4.55a: Relationship between field EC_a and percentage total nitrogen in the soils of cacao farm during the wet season

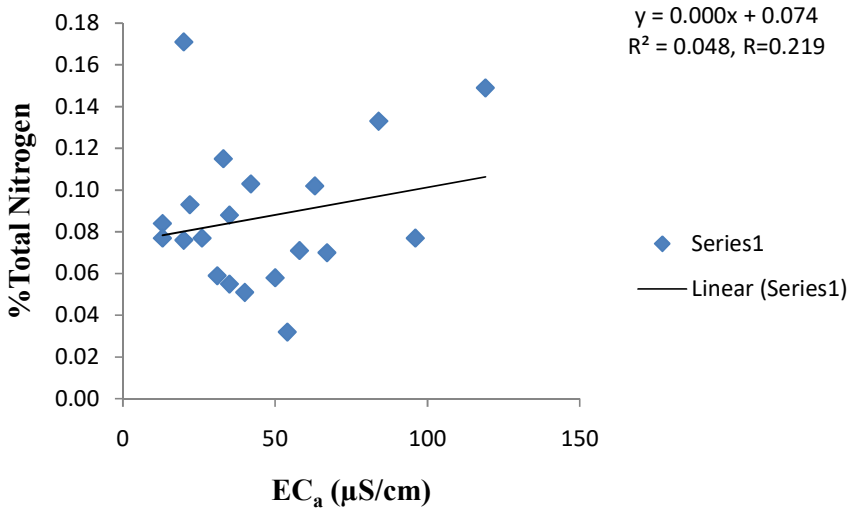

Figure 4.55b: Relationship between field EC_a and percentage total nitrogen in the soils of cacao farm during the dry season

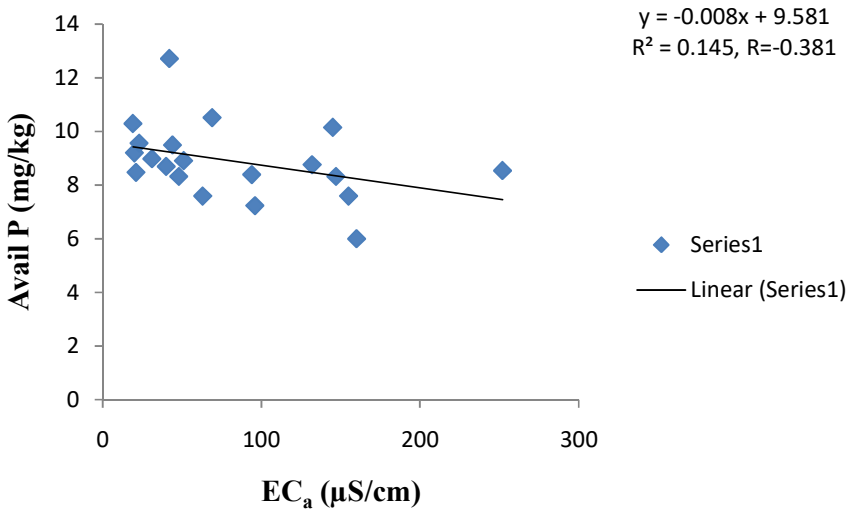

Figure 4.56a: Relationship between field EC_a and available phosphorus in the soils of cacao farm during the wet season

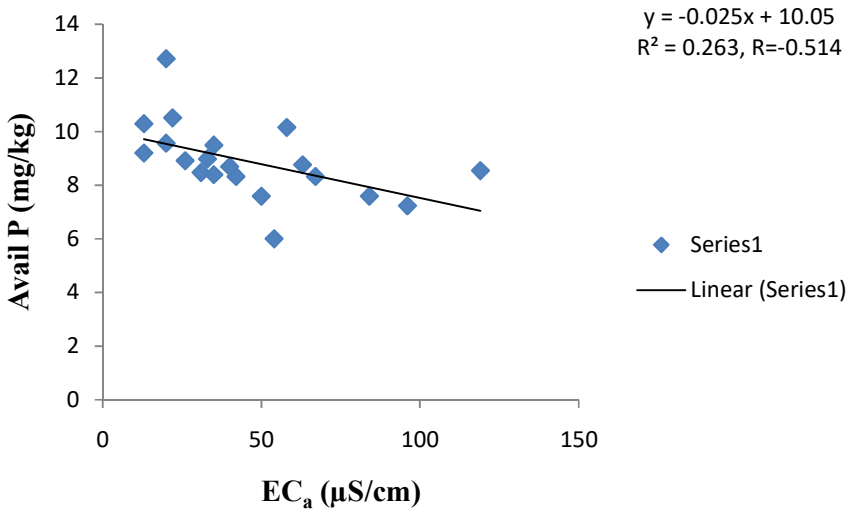

Figure 4.56b: Relationship between field EC_a and available phosphorus in the soils of cacao farm during the dry season

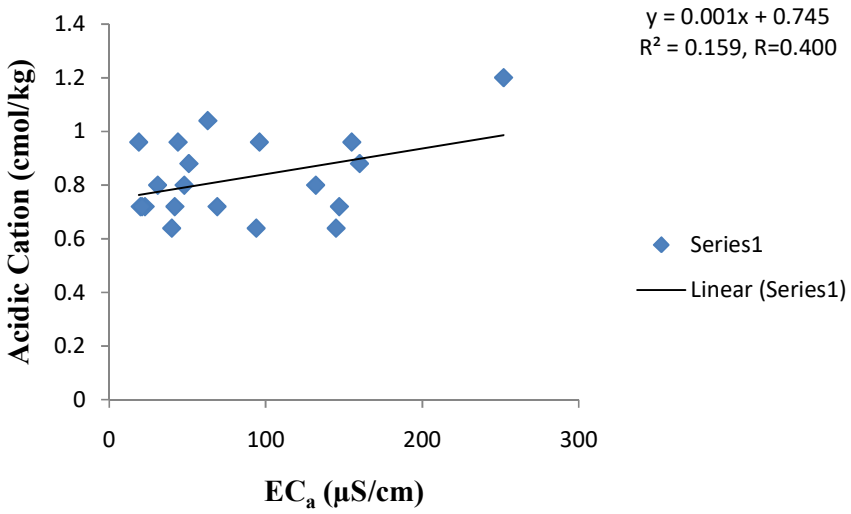

Figure 4.57a: Relationship between field EC_a and acidic cation in the soils of cacao farm during the wet season

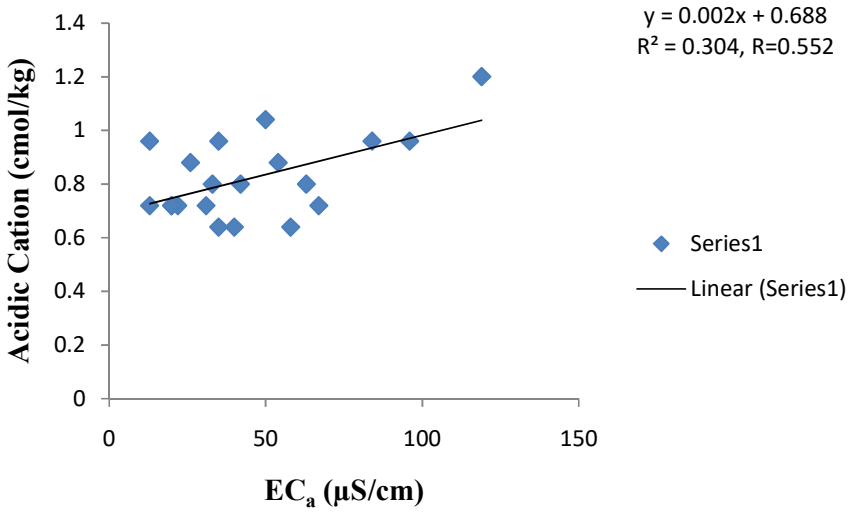

Figure 4.57b: Relationship between field EC_a and acidic cation in the soils of cacao farm during the dry season

Strong positive relationship iwas noticed between calcium and EC_a in the wet and dry seasons with coefficient of 0.9 and 0.7 respectively (Figs. 4.58a and b). 71.4% and 55.1% of the data were perfectly engaged in the correlation exercise in which there was great chunk of the ions participating in the fluid conductivity. Medeiros *et al*. (2018) also reported positive correlation between calcium and EC measured at depth 20 cm, 40 cm and 60 cm. Also positive correlations were reported from its interaction with apparent electrical conductivity by Peralta and Costa (2013), Heil and Schmidhalter (2017). This suggests that Ca is one of the dominant divalent ions in soil solution as a result of its large hydrated radius responsible for its easy dislodge from soil charges-CEC (Gransee and Führs, 2013).

Coefficient of determination (R^2) indicates that 39.0% and 42.9% of the magnesium ions were involved in determining the coefficient of correlation between the two parameters. Strong positive coefficient was generated from their interaction (Korsaeth, 2005; Rodríguez-Pérez *et al.,* (2011)), and their coefficients (Figs. 4.59a and b) are 0.6 and 0.7 in the wet and dry periods respectively. Although group II metals are not good conductor as group I metals but due to S-P hybridisation in which the S and P electron shells overlap, this avail the metal access to the unfilled P-subshell and finally aiding its electrical conductivity (Garcia and Damask, 1991). Magnesium has smaller ionic radius compare to that of Ca, K and Na, and its hydrated radius is larger, this made magnesium to be less strongly bounded to soil charges which was responsible for higher magnesium concentration in soil solution with increasing mobility and the mobility leads to electrical conductivity (Gransee and Führs, 2013).

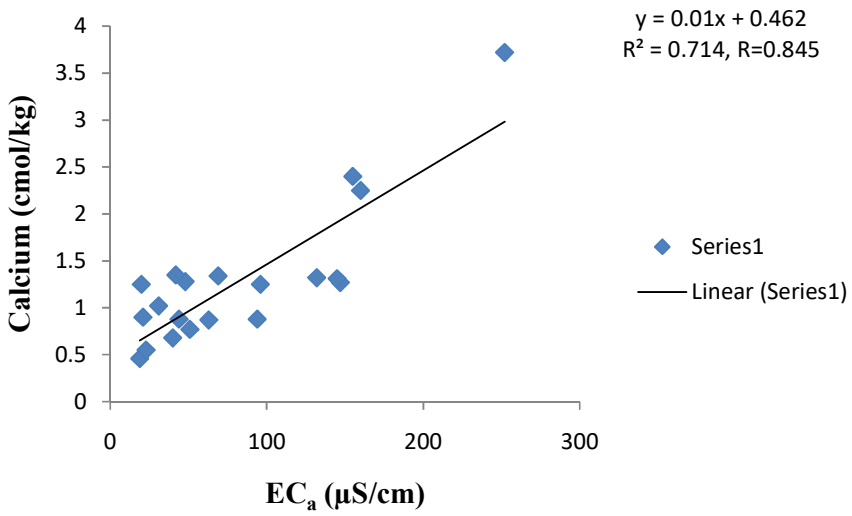

Figure 4.58a: Relationship between field EC_a and calcium in the soils of cacao farm during wet season

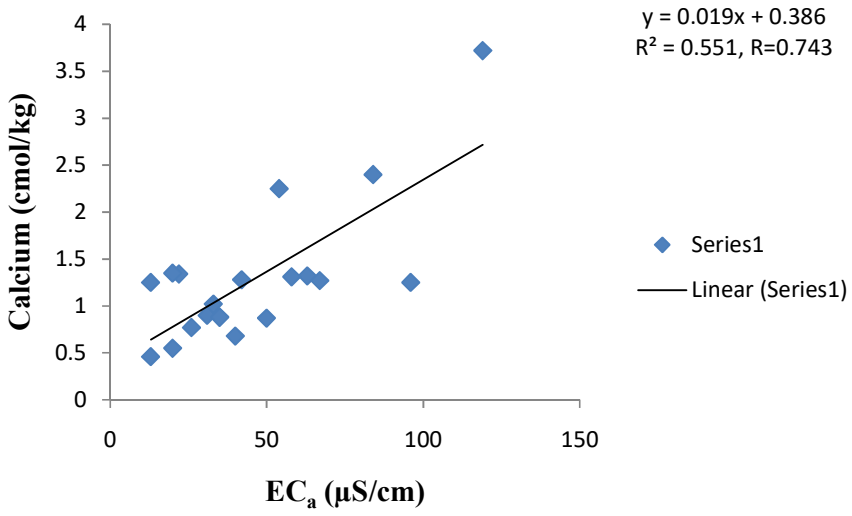

Figure 4.58b: Relationship between field EC_a and calcium in the soils of cacao farm during the dry season

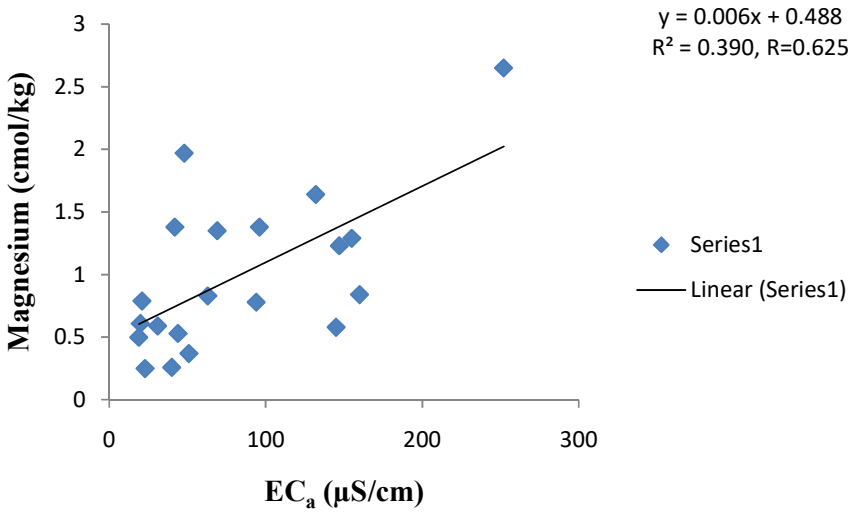

Figure 4.59a: Relationship between field EC_a and magnesium in the soils of cacao farm during the wet season

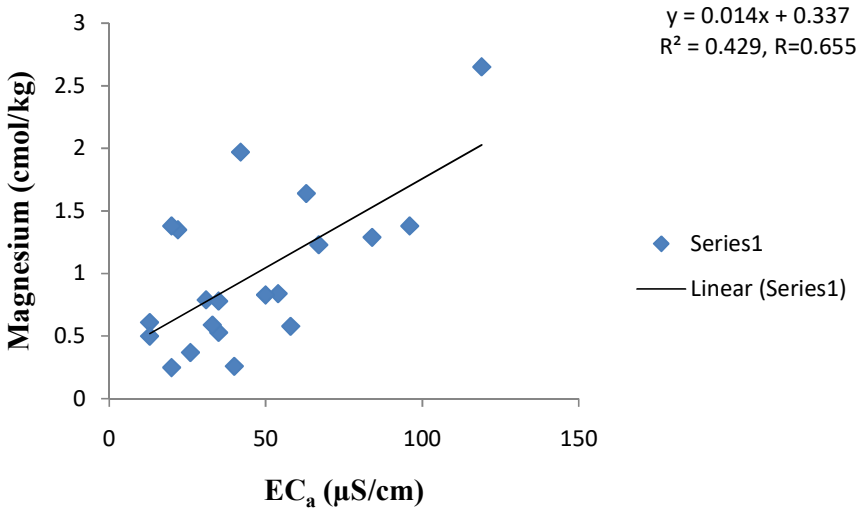

Figure 4.59b: Relationship between field EC_a and magnesium in the soils of cacao farm during the dry season

Weak positive correlation was established from the interaction of potassium ions with the electrical conductivity (EC_a), resultant coefficients of 0.3 were generated from the interaction at both seasons (Figs. 4.60a and b). 6.2% and 8.0% of potassium and EC_a data were matched perfectly with each other in the wet and dry periods respectively. This gives an indication that it has a less influence on the conductivity of the medium. Its strong adsorption onto clay surface was due to decrease in hydrated radius compare to other cations ($<Na^{+}<Ca^{2+}<Mg^{2+}<Al^{3+}$) (Gransee and Führs, 2013). Potassium contributes less to the conductivity of the soil medium as suggested by the coefficient of determination because of its reduced mobility in which it is strongly adsorbed onto clay surface (Olson-Rutz and Jones, 2018).

Contribution of Na^{+} ions to the conductivity of soil unit in the farm was regarded as weak, as determined from the cross plot of its data with the measured EC_a, its coefficient was 0.3 at both seasons (Figs. 4.61a and b). 9.5% and 6.6% of the data fit perfectly, thus its influence on the conductivity of soil solution is less. UNSW (2007) reported that cations with small hydrated radii are strongly adsorbed onto clay surface because adsorption strength increases with decreasing hydrated radius of cation.

Cation exchange capacity (CEC) was derived from the combination of the acidic cation and basic cations. Correlating the CEC with the EC_a, a strong positive relationship was deduced with resultant coefficients of 0.8 at both seasons (Figs 4.62a and b). Data interaction shows 61.1% and 57.4% of EC_a and CEC data matched completely, suggesting a greater influence on the measured EC_a. Positive correlations were also reported by Korsaeth (2005) and Peralta and Costa (2013).

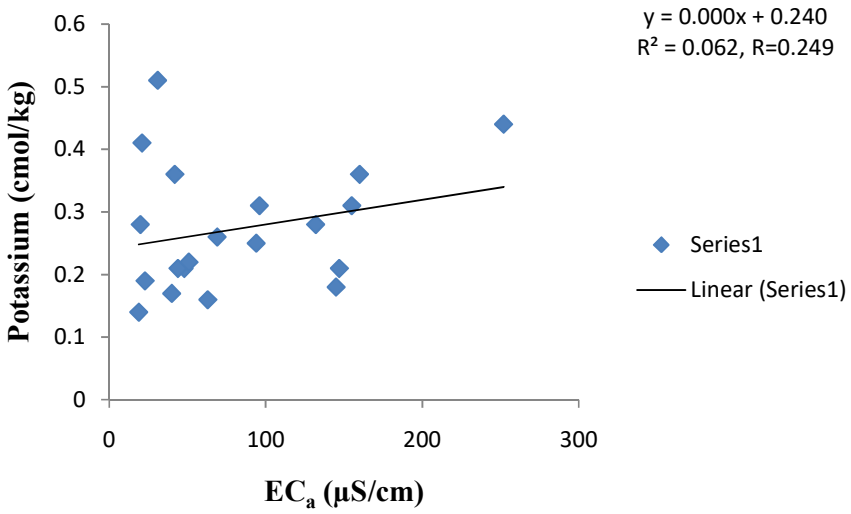

Figure 4.60a: Relationship between field EC_a and potassium in the soils of cacao farm during the wet season

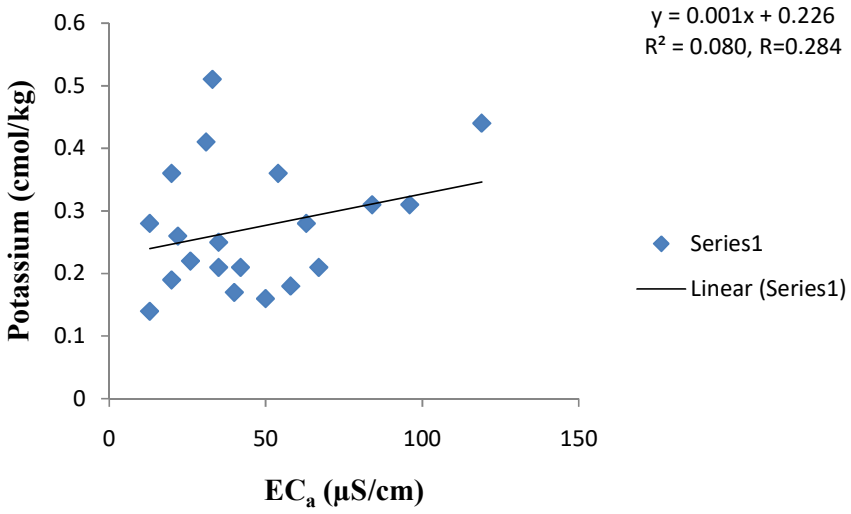

Figure 4.60b: Relationship between field EC_a and potassium in the soils of cacao farm during the dry season

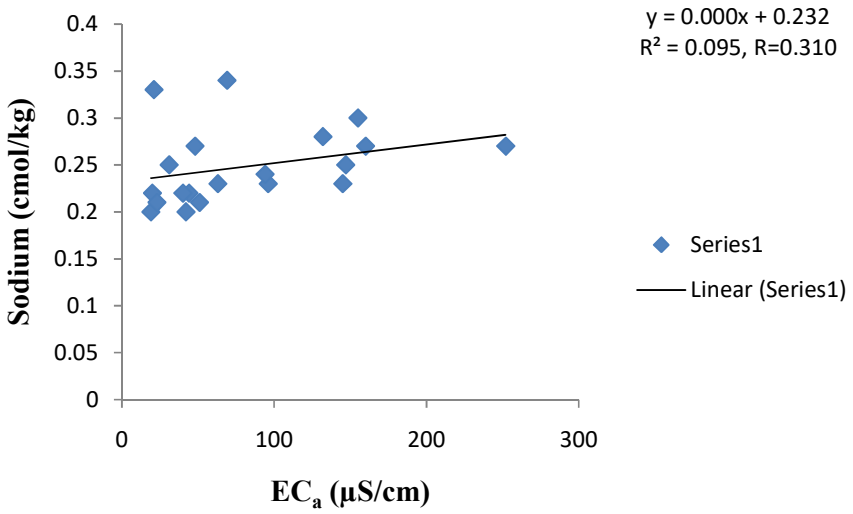

Figure 4.61a: Relationship between field EC_a and sodium in the soils of cacao farm during the wet season

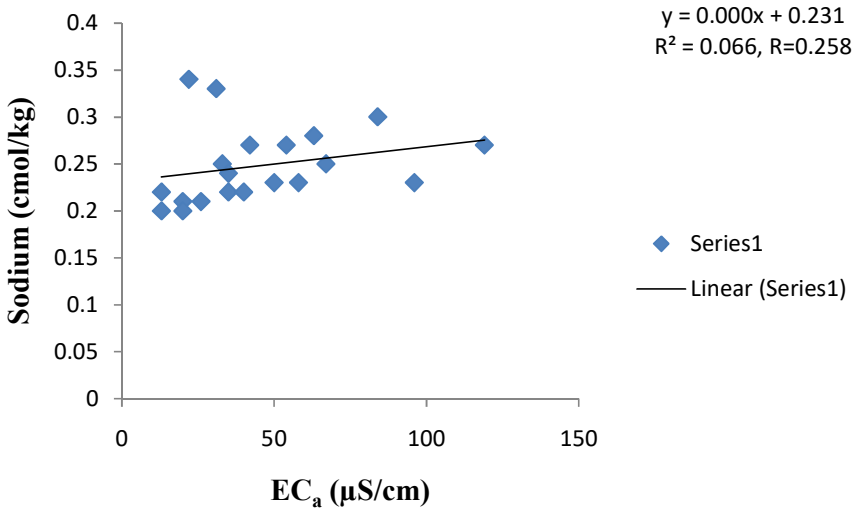

Figure 4.61B: Relationship between field EC_a and sodium in the soils of cacao farm during the dry season

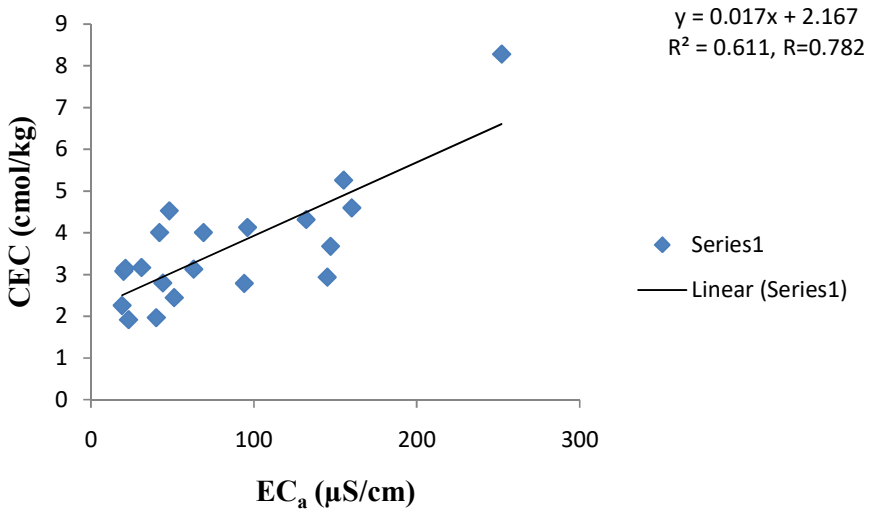

Figure 4.62a: Relationship between field EC_a and cation exchange capacity in the soils of cacao farm during the wet season

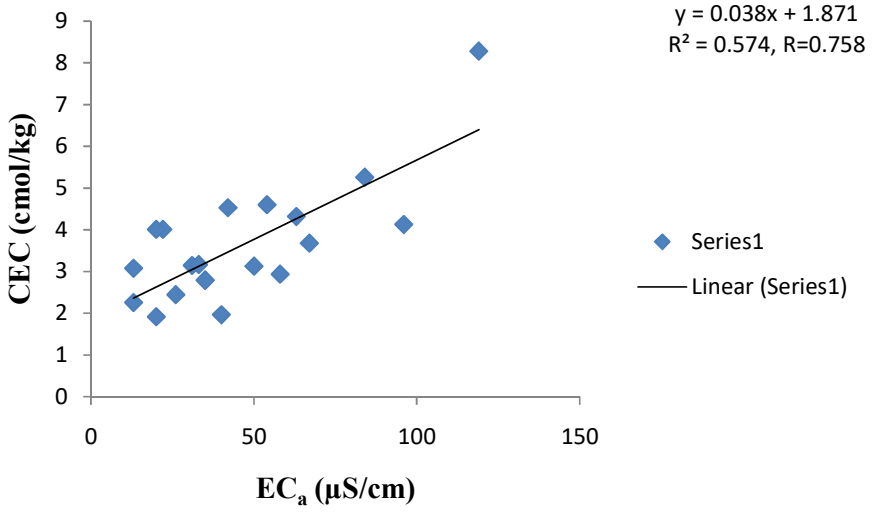

Figure 4.62b: Relationship between field EC_a and cation exchange capacity in the soils of cacao farm during the dry season

(ii) **Kola Farm**

An attempt was made to determine the efficiency and effectiveness of EC_a values obtained via field measurement by correlating it with the laboratory determined EC readings in order to validate its reliability as useful soil fertility check. Strong positive coefficients were deduced from their interaction in the wet (0.733) and dry (0.765) seasons. Also 53.8% and 58.5% of the data were involved in establishing the correlation (Figs 4.63a and b).

A very weak correlation coefficient was generated from the relationship between EC_a and organic carbon percentage; the values (Figs 4.64a and b) include 0.019 and 0.096 in the wet and dry seasons respectively, determination coefficient showed that a negligible part of data partook in the correlation analysis. Clarke *et al*. (2005) and Monteiro *et al*. (2013) reported that positive correlation existed from the interaction of EC with the dissolved organic carbon, more so organic anions are weak acids contributing to the acidity of soil solution and that EC is a reliable tool in assessing organic carbon present in a medium. Similar output will be generated for the interaction between EC_a and organic matter as noted with the organic carbon because organic carbon can be converted to organic matter through a conversion factor of 1.724, therefore similar correlation trend will be established. Ozlu and kumar (2018) suggested that the presence of organic matter in soil will result in soil compaction decrease which restricts soil erosion thereby establishing a stabilised soil structure.

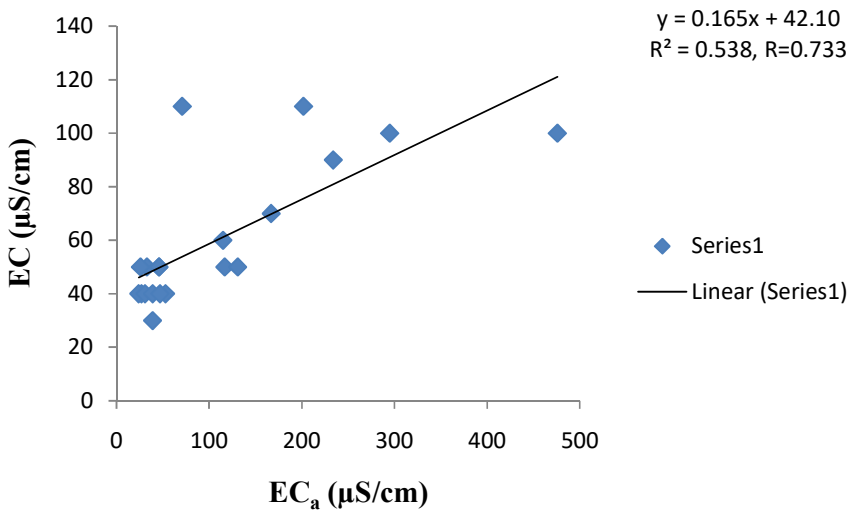

Figure 4.63a: Relationship between EC-lab and field EC_a in the kola farm during the wet season

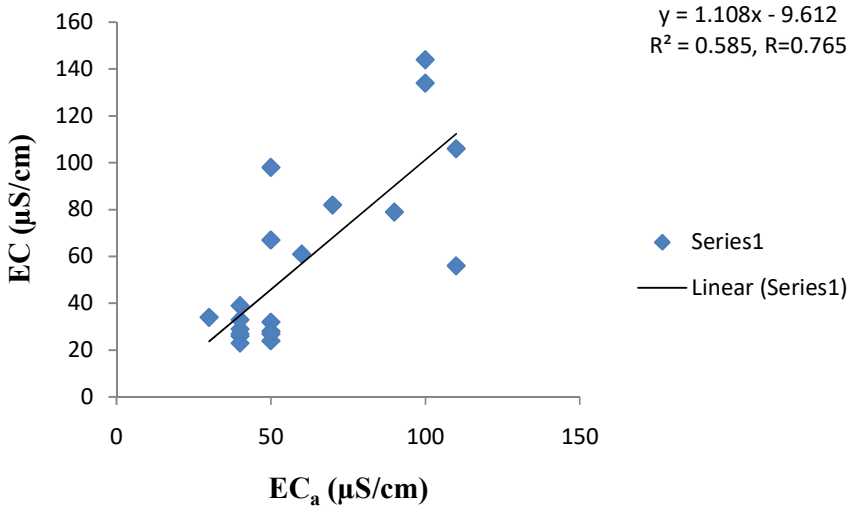

Figure 4.63b: Relationship between EC-lab and field EC_a in the kola farm during the dry season

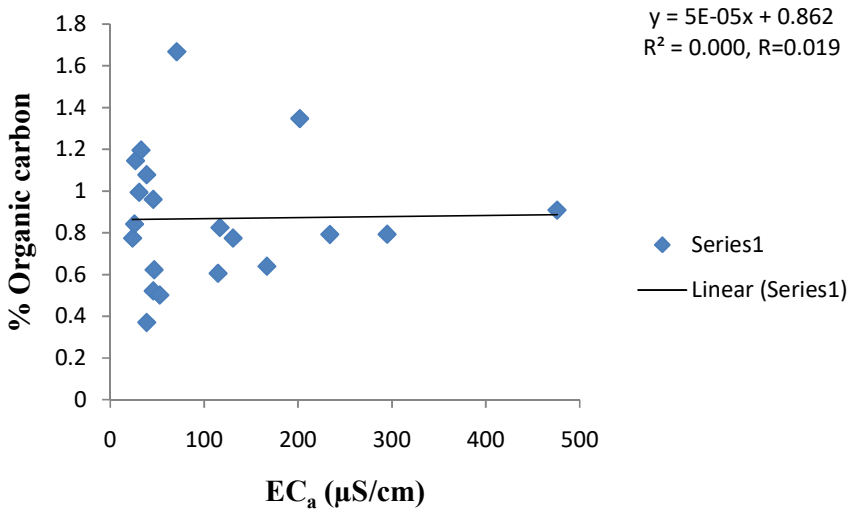

Figure 4.64a: Relationship between field EC_a and percentage organic carbon in the soils of kola farm during the wet season

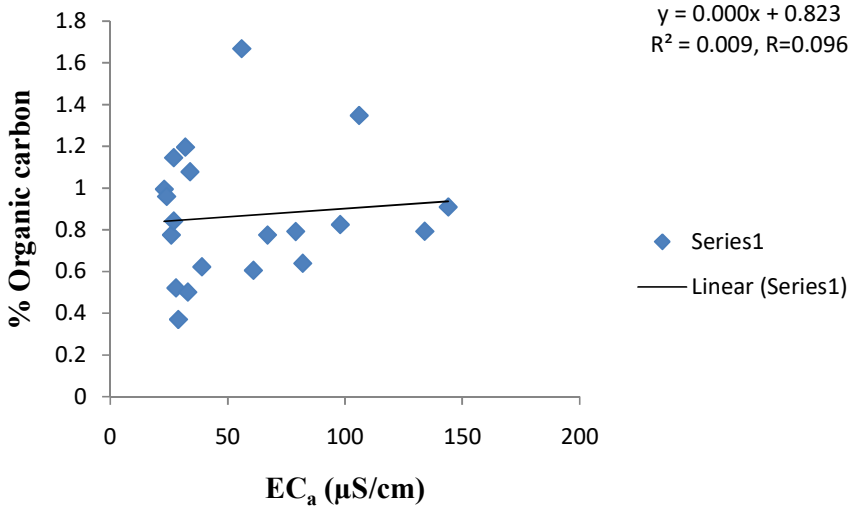

Figure 4.64b: Relationship between field EC_a and percentage organic carbon in the soils of kola farm during the dry season

Weak relationship exists between the ECa and the total nitrogen in kola soil such that the coefficients (R) were 0.134 and 0.215 in the wet and dry periods respectively (Figs 4.65a and b). Coefficients of determination (R^2) in the wet and dry periods were 0.018 and 0.046 respectively. Findings of Pearce and Palmer (1999) and Heil and Schmidhalter (2017) also supported the positive relationship projected from concentration of nitrogen with EC_a. Nemali (2018) also reported similar trend such that rise in nitrogen-concentration led to an increase in electrical conductivity.

Electrical conductivity recorded from the field was not being influenced by the concentration of phosphorus content in the soil. Moderate correlation occurred between EC_a and available phosphorus but negative coefficients were observed from their interaction, -0.455 and -0.413 in the wet and dry periods respectively (Figs 4.66a and b). Determination coefficient relates the percentage of data involved in the analysis to be 20.7% in the wet season and 17.0% in the dry season. Negative correlation was reported by Kim *et al*. (2007) between EC and concentration of phosphorus and that denitrification must have taken place ahead before phosphorus was released so that direct interaction can occur between EC and phosphorus.

The result of the correlation analysis showed that weak positive coefficients were generated from interaction of EC_a with acidic cation, 0.096 and 0.152 in the wet and dry season (Figs 4.67a and b) respectively. Approximately 1.0% and 2.3% of the data were perfectly marched as observed from the coefficient of determination. Acidic cations are not required plant nutrient, their concentration could be hazardous to plant growth when the pH value is below 5.5 (Botta, 2015) because acidic cation tends to replace the leached base cation thereby resulting in soil acidity (FAO and ITPS, 2015). The weak correlation coefficients as well as the measured mean pH value of 6.92 in the kola soil indicate that acidic cation is not contributing greatly to the electrical conductivity of the soil medium.

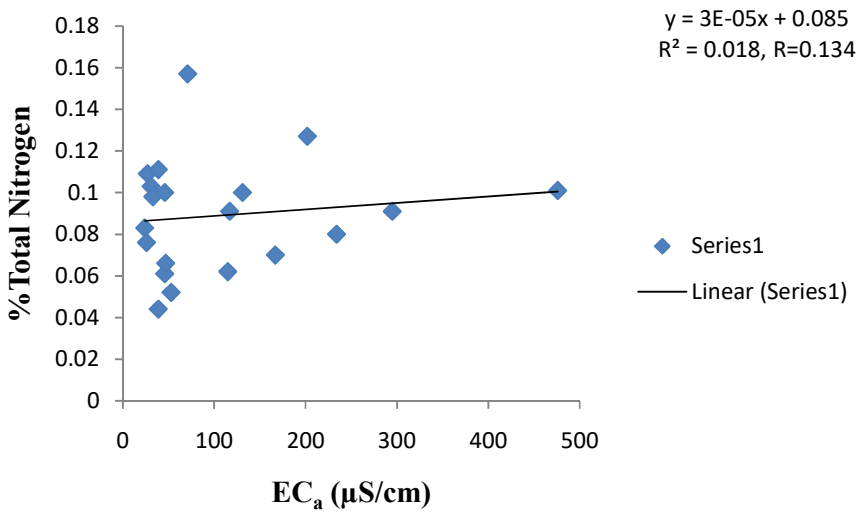

Figure 4.65a: Relationship between field EC_a and percentage total nitrogen in the soils of kola farm during the wet season.

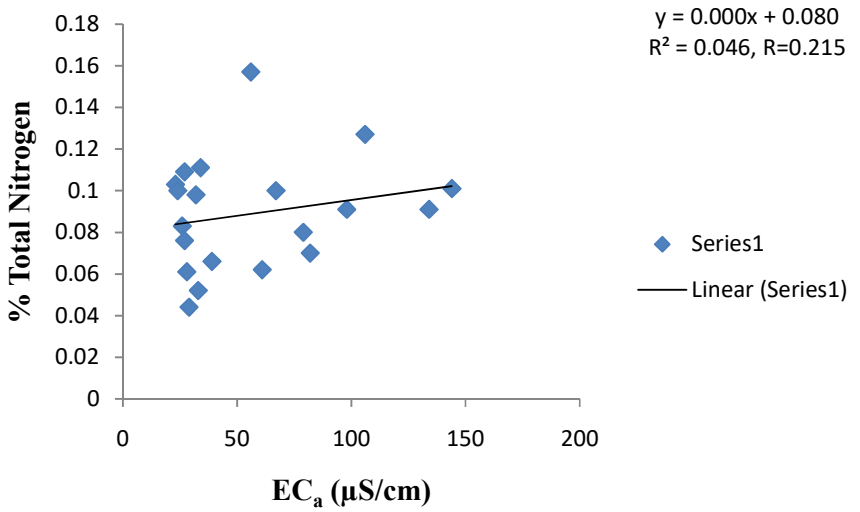

Figure 4.65b: Relationship between field EC_a and percentage total nitrogen in the soils of kola farm during the dry season

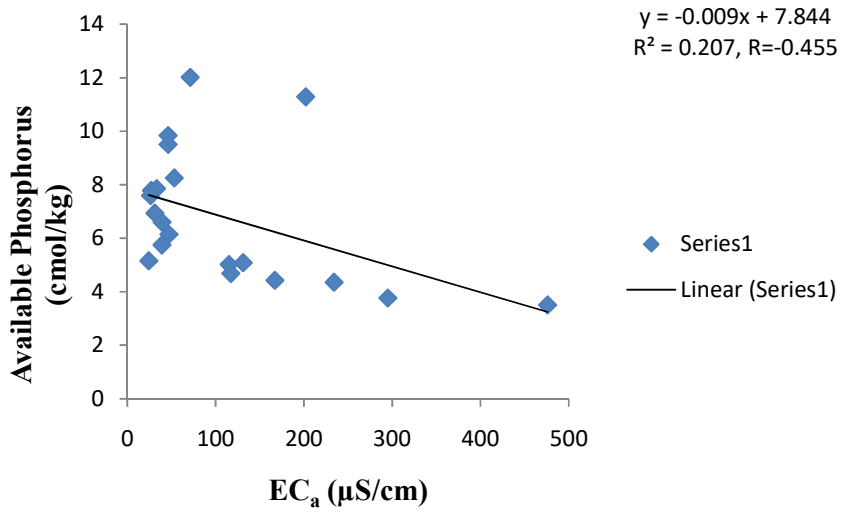

Figure 4.66a: Relationship between field EC_a and available phosphorus in the soils of kola farm during the wet season

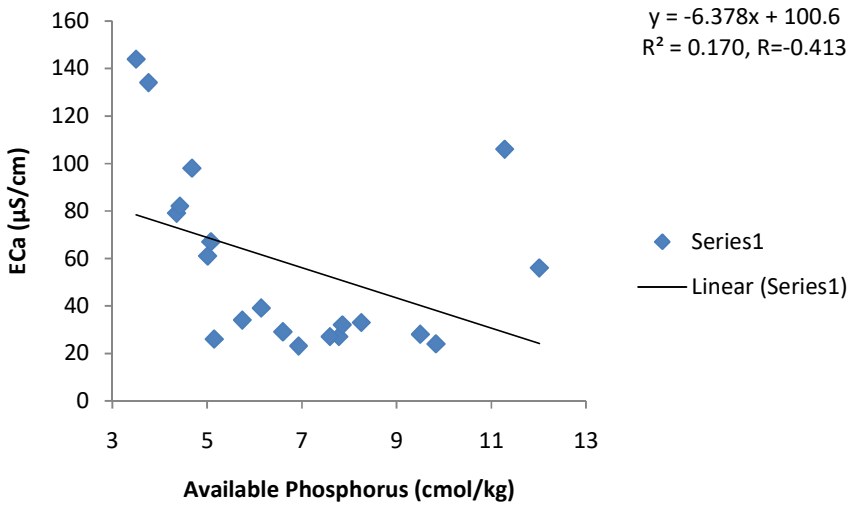

Figure 4.66b: Relationship between field EC_a and available phosphorus in the soils of kola farm during the dry season

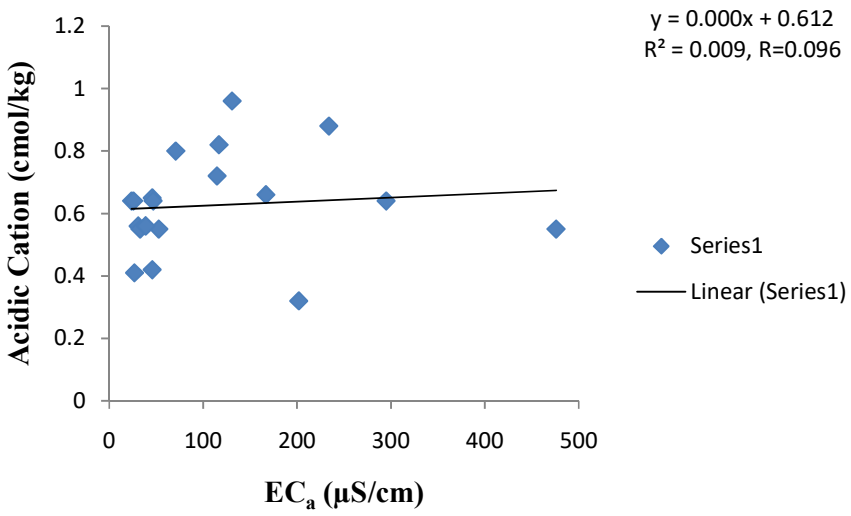

Figure 4.67a: Relationship between field EC_a and acidic cation in the soils of kola farm during the wet season

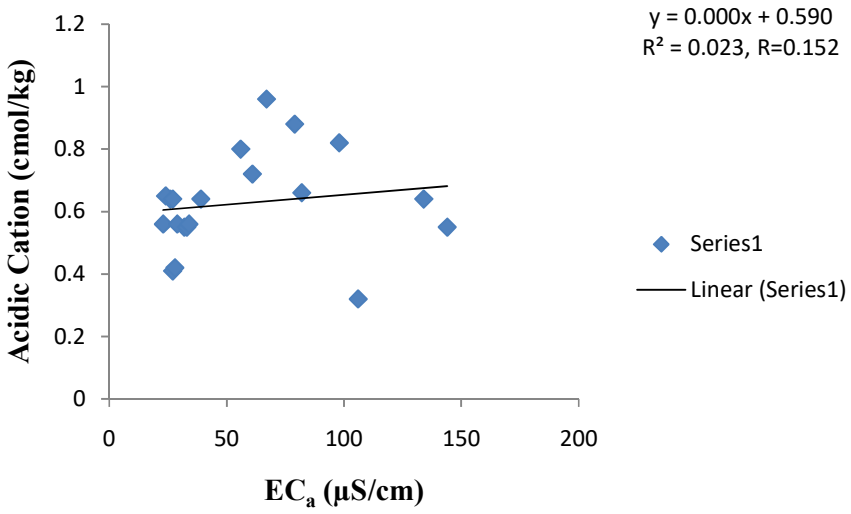

Figure 4.67b: Relationship between field EC_a and acidic cation in the soils of kola farm during the dry season

Percentage of data engaged in relating calcium with EC_a varied between 82.65% and 84.6% for both seasons (Figs 4.68a and b), with strong correlation coefficients of 0.909 and 0.920 in the wet and dry seasons respectively. Mobility of calcium ions is due to its high hydrated radius (0.410) which made it to be easily dislodged from clay surface while cations with small hydrated radius are strongly adsorbed onto the class surface (UNSW, 2007), thereby aiding the conductivity of the medium. Sonon *et al*. (2015) reported that plants growth will not be restricted in the presence of abundance of calcium ions due to the fact that it promotes good aeration and aids water infiltrating the soil medium; invariably connoting that those soils in high EC_a support healthy growth of kola trees.

Strong positive correlation was also generated from the relationship between magnesium and EC_a, such that the coefficients were 0.895 and 0.921 in the wet and dry periods respectively (Figs 4.69a and b). Percentages of 80.1% and 84.8% of the data were related together from the interaction of magnesium ions in soils with the EC_a data acquired during wet and dry seasons respectively. Positive correlation was also noticed by Rodríguez-Pérez *et al.,* (2011). Magnesium is one of the dominant divalent cations, because of its high hydrated radius (0.430) according to UNSW (2007) which made it to detach from the soil charges, and therefore resulting in high mobility (Gransee and Führs, 2013). Mobility of water-soluble magnesium increases with an increase in water content aiding its migration which is dependent on soil texture and rainfall (Yan and Hou, 2018).

Nearly uniform coefficients were generated from the relationship of EC_a with potassium at both seasons; a coefficient of 0.530 was deduced from their interaction in the wet period and 0.536 in the dry section (Figs 4.70a and b) and the correlation was moderate. 28.1% and 28.6% of the data involved in the interaction matched perfectly. Potassium has the least hydrated radius (0.33) compare to other cations in group 1 and group 2 (UNSW 2007). It is strongly adsorbed onto the clay surface due to its hydrated radius, its mobility is a function of soil texture, and it is highly mobile in coarse sand, moderate in loam soil and less in clay soil (Oldham, 2015).

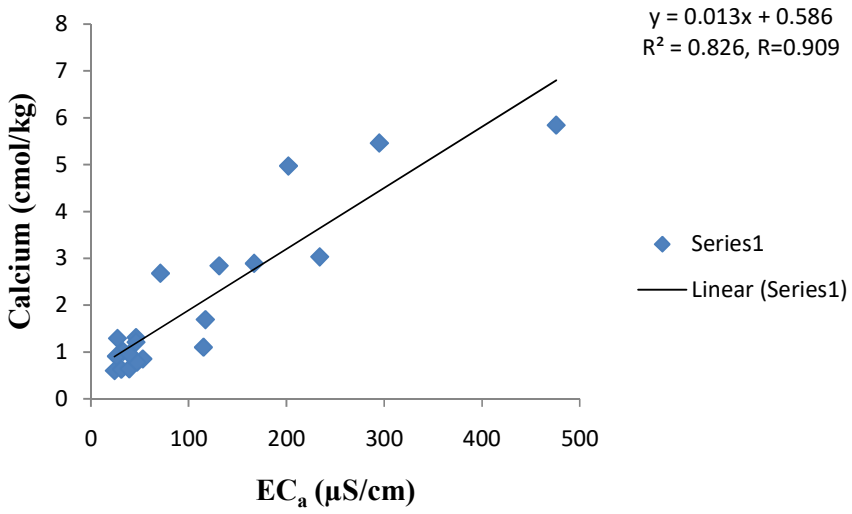

Figure 4.68a: Relationship between field EC_a and calcium in the soils of kola farm during the wet season

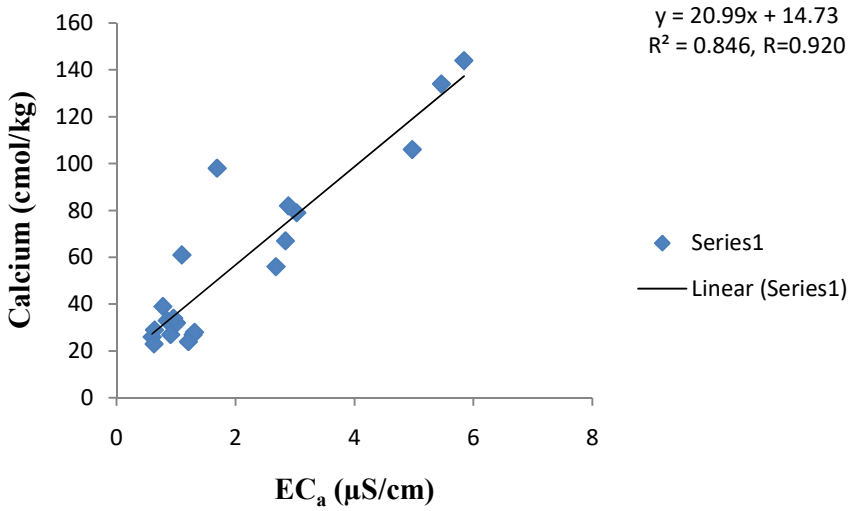

Figure 4.68b: Relationship between field EC_a and calcium in the soils of kola farm during the dry season

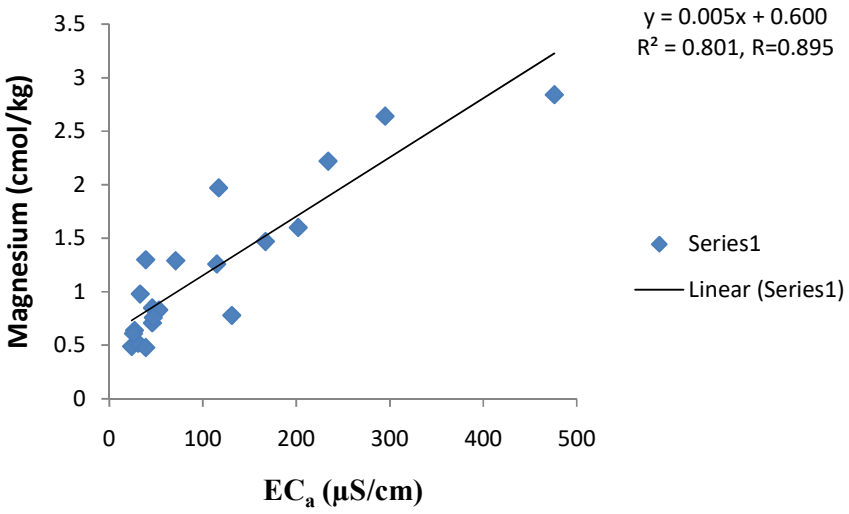

Figure 4.69a: Relationship between field EC_a and magnesium in the soils of kola farm during the wet season.

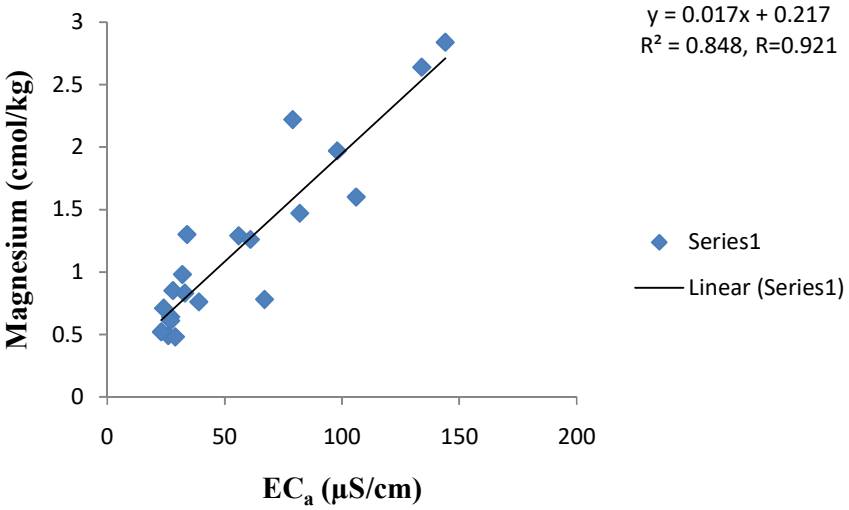

Figure 4.69b: Relationship between field EC_a and magnesium in the soils of kola farm during the dry season.

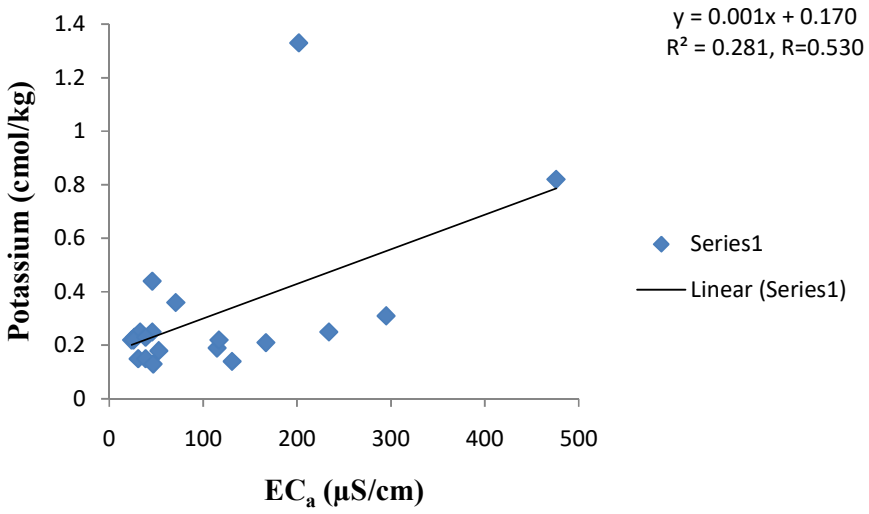

Figure 4.70a: Relationship between field EC_a and potassium in the soils of kola farm during the wet season.

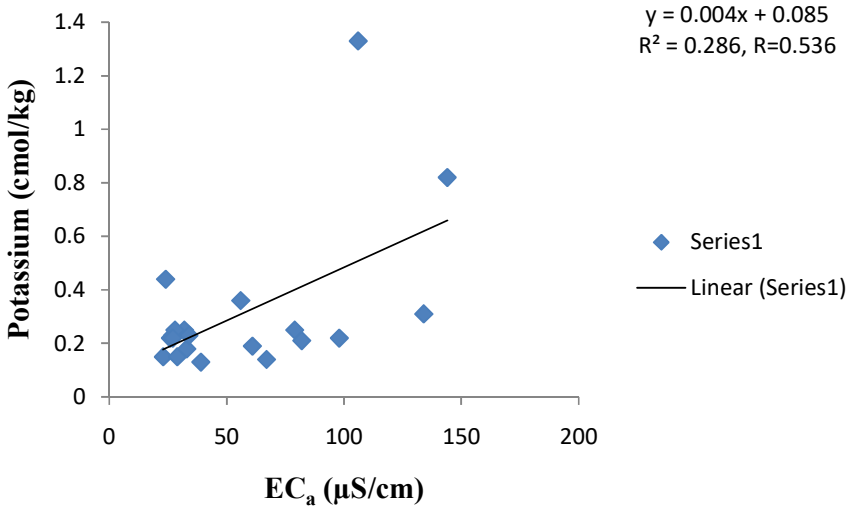

Figure 4.70b: Relationship between field EC_a and potassium in the soils of kola farm during the dry season.

Coefficients of 0.583 and 0.673 were generated from the interaction of sodium with EC_a values measured in the wet and dry seasons respectively (Figs 4.71a and b). Determination coefficient from the plot of sodium values obtained via chemical assessment of the soil with the measured EC_a values in the wet and dry season were 34.0% and 45.3% respectively. Its hydrated radius was 0.36 (UNSW, 2007) and also has high affinity to be adsorbed onto clay surface but not as strong as that of the potassium.

A very strong correlation exists between cation exchange capacity (CEC) and EC_a value, coefficients of 0.930 and 0.951 occurred from their interaction in the wet and dry seasons respectively (Figs 4.72a and b). 86.5% and 90.4% of these parameters were engaged in the plot suggesting majority of cations (acidic and base) were contributing to the electrical conductivity measured in the soil medium. Positive correlations were reported from the interaction of CEC with EC_a by Korsaeth (2005), and Heil and Schmidhalter (2017).

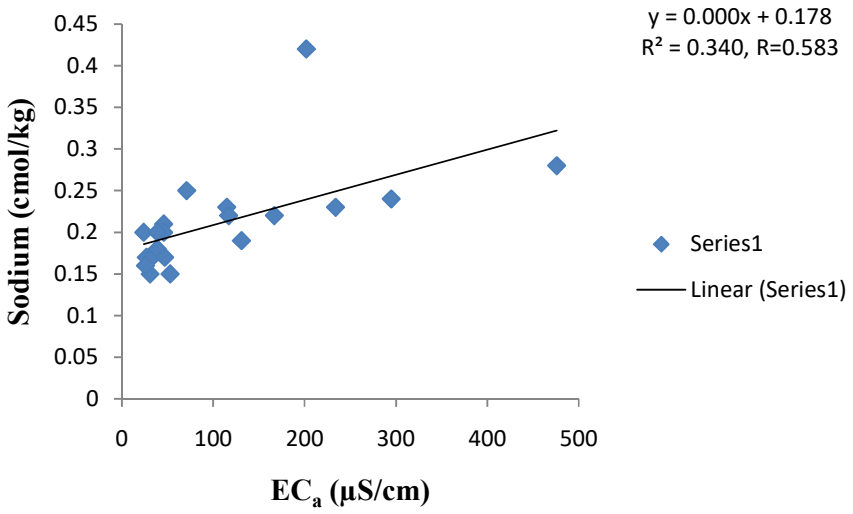

Figure 4.71a: Relationship between field EC_a and sodium in the soils of kola farm during the wet season.

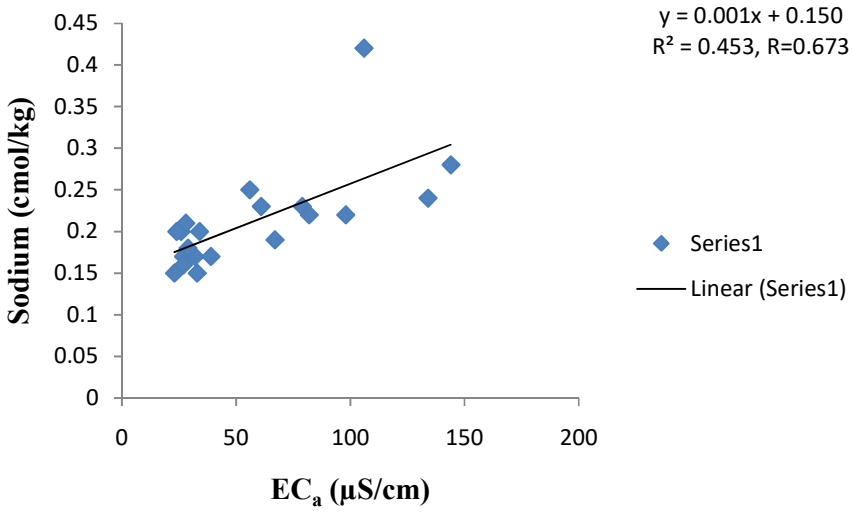

Figure 4.71b: Relationship between field EC_a and sodium in the soils of kola farm during the dry season.

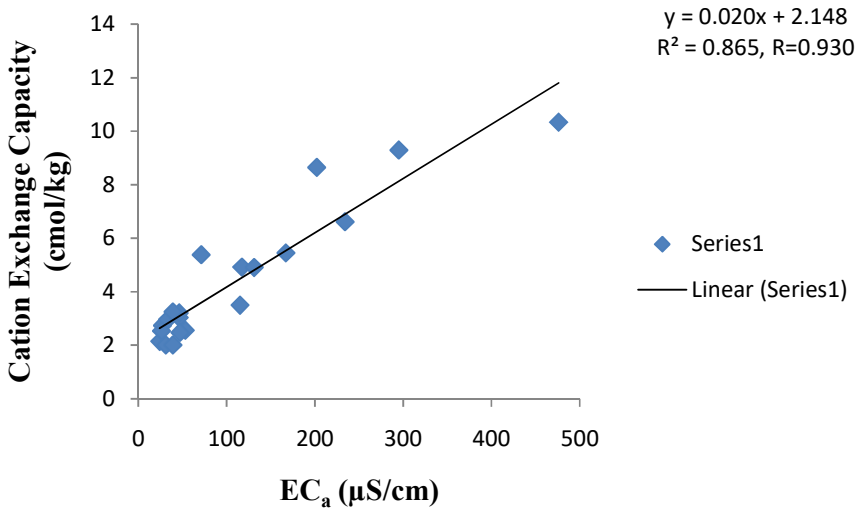

Figure 4.72a: Relationship between field EC_a and CEC in the soils of kola farm during the wet season

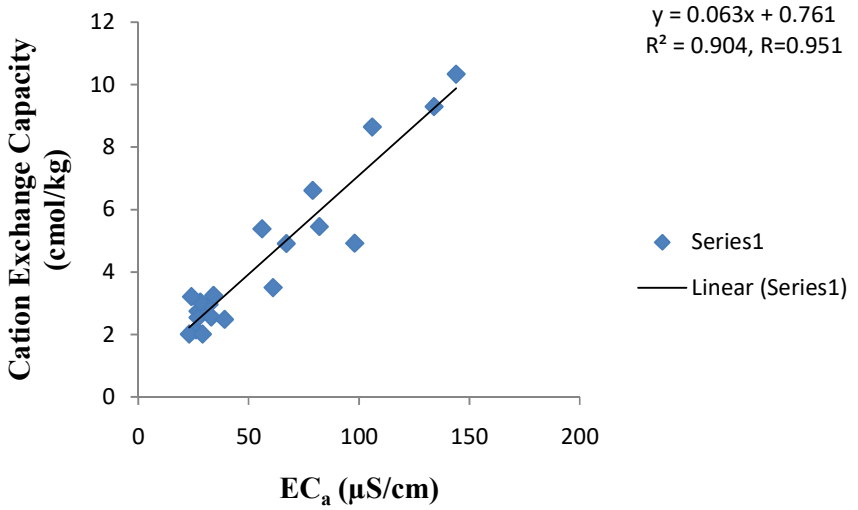

Figure 4.72b: Relationship between field EC_a and CEC in the soils of kola farm during the dry season

4.8 Soil X-Ray Diffraction (XRD) Assessment

XRD analysis reveals the prevailing clay mineral to be kaolinite and occurrence of montmorillonite and nontronite as trace across the two farms. Non-clay minerals include quartz, microcline, albite, muscovite, biotite, oligoclase, corderite and coquimbite.

4.8.1 Mineralogical Composition of Fine Fraction in the Cacao Soils

X-ray diffractograms highlight the quantity of mineral assemblage in the fine fractions, dominant clay mineral in the low EC_a section (Figs 4.73 and 4.74) is kaolinite and it ranges from 4.7% to 11.3% and its equitable percentage was 8.0% as subordinate whereas montmorillonite occurred as trace with its distribution ranging from 0- 0.1% (Okunlola and Owoyemi, 2015). Quantity of quartz varies from 61.1% to 67.2%, its mean percentage was 64.2% (dominant). Microcline content in the fine soil sample ranges between 14.2% and 24.6%, on the average it was 19.4% (subordinate). Other minerals in this segment include muscovite (2.9%-5.7%), corderite (0.4%-1.2%) and oligoclase (1.3%-5.4%).

Region of moderate EC_a (Figs 4.75 and 4.76) has kaolinite as the major clay mineral varying between 14.9% and 28.4%, 21.7% is the prevailing percentage occurring as subordinate whereas nontronite (0-7.1%) also occurred as the trace clay mineral. Quartz is the dominant mineral ranging from 49.2% to 51.2% with a mean percentage of 50.2%, while microcline fraction varies from 15.3% to 16.1% and its average percentage was 15.7 occurring as subordinate. Other minerals include corderite (0-9.3%), albite (0.4%-1.5%) and biotite (1.0%-4.0%)

Section of high EC_a (Figs 4.77 and 4.78) in the cacao plant has kaolinite as the abundant clay mineral varying between 23.9% and 38.3% with an average quantity of 31.1%, montmorillonite (0-4.5%) occurs as trace in the fine fraction. Percentage of quartz ranges from 30.5% to 52.7%, with a mean percent of 41.3% signifying abundance fraction. Proportion of microcline in the sample was between 9.8% and 20.3% with a common percentage of 15.1 (subordinate). Corderite and muscovite proportions in the fine fraction vary from 0.5% to 6.4% and 0% to 10.1% respectively. Percentage contributions from oligoclase (0.4%), albite (1.7%) and biotite (1.0%) are regarded as trace in quantity.

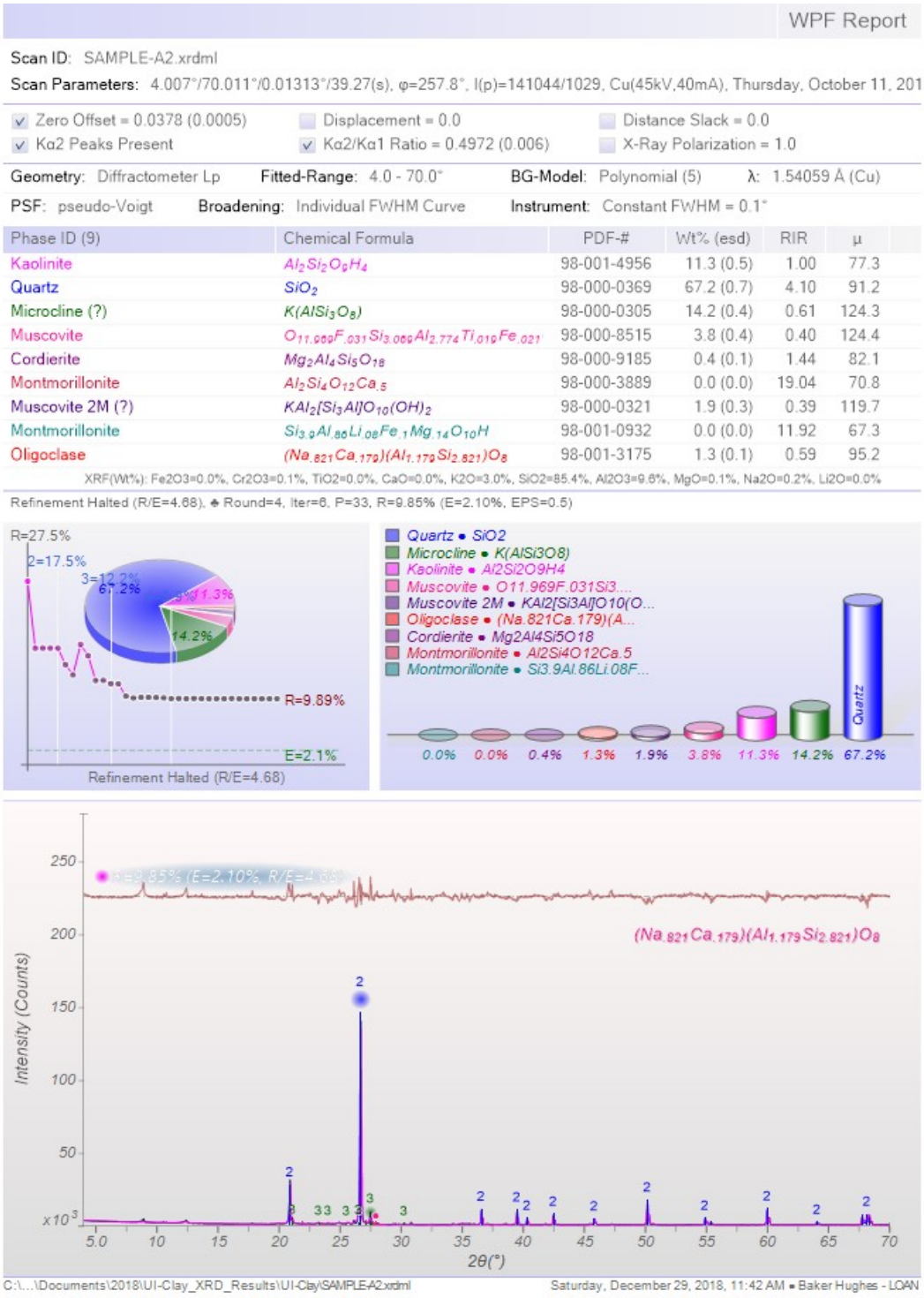

Figure 4.73: X-ray diffraction result of soil-fine fraction in the low EC_a region of cacao plot (Sample A2)

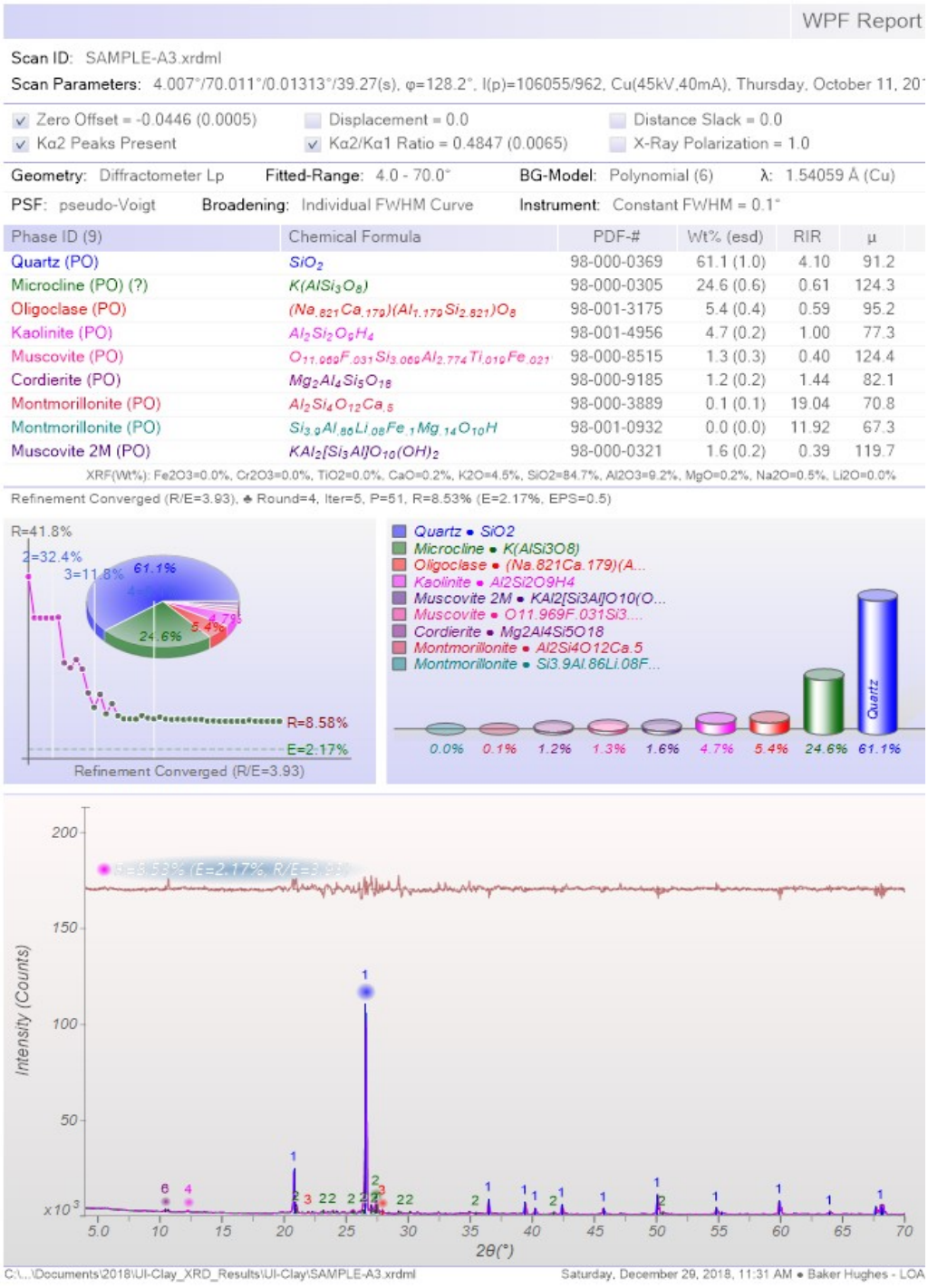

Figure 4.74: X-ray diffraction result of soil-fine fraction in the low EC_a region of cacao plot (Sample A3)

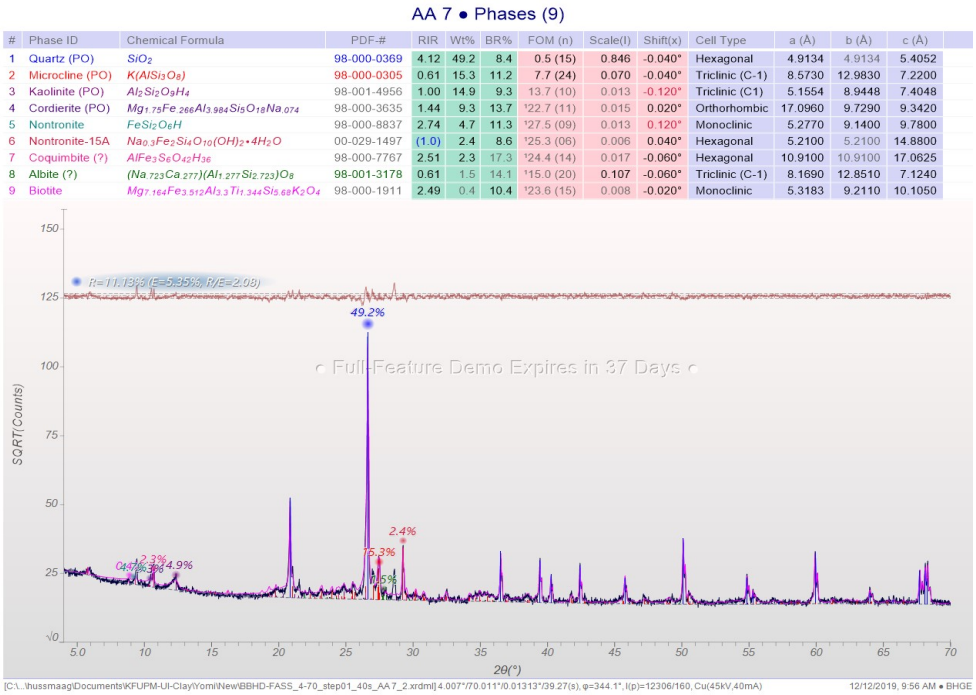

Figure 4.75: X-ray diffraction result of soil-fine fraction in the moderate EC_a region of cacao plot (Sample AA7)

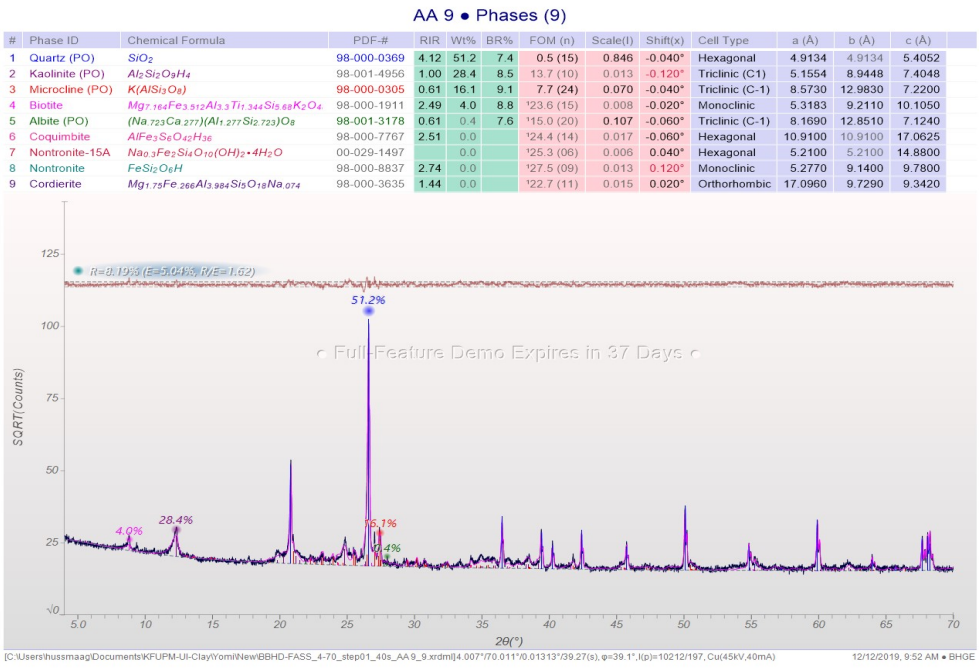

Figure 4.76: X-ray diffraction result of soil-fine fraction in the moderate EC_a region of cacao plot (Sample AA9)

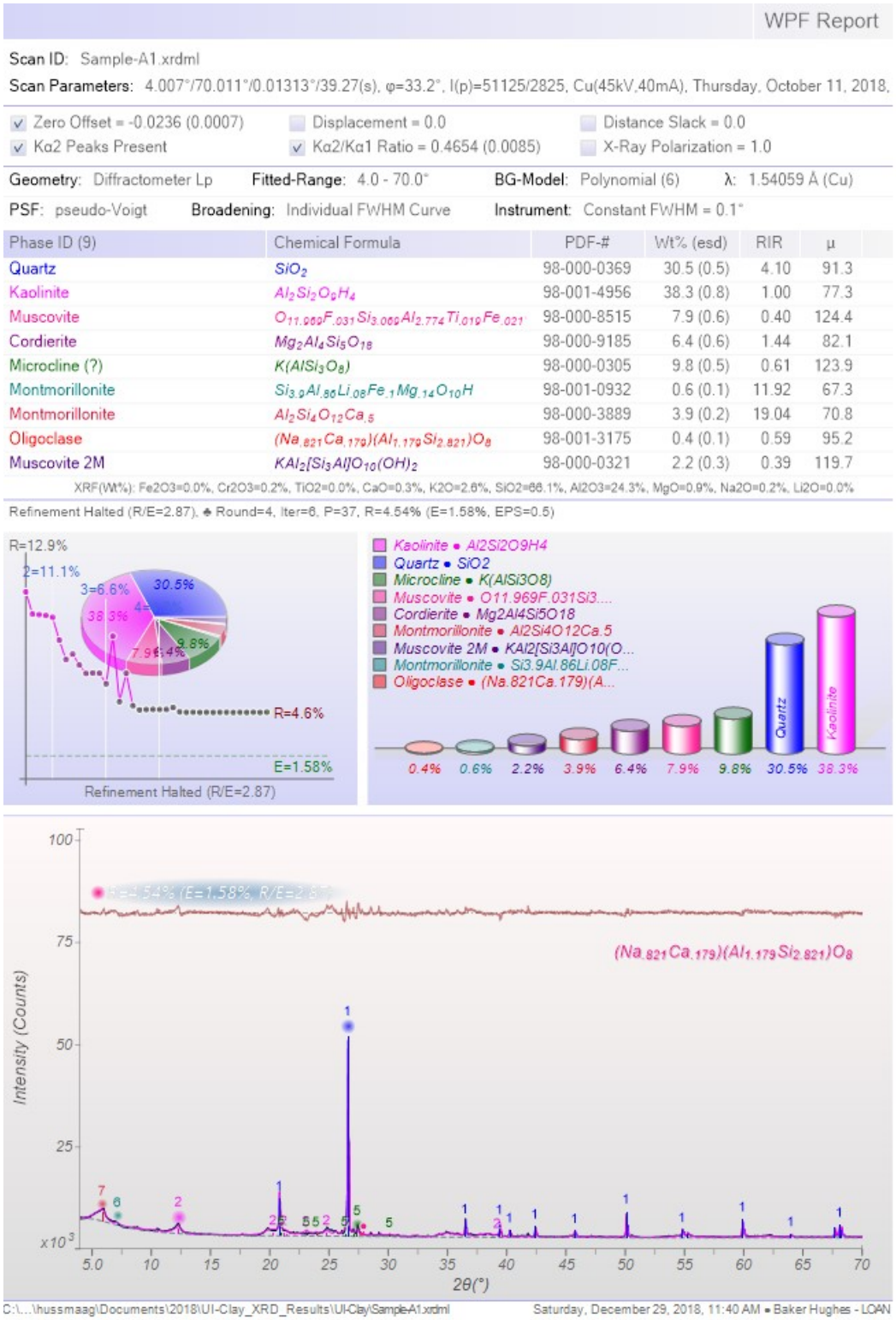

Figure 4.77: X-ray diffraction result of soil-fine fraction in the high EC_a region of cacao plot (Sample A1)

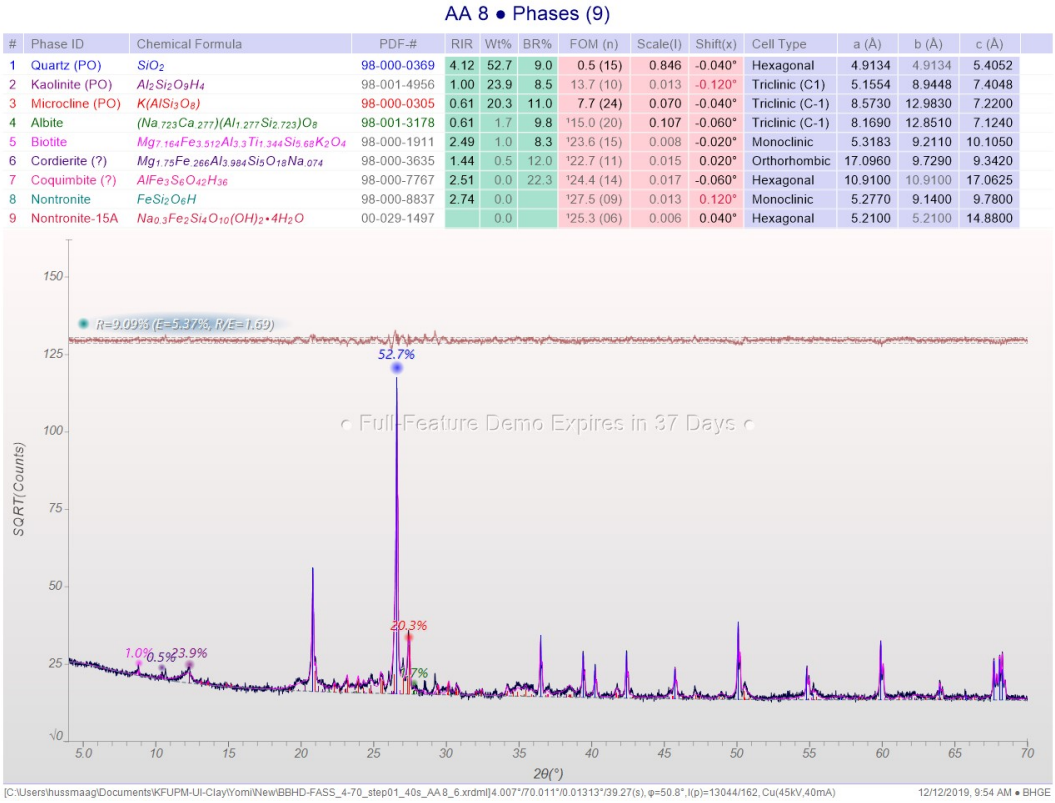

Figure 4.78: X-ray diffraction result of soil-fine fraction in the high EC_a region of cacao plot (Sample AA8)

Analysis of average mineral distribution across three segments in the cacao plot shows that the quantity of quartz decreases from region of low EC_a (64.2%) through the moderate EC_a (50.2%) section down to the high ECa segment (41.3%). Quantity of microcline is highest (19.4%) in the low EC_a section, intermediate (15.7%) in the moderate EC_a region and low (15.1%) in the high EC_a; microcline was in subordinate class. It is worthy to note that the quantity of kaolinite increases from low EC_a area to high EC_a segment; kaolinite in the low EC_a segment was 8%, it is 21.7% in the moderate ECa and both contents are in the subordinate class (5-25%) whereas highest percentage of kaolinite (31.1%) was noted to be in abundant quantity (25-50%) in the high EC_a zone.

Ratio of kaolinite distribution across the moderate EC_a and high EC_a sections are approximately (≈) three and four times respectively with respect to the low EC_a segment. Average quartz content in the low EC_a region approximately doubles the fraction in the high EC_a area. Grisso *et al.* (2009) reported that EC of sand is low and sand constitutes 85% of quartz, quartz particles have been regarded as good insulator of electric current and it dominates sand and silt fractions whereas clay fraction transmits current and it is composed of clay mineral and organic matter (Allred *et al*., 2008); quartz has negligible conductivity of 58 nS/m (Manoucheri, 2002). In furtherance to this, the EC of silt was regarded as medium while that of the clay was high (Grisso *et al.,* 2009); kaolinite has its electrical conductivity to be 0.2 S/m (Kibria and Hossain, 2019).

Conclusion reached by Revil and Glover (1998) was that surface conductance of clay is about four higher than that of the quartz; clay has large surface area with porous pores than the sandier material and soil having high clay content has higher EC reading (Hawkins *et al.,* 2017). Fraction with greatest surface area controls the behaviour and performance (properties) of soil. Besra *et al.* (2000) deduced that kaolin has high capacity to retain water because it is porous and permeable whereas quartz has low porosity coupled with high permeability hence low water retention capacity. Soil characterised with high proportion of quartz will hold less water compared to that with much more clay content when they are both saturated account for water content variation across the three segments, even when the contents are supplied with same amount of soluble ions, concentration of dissolved nutrients will vary, thereby impacting different plant productivity rate.

4.8.2 Mineralogical Composition of Fine Fraction in the Kola Soils

Dominance of kaolinite spread throughout the EC_a regions, while montmorillonite occurs as a trace. Non-clay minerals include quartz, muscovite, corderite, microcline, oligoclase and biotite. Mineralogical composition in the fine fraction of soils from low EC_a (Figs 4.79 and 4.80) in the kola plot as determined by diffractograms peaks indicates that kaolinite (14.8%-20.9%) was classified as subordinate clay mineral with a prevailing percentage of 17.9%. Quartz distribution varies between 38.2% and 42.3%, average percentage of quartz peculiar to this region was 40.3% and its presence in the soil fraction connotes abundance. The average quantity of microcline was subordinate (20.5%), it varies from 18.1% to 22.8%. Other minerals have varying proportion are: oligoclase (0-9.0%), muscovite (3-10.4%), and albite (0-19.9%).

Mineralogical assessment of fine fraction in the soil of moderate EC_a area (Figs 4.81 and 4.82) showed that kaolinite ranges from 14.5% to 26.7% and its mean percentage was 20.6 (subordinate category). Average proportion of quartz was 43.1% (abundant class) and it varies from 38.8% to 47.4%. Microcline has a mean quantity of 15.5% (subordinate class) and its distribution ranges between 13.7% and 17.3%. Percentage composition of albite varies between 18.3% and 20.7% with a mean of 19.5%. Muscovite ranges from 0 to 1.1% and corderite ranges from 0 to 1.4%, both occurring in trace quantity.

Zone of high EC_a has varying mineral assemblage including kaolinite as the clay mineral with the highest quantity and it varies from 33.9% to 41.2% with a mean percentage of 37.6 (Figs 83 and 84). Average percentage of quartz in this region was 22.5 (subordinate category) while it ranges from 14.3% to 30.7%. Microcline has its composition between 6.8% and 12.9% with a common percentage of 9.9 (subordinate class). Quantity of muscovite also ranges from 7.5% to 22.6% and its mean was 15.1%. Proportion of oligoclase ranged between 9.4% and 13.9% and has an average constituent of 11.7%. Corderite has an average percentage of 2.9% and it varies from 0.6% to 5.1% while montmorillonite ranges from 0.3% to 0.6%.

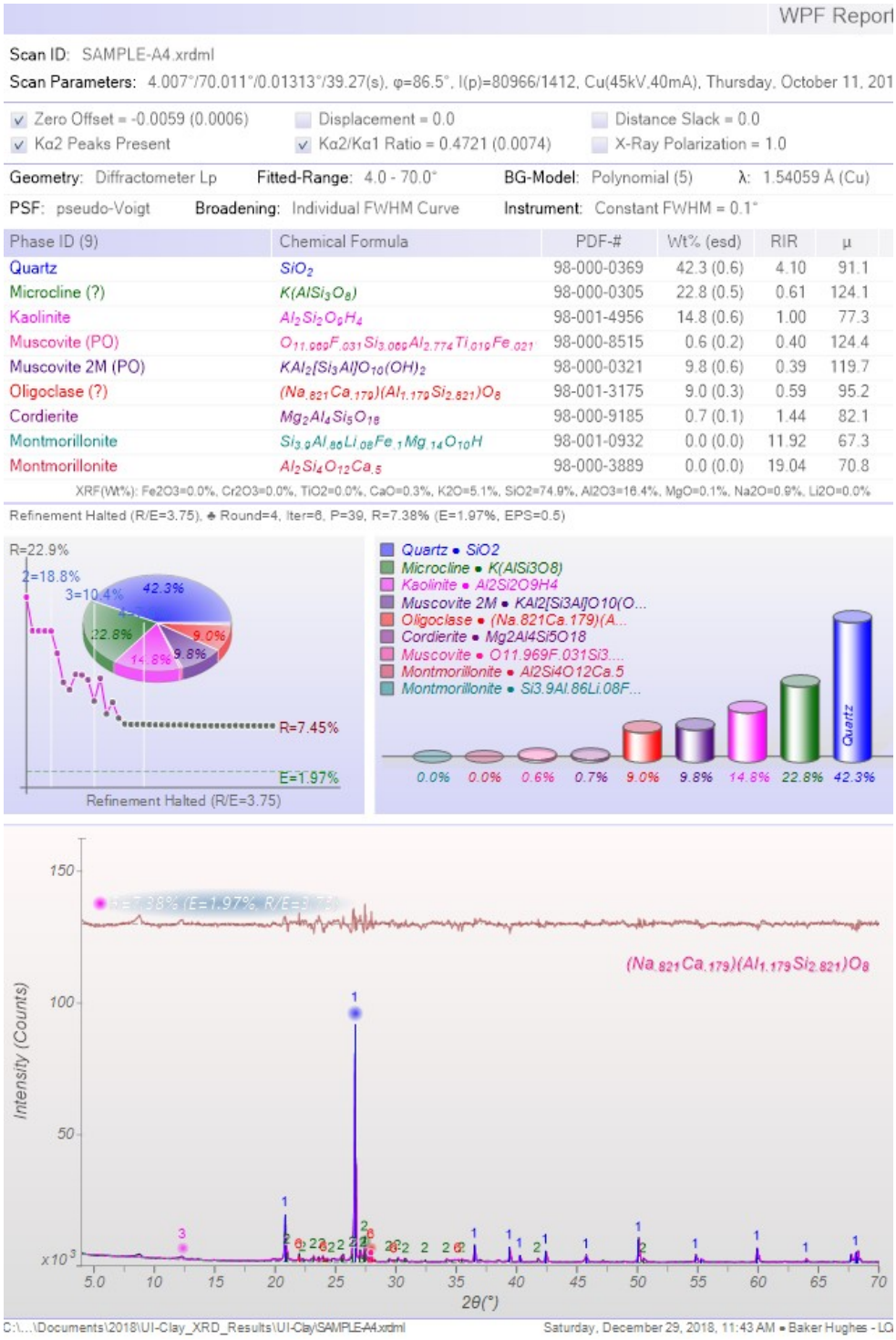

Figure 4.79: X-ray diffraction result of soil-fine fraction in the low EC_a region of kola plot (Sample A4)

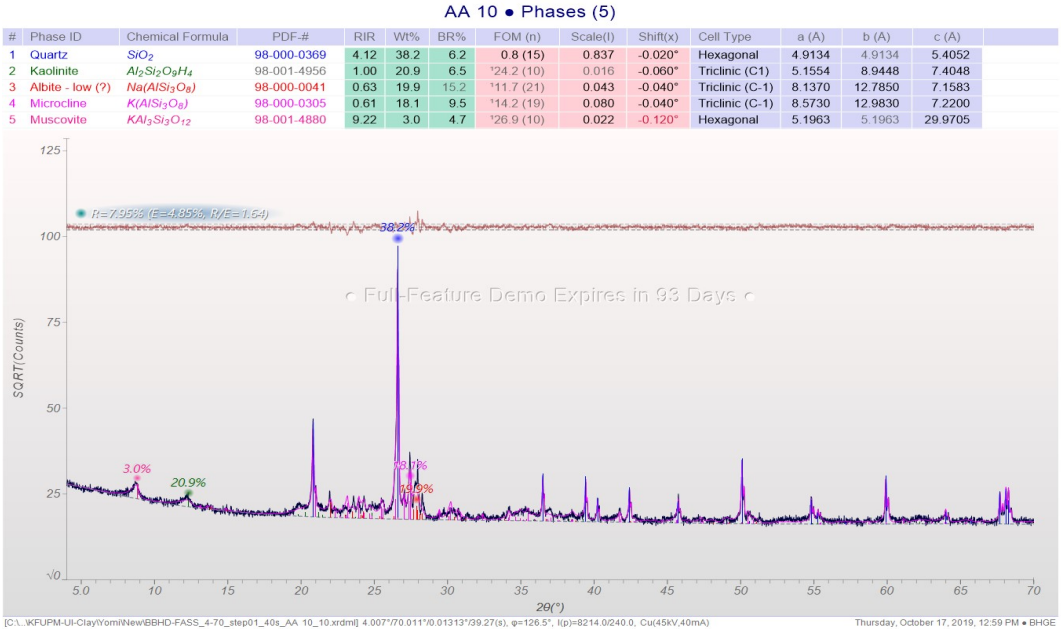

Figure 4.80: X-ray diffraction result of soil-fine fraction in the low EC_a region of kola plot (Sample AA 10)

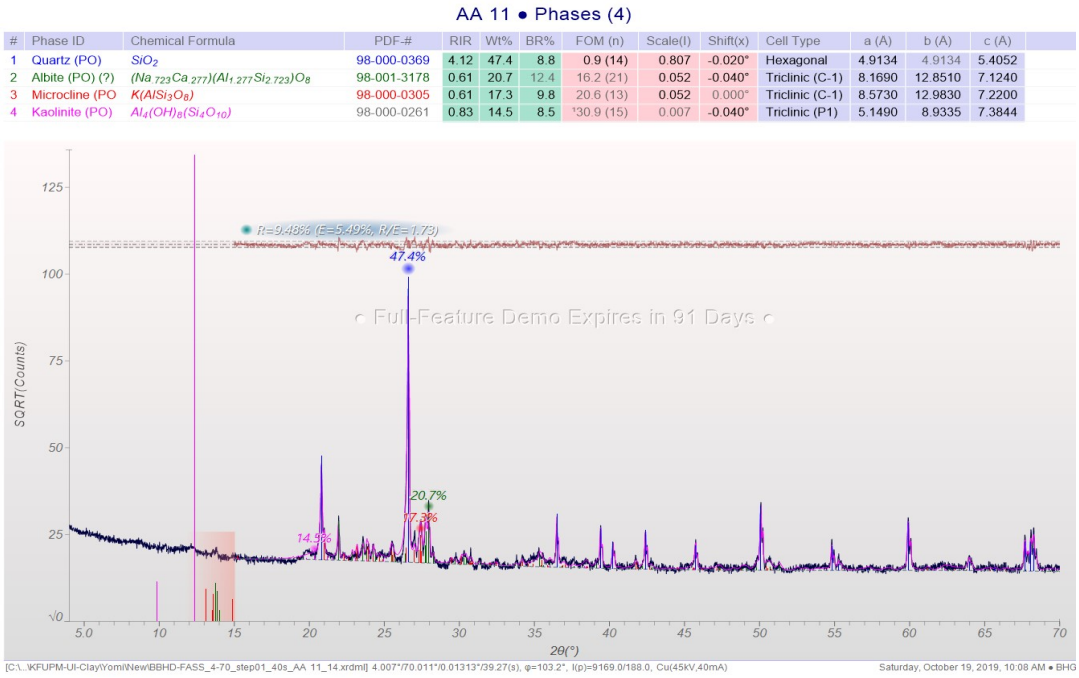

Figure 4.81: X-ray diffraction result of soil-fine fraction in the moderate ECa region of kola plot (Sample AA 11).

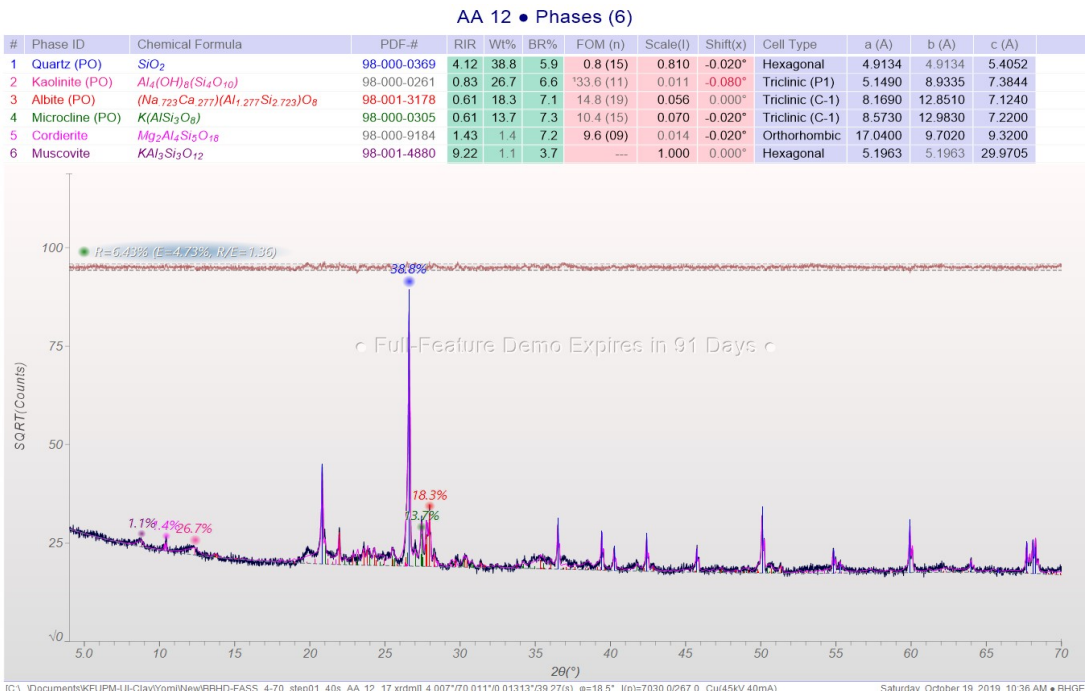

Figure 4.82: X-ray diffraction result of soil-fine fraction in the moderate EC_a region of kola plot (Sample AA 12)

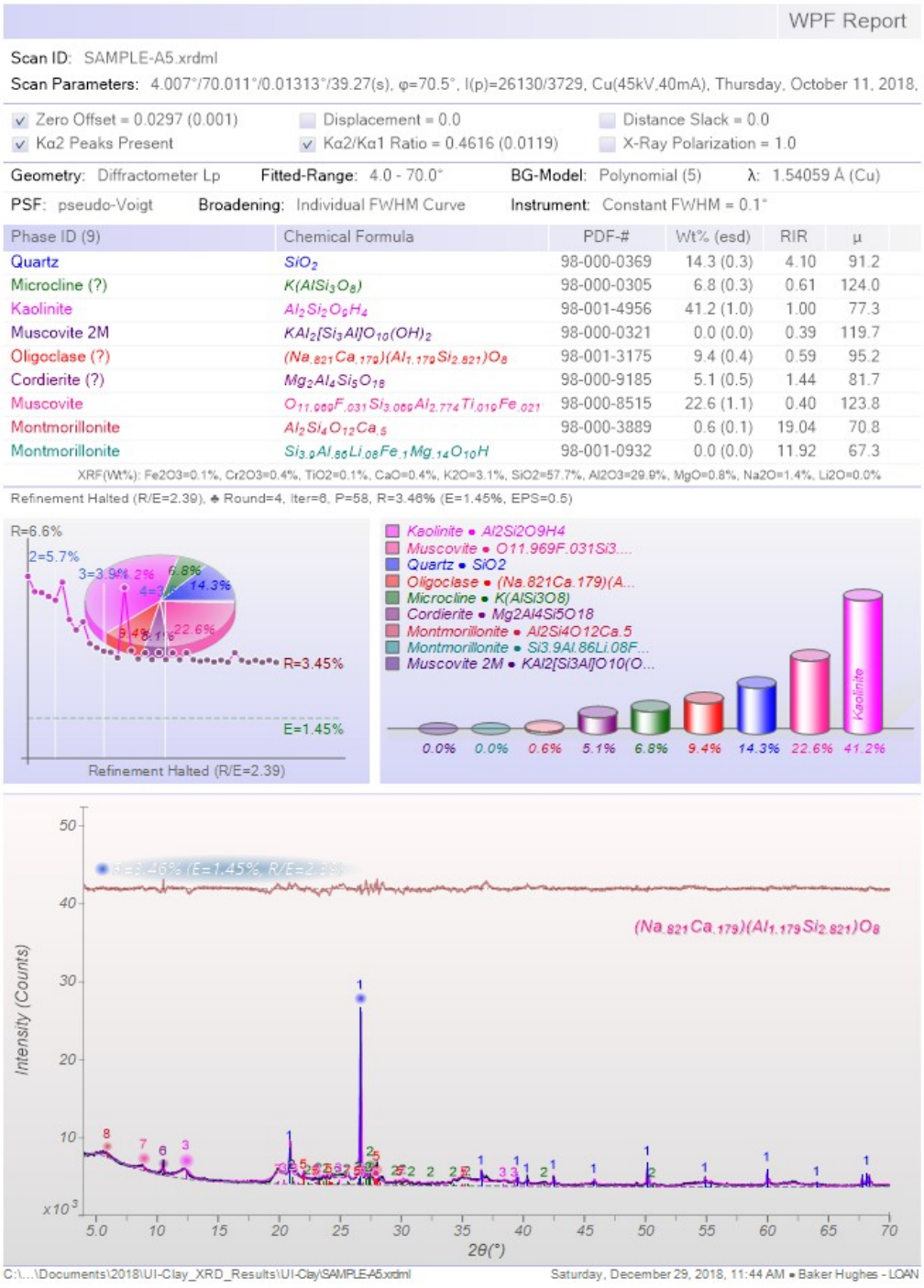

Figure 4.83: X-ray diffraction result of soil-fine fraction in the high EC_a region of kola plot (Sample A5)

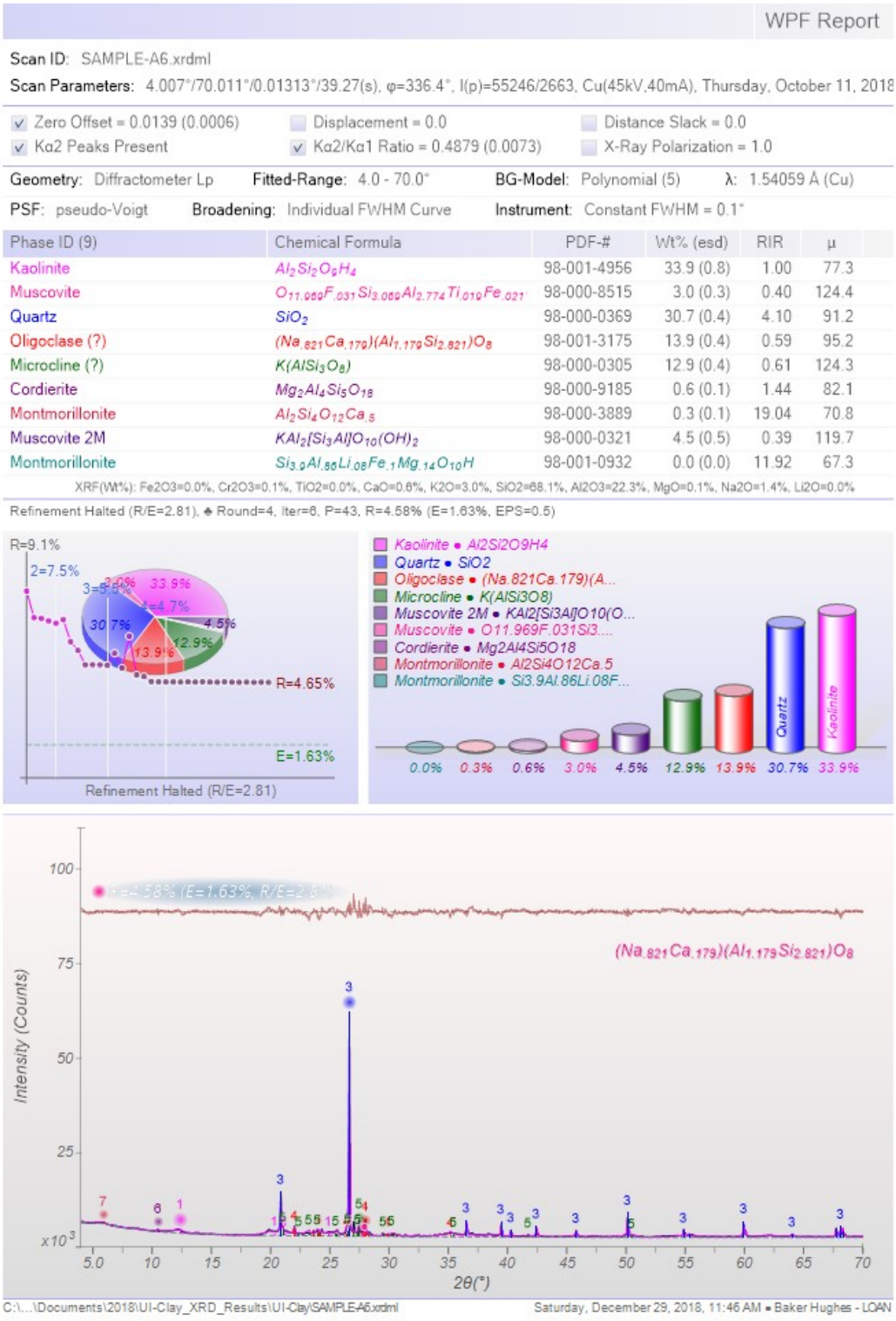

Figure 4.84: X-ray diffraction result of soil-fine fraction in the high EC_a region of kola plot (Sample A6)

Average percentage contribution was used in analysing the varying proportion and implication on plant productivity. It was observed that the content of microcline decreases from low EC_a area (20.5%) to the region of moderate EC_a (15.5%) and finally a low mean fraction (9.9%) in the high EC_a area. Contents of microcline in the moderate and low EC_a areas are approximately twice its proportion in the high EC_a section. Quantity of kaolinite across the EC_a segments is vice-versa with respect to microcline distribution. Low content (17.9%) of kaolinite was noted in the low EC_a zone, and intermediate proportion (20.6%) was present in the moderate EC_a section while the highest quantity (37.6%) was situated in the high EC_a section. Similarly quantity of kaolinite in the high EC_a doubles the proportion within the low EC_a area while a slight increase above that obtained in low EC_a was observed in the moderate EC_a section.

Highest amount of quartz (43.1%) was recorded in the moderate EC_a sector, intermediate proportion (40.3%) in the low EC_a portion but the lowest amount (22.5%) was observed in the high EC_a area. The XRD results reveal that the quantity of quartz in the moderate and low EC_a areas roughly doubles the content in the high ECa division. Electrical conductivity of quartz was reported to be insignificant (58 nS/m) according to Manoucheri (2002) and Pandey *et al*. (2015) reported that the EC of dry sand is extremely low but rises for a slight increase in water content whereas Kibria and Hossain (2019) found the EC of kaolinite to be 0.2 S/m. This could be attributed to the presence of cation attached to the surface area of kaolinite clay and the surface conductance was confirmed by Revil and Glover (1998) to be four times as much as that of quartz.

Zones with high fraction of kaolinite and a lesser amount of quartz have the ability to retain soil nutrient and water. This has aided quality health growth of kola-nut tree found within it whereas regions with high quartz substance and low quantity of kaolinite are characterised with stunted growth due to inability of the soil to retain water and plant nutrient. Moderate growth was observed in the moderate EC_a area despite high proportion of quartz in it, but inward examination reveals that kaolinite content was higher than that of the low EC_a zone, thus giving it an edge over it in terms of soil nutrient retention and water holding capacity.

CHAPTER FIVE

SUMMARY, CONCLUSIONS AND RECOMMENDATIONS

5.1 Summary

This study was anchored on the use of physical properties to establish soil productivity status/index, based on the rare documentation of its applicability in Nigeria agricultural system. The principal tool of investigation was the electrical conductivity of the soil. Cocoa Research Institute of Nigeria (CRIN) was chosen as the research station, based on the observations noticed on some of her research farms; these include varying pods production by cacao trees and uneven growth experienced by kola nut trees planted at the same time on same farmland. Soil EC_a mapping is an indirect approach of analyzing soil properties which has advantages of rapid data acquisition, large sampling density, data reliability, and economical advantage compared to the huge cost of carrying out geochemical analyses coupled with its time-consuming nature.

Findings made from the study could be highlighted as follow:

1) Biotite granite gneiss is the rock that underlain the research farms and trends in the north-south direction. The average feldspar content is twice the component of the quartz mineral.

2) Distribution of EC_a varies significantly with the volumetric water content such that the area of high EC_a corresponds to high VWC and vice versa. EC_a map has aided in classifying the farms into management sections (high, moderate, and low). Thus, EC_a is useful in predicting water content in soils due to the high correlation coefficient generated between these variables.

3) Heat regime influenced the electrical conductivity of ions present in soil and soil with high moisture content has a linear relationship with volumetric heat capacity and thermal

conductivity and inversely related to thermal diffusivity. Section of low thermal conductivity and volumetric heat capacity and high thermal diffusivity are characterised with fewer cacao pods production and stunted growth of kola nut trees.

4) Low permeability was noticed in the most electrically conductive soils. Low permeable soil has high nutrient retention and high water holding capacity, thereby preventing leaching of soil nutrients. Highly permeable soils in low EC_a permits low nutrient withholding as water drained easily through it, this is responsible for the underdeveloped growth of kola nut tree and less cacao pod production

5) Loamy sand, sandy loam, and sandy clayey loam were three soil textural classes identified from the farms. Soils in the region of the high EC_a have high clay and silt fractions and low sand constituent. Clay content decreases from the region of high EC_a to moderate EC_a section, then finally to low EC_a area. Zone with high clay fraction favours nutrient retention as well as the ability to retain soil water and vice versa.

6) Soil pH in both farms favours the availability of soil nutrients for plant uptake, concentrations of Ca, Mg, K, Na, and CEC value were high in the region of high EC_a at both farms, organic carbon, organic matter, total nitrogen, and available P are almost evenly distributed across the three regions. High EC_a is more inundated with base saturation and it is a non-sodic soil that promotes nutrient retention, good aeration, and drainage but soils in low EC_a (cacao and kola fields) and moderate EC_a (cacao farm) are sodic permitting leaching of nutrient and prone to erosion.

7) There was an agreement between the CEC generated clay type and XRD clay mineralogy (kaolinite). Soil enrichment was dependent on its mineralogy; kaolinite, microcline, and quartz are the dominant mineral phase in the soils of kola and cacao farms. Areas with large quantity of kaolinite clay and less of quartz and microcline have a greater tendency to retain soil moisture and nutrient, thus healthy plant growth and enhanced pods production are noticed in High EC_a regions.

The viariations noticed in soil's productivity of the cacao and kola farms were due to variation observed in soil texture. Soil texture played a major role in determining the nutrient retention capability, soil moisture infiltration rate together with its retention

capacity and the quantity of clay mineral present determines the cation exchange capacity of the adsorbed cations.

5.2 Conclusions

The petrographic analysis revealed the mineral components in the rock, the rock's nomenclature is biotite granite gneiss and possible end product of the minerals via weathering could be substantiated. The mineral constituents in rock play a major role in the subsequent soil being formed from the breakdown of the crystalline rock and it could used to assess their productivity. The possible clay mineral that would be generated if the minerals weather is kaolinite and this agrees with the results of XRD analysis.

EC_a map has aided in describing the field condition, strong correlations exist between EC_a and VWC during wet and dry seasons indicating that EC_a is a good indicator of relative variation of water content in soil and this was also confirmed by the EC_a and VWC maps exhibiting the similar distribution of EC_a and water content. The soils in both farms are regarded to be non-saline; area of high moisture content has more dissolved solutes, a large proportion of clay, better water retention, that is, low permeability and provides an insight into soil textural variation. EC_a map has helped in combining areas with similar soil property being grouped together for further soil sampling and examination. Mapping the soil EC_a around the kola and cacao fields has given information on the changes in the soil conditions and area in which utmost attention needed should be given.

Thermal conductivity and volumetric heat capacity increase with soil moisture content whereas thermal diffusivity reduces with an increase in soil moisture, these properties aided in mapping out variations in soil moisture content. It could be also deduced that rise in temperature possibly aid the mobility of ions in solution and lowering the viscosity of water, thereby making the dissolved nutrient available for plant uptake. The correlation analyses of thermal properties with electrical conductivity and volumetric water content indicated a weak to a strong relationship between them but better correlation existed with volumetric heat capacity. Areas of high thermal conductivity, high volumetric heat capacity and low diffusivity at both cacao and kola fields turned out to be regions of better

pods yield and healthy growth. It was discovered that correlation coefficients generated from the interaction of EC_a/VWC data with volumetric heat capacity and thermal diffusivity for the duration of rainy were higher than those coefficients derived during dry period whereas the relation of EC_a/VWC with thermal conductivity during the wet season was weak but numerically higher coefficients were noted in the dry term.

It can be inferred that a high electrically conductive section tends to retain soil moisture over time than a less electrically conductive unit; thus, water was made available for root uptake of the crops. Soil horizon in the root zone of the low EC segment allows the discharge of water percolating through it. There is a gradual reduction in water content across the medium to low EC_a section; therefore less pod production was accounted for by cacao trees situated within these portions. Stunted growth noticed in kola trees was due to the inability of soil horizon to retain water and less affinity to hold the elements within it, thus less electrical activity as a result of leaching of these elements from the soil unit of low EC_a. Highly conductive soils are characterized by high water holding capacity than the less conductive soil unit. More so, the dissolved nutrient is also available for plant growth by reducing the effect of soil leaching. Kola and cacao trees thrive in the region of low permeability than the highly permeable section because soil nutrients are made available in solution to plants and their mobility was responsible for the increase in electrical activity; and strong affinity exists between the nutrients and the low permeable soil unit.

The soil of low water-holding capacity and high permeability permits leaching of its nutrients due to low nutrient-retention capacity. Failure of cacao trees within the low conductive section to produce sufficient cacao pods unlike those situated within high conductive terrain could be attributed to low availability of water and nutrients due to leaching. Variations in hydraulic conductivity observed across the cacao and kola plots have shown that electrical conductivity was a crucial tool in assessing soil permeability and its fertility. The electrical conductivity of a medium can be used in predicting the permeability of the soil's horizon; the higher the electrical conductivity of a soil unit, the lower the permeability of the medium.

Three textural classes were established from soils in the cacao farm, namely loamy sand, sandy loam, and sandy clayey loam while two classes (loamy sand and sandy loam) were instituted from soils in the kola plot. Loamy sand was found within the low and moderate EC_a sections, sandy clayey loam was situated in the high EC_a segment while sandy loam cut across the low, moderate, and high EC_a areas. The proportion of the soil particle size was used to adjudge its fertility; the region of high ECa has a high quantity of clay and silt fraction with less content of sand relative to the moderate and low EC_a divisions. Fine fractions have a large surface area than the coarse fragment of less surface area, thereby resulting in a large catchment/retention area for water and soil nutrients in solution.

Areas of a large quantity of clay and silt contents have high EC_a value due to its low permeability resulting in high water-holding capability and nutrient retention capacity than the moderate and low EC_a parts which are characterised with quick water drain leading to leaching of soil nutrient. Correlation analysis between the various particle size and electrical conductivity revealed that clay and silt particles have a positive relationship with electrical conductivity while an inverse relation was established between sand fraction and EC_a. The electrical conductivity technique can be used to map out areas of soil textural variation because its measurement was based on the porosity of the medium, nature of pore fluid, and resistivity of the mineral grains. Zones with abundant pore fluid filling the pore spaces tend to be more conductive than sections with less pore fluid; therefore, soils with high water holding capacity tend to be conductive whereas those having less water retention capability are characteristically more resistive.

Soils in the farms were divided into three zones; high, moderate, and low based on field EC_a measurement. The mean concentration of hydrogen ion across the soils was adequate for the availability of soil nutrients required for plant consumption and its variability was low in both farms suggesting nearly uniform concentration and presence of non-toxic elements in soil solution. Moderate variability was noticed in EC, organic carbon, organic matter, total nitrogen, available phosphorus, acidity, sodium, CEC at both farms, the concentrations of calcium and potassium are highly variable in kola soil but moderate in the cacao field whereas magnesium was high in the cacao plot but moderate in kola plot.

Region of high EC_a has electrical conductivity determined from the laboratory to be approximately double the conductivity in the moderate EC_a and low EC_a sections in the cacao field while kola soils exhibit similar concentration in the high EC_a and moderate EC_a areas but the conductivity of high EC_a segment was nearly twofold that of low EC_a district. It serves as a pointer that there is a presence of more soluble ions in soil solution around high EC_a area than the moderate and low EC_a regions. This shows that region of high EC_a is more fertile than other segments; less concentration of ions may be responsible for the stunted growth and fewer pods production being experienced by crops in the low EC_a district.

The proportion of organic carbon, organic matter, and total nitrogen was nearly equal in both farms but the available phosphorus was below the limit required for adequate plant growth. Calcium content across all the segments at both fields as classified as low; its concentration in the high EC_a area doubles its content in the moderate and low EC_a zones for the cacao soil while its concentration in high EC_a is more than thrice the content in the low EC_a segment and twice the content of moderate EC_a region for the kola field. Magnesium concentration in the high EC_a area was in the moderate range for cacao plants but in the moderate EC_a and low EC_a segments, their concentration was regarded as low. The proportion of magnesium in high EC_a doubles the concentration in the low EC_a and almost one and a half in the moderate EC_a region. Kola soils have magnesium concentration in the high and moderate EC_a regions to be moderate whereas it is low in low EC_a section, the region of high EC_a has it magnesium content to be two and half times that of the magnesium distribution in low EC_a and almost twice the content in moderate EC_a area. All the potassium concentration in the three sections of the cacao farm is in a low category while its concentration in the high EC_a division was considered to be medium for the kola field which approximately doubles the potassium content in the low and moderate EC_a segments. Though sodium is not regarded as an essential nutrient for plants, its distribution is enormous in high EC_a than other zones for both fields.

The cation exchange capacity of soil in the moderate EC_a and high EC_a zones was considered to be moderate whereas it was low in the low EC_a segment for the farms and CEC values suggest the clay type to be kaolinite in all the regions. Region of high EC_a

was more conductive, has a high proportion of calcium, magnesium, and potassium. The concentration of these soil nutrients gave the most conductive section an edge over the moderate and low EC_a segments resulting in healthy growth and pods production in high EC_a section but stunted growth and fewer pods in low EC_a zone. This suggests that soils in the moderate and high EC_a areas are more fertile than the low EC_a soil, this was justified by the base saturation such that high EC_a zone was more saturated than low EC_a while soils in the moderate EC_a area are more saturated with base cations than the low EC_a segment. High EC_a area was more flooded with base saturation and it is a non-sodic soil but soils in low EC_a (cacao and kola fields) and moderate EC_a (cacao farm) are sodic; non-sodic soil prevents leaching of soil nutrients coupled with good aeration and drainage whereas sodic soil is characterised with poor drainage and aeration and they are susceptible to leaching via erosion. Leaching of soil nutrients was responsible for the reduction in the fertility content of the soil.

The electrical conductivity of soil medium is a function of the dissolved ions present in it; the conductivity was partially influenced by the concentrations of organic carbon, organic matter, percentage total nitrogen (all fields), potassium and sodium (cacao soil) and acidic cation (kola soil) due to their weak interaction with the EC_a as observed from their plots. The content of available phosphorus does not contribute to the electrical conductivity of soil's solution as noticed from its inverse relationship with the EC_a at both seasons. Moderate and high coefficients were generated from the interaction of acidic cation, calcium, magnesium and the CEC at large with the EC_a for cacao soil while all the base cations together with the resultant CEC greatly influenced the electrical conductivity measured in the kola soil unit, thus, contributing to the bulk of the electrical conductivity in the soil medium.

Kaolinite, quartz, and microcline are the dominant mineral phase in soils of cacao and kola fields respectively. A high quantity of quartz and less proportion of kaolinite was responsible for low water retention, thereby contributing to leaching of soil nutrients in the low EC_a zone. An increase in the quantity of kaolinite and less of quartz content to that of low EC_a medium was responsible for the average pods' productivity in the moderate EC_a section due to better water and nutrient retention capabilities. A high proportion of

kaolinite and a low fraction of quartz and microcline aided soil nutrient and water retention, thus confirming high pod productivity being experienced by the cacao plants within this zone.

Soil nutrient enrichment is a function of combining mineralogy of the weathered parent rock, kola soil with a high quantity of kaolinite and low content of quartz can adsorb more cations onto its surface than soils having low kaolinite fraction and much quartz. Soils in the region of low EC_a are characterised with high quartz content and less of kaolinite which was accountable for less nutrient retention and low water-holding capability, that is, it encourages leaching of nutrients, thus stunted growth of kola plant is observed. Healthy growth of kola nut trees noted in the high EC_a area was due to the presence of more kaolinite and less of quartz, thereby supporting nutrients retention and better water-holding capacity relative to soils in the low EC_a section.

5.3 Recommendations

The introduction of organic matter through the application of organic manure will help in reworking the textural differences in the regions of low and moderate EC_a. Thereby aiding nutrient retention and reducing nutrient leaching in soils; also stabilizing soil from run-off losses and preventing soil erosion. Phosphorus content in the farms should be improved as the soils are deficient in this nutrient.

There is a need to employ other geophysical techniques relevant to the field of agriculture to establish various soil properties aiding its productivity. Aerial satellite imageries, seismic refraction, ground penetrating radar (GPR), electromagnetic induction (EMI) and time domain reflectometry (TDR) should be adequately engaged as non-invasive sensors in ascertaining the physical properties of soil. Efforts should be intensified on the use of physical laws in predicting and controlling unfavourable physical conditions responsible for the degradation of agricultural soils.

5.4 Contributions to Knowledge

(1) One of the major contributions of this study has shown that electrical resistivity technique has the capability to assess the porosity, thermal properties, soil texture, mineralogy, chemical constituent and moisture content of soil; these are attributes being assessed in soil for its productive potential. Having fulfilled these criteria, the technique should be adapted into Nigerian agricultural farming practices as a useful alternative in evaluating soil management zone to wholesome geochemical assessment which is laborious and time consuming.

Therefore, the study has established that electrical conductivity contrast is a qualitative evaluator from which geochemical data point could be streamlined in the assessment of soil's productivity.

(2) This technique allows dense sampling of the agricultural site and serves as viable pilot, from which geochemical data point could be streamlined, and thereby reducing cost that would have been expended on geochemical estimation if it was to be carried out at all the resistivity points. Thus, it is cost effective and efficient in characterising the soil properties, which is synonymous with nutrient variation. It will also avail the opportunity of rapid data acquisition, coverage extent, and data reliability in mapping out the soil conductivity contrast.

(3) This research has revealed that soil apparent electrical conductivity is a useful alternative to wholesome geochemical assessment which is laborious, costly and time consuming; thus necessitating its adoption into Nigerian agricultural farming practices.

REFERENCES

Abdullahi M, Singh U.K. and Modibbo U.M. 2019. Crustal structure of southern Benue Trough, Nigeria from 3D inversion of gravity data. *Journal of Geology and Mining Research,* Vol. 11(4): 39-47, DOI: 10.5897/JGMR2018.0299

Abu-Hamdeh N.H. 2001. SW—Soil and water: measurement of the thermal conductivity of sandy loam and clay loam soils using single and dual probes. *Journal of Agricultural Engineering Research* 80.2: 209–216.

Adebowale L.A. and Odesanya B.O. 2015. Effects of kola cultivation on soil fertility status of selected kolanut plantation in Ogun state, western Nigeria. *International Research Journal of Agricultural Science and soil science* 5.5: 129-136.

Adelekan I.0. and Bolarinwa O. 2009. Local knowledge of climatic conditions and agricultural activities in southwestern Nigeria. *Journal of Science Research*, vol. 8: 56-60

Adeniyi M.O., Oshunsanya S.O. and Nymphas E.F. 2012. Validation of analytical algorithms for the estimation of soil thermal properties using de Vries model. *American Journal of Scientific and Industrial Research*, vol. 3(2): 103-114.

Adepitan, J. O., Falayi, E. O. and Ogunsanwo, F.O. 2017. Confirmation of Climate Change in Southwestern Nigeria through Analysis of Rainfall and Temperature Variations over the Region. *Covenant Journal of Physical & Life Sciences (CJPL)* Vol. 5 (1): 37-51.

Adewole M.B. and Adeoye G.O. 2014. Assessment of soil properties and crop yield under agroforestry in the traditional farming system. *African Journal of Agricultural Research* 9.27: 2119-2123.

Afolagboye, L.O., Talabi, A.O. and Akinola, O.O. 2016. Evaluation of selected basement complex rocks from Ado-Ekiti, SW Nigeria, as source of road construction aggregates. *Bull Eng Geol Environ* vol. 75**:** 853–865. https://doi.org/10.1007/s10064-015-0766-1

Aga T. and Haruna A. I. 2019. The field geology and petrography of the kofayi younger granite complex, central Nigeria. *International Journal of Advanced Geosciences*, vol. 7(2): 95-103.

Ajigo, I.O., Odeyemi, I.B. and Ademeso, O.A. 2019. Field geology and structures of migmatitic gneisses around ibillo-okene area, southwest Nigeria. *Journal of Environment and Earth Science* . vol.9 (2): 59-72.

Akande S.O. 2006. Paleofluids circulation in the basement complex: implication for base metal mineralization in Nigeria mineral belt. In: O.Oshin (editor), the basement complex of Nigeria and its mineral resources, Akin Jinad and Co Press, Ibadan. 87-106.

Akinola O.O. and OlaOlorun O.A. 2021. Lithological features and chemical characterization of metamorphosed carbonate rocks in Igue, Southwestern Nigeria. *Journal of Geology and Mining Research*, vol. 13(1):11-20. DOI: 10.5897/JGMR2020.0349

Al-Ani T. and Sarapää O. 2008. Clay and clay mineralogy: physical – chemical properties and industrial uses. Geologian Tutkuskeskus M19/3232/2008/41. 1-95.Retrieved on 23rd September, 2019 from https://www.coursehero.com/file/28844025/m19-3232-2008-41pdf/

Ali B., Cengiz K. and Hasan E. 2009. Measurements of apparent electrical conductivity and water content using a resistivity meter. *International Journal of Physical Sciences* 4.12: 784-795.

Allred B.J., Groom D., Ehsani M.R. and Daniels J.J. 2008. Resistivity method. In: Allred B.J., Daniels J.J. and Ehsani M.R. (editors), handbook of agricultural geophysics, CRC Press, Taylor and Francis Group. 85-108.

Allred B.J. and Smith B. D. 2010. Introduction to JEEG agricultural geophysics special issue. *Journal of Environmental and Engineering Geophysics* 15.3: v-vi.

Amidu S.A. and Dunbar J.A. 2007. Geoelectric studies of seasonal wetting and drying of a Texas Vertisol. *Vadose Zone Journal* 6.3: 511-523.

Amidu S.A. and Olayinka A.I. 2006. Environmental assessment of sewage disposal systems using 2d electrical-resistivity imaging and geochemical analysis: A case study from Ibadan, Southwestern Nigeria. *Environmental & Engineering Geoscience* 12.3: 261–272.

Amos-Tautua B.M.W., Onigbinde A.O. and Ere D. 2014. Assessment of some heavy metals and physicochemical properties in surface soils of municipal open waste dumpsite in Yenagoa, Nigeria. *African Journal of Environmental Science and Technology* 8.1: 41-47.

Archie G.E. 1942. The electrical resistivity log as an aid to determining some reservoir characteristics. *Trans. A.I.M.E.*, 146: 389-409.

Arévalo-Gardini E., Canto M., Alegre J., Loli O., Julca A., Baligar V. 2015. Changes in soil physical and chemical properties in long term improved natural and traditional agroforestry management systems of cacao genotypes in peruvian amazon. *PLoS ONE* 10.7: e0132147. doi:10.1371/journal.pone.0132147.

Asadullah S., Muhammad S.M., Ali A.M., Shafi M.K. and Abdul L.Q. 2014. Determination of saturated hydraulic conductivity of different soil texture materials. *IOSR Journal of Agriculture and Veterinary Science* 7.12: 56-62.

Asif A.R., Ali S.S., Noreen N., Ahmed W., Khan S., Khan M.Y. and Waseem M. 2016. Correlation of electrical resistivity of soil with geotechnical engineering parameters at Wattar area district Nowshera, Khyber Pakhtunkhwa, Pakistan. *Journal of Himalayan Earth Sciences* 49.1: 124-130.

Ayanlade A., Radeny M., Morton J.F. and Muchaba T. 2018. Rainfall variability and drought characteristics in two agro-climatic zones: An assessment of climate change challenges in Africa. *Science of the Total Environment*, 630 (2018):728–737.

Ayodele O.S. 2015. The Geology, Geochemistry and Petrogenetic Studies of the Precambrian Basement Rocks around Iworoko, are and Afao Area, Southwestern Nigeria. *Journal of Environment and Earth Science* . vol.5 (3): 58-66.

Ayodele O.S. and Akinyemi S.A. 2014. Petrostructural and Mineralogical Assessment of the Precambrian Rocks in Ikere Area, Southwestern Nigeria. *Asian Review of Environmental and Earth Sciences*, Vol. 1 (3): 66-83.

Bai W., Kong L. and Guo A. 2013. Effects of physical properties on electrical conductivity of compacted lateritic soil. *Journal of Rock Mechanics and Geotechnical Engineering* 5: 406-411. http://dx.doi.org/10.1016/j.jrmge.2013.07.003

Balogun O.B. 2019. Tectonic and structural analysis of the Migmatite–Gneiss–Quartzite complex of Ilorin area from aeromagnetic data, *NRIAG Journal of Astronomy and Geophysics*, vol. 8(1): 22-33. DOI:10.1080/20909977.2019.1615795

Barry-Macaulay D., Bouazza A., Singh R.M. and Wang B. 2014. Thermal properties of some Melbourne soils and rocks. *Australian Geomechanics* 49.2: 31-44

Behera S.K., Suresh K., RaoB.N., Mathur R.K., Shukla A.K., Manorama K., Ramachandrudu K. and Harinarayana P. 2016. Spatial variability of some soil properties in west coastal area of India having oil palm (*Elaeis guineensis* Jacq.) plantations. *Solid Earth Discussions* Retrieved on 18th October, 2018 from doi:10.5194/se-2016-9

Belachew T. and Abera Y. 2010. Assessment of soil fertility status with depth in wheat growing highlands of Ethiopia. *World Journal of Agricultural Sciences* 6.5: 525-531

Benkheli J., Mascle J. and Guiraud M. 1998. Sedimentary and structural characteristics of the cretaceous along the Côte d'ivoire-Ghana transform margin and in the Benue Trough: A comparison. In: Mascle, J., Lohmann, G.P., and Moullade, M. (Eds.), 1998 *Proceedings of the Ocean Drilling Program, Scientific Results,* vol. 159: 93-99.

Bertermann D. and Schwarz H. 2017. Laboratory device to analyse the impact of soil properties on electrical and thermal conductivity. *International Agrophysics,* vol.31: 157-166. doi: 10.1515/intag-2016-0048

Besra L., Sengupta D.K. and Roy S.K. 2000. Particle characteristics and their influence on dewatering of kaolin, calcite and quartz suspensions. *International Journal of Mineral Processing* 59: 89–112

Bolarinwa A.T., Idakwo S.O. and Bish D.L. 2019. Rare-earth and trace elements and hydrogen and oxygen isotopic compositions of Cretaceous kaolinitic sediments from the Lower Benue Trough, Nigeria: provenance and paleoclimatic significance. *Acta Geochim.* https://doi.org/10.1007/s11631-019-00328-y

Bonde, D.S, Rai J.K., Joshua, B.W. and Abbas M. 2014. Basement depth estimates of Sokoto sedimentary basin, Northwestern Nigeria,using spectral depth analysis. *Journal of Chemistry and Material Science (DRCMS*), Vol.2 (2):21-26

Botta C. 2015. Understanding your soil test step by step. Yea River Catchment Landcare Group. 1-49.

Bozkurt A., Kurtulus C. and Endes H. 2009. Measurements of apparent electrical conductivity and water content using a resistivity meter. *International Journal of Physical Sciences* 4.12: 784-795.

Brandon T.L. and Mitchel J.K. 1989. Factors influencing thermal resistivity of sands. *J. Geotech. Engr*. 115: 1683-1698.

Brevik E.C., Fenton T.E. and Horton R. 2004. Effect of daily soil temperature fluctuations on soil electrical conductivity as measured with the geonics EM-38. *Precision Agriculture* 5: 145–152.

Brevik E C., Fenton T.E. and Lazari A. 2006. Soil electrical conductivity as a function of soil water content and implications for soil mapping. *Precision Agric.* 7: 393-404.

Brillante L., Mathieu O., Bois B., van Leeuwen C. and Lévêque J. 2015. The use of soil electrical resistivity to monitor plant and soil water relationships in vineyards. *Soil* 1: 273–286.

Brocca L., Ciabatta L., Massari C., Camici S. and Tarpanelli A. 2017. Soil moisture for hydrological applications: Open questions and new opportunities. Water 2017, 9, 140; doi:10.3390/w9020140.

Carvalho P.S.M., Franco L.B., Silva S.A., Sodré G.A., Queiroz D.M. and Lima J.S.S. 2016. Cacao crop management zones determination based on soil properties and crop yield. *Revista Brasileira de Ciencia do Solo.*2016;40:e0150520. https://doi.org/10.1590/18069657rbcs20150520

Cassiani G., Giustiniani M., Ferraris S., Deiana R. and Strobbia C. 2009. Time-lapse surface-to-surface GPR measurements to monitor a controlled infiltration experiment. *Bollettino di Geofisica Teorica ed Applicata* 50.2: 209-226.

Chaudhari P.R., Ahire D.V., Chkravarty M. and Maity S. 2014. Electrical conductivity as a tool for determining the physical properties of Indian soils. *International Journal of Scientific and Research Publications*, vol. 4(4):1-4.

Chen G., Wang S., Huang X., Hong J., Du L., Zhang L., and Ye L. 2015. Environmental factors affecting growth and development of Banlangen (Radix Isatidis) in China. *African Journal of Plant Science* 9.11: 421-426.

Chenhui L., Libo Z., Jinhui P., Chandrasekar S., Bingguo L., Hongying X., Junwen Z. and Lei X. 2013. Temperature and moisture dependence of the dielectric properties of silica sand. *Journal of Microwave Power and Electromagnetic Energy* 47.3:199-209. doi: 10.1080/08327823.2013.11689858

Chineke T.C., Jagtap S.S. and Nwofor O. 2010. West African monsoon: is the August break “breaking” in the eastern humid zone of southern Nigeria? *Climatic Change* (2010) 103:555–570. DOI 10.1007/s10584-009-9780-2

Clarke N., Røsberg I. and Aamlid D. 2005. Concentrations of dissolved organic carbon along an altitudinal gradient from Norway spruce forest to the mountain birch/alpine ecotone in Norway. *Boreal Environment Research* 10: 181-189.

Clay D. E., Chang J., Malo D. D., Carlson C. G. Reese C., Clay S. A., Ellsbury M. and Berg B. 2001. Factors influencing spatial variability of soil apparent electrical conductivity. *Agronomy, Horticulture and Plant Science Faculty Publications*. 206. https://openprairie.sdstate.edu/plant_faculty_pubs/206

Corwin D.L., Kaffka S.R., Hopmans J.W., Mori Y., van Groenigen J.V., van Kessel C., Lesch S.M. and Oster J.D. 2003. Assessment and field-scale mapping of soil quality properties of a saline-sodic soil. *Geoderma* 114: 231-259.

Corwin D.L. and Lesch S.M. 2003. Application of soil electrical conductivity to precision agriculture: Theory, principles and guidelines. *Agronomy Journal* 95.3: 455-471.

Corwin D.L. and Lesch S.M. 2005a. Apparent soil electrical conductivity measurements in agriculture. *Computers and Electronics in Agriculture* 46: 11–43.

_____2005b. Characterizing soil spatial variability with apparent soil electrical conductivity part II. Case study. *Computers and electronics in agriculture* 46: 135-152.

Corwin D.L. and Lesch S.M. 2013. Protocols and Guidelines for Field-scale Measurement of Soil Salinity Distribution with ECa-Directed Soil Sampling. *Journal of Environmental and Engineering Geophysics* 18.1: 1–25.

Corwin D.L., Lesch S.M., Oster J.D. and Kaffa S.R. 2006. Monitoring management-induced spatio-temporal changes in soil quality through soil sampling directed by apparent electrical conductivity. *Geoderma* 131.3-4: 369-387.

Corwin D.L. and Yemoto K. 2017. Salinity: electrical conductivity and total dissolved solids. *Methods of Soil Analysis* 2. Retrieved on 18th November, 2019 from doi:10.2136/msa2015.0039

Cosenza P., Guérin R. and Tabbagh A. 2003. Relationship between thermal conductivity and water content of soils using numerical modeling. *European Journal of Soil Science*, vol. 54, 581–587

Costa M.M., Queiroz D.M., Pinto F.A.C., Reis E.F.D. and Santos N.T. 2014. Moisture content effect in relationship between apparent electrical conductivity and soil attributes. *Acta Scientiarum Agronomy* 36.4: 395-401.

Crouse, D.A. 2018. Soils and Plant Nutrients, Chapter 1. In: K.A. Moore, and. L.K. Bradley (eds). North Carolina Extension Gardener Handbook. NC State Extension, Raleigh, NC. Retrieved on 8th March, 2020 from https://content.ces.ncsu.edu/extension-gardener-handbook/1-soils-and-plant-nutrients

Curado L.F.A., Rodrigues T.R., De Oliveira A. G., Novais J.W.Z., De Paulo I.J.C. and Nogueira M.S.B.E. 2013. Analysis of thermal conductivity in a seasonal flooded forest in the northern Pantanal. *Revista Brasileira de Meteorological* 28.2: 125-128

Dada S.S. 2006. Proterozoic evolution of Nigeria. In: O.Oshin (editor), the basement complex of Nigeria and its mineral resources, Akin Jinad and Co Press, Ibadan. 29-44.

Danbatta U.A. 2010. On the evolution of the kazaure schist belt of nw nigeria: a re-interpretation. *Global Journal of Geological Sciences* vol 8(2): 207-216.

Danbatta U.A. and Garba M.L. 2007. Geochemistry and petrogenesis of Precambrian amphibolites in the Zuru schist belt, northwest Nigeria. Journal of Mining and Geology, vol. 43(1): 23-30.

Dec D., Dörner J. and Horn R. 2009. Effect of soil management on their thermal properties**.** *J. Soil Sc. Plant Nutr*. 9.1: 26-39

Di Sipio E. and Bertermann B. 2018. Thermal properties variations in unconsolidated material for very shallow geothermal application (ITER project). *International Agrophysics,* vol. 32:149-164

Doerge T. 1999. Defining management zones for precision farming. *Crop Insights* 8.21: 1-5.

Dong X., Xu W., Zhang. and Daniel I. Leskovar D.I. 2016. Effect of irrigation timing on root zone soil temperature, root growth and grain yield and chemical composition in corn. *Agronomy* 2016, 6, 34. Retrieved on 16th June, 2017 from https://doi.org/10.3390/agronomy6020034

Dong Y., McCartney J.S. and Lu N. 2015. Critical review of thermal conductivity models for unsaturated soils. *Geotech. Geol Eng*. DOI 10.1007/s10706-015-9843-2

Dontsova K. and Norton L.D. 2001. Effects of exchangeable Ca:Mg ratio on soil clay flocculation, infiltration and erosion. In: D.E. Stott, R.H. Mohtar and G.C. Steinhardt (eds). 2001. Sustaining the Global Farm. Selected papers from the 10th Internattional Soil Conservation Organisation Meeting held May 24-29, 1999 at Purdue University and the USDA-ARS National Soil Erosion Research Laboratory, pg 580-585.

Edwards L.S. 1977. A modified pseudosection for resistivity and induced polarization. *Geophysics* 42: 1020-1036.

Egesi N. 2019. Petrography and structural features of migmatites, granites and granite gneisses at osokom and its environs Bansara area Southeastern Nigeria. *The Pacific Journal of Science and Technology*. Vol. 20 (1): 356-364.

Ekine, A.S.and Onuoha, K. M. 2010. Seismic geohistory and differential interformational velocity analysis in the Anambra Basin, Nigeria. *Earth Sci. Res. Journal*, vol. 14(1)):88-99.

Ekwue E.I. and Bartholomew J. 2011. Electrical conductivity of some soils in Trinidad as affected by density, water and peat content. *Biosystems Engineering* 108: 95-103.

Ekwue E.I., Stone R.J., Peters E.J. and Rampersad S. 2015. Thermal conductivities of some agricultural soils in Trinidad as affected by density, water and peat content. *The West Indian Journal of Engineering* 38.1: 61-69.

Elhakim A.F. 2016. Estimation of soil permeability. *Alexandria Engineering Journal* 55: 2631-2638.

El-Nafaty J.M. 2015. Geology and petrography of the rocks around Gulani Area, Northeastern Nigeria. *Journal of Geology and Mining Research*, vol. 7(5):41-57. DOI: 10.5897/JGMR15.0222

El-Naggar A.G., Hedley C.B., Horne D., Roudier P. and Clothier B. 2017. Using electrical conductivity imaging to estimate soil water content. In: Science and policy: nutrient management challenges for the next generation. (Eds L. D. Currie and M. J. Hedley). http://flrc.massey.ac.nz/publications.html. Occasional Report No. 30. Fertilizer and Lime Research Centre, Massey University, Palmerston North, New Zealand. 13 pages.

Elueze A.A., Jimoh A.O. and Aromolaran O.K. 2015. Compositional characteristics and functional applications of Obajana marble deposit in the Precambrian Basement Complex of central Nigeria. *Ife Journal of Science* 17.3: 591-603.

Eluwole A.B. 2016. In-situ soil resistivity measurements as indices for selected topsoil properties and maize yield prediction in a basement complex terrain of Ado-Ekiti, southwestern Nigeria. Unpublished Ph.D. thesis, Department of Geology, Obafemi Awolowo University, Ile-Ife, Nigeria, 342pp

Fagbenro A.W. and Woma T.Y. 2013. Quantitative Use of Surface Resistivity Data for Aquifer Hydraulic Parameter Estimation. A review. *International Journal of Engineering Research & Technology (IJERT)*, vol. 2(11): 342-348.

FAO and ITPS 2015.Status of the world's soil resources (SWSR)-main report. Food and Agriculture Organisation of the United Nations and Intergovernmental Technical Panel on soils, Rome, Italy. 1-607

Farouki O.T. 1986. Thermal properties of soils. Series on rock and soil mechanic. Trans. Tech. Publ., Clausthal-Zellerfield, Germany, vol. 11, 136p.

Fashae O., Olusola A. and Adedeji O. 2017. Geospatial analysis of changes in vegetation cover over Nigeria. *Bulletin of Geography. Physical Geography Series* 2017, 13 (2017): 17-28 http://dx.doi.org/10.1515/bgeo-2017-0010.

Fernando J. 2008. Determination of coefficient of permeability from soil percolation test. 12th International Conference of International Association for Computer Methods and Advances in Geomechanics (IACMAG) 1-6 October, 2008 Goa, India. 1324-1331.

Food and Agriculture Organisation (FAO). 2008. Guide to laboratory establishment for plant nutrient analysis. FAO fertilizer and plant nutrition bulletin 19, 1-204.

Fraisser C.W., Sudduth K.A. and Kitchen N.R. 2001. Delineation of site-specific management zones by unsupervised classification of topographic attributes and soil electrical conductivity. *American Society of Agricultural Engineers* 44.1: 155-166.

Friedman S.P. 2005. Soil properties influencing apparent electrical conductivity: a review. *Computers and Electronics in Agriculture* 46: 45-70.

Garcia N. and Damask A.1991. Physics for computer science students: with emphasis on atomic and semiconductor physics. New York, Springer-Verlag.

Gardner C.M.K., Laryea K.B. and Unger P.W. 1999. Soil physical constraints to plant growth and crop production. Land and water development division Food and Agriculture Organization of the United Nations. AGL/MISC/24/99

Gholizadeh A., Soom M.A.M., Anuar A.R. and Wayayok Aimrun W. 2012. Relationship between apparent electrical conductivity and soil physical properties in a Malaysian paddy field. *Archives of Agronomy and Soil Science*, vol. 58(2):155-168. http://dx.doi.org/10.1080/03650340.2010.509132

Ghuman, B.S. and Lal R. 1985. Thermal conductivity, thermal diffusivity and thermal capacity of some Nigerian soils. *Soil Science* 139.1: 74-80.

Gleeson T., Smith L., Moosdorf N., Hartmann J., Dürr H.H., Manning A.H., van Beek L.P.H., and Jellinek A.M. 2011. Mapping permeability over the surface of the Earth. *Geophysical Research Letters* 38 L02401 retrieved on 20th October, 2017 from doi:10.1029/2010GL045565

Goto S. and Matsubayashi O. 2009. Relations between the thermal properties and porosity of sediments in the eastern flank of the Juan de Fuca Ridge. *Earth Planets Space* 61: 863–870.

Gransee A. and Führs H. 2013. Magnesium mobility in soils as a challenge for soil and plant analysis, magnesium fertilization and root uptake under adverse growth conditions. *Plant Soil* 368: 5–21. doi 10.1007/s11104-012-1567-y

Gregory K.J., Simmons I.G., Brazel A.J., Day J.W., Keller E.A. Sylvester A.G. and Yānez-Arancibia. 2009. Soil science: In environmental sciences: A student's comparison. SAGE publication ltd, London. Dx.doi.org/10.4135/9781446216187.n34

Grisso R.B., Alley M., Wysor W.G., Holshouser D. and Thomason W. 2009. Precision farming tools: soil electrical conductivity communications and marketing, College of Agriculture and Life Sciences, Virgnia Polytechnic Institute and State University. Retrieved on 23rd December, 2017 from www.ext.vt.edu

Guo Y., Huang J., Shi Z. and Li H. 2015. Mapping Spatial Variability of Soil Salinity in a Coastal Paddy Field Based on Electromagnetic Sensors. *PLoS ONE* 10.5: e0127996. doi:10.1371/journal.pone.0127996

Hamdhan I.N and Barry G. Clarke B.G. 2010. Determination of thermal conductivity of coarse and fine sand soils. Retrieved on 16th May, 2017 from Proceedings of World Geothermal Congress 2010, Bali, Indonesia, 25-29 April 2010.

Haruna I.V. 2016. Lithology and field relationships of the granitoids of Bauchi district, northeastern Nigeria. International Research Journal of Earth Sciences, vol. 4(6): 31-40.

Haskell D.E, Flaspohler D.J., Webster C.R. and Meyer M.W. 2010.Variation in soil temperature, moisture, and plant growth with the addition of downed woody material on lakeshore restoration sites. *Restoration Ecology.* doi: 10.1111/j.1526-100X.2010.00730.x

Hatfield J. L. and Prueger J.H. 2015. Temperature extremes: Effect on plant growth and development. Weather and Climate Extremes, vol. 10:4-10.

Hawkins E., Fulton J. and Port K. 2017. Using soil electrical conductivity (EC) to delineate field variation. College of Food, Agricultural and Environmetal Sciences, Ohio State University. Retrieved on 20th December, 2017 from https://ohioline.osu.edu/factsheet/fabe-565.

He Y., DeSutter T.M. and Clay D.E. 2013. Dispersion of Pure Clay Minerals as Influenced by Calcium/Magnesium Ratios, Sodium Adsorption Ratio, and Electrical Conductivity. *Soil Science Society of America Journal* 77: 2014–2019

Heil K. and Schmidhalter U. 2017. The application of EM38: determination of soil parameters, selection of soil sampling points and use in agriculture and archaeology. Sensors, 17:2540. doi:10.3390/s17112540

Hillel D. 2004. Introduction to environmental soil physics, Elsevier Academic Press, USA. 145pp

Ho S.Y., Wasli M.E.B. and Perumal M. 2019. Evaluation of physicochemical properties of sandy-textured soils under smallholder agricultural land use practices in Sarawak, East Malaysia. *Applied and Environmental Soil Science.* Retrieved on 16th March, 2020 from doi.org/10.1155/2019/7685451

Horneck, D.A., Sullivan, D.M. Owen, J.S., Hart, J.M. 2011. Soil test interpretation guide. Oregon State University Extension Service, EC 1478, USA. 12p. Retrieved on 6th September, 2019. https://catalog.extension.oregonstate.edu/ec1478.

Hossain Z. and Cohen A.J. 2012. Relationship among porosity, permeability, electrical and elastic properties. SEG Las Vegas 2012 Annual Meeting. Retrieved on 6th September, 2019. from http://dx.doi.org/10.1190/segam2012-1496.1

Hossain M.B., Lamb D.W., Lockwood P.V. and Frazier P. 2010. EM38 for volumetric soil water content estimation in the rootzone of deep vertosol soils. *Computers and Electronics in Agriculture* 74:100-109.

Ibiremo O.S., Daniel M.A., Iremiren G.O. and Fagbola O. 2011. Soil fertility evaluation for cocoa production in southeastern Adamawa state, Nigeria. *World Journal of Agricultural Sciences* 7.2: 218-223.

Ibrahim A., Toyin A. & Sanni Z. J. 2015. Geological characteristics and petrographic analysis of rocks of Ado-Awaiye and its environs, Southwestern Nigeria. *International Journal of Applied Science and Mathematical Theory*, 28-47.

Inthavong T., Fukai S. and Tsubo M. 2011. Spatial Variations in Water Availability, Soil Fertility and Grain Yield in Rainfed Lowland Rice: A Case Study from Savannakhet Province, Lao PDR, *Plant Production Science* 14.2: 184-195. doi: 10.1626/pps.14.184

Jaja N. 2016. Understanding the texture of your soil for agricultural productivity. Virginia State University, Virginia Cooperative Extension, publication CSES-162P. Retrieved on 30th August 2019 from www.ext.vt.edu.

Kasidi, S. 2019. Determination of Curie Point Depth, Heat Flow and Geothermal Gradient from High Resolution Aeromagnetic Data around Lamurde Area, Adamawa State, North-Eastern Nigeria. *Open Journal of Geology*, vol. 9:829-838. https://doi.org/10.4236/ojg.2019.911093

Khadka D., Lamichhane S., Bhantana P., Ansari A.R., Joshi S. and Baruwal P. 2018. Soil fertility assessment and mapping of chungbang farm, Pakhribas, Dhankuta, Nepal. *Advances in Plants and Agricultural Research* 8.3: 219–227. doi: 10.15406/apar.2018.08.00317

Khattak R.A. and Hussain Z. 2007. Evaluation of soil fertility status and nutrition of orchards. *Soil & Environ.* 26.1: 22-32

Kibria G. and Hossain S. 2019. Electrical resistivity of compacted clay minerals. *Environmental Geotechnics*, 6.1: 18–25. https://doi.org/10.1680/jenge.16.00005

Kim K., Yoo J., Kim S., Lee H.S., Ahn K. and Kim I.S. 2007. Relationship between the electric conductivity and phosphorus concentration variations in an enhanced biological nutrient removal process. *Water Science and Technology* 55.1-2: 203-208

Kirkby, A., Heinson G. and Krieger L. 2016. Relating permeability and electrical resistivity in fractures using random resistor network models, *Journal of Geophysical Research Solid Earth* 121: 1546–1564. doi:10.1002/2015JB012541.

Kizito F., Campbell C.S., Campbell G.S., Cobos D.R., Teare B.L., Carter B.,and Hopmans J.W. 2008. Frequency, electrical conductivity and temperature analysis of a low cost capacitance soil moisture sensor. *Journal of Hydrology* 352: 367-378.

Kodešová R., Vlasáková M., Fér M., Teplá D., Jakšík O., Neuberger P., Adamovský R. 2013. Thermal properties of representative soils of the Czech Republic. *Soil Water Res*., vol. 8: 141–150.

Kool D., Tong B., Tian Z., Heitman J.L., Sauer T.J. and Horton R. 2019. Soil water retention and hydraulic conductivity dynamics following tillage. *Soil and Tillage Research* 193: 95-100.

Korsaeth A. 2005. Soil apparent electrical conductivity (ECa) as a means of monitoring changesin soil inorganic N on heterogeneous morainic soils in SE Norway during two growing seasons. *Nutrient Cycling in Agroecosystems* vol.72: 213–227. DOI 10.1007/s10705-005-1668-6

Kurowska E. and Schoeneich K. 2010. Geothermal Exploration in Nigeria. Proceedings World Geothermal Congress 2010 Bali, Indonesia, 25-29 April 2010. Retrieved on 9th October, 2021.

Lambot S., Slob E., Chavarro D., Lubczynski M. and Vereecken H. 2008. Measuring soil surface water content in irrigated areas of southern Tunisia using full-waveform inversion of proximal GPR data. *Near Surface Geophysics* 6: 403-410.

Li K., Shapiro M., Horne R.N., Ma S., Hajari A. and Mudhhi M. 2014. *In situ* estimation of relative permeability from resistivity measurements. *Petroleum Geoscience* 20: 143–151. http://dx.doi.org/10.1144/petgeo2013-002

Lide D.R. 2007. CRC Handbook of Chemistry and Physics, 88th edition. CRC Press, London. 5-71.

Lipiec, J., C. Doussan, A. Nosalewicz and Kondracka K. 2013. Effect of drought and heat stresses on plant growth and yield: A review. *International Agrophysics* 27: 463-477. doi: 10.2478/intag-2013-0017

Loke M.H. 2000. Electrical imaging surveys for environmental and engineering studies: A pratical guide to 2-D and 3-D surveys, 61pp.

Manoucheri H.R., Rao K.H. and Forssberg K. S. E. 2002. Triboelectric charge, electrophysical properties and electrical beneficiation potential of chemically treated feldspar, quartz and wollastonite. *Magnetic and Electrical Separation* 11.1-2: 9-32.

Mäntynen M. 2001. Temperature correction coefficients of electrical conductivity and of density measurements for saline groundwater. Posiva Oy Working Report 2001-15, Töölönkatu 4, FIN-00100 Helsinki, Finland. https://www.google.com/url?sa=t&rct=j&q=&esrc=s&source=web&cd=1&cad=rja&uact=8&ved=2ahUKEwiKu4G6pMXpAhX5BGMBHTBDBFUQFjAAegQIAxAB&url=http%3A%2F%2Fwww.posiva.fi%2Ffiles%2F2094%2FPOSIVA-2001-15_Working-report_web.pdf&usg=AOvVaw10wyc8HeMU8Brk-OToQxny

Marshall W.L. 1987. Electrical conductance of liquid and supercritical water evaluated at 0˚C and 0.1 MPa to high temperatures and pressures: reduced state relationships. *Journal of Chemical and Engineering Data* 32: 221-226.

McCauley A., Jones C. and Jacobsen J. 2005. Basic soil properties. Soil and water management module 1 Montana State University, Extension Service Continuing Education Series, pg1-12. Retrieved on 18th November, 2017. www.montana.edu/publications/

McCutcheon M.C., Farahani H.J., Stednick J.D., Buchleiter G.W. and Green T.R. 2006. Effect of Soil Water on Apparent Soil Electrical Conductivity and Texture Relationships in a Dryland Field. *Biosystems Engineering*, vol. 94 (1):19–32. doi:10.1016/j.biosystemseng.2006.01.002

Medeiros W.N., Valente D.S.M, Queiroz D.M., Pinto F.A.C and Assis I.R. 2018. Apparent soil electrical conductivity in two different soil types. *Revista Ciência Agronômica* 49.1: 43-52. doi: 10.5935/1806-6690.20180005

Milsom J. 2003. Field geophysics: the geological field guide series. John Wiley and Sons Ltd, pg 97-116.

Miyamoto T., Kameyama K. and Iwata Y. 2015. Monitoring electrical conductivity and nitrate concentrations in Andisol field using time domain reflectometry. *Japan Agricultural Research Quarterly (JARQ),* vol. 49(3):261-267.

Molin J.P. and Faulin G.D.C. 2013. Spatial and temporal variability of soil electrical conductivity related to soil moisture. *Scientia. Agricola* 70.1: 1-5.

Mommer L. 1999. The water relations in cacao (Theobroma cacao L.): modelling root growth and evapotranspiration. M.Sc. Thesis Department of Theoretical Production Ecology, Wageningen Agricultural University, Netherlands. 57pp

Monteiro M.T.F., Oliveira S.M., Luizão F.J., Cândido L.A., Ishida F.Y. and Tomasella J. 2013. Dissolved organic carbon concentration and its relationship to electrical conductivity in the waters of a stream in a forested Amazonian blackwater catchment, *Plant Ecology & Diversity*. Retrieved on 9th June, 2018 from doi:10.1080/17550874.2013.820223

Moore R.D., Richards G. and Story A. 2008. Electrical conductivity as an indicator of water chemistry and hydrologic process. *Streamline Watershed Management Bulletin* 11.2: 25-29

Moral F.J. and Rebollo F.J. 2017. Characterization of soil fertility using the Rasch model. *Journal of soil science and plant nutrition* 17.2: 486-498.

Moral F.J., Terrón J.M. and Marques da Silva J.R. 2010. Delineation of management zones using mobile measurements of soil apparent electrical conductivity and multivariate geostatistical techniques. *Soil and Tillage Research* 106: 335-343.

Mueller T.G., Hartsock N.J., Stombaugh T.S., Shearer S.A., Cornelius P.L. and Barnhisel R.I. 2003. Soil electrical conductivity map variability in limestone soils overlain by loess. *Agronomy Journal* 95: 496–507.

Mukungurutse C.S., Nyapwere N., Manyanga A.M. and Mhaka L. 2018. Pedological characterization and classification of typical soils of Lupane district, Zimbabwe. International *Journal of Journal of Plant and Soil Sciences* 22.3: 1-12. doi: 10.9734/IJPSS/2018/39609

Musa H.I., Hassan L., Shamsuddin Z.H., Panchadcharam C., Zakaria Z., Abdul Aziz S. 2016. Physicochemical properties influencing presence of Burkholderia pseudomallei in soil from small ruminant farms in Peninsular Malaysia. *PLoS ONE* 11.9: e0162348. Retrieved on 20th November, 2018 from doi:10.1371/journal.pone.0162348

Mzuku M., Khosla R., Reich R., Inman D., Smith F. and MacDonald L. 2005. Spatial variability of measured soil properties across site-specific management zones. *Soil Science Society of American Journal* 69: 1572-1579.

Nemali K. 2018. Details of electrical conductivity measurements in greenhouse production. Purdue University, Purdue Horticulture and Landscape Architecture-Purdue Extension. Retrieved on 27th September, 2019 from www.ag.purdue.edu/HLA

Nigeria Geological Survey Agency (N. G. S. A.), 2009. The Geological Map of Nigeria. A publication of Nigeria Geological Survey Agency, Abuja, Nigeria.

Nijp J.J., Metselaar K., Limpens J., Gooren H.P.A., van der Zee S.E.A.T.M. 2017. A modification of the constant-head permeameter to measure saturated hydraulic conductivity of highly permeable media. *MethodsX* 4: 134–142. http://dx.doi.org/10.1016/j.mex.2017.02.002

Nord R.S. 2018. Conductivity and chemical reactions. Experiment 5-conductivity, Eastern Michigan University. Retrieved on 27th September, 2019 from www.emich.edu/chemistry/genchemlab/documents/5conductivity_and_reactions.pdf

Nyugen T.T. and Marschner P. 2013. Addition of a fine textured soil to compost to reduce leaching in a sandy soil. *Soil Research* 51: 232-239.

Obaje N.G. 2009. Geology and mineral resources of Nigeria, lecture notes in earth Sciences. Retrieved on 30th November, 2019 from doi 10.1007/978-3-540-92685-6

Obaje N.G., Balogun D. O.,. Idris-Nda A,. Goro I. A., Ibrahim S. I., Musa M. K., Dantata S. H., Yusuf I., Mamud-Dadi N and Kolo I. A. 2013. Preliminary integrated hydrocarbon prospectivity evaluation of the bida basin in north central Nigeria. *Petroleum Technology Development Journal*, vol.3 (2): 36-65.

Obaje N.G., Musa M.K., Odoma A. N., and Hamza H. 2011. The Bida Basin in north-central Nigeria: sedimentology and petroleum geology. *Journal of Petroleum and Gas Exploration Research,* vol. 1(1): 001-013.

Ocan O.O. 2006. Contribution of Professor M.A.O. Rahaman to the understanding of the Precambrian geology of Nigeria. In: O.Oshin (editor), the basement complex of Nigeria and its mineral resources, Akin Jinad and Co Press, Ibadan. 3-11.

Odekunle T.O. 2004. Rainfall and the length of the growing season in Nigeria. *International Journal of Climatology*, vol. 24: 467–479.

Ogeh J.S. and Ipinmoroti R.R. 2015. Soil organic carbon dynamics under different plantation crops of different ages in tropical oxic Paleustalf. *University of Mauritius Research Journal* 21: 1-14.

Okoffo, E.D., Ofori, A., Nkoom, M. and Bosompem, O.A. 2016. Assessment of the physicochemical characteristics of soils in major cocoa producing areas in the Dormaa West District of Ghana, *International Journal of Scientific & Technology Research* 5.2: 62-68.

Oladunjoye M.A. and Sanuade O.A. 2012. Thermal diffusivity, thermal effusivity and specific heat of soils in Olorunsogo power plant, southwestern Nigeria. *IJRRAS* 13.2: 502-521.

Oladunjoye, M.A., Sanuade, O.A. and Olaojo, A.A. 2013. Variability of soil thermal properties of a seasonally cultivated agricultural teaching and research farm, University of Ibadan, south-western Nigeria. *Global Journal of Science* 13.8: 41-63.

Olatunji A.S. and Jimoh R. O. 2016. Geochemical Study of Tourmalines from Some Parts of Southwestern Nigeria. *International Research Journal of Geology and Mining (IRJGM)* vol. 6(1): 009 – 0027. DOI: http://dx.doi.org/10.14303/irjgm.2016.107

Olarewaju V.O. 2006. The charnockitic intrusives of Nigeria. In: O.Oshin (editor), the basement complex of Nigeria and its mineral resources, Akin Jinad and Co Press, Ibadan. 45-70.

Oldham L. 2015. Potassium in Mississippi. Mississippi State University Extension Service. Information Sheet 894 (POD-09-15), Retrieved on 9th October, 2019 from https://www.google.com/url?sa=t&rct=j&q=&esrc=s&source=web&cd=1&cad=rja&uact=8&ved=2ahUKEwjMiYHMq8XpAhURtRoKHWnJDz0QFjAAegQIBRAB&url=https%3A%2F%2Fextension.msstate.edu%2Fsites%2Fdefault%2Ffiles%2Fpublications%2Finformation-sheets%2Fis0894_1.pdf&usg=AOvVaw0It0tqHYZ_beH24nzeuf3Z

Oleschko K., Korvin G., Muñoz A., Velazquez J., Miranda M. E., Carreon D., Flores L., Martínez M., Velásquez-Valle M., Brambila F., Parrot J.-F., and Ronquillo G. 2008. Mapping soil fractal dimension in agricultural fields with GPR. *Nonlinear Processes in Geophysics* 15: 711–725.

Oli I.C., Okeke O.C., Abiahu C.M.G., Anifowose F.A. and Fagorite V.I. 2019. A Review of the Geology and Mineral Resources of Dahomey Basin, Southwestern Nigeria. Internationational Journal of Environmental Science and Natural Resources. vol. 21(1): 36-40.

Olorunfemi I.E., Fasinmirin J.T. and Akinola F.F. 2018. Soil physico-chemical properties and fertility status of long-term land use and cover changes: A case study in Forest vegetative zone of Nigeria. *Eurasian Journal of Soil Science* 7.2: 133-150.

Olson-Rutz K. and Jones C. 2018. Soil nutrient management for forages: Phosphorus, potassium, sulphur and micronutrient. Montana State University Extension Service, EB0217. Retrieved on 9th October, 2019 from www.landresources.montana.edu/pdf/pub/foragePKSMEBO217

Okunlola O.A. 2006. Regional metallogeny of rare metals (Ta-Nb) mineralization in Precambrian pegmatites of Nigeria. In: O.Oshin (editor), the basement complex of Nigeria and its mineral resources, Akin Jinad and Co Press, Ibadan. 107-126.

Okunlola O.A. & Owoyemi K.A. 2015. Compositional characteristics of geophagic clays in parts of southern Nigeria, *Earth Science Research* 4.2: 1-15.

Omer A. and Omer A.M. 2014. Soil thermal properties and the effects of groundwater on closed loops. *International Journal of Sustainable Energy and Environmental Research,* vol. 3(1): 34-52

Omosanya K.O., Sanni R.A., Laniyan T.A., Mosuro G., Omosanya and Falana L. 2012. Petrography and Petrogenesis of Pre-Mesozoic rocks, Ago-Iwoye NE, SW Nigeria. In: (Ed.) Gordon S. Lister, *Journal of the Virtual Explorer*, Vol. 40 (1):1-18. doi: 10.3809/jvirtex.2012.00313.

Othaman N.N.C., Md Isa M.N., Hussin R., Ismail R.C. , Md Naziri S.Z., Murad S.A.Z., Harun A. and Ahmad M.I. 2020. Development of Soil Electrical Conductivity (EC) Sensing System in Paddy Field. *Journal of Physics*: 5th International Conference Series 1755 (2021) 012005 IOP Publishing doi:10.1088/1742-6596/1755/1/012005

Oyediran I.A. and Adeyemi G.O. 2012. Geochemical Assessment of a Proposed Landfill in Ibadan, Southwestern Nigeria. *The Pacific Journal of Science and Technology* 13.1: 640-651.

Oyeyiola G.P. and Agbaje A.B. 2013. Physicochemical analysis of a soil near microbiology laboratory at the University of Ilorin, main campus. *Journal of Natural Sciences Research* 3.6: 78-81.

Ozcep F., Yıldırım E., Tezel O., Asci M. and Karabulut S. 2010. Correlation between electrical resistivity and soil-water content based artificial intelligent techniques. *International Journal of Physical Sciences* 5.1: 47-56.

Ozlu E. and Kumar S. 2018. Response of soil organic carbon, pH, electrical conductivity and water stable aggregates to long term annual manure and inorganic fertilizer. *Soil Science Society of America Journal*. Retrieved on 9th October, 2019 from doi.10.2136./sssaj2018.02.0082, pg1243-1251

Pandey L. M. S., Shukla S. K. and Habibi D. 2015. Electrical resistivity of sandy soil. *Géotechnique Letters* 5: 178–185. http://dx.doi.org/10.1680/jgele.15.00066

Parsons, T.L. and Zwanzig, H.V. 2003. Mineral modes of gneiss along the Thompson Nickel Belt–Kisseynew domain boundary, Manitoba (parts of NTS 63J, 63O, 63P, 64A and 64B); in Report of Activities 2003, Manitoba Industry, Trade and Mines, Manitoba Geological Survey, p. 132–136.

Pearce B. and Palmer G. 1999. Using conductivity meters for nitrogen management in float systems. College of Agriculture, University of Kentucky, Cooperative Extension Service AGR-174. issue 5-1999. Retrieved on 27th September, 2019 from http://www.ca.uky.edu.

Pedrera-Parrilla A., Brevik E. C., Giráldez J. V. and Vanderlinden K. 2016. Temporal stability of electrical conductivity in a sandy soil. *International Agrophysics* 30: 349-357. doi: 10.1515/intag-2016-0005

Peralta N.R. and Costa J.L. 2013. Delineation of management zones with soil apparent electrical conductivity to improve nutrient management. *Computers and Electronics in Agriculture*, vol. 99: 218–226.

Peralta N.R., Costa J.L., Balzarini M. and Angelini H. 2013. Delineation of management zones with measurements of soil apparent electrical conductivity in the southeastern pampas. *Canadian Journal of Soil Science* 93: 205-218. doi:10.4141/CJSS2012-022

Proffitt T. 2014. Assessing soil quality and interpreting soil test results. Retrieved on 2nd September, 2019 from www.winewa.asn.au

Qing Z., Jie T., Zhaoyang L., Wei Y. and Yucong D. 2018. The influence of soil physico-chemical properties and enzyme activities on soil quality of saline-alkali agroecosystems in western Jilin Province, China. *Sustainability*, 10, 1529. doi:10.3390/su10051529

Rahaman M.A.O. 2006a. Nigeria's solid mineral endowment and sustainable development. In: O.Oshin (editor), the basement complex of Nigeria and its mineral resources, Akin Jinad and Co Press, Ibadan. 139-168.

_____ 2006b. The government, us and the attainment of our twin goals (increasing the nation's wealth and improving the quality of life of the citizenry). In: O.Oshin (editor), the basement complex of Nigeria and its mineral resources, Akin Jinad and Co Press, Ibadan. 169-186.

_____ 2006c. Nigeria's solid mineral endwonment and sustainable development. In: O.Oshin (editor), the basement complex of Nigeria and its mineral resources, Akin Jinad and Co Press, Ibadan. 139-168.

Rahman T., Lebedev M., Zhang Y., Barifcani A., and Iglauer S. 2017. Influence of rock microstructure on its electrical properties: an analysis using x-ray microcomputed tomography. *Energy Procedia* 114: 5023–5031

Revil A. and Glover P.W.J. 1998. Nature of surface electrical conductivity in natural sands, sandstones, and clays. *Geophysical Research Letters* 25.5: 691-694

Reynolds J.M. 1997. An introduction to applied and environmental geophysics. Wiley and Sons, New York, pp 415.

Rhoades J.D., Manteghi N.A., Shouse P.J. and Alves W.J. 1989. Soil electrical conductivity and soil salinity: new foundations and calibrations. *Soil Science Society of America Journal* 53.2: 433-439.

Ribeiro M.A.Q., de Almeida A.F., Mielke M.S., Gomes F.P., Pires M.V. and Baligar V.C. 2013. Aluminum effects on growth, photosynthesis, and mineral nutrition of cacao genotypes, *Journal of Plant Nutrition* 36.8: 1161-1179.

Ritchey E., McGrath J. and Gehring D. 2015. Determining Soil Texture by Feel. University of Kentucky College of Agriculture, Food and Environment Cooperative Extension Service AGR-127. Retrieved on 16th July, 2019 from www.ca.uky.edu.

Rodríguez-Pérez J.R., Plant R.E, Lambert J. and Smart D.R. 2011. Using apparent soil electrical conductivity (ECa) to characterize vineyard soils of high clay content. *Precision Agric* (2011) 12:775–794 DOI 10.1007/s11119-011-9220-ys

Rubio C.M. 2015. Effects on the relationship between thermal conductivity and moisture for a stony sandy soil. *European Journal of Environmental and Safety Sciences* 3.1: 10-16.

Ryšan L. and Šařec O. 2008. Research of correlation between electric soil conductivity and yield based on the use of GPS technology. *RES. AGR. ENG.,* vol. 54, (3): 136–147.

Samouëlian, A., Cousin I., Tabbagh A., Bruand A., Richard G. 2005. Electrical resistivity survey in soil science: a review. *Soil & Tillage Research* 83: 173–193

Scherer T.F., Franzen D., and Cihacek L. 2013. Soil, Water and Plant Characteristics Important to Irrigation. Retrieved on 4th October, 2017 from *https://www.ag.ndsu.edu/publications/crops/soil-water-and-plant characteristics-important-to-irrigation/ae1675.pdf* ***AE1675*** *(Revised).*

Schoeneberger P.J., Wysocki D.A., Benham E.C. and Soil Survey Staff. 2012. Field book for describing and sampling soils, Version 3.0. Natural Resources Conservation Service, National Soil Survey Center, Lincoln, NE. ix + 9-14pp Retrieved on 19th September 2017 from https://www.google.com/url?sa=t&rct=j&q=&esrc=s&source=web&cd=&cad=rja&uact=8&ved=2ahUKEwjSgNuun8bpAhVHQxUIHfhdBEcQFjAAegQIBhAB&url=https%3A%2F%2Fwww.nrcs.usda.gov%2FInternet%2FFSE_DOCUMENTS%2Fnrcs142p2_052523.pdf&usg=AOvVaw0Lfj2UeibO5Ldk4N87Tuq-

Schoonover J.E. and Crim J.F. 2015. An Introduction to Soil Concepts and the Role of Soils in Watershed Management. *Journal of Contemporary Water Research & Education*, Issue 154, Pages 21-47.

Sharu M.B., Yakubu M., Noma S.S. and Tsafe A.I. 2013. Characterization and classification of soils on an agricultural landscape in Dingyadi district, Sokoto state, Nigeria. *Nigerian Journal of Basic and Applied Science* 21.2: 137-147. http://dx.doi.org/10.4314/njbas.v21i2.9

Shein. E. V. and Mady A.Y. 2016. Soil thermal parameters assessment by direct method and mathematical models. *Journal of Soil Science and Environmental Management* 7.10: 166-172.

Shin J.H. and Son J.E. 2015. Changes in electrical conductivity and moisture content of substrate and their subsequent effects on transpiration rate, water use efficiency, and plant growth in the soilless culture of Paprika (*Capsicum annuum* L.). *Hort. Environ. Biotechnol*. 56.2: 178-185. doi 10.1007/s13580-015-0154-6

Siqueira G.M., Dafonte J.D., Armesto M.V. and e Silva E.F.F. 2014. Using multivariate geostatistics to access patterns of spatial dependence of apparent soil electrical conductivity and selected soil properties. *The Scientific World Journal*, volume 2014. Retrieved on 6th September, 2017 dx.doi.org/10.1155/2014/712403

Siqueira G.M., Dafonte J.D., González A.P., Armesto M.V., e Silva Ê.F.F, Costa M.K.L. and Silva R.A. 2016. Measurement of apparent electrical conductivity of soil and the spatial variability of soil chemical properties by electromagnetic induction. African *Journal of Agricultural Research*, Vol. 11(39): 3751-3762. DOI: 10.5897/AJAR2016.11088

Smarsly K. 2013. Agricultural ecosystem monitoring based on autonomous sensor systems. 2013 Second International Conference on Agro-Geoinformatics (Agro-Geoinformatics) 12-16 Aug. 2013, IEEE. Retrieved on 8th August, 2017 from doi**:** 10.1109/Argo-Geoinformatics.2013.6621952.

Sonon L.S., Kissel D.E., and Saha U. 2014. Cation exchange capacity and base saturation. University of Georgia *UGA-Extension Circular 1040. Retrieved on 3rd August, 2019 from https://extension.uga.edu/publications/detail.html?number=C1040&title=Cation%20Exchange%20Capacity%20and%20Base%20Saturation*

Sonon L.S., Saha U. and Kissel D.E. 2015. Soil salinity- testing, data interpretation and recommendation. University of Georgia Agricultural and Environmental Services Laboratories, UGA extension circular 1019. *Retrieved on 1st October, 2019 from* https://extension.uga.edu/publications/detail.html?number=C1019&title=Soil%20Salinity%20Testing,%20Data%20Interpretation%20and%20Recommendations

Sriraam A.S., Samath T.R.J. and Raghunandan M.E. 2016. Electrical conductivity of compacted kaolin. International Conference on Geomechanics, Geo-energy and Geo-resources, IC3G 2016, 6p. Retrieved on 4th September, 2019 from https://www.researchgate.net/publication/313713971_Electrical_conductivity_of_compacted_kaolin

Suarez D.L. and Gonzalez-Rubio A. 2017. Effects of the dissolved organic carbon of treated municipal wastewater on soil infiltration as related to sodium adsorption ratio and pH. *Soil Science Society of America Journal* 81: 602–611.

Sudhir B. and Pradeep K.J. 2014. Correlation between electrical resistivity and water content of sand- a statistical approach. *American International Journal of Research in Science, Technology, Engineering and Mathematics* 6.2: 115-121.

Szentes, G. 2009. Granite formations and granite cavities in northern Nigeria. *Cadernos Lab. Xeolóxico de Laxe Coruña*, vol. 34: 13 – 26.

Terzaghi, K. and Peck R.B. 1967. Soil Mechanics in Engineering Practice. New York: J. Wiley and Sons, Inc.

Tessy, P.C. and Renuka, G. 2008. Thermal diffusivity of soils in iso-hyperthermic temperature regime by harmonic analysis. *Indian Journal of Radio and Space Physics* 37: 360-365.

Tkaczyk P., Bednarek W., Dresler S. and Krzyszozak J. 2018. The effect of some soil physicochemical properties and nitrogen fertilization on winter wheat yield. *Acta Agroph*. 25.1: 107-116.

UNSW. 2007. Soil properties: Exchangeable cations. terraGIS. Retrieved on 2nd October, 2019 from www.terragis.bees.unsw.edu.ac/terraGIS_soil/sp_exchangeable_cations.html

USDA Natural Resources Conservation Service. 2011. Soil Quality Indicators. Retrieved on 19th September, 2017 from https://www.nrcs.usda.gov/wps/portal/nrcs/detail/soils/health/assessment/?cid=stelprdb1237387.

van Lier Q. J. and Durigon A. 2012. Soil thermal diffusivity estimated from data of soil temperature and single soil component properties. *R. Bras. Ci. Solo* 37: 106-112.

van Vliet J.A., Slingerland M. and Giller K.E. 2015. Mineral nutrition of cocoa. A review. Wageningen University and Research Centre, Wageningen, 57pp.

Wang J., Zhang X. Du L. 2017. A laboratory study of the correlation between the thermal conductivity and electrical resistivity of soil. *Journal of Applied Geophysics*, vol. 145: 12–16.

Wardani A.K. and Purqon A. 2016. Thermal conductivity prediction of soil in complex plant soil system using artificial neural networks. *Journal of Physics: Conference Series 739 (2016) 012007.* Retrieved on 15th August, 2018 from doi:10.1088/1742-6596/739/1/012007

Warrick A.W. and Nielsen R.R. 1980. Spatial variability of soil physical properties in the field. In: D. Hillel (Ed) Application of soil physics, Academic Press, New York, NY, USA.

Watanabe Y., Kikuno H., Asiedu R., Masunaga T. and Wakatsuki T. 2015. Comparison of physicochemical properties of soils under contrasting land use systems in southwestern Nigeria. *JARQ* 49.4: 319–331.

Wayne B., Quirine K., Steve A., Steve P., Jonathan R., Renuka R., and Steve D. 2007. "Soil Texture." Agronomy Fact Sheet Series, Fact Sheet 29. Department of Crop Sciences, College of Agriculture & Life Sciences, Cornell University Cooperative Extension. Retrieved on 23rd August 2019 from http://water.rutgers.edu/Rain_Gardens/factsheet29.pdf.

White A.F., Bullen T.D., Schulz M.S., Blum A.E., Huntington T.G., and Peters N.E. 2001. Differential rate of feldspar weathering in granitic regoliths. *Geochimica et Cosmochimica Acta*, vol. 65(1): 847-869

White P.J. and Broadley M.R. 2003. Calcium in plants. *Annals of Botany*, vol. 92: 487-511

Widjonarko N.E. 2016. Introduction to advanced X-ray diffraction techniques for polymeric thin films. *Coatings*, 6 (54). Retrieved on 18th August 2019 from doi:10.3390/coatings6040054

Wilson M.J. 2004. Weathering of the primary rock-forming minerals: processes, products and rates. *Clay Minerals*, vol. 39: 233–266

Wodaje A. and Abebaw A. 2014. Analysis of selected physicochemical parameters of soils used for cultivation of garlic (*Allium sativum* L.). *Science, Technology and Arts Research Journal (International Journal of Wollega University, Ethiopia)* 3.4: 29-35.

Woods End Research Laboratory's. 1996. A Basic Guide for Interpreting Soil Test Values. SEPTEMBER / OCTOBER 1997 BIODYNAMICS Farming and Gardening in the 21st Century, pg 27-31.

Yan B. and Hou Y. 2018. Effect of soil magnesium on plants: a review. *Earth and Environmental Science*, Retrieved on 23rd December 2019 from doi.10.1088/1755-1315/170/2/022168

Yusof N.Q.A.M. and Zabidi H. 2016. Correlation of mineralogical and textural characteristics with engineering properties of granitic rock from Hulu Langat, Selangor. *Procedia Chemistry*, vol. 19: 975 – 980.

Zhou X., Liu D., Bu H., Deng L., Liu H., Yuan P., Du P. and Song H. 2018. XRD-based quantitative analysis of clay minerals using reference intensity ratios, mineral intensity factors, Rietveld, and full pattern summation methods: A critical review. *Solid Earth Sciences* 3: 16-29.

APPENDICES

Respresentative data from some selected stations

Table 5.1: Electrical conductivity of soil in the cocoa farm during the wet season

Line 1			Line 4			Line 7		
Northing	Easting	EC (µS/cm)	Northing	Easting	EC (µS/cm)	Northing	Easting	EC (µS/cm)
7.22201	3.86123	20	7.22205	3.8613	27	7.22207	3.86141	19
7.22198	3.86123	24	7.22204	3.86132	23	7.22203	3.86142	34
7.22196	3.86122	30	7.222	3.86132	33	7.22202	3.8614	24
7.22194	3.86122	26	7.22198	3.8613	18	7.22199	3.86143	23
7.22189	3.86123	18	7.22195	3.86132	16	7.22196	3.86141	34
7.22189	3.86124	22	7.22192	3.86131	28	7.22192	3.86142	227
7.22188	3.86124	36	7.22188	3.86132	35	7.2219	3.86142	58
7.22186	3.86122	41	7.22187	3.86128	103	7.22186	3.8614	71
7.22183	3.86122	74	7.22183	3.86132	344	7.22183	3.86141	104
7.22182	3.86122	66	7.22179	3.86132	134	7.22181	3.86141	73
7.22177	3.86121	51	7.22177	3.86131	82	7.22179	3.86142	55
7.22173	3.86122	46	7.22174	3.86128	93	7.22175	3.8614	48
7.22171	3.86121	48	7.22173	3.86131	93	7.22173	3.86142	44
7.2217	3.86121	39	7.2217	3.86134	114	7.22171	3.86141	36
7.22166	3.86121	51	7.22167	3.86132	75	7.22169	3.8614	48
7.22164	3.86122	96	7.22163	3.86131	64	7.22165	3.8614	57
7.22161	3.86122	146	7.2216	3.86132	102	7.22163	3.86139	54
7.2216	3.86121	211	7.22158	3.86128	231	7.22159	3.8614	49
7.22156	3.86121	155	7.22155	3.86131	247	7.22157	3.8614	160
7.22154	3.86121	76	7.22152	3.86131	170	7.22154	3.86139	116
7.22152	3.86121	109	7.2215	3.8613	125	7.22151	3.86138	88
7.2215	3.86122	191	7.22147	3.86127	169	7.22148	3.86139	73
7.22147	3.86123	75	7.22144	3.86127	102	7.22145	3.86139	68
7.22145	3.86122	116	7.2214	3.86129	162	7.22142	3.86138	80
7.22139	3.86121	252	7.22138	3.86127	83	7.22139	3.86138	71
7.22137	3.8612	90	7.22136	3.86129	103	7.22136	3.86138	73
7.22134	3.86121	108	7.22134	3.86128	135	7.22133	3.86138	109
7.22133	3.8612	102	7.22132	3.86128	131	7.2213	3.86138	126
7.22129	3.86119	37	7.22128	3.8613	93	7.22128	3.86138	97
7.22125	3.86119	52	7.22125	3.86129	49	7.22125	3.86139	101
7.22124	3.86119	52	7.22121	3.8613	42	7.22123	3.8614	96
7.22119	3.86122	79	7.22119	3.86128	101	7.2212	3.86139	120
7.22119	3.86121	67	7.22117	3.86126	122	7.22116	3.86138	159
7.22116	3.8612	84			95	7.22113	3.86138	119

*EC- Electrical conductivity

Table 5.1 cont'd

Line 10			Line 13			Line 16		
Northing	Easting	EC (µS/cm)	Northing	Easting	EC (µS/cm)	Northing	Easting	EC (µS/cm)
7.2221	3.8615	40	7.22206	3.86154	69	7.22206	3.86163	164
7.22205	3.86148	44	7.22202	3.86154	76	7.22201	3.86164	108
7.22203	3.86148	34	7.222	3.86156	49	7.22198	3.86164	113
7.22199	3.86148	22	7.22197	3.86156	71	7.22196	3.86164	110
7.22198	3.86147	15	7.22195	3.86154	28	7.22193	3.86164	109
7.22196	3.86148	21	7.22193	3.86154	36	7.22191	3.86164	72
7.22192	3.86147	37	7.22189	3.86154	69	7.22188	3.86164	89
7.2219	3.86147	50	7.22187	3.86154	37	7.22186	3.86163	61
7.22188	3.86147	44	7.22185	3.86155	49	7.22183	3.86163	44
7.22183	3.86148	78	7.22182	3.86156	39	7.22179	3.86163	73
7.22181	3.86149	74	7.2218	3.86155	45	7.22177	3.86163	45
7.22177	3.86148	75	7.22178	3.86154	50	7.22174	3.86164	37
7.22175	3.86146	39	7.22175	3.86154	80	7.22172	3.86164	21
7.22173	3.86145	31	7.22173	3.86155	76	7.22169	3.86164	28
7.2217	3.86145	31	7.22171	3.86154	36	7.22166	3.86163	21
7.22167	3.86147	33	7.22169	3.86154	31	7.22163	3.86163	28
7.22164	3.86147	21	7.22164	3.86155	37	7.2216	3.86164	35
7.22162	3.86144	43	7.2216	3.86155	30	7.22157	3.86163	39
7.22159	3.86147	28	7.22158	3.86155	23	7.22155	3.86164	72
7.22157	3.86145	39	7.22154	3.86154	30	7.22152	3.86164	45
7.22154	3.86145	24	7.22151	3.86155	28	7.22149	3.86163	45
7.22151	3.86147	25	7.22148	3.86156	27	7.22146	3.86164	49
7.22148	3.86145	31	7.22145	3.86155	29	7.22142	3.86163	70
7.22145	3.86146	41	7.22143	3.86154	37	7.22139	3.86164	69
7.22143	3.86146	62	7.22141	3.86154	40	7.22136	3.86163	48
7.2214	3.86144	71	7.22139	3.86153	51	7.22133	3.86163	55
7.22137	3.86146	55	7.22135	3.86153	40	7.2213	3.86163	52
7.22133	3.86147	74	7.2213	3.86153	28	7.22128	3.86164	43
7.22129	3.86146	73	7.22128	3.86154	35	7.22125	3.86163	46
7.22126	3.86144	70	7.22126	3.86154	25	7.22123	3.86163	33
7.22124	3.86146	59	7.22123	3.86153	21	7.22121	3.86162	23
7.22121	3.86147	116	7.2212	3.86153	41	7.22117	3.86162	58
7.22119	3.86146	113	7.22118	3.86153	57	7.22115	3.86162	39
7.22113	3.86145	97	7.22116	3.86153	28	7.2211	3.86162	39

Table 5.1 cont'd

Line 19			Line 22			Line 25		
Northing	Easting	EC (µS/cm)	Northing	Easting	EC (µS/cm)	Northing	Easting	EC (µS/cm)
7.22208	3.86171	132	7.22207	3.86181	134	7.22201	3.8619	145
7.22206	3.86171	88	7.22205	3.86181	113	7.22199	3.8619	73
7.22202	3.86173	148	7.22203	3.86181	65	7.22197	3.86189	74
7.22199	3.86173	56	7.222	3.8618	68	7.22195	3.86189	100
7.22196	3.86173	47	7.22198	3.8618	69	7.2219	3.86189	65
7.22194	3.86172	57	7.22195	3.86181	42	7.22188	3.86188	68
7.22192	3.86172	75	7.2219	3.8618	42	7.22186	3.86187	72
7.2219	3.86171	52	7.22188	3.86181	20	7.22183	3.86188	78
7.22186	3.86171	37	7.22186	3.8618	18	7.22181	3.86189	99
7.22182	3.86172	36	7.22183	3.8618	32	7.22179	3.86188	61
7.22178	3.86171	98	7.2218	3.8618	40	7.22177	3.86188	35
7.22175	3.86171	111	7.22177	3.8618	56	7.22174	3.86187	46
7.22171	3.8617	63	7.22172	3.8618	40	7.2217	3.86187	42
7.22169	3.86171	120	7.22169	3.86179	32	7.22168	3.86188	27
7.22167	3.86171	121	7.22167	3.8618	52	7.22164	3.86188	28
7.22164	3.86171	142	7.22165	3.8618	51	7.2216	3.86187	18
7.2216	3.86172	184	7.22163	3.86179	52	7.22157	3.86188	36
7.22158	3.86172	194	7.2216	3.86179	66	7.22154	3.86187	34
7.22156	3.86172	147	7.22156	3.86179	54	7.22152	3.86187	35
7.22154	3.86172	141	7.22155	3.8618	43	7.2215	3.86187	36
7.22151	3.86171	108	7.22153	3.86179	58	7.22147	3.86187	33
7.22147	3.86171	115	7.2215	3.86179	67	7.22145	3.86187	30
7.22142	3.86171	95	7.22147	3.86179	71	7.22141	3.86188	27
7.22138	3.86171	66	7.22143	3.86179	47	7.22138	3.86188	23
7.22135	3.8617	41	7.22141	3.86179	47	7.22135	3.86187	31
7.22132	3.8617	67	7.22137	3.86179	62	7.22133	3.86187	54
7.22129	3.8617	64	7.22134	3.8618	114	7.2213	3.86188	54
7.22127	3.8617	37	7.22131	3.8618	86	7.22127	3.86187	64
7.22125	3.86171	23	7.22129	3.86179	45	7.22125	3.86186	43
7.22123	3.8617	38	7.22126	3.86179	182	7.2212	3.86186	36
7.22121	3.86171	51	7.22123	3.86178	110	7.22118	3.86187	94
7.22119	3.8617	39	7.22119	3.86179	108	7.22115	3.86187	59
7.22114	3.8617	36	7.22116	3.86179	73	7.22111	3.86186	40
7.22112	3.8617	57	7.22114	3.86178	76	7.22109	3.86186	54

Table 5.1 cont'd

Line 27		
Northing	Easting	EC (µS/cm)
7.22199	3.86194	231
7.22196	3.86194	136
7.22193	3.86194	165
7.22191	3.86194	137
7.22188	3.86193	84
7.22186	3.86193	104
7.22183	3.86193	95
7.2218	3.86194	99
7.22177	3.86193	71
7.22174	3.86193	57
7.22171	3.86193	41
7.22169	3.86194	34
7.22165	3.86195	26
7.22161	3.86194	22
7.22159	3.86194	50
7.22157	3.86194	48
7.22154	3.86193	29
7.22152	3.86193	36
7.22149	3.86192	44
7.22147	3.86193	21
7.22142	3.86192	19
7.2214	3.86193	22
7.22136	3.86193	28
7.22134	3.86193	33
7.22131	3.86194	35
7.22128	3.86193	51
7.22126	3.86193	57
7.22124	3.86193	70
7.22122	3.86192	70
7.22117	3.86193	101
7.22114	3.86192	85
7.22112	3.86192	73
7.2211	3.86191	61

Table 5.2: Volumetric water content of soil in the cocoa farm during the wet season

Line 1			Line 4			Line 7		
Northing	Easting	VWC (%)	Northing	Easting	VWC (%)	Northing	Easting	VWC (%)
7.22201	3.86123	10	7.22205	3.8613	14	7.22207	3.86141	9
7.22198	3.86123	12	7.22204	3.86132	23	7.22203	3.86142	14
7.22196	3.86122	13	7.222	3.86132	28	7.22202	3.8614	12
7.22194	3.86122	12	7.22198	3.8613	19	7.22199	3.86143	11
7.22189	3.86123	8	7.22195	3.86132	20	7.22196	3.86141	14
7.22189	3.86124	11	7.22192	3.86131	40	7.22192	3.86142	63
7.22188	3.86124	14	7.22188	3.86132	26	7.2219	3.86142	20
7.22186	3.86122	15	7.22187	3.86128	29	7.22186	3.8614	27
7.22183	3.86122	27	7.22183	3.86132	50	7.22183	3.86141	42
7.22182	3.86122	25	7.22179	3.86132	51	7.22181	3.86141	27
7.22177	3.86121	19	7.22177	3.86131	34	7.22179	3.86142	19
7.22173	3.86122	17	7.22174	3.86128	47	7.22175	3.8614	17
7.22171	3.86121	16	7.22173	3.86131	26	7.22173	3.86142	15
7.2217	3.86121	14	7.2217	3.86134	24	7.22171	3.86141	14
7.22166	3.86121	19	7.22167	3.86132	30	7.22169	3.8614	17
7.22164	3.86122	39	7.22163	3.86131	35	7.22165	3.8614	20
7.22161	3.86122	52	7.2216	3.86132	19	7.22163	3.86139	19
7.2216	3.86121	67	7.22158	3.86128	29	7.22159	3.8614	17
7.22156	3.86121	55	7.22155	3.86131	36	7.22157	3.8614	56
7.22154	3.86121	29	7.22152	3.86131	53	7.22154	3.86139	46
7.22152	3.86121	44	7.2215	3.8613	58	7.22151	3.86138	36
7.2215	3.86122	59	7.22147	3.86127	48	7.22148	3.86139	26
7.22147	3.86123	28	7.22144	3.86127	44	7.22145	3.86139	25
7.22145	3.86122	46	7.2214	3.86129	44	7.22142	3.86138	30
7.22139	3.86121	64	7.22138	3.86127	49	7.22139	3.86138	26
7.22137	3.8612	38	7.22136	3.86129	56	7.22136	3.86138	27
7.22134	3.86121	43	7.22134	3.86128	55	7.22133	3.86138	45
7.22133	3.8612	41	7.22132	3.86128	58	7.2213	3.86138	48
7.22129	3.86119	14	7.22128	3.8613	46	7.22128	3.86138	39
7.22125	3.86119	18	7.22125	3.86129	29	7.22125	3.86139	40
7.22124	3.86119	19	7.22121	3.8613	42	7.22123	3.8614	39
7.22119	3.86122	39	7.22119	3.86128	41	7.2212	3.86139	48
7.22119	3.86121	25	7.22117	3.86126	35	7.22116	3.86138	55
7.22116	3.8612	33				7.22113	3.86138	48

*VWC-Volumetric water content

Table 5.2 cont'd

Line 10			Line 13			Line 16		
Northing	Easting	VWC (%)	Northing	Easting	VWC (%)	Northing	Easting	VWC (%)
7.2221	3.8615	14	7.22206	3.86154	25	7.22206	3.86163	57
7.22205	3.86148	17	7.22202	3.86154	29	7.22201	3.86164	43
7.22203	3.86148	13	7.222	3.86156	18	7.22198	3.86164	44
7.22199	3.86148	10	7.22197	3.86156	26	7.22196	3.86164	44
7.22198	3.86147	4	7.22195	3.86154	13	7.22193	3.86164	43
7.22196	3.86148	11	7.22193	3.86154	14	7.22191	3.86164	27
7.22192	3.86147	14	7.22189	3.86154	26	7.22188	3.86164	36
7.2219	3.86147	18	7.22187	3.86154	14	7.22186	3.86163	22
7.22188	3.86147	15	7.22185	3.86155	17	7.22183	3.86163	15
7.22183	3.86148	28	7.22182	3.86156	14	7.22179	3.86163	28
7.22181	3.86149	28	7.2218	3.86155	16	7.22177	3.86163	16
7.22177	3.86148	27	7.22178	3.86154	18	7.22174	3.86164	14
7.22175	3.86146	14	7.22175	3.86154	30	7.22172	3.86164	10
7.22173	3.86145	13	7.22173	3.86155	28	7.22169	3.86164	13
7.2217	3.86145	13	7.22171	3.86154	14	7.22166	3.86163	11
7.22167	3.86147	14	7.22169	3.86154	13	7.22163	3.86163	13
7.22164	3.86147	10	7.22164	3.86155	14	7.2216	3.86164	14
7.22162	3.86144	15	7.2216	3.86155	13	7.22157	3.86163	14
7.22159	3.86147	13	7.22158	3.86155	11	7.22155	3.86164	28
7.22157	3.86145	14	7.22154	3.86154	13	7.22152	3.86164	16
7.22154	3.86145	12	7.22151	3.86155	13	7.22149	3.86163	16
7.22151	3.86147	12	7.22148	3.86156	12	7.22146	3.86164	18
7.22148	3.86145	13	7.22145	3.86155	13	7.22142	3.86163	26
7.22145	3.86146	14	7.22143	3.86154	14	7.22139	3.86164	26
7.22143	3.86146	23	7.22141	3.86154	15	7.22136	3.86163	17
7.2214	3.86144	26	7.22139	3.86153	18	7.22133	3.86163	19
7.22137	3.86146	19	7.22135	3.86153	14	7.2213	3.86163	18
7.22133	3.86147	28	7.2213	3.86153	13	7.22128	3.86164	15
7.22129	3.86146	26	7.22128	3.86154	14	7.22125	3.86163	16
7.22126	3.86144	25	7.22126	3.86154	12	7.22123	3.86163	14
7.22124	3.86146	21	7.22123	3.86153	11	7.22121	3.86162	12
7.22121	3.86147	45	7.2212	3.86153	14	7.22117	3.86162	21
7.22119	3.86146	45	7.22118	3.86153	20	7.22115	3.86162	14
7.22113	3.86145	39	7.22116	3.86153	13	7.2211	3.86162	14

Table 5.2 cont'd

Line 19			Line 22			Line 25		
Northing	Easting	VWC (%)	Northing	Easting	VWC (%)	Northing	Easting	VWC (%)
7.22208	3.86171	51	7.22207	3.86181	50	7.22201	3.8619	54
7.22206	3.86171	34	7.22205	3.86181	44	7.22199	3.8619	26
7.22202	3.86173	53	7.22203	3.86181	24	7.22197	3.86189	28
7.22199	3.86173	19	7.222	3.8618	26	7.22195	3.86189	43
7.22196	3.86173	17	7.22198	3.8618	25	7.2219	3.86189	25
7.22194	3.86172	20	7.22195	3.86181	15	7.22188	3.86188	27
7.22192	3.86172	28	7.2219	3.8618	15	7.22186	3.86187	27
7.2219	3.86171	18	7.22188	3.86181	10	7.22183	3.86188	29
7.22186	3.86171	14	7.22186	3.8618	9	7.22181	3.86189	39
7.22182	3.86172	14	7.22183	3.8618	14	7.22179	3.86188	23
7.22178	3.86171	37	7.2218	3.8618	15	7.22177	3.86188	14
7.22175	3.86171	43	7.22177	3.8618	19	7.22174	3.86187	17
7.22171	3.8617	23	7.22172	3.8618	15	7.2217	3.86187	15
7.22169	3.86171	48	7.22169	3.86179	14	7.22168	3.86188	13
7.22167	3.86171	46	7.22167	3.8618	18	7.22164	3.86188	13
7.22164	3.86171	51	7.22165	3.8618	18	7.2216	3.86187	8
7.2216	3.86172	59	7.22163	3.86179	18	7.22157	3.86188	14
7.22158	3.86172	59	7.2216	3.86179	25	7.22154	3.86187	14
7.22156	3.86172	51	7.22156	3.86179	19	7.22152	3.86187	14
7.22154	3.86172	51	7.22155	3.8618	15	7.2215	3.86187	14
7.22151	3.86171	42	7.22153	3.86179	21	7.22147	3.86187	13
7.22147	3.86171	43	7.2215	3.86179	25	7.22145	3.86187	13
7.22142	3.86171	37	7.22147	3.86179	22	7.22141	3.86188	13
7.22138	3.86171	25	7.22143	3.86179	17	7.22138	3.86188	12
7.22135	3.8617	15	7.22141	3.86179	17	7.22135	3.86187	13
7.22132	3.8617	25	7.22137	3.86179	23	7.22133	3.86187	19
7.22129	3.8617	24	7.22134	3.8618	43	7.2213	3.86188	19
7.22127	3.8617	14	7.22131	3.8618	32	7.22127	3.86187	24
7.22125	3.86171	11	7.22129	3.86179	16	7.22125	3.86186	15
7.22123	3.8617	14	7.22126	3.86179	58	7.2212	3.86186	14
7.22121	3.86171	18	7.22123	3.86178	44	7.22118	3.86187	39
7.22119	3.8617	14	7.22119	3.86179	44	7.22115	3.86187	21
7.22114	3.8617	13	7.22116	3.86179	27	7.22111	3.86186	14
7.22112	3.8617	20	7.22114	3.86178	29	7.22109	3.86186	19

Table 5.2 cont'd

Line 27		
Northing	Easting	VWC (%)
7.22199	3.86194	64
7.22196	3.86194	52
7.22193	3.86194	55
7.22191	3.86194	51
7.22188	3.86193	33
7.22186	3.86193	43
7.22183	3.86193	37
7.2218	3.86194	39
7.22177	3.86193	27
7.22174	3.86193	20
7.22171	3.86193	14
7.22169	3.86194	14
7.22165	3.86195	13
7.22161	3.86194	11
7.22159	3.86194	18
7.22157	3.86194	17
7.22154	3.86193	13
7.22152	3.86193	14
7.22149	3.86192	16
7.22147	3.86193	11
7.22142	3.86192	10
7.2214	3.86193	11
7.22136	3.86193	13
7.22134	3.86193	14
7.22131	3.86194	14
7.22128	3.86193	18
7.22126	3.86193	20
7.22124	3.86193	26
7.22122	3.86192	26
7.22117	3.86193	42
7.22114	3.86192	31
7.22112	3.86192	28
7.2211	3.86191	21

Table 5.3: Electrical conductivity of soil in the cocoa farm during the dry season

Line 2			Line 5			Line 8		
Northing	Easting	EC (µS/cm)	Northing	Easting	EC (µS/cm)	Northing	Easting	EC (µS/cm)
7.22204	3.86125	19	7.22204	3.86136	39	7.22209	3.86144	15
7.222	3.86125	19	7.22202	3.86135	28	7.22207	3.86142	12
7.22198	3.86127	19	7.22201	3.86136	25	7.22205	3.86142	12
7.22197	3.86126	15	7.22199	3.86136	30	7.22202	3.86145	13
7.22195	3.86126	13	7.22197	3.86136	58	7.22199	3.86144	15
7.22193	3.86127	15	7.22194	3.86137	32	7.22197	3.86142	19
7.22191	3.86125	23	7.22191	3.86136	63	7.22194	3.86143	18
7.22187	3.86125	132	7.22188	3.86135	73	7.22191	3.86143	28
7.22185	3.86125	267	7.22185	3.86136	75	7.22187	3.86143	30
7.22183	3.86124	131	7.22179	3.86135	68	7.22184	3.86143	32
7.22179	3.86127	97	7.22175	3.86133	42	7.22182	3.86143	34
7.22176	3.86124	97	7.22173	3.86137	39	7.22179	3.86144	28
7.22172	3.86125	100	7.22171	3.86135	60	7.22177	3.86143	25
7.2217	3.86128	118	7.22169	3.86136	46	7.22173	3.86143	39
7.22168	3.86126	49	7.22167	3.86136	43	7.22171	3.86143	38
7.22166	3.86124	57	7.22164	3.86137	96	7.22168	3.86142	38
7.22164	3.86125	94	7.22162	3.86135	37	7.22165	3.86142	45
7.22161	3.86127	201	7.22159	3.86134	71	7.22162	3.8614	29
7.22156	3.86126	182	7.22156	3.86134	81	7.22159	3.86142	24
7.22154	3.86124	118	7.22153	3.86134	104	7.22157	3.86141	45
7.22151	3.86124	101	7.22149	3.86135	99	7.22154	3.86141	66
7.22148	3.86125	109	7.22147	3.86135	71	7.2215	3.86141	43
7.22145	3.86124	73	7.22144	3.86136	103	7.22147	3.86141	42
7.22142	3.86123	92	7.22142	3.86135	116	7.22145	3.86141	48
7.22139	3.86124	58	7.22139	3.86132	78	7.22142	3.86141	47
7.22137	3.86123	78	7.22137	3.86131	100	7.2214	3.8614	61
7.22135	3.86125	79	7.22134	3.86131	83	7.22137	3.8614	55
7.22133	3.86122	91	7.22132	3.86132	72	7.22135	3.8614	56
7.22131	3.86121	44	7.22128	3.86134	74	7.22131	3.8614	73
7.22128	3.86121	16	7.22126	3.86132	68	7.22128	3.8614	59
7.22124	3.86123	18	7.22124	3.86131	73	7.22126	3.8614	65
7.22122	3.86123	51	7.2212	3.86132	45	7.22124	3.86143	67
7.22121	3.86122	47	7.22117	3.86132	59	7.22121	3.86141	81
7.22119	3.8612	57						

*EC-Electrical conductivity

Table 5.3 cont'd

Line 11			Line 14			Line 17		
Northing	Easting	EC (µS/cm)	Northing	Easting	EC (µS/cm)	Northing	Easting	EC (µS/cm)
7.22208	3.86149	22	7.22205	3.86158	19	7.22206	3.86167	167
7.22206	3.8615	19	7.22202	3.86157	21	7.22203	3.86166	93
7.22204	3.8615	15	7.222	3.8616	16	7.22201	3.86167	47
7.22202	3.8615	14	7.22198	3.86158	22	7.22199	3.86166	62
7.22198	3.86151	10	7.22195	3.86158	29	7.22196	3.86167	83
7.22194	3.86148	12	7.22193	3.86158	28	7.22192	3.86166	45
7.22192	3.86151	23	7.22191	3.86159	40	7.22189	3.86167	47
7.2219	3.8615	28	7.22187	3.86159	26	7.22187	3.86167	36
7.22187	3.86151	47	7.22183	3.86159	24	7.22182	3.86166	49
7.22185	3.8615	42	7.2218	3.86158	25	7.2218	3.86166	59
7.22183	3.86151	48	7.22178	3.86159	24	7.22177	3.86165	37
7.2218	3.86152	57	7.22174	3.86159	15	7.22172	3.86166	28
7.22177	3.8615	34	7.22172	3.86158	16	7.22168	3.86166	30
7.22174	3.8615	23	7.22167	3.86158	20	7.22166	3.86166	36
7.22172	3.86149	16	7.22165	3.86158	30	7.22163	3.86166	63
7.22169	3.86151	16	7.22162	3.86158	64	7.2216	3.86166	32
7.22167	3.86149	16	7.22159	3.86158	24	7.22158	3.86165	28
7.22163	3.86151	13	7.22156	3.86158	20	7.22154	3.86166	30
7.2216	3.86151	22	7.22154	3.86158	20	7.22152	3.86166	27
7.22157	3.86151	18	7.22151	3.86158	16	7.2215	3.86166	34
7.22153	3.86151	16	7.22149	3.86158	22	7.22146	3.86166	47
7.22151	3.8615	21	7.22146	3.86157	26	7.22144	3.86166	32
7.22148	3.86151	38	7.22144	3.86158	28	7.2214	3.86166	25
7.22143	3.86151	38	7.22141	3.86157	27	7.22137	3.86166	18
7.22141	3.8615	34	7.22138	3.86158	30	7.22133	3.86166	19
7.22137	3.86149	40	7.22136	3.86158	27	7.2213	3.86165	44
7.22135	3.8615	43	7.22133	3.86156	26	7.22128	3.86165	22
7.22133	3.8615	52	7.2213	3.86157	32	7.22124	3.86166	22
7.2213	3.86148	53	7.22126	3.86158	26	7.22122	3.86165	30
7.22127	3.86148	57	7.22123	3.86158	25	7.22118	3.86164	21
7.22124	3.86149	70	7.22121	3.86157	23	7.22117	3.86165	24
7.2212	3.86149	76	7.22118	3.86156	25	7.22115	3.86166	28
7.22118	3.86149	48	7.22116	3.86156	21	7.2211	3.86165	35
7.22116	3.86148	58						

Table 5.3 cont'd

Line 20			Line 22		
Northing	Easting	EC (µS/cm)	Northing	Easting	EC (µS/cm)
7.22207	3.86173	51	7.22207	3.86181	97
7.22203	3.86174	61	7.22205	3.86181	59
7.222	3.86175	49	7.22203	3.86181	35
7.22198	3.86176	19	7.222	3.8618	24
7.22196	3.86176	15	7.22198	3.8618	25
7.22192	3.86176	23	7.22195	3.86181	18
7.2219	3.86176	31	7.2219	3.8618	20
7.22188	3.86174	23	7.22188	3.86181	16
7.22184	3.86175	32	7.22186	3.8618	14
7.2218	3.86175	30	7.22183	3.8618	24
7.22178	3.86175	27	7.2218	3.8618	32
7.22176	3.86175	37	7.22177	3.8618	33
7.22172	3.86175	56	7.22172	3.8618	28
7.2217	3.86175	44	7.22169	3.86179	35
7.22167	3.86174	114	7.22167	3.8618	44
7.22164	3.86174	90	7.22165	3.8618	84
7.22162	3.86174	85	7.22163	3.86179	35
7.22159	3.86174	86	7.2216	3.86179	39
7.22156	3.86174	77	7.22156	3.86179	40
7.22153	3.86174	53	7.22155	3.8618	28
7.22151	3.86174	87	7.22153	3.86179	47
7.22146	3.86174	67	7.2215	3.86179	48
7.22143	3.86174	96	7.22147	3.86179	30
7.2214	3.86174	73	7.22143	3.86179	28
7.22137	3.86174	58	7.22141	3.86179	30
7.22135	3.86173	66	7.22137	3.86179	35
7.22131	3.86173	45	7.22134	3.8618	70
7.22128	3.86173	37	7.22131	3.8618	46
7.22126	3.86173	55	7.22129	3.86179	34
7.22124	3.86173	33	7.22126	3.86179	40
7.22121	3.86173	30	7.22123	3.86178	63
7.22119	3.86173	40	7.22119	3.86179	73
7.22116	3.86173	33	7.22116	3.86179	55
7.22114	3.86173	24	7.22114	3.86178	48

Table 5.3 cont'd

Line 25			Line 27		
Northing	Easting	EC (µS/cm)	Northing	Easting	EC (µS/cm)
7.22201	3.8619	58	7.22199	3.86194	155
7.22199	3.8619	37	7.22196	3.86194	103
7.22197	3.86189	41	7.22193	3.86194	74
7.22195	3.86189	69	7.22191	3.86194	79
7.2219	3.86189	42	7.22188	3.86193	57
7.22188	3.86188	35	7.22186	3.86193	64
7.22186	3.86187	47	7.22183	3.86193	48
7.22183	3.86188	59	7.2218	3.86194	36
7.22181	3.86189	46	7.22177	3.86193	34
7.22179	3.86188	29	7.22174	3.86193	20
7.22177	3.86188	29	7.22171	3.86193	20
7.22174	3.86187	21	7.22169	3.86194	14
7.2217	3.86187	20	7.22165	3.86195	36
7.22168	3.86188	26	7.22161	3.86194	35
7.22164	3.86188	18	7.22159	3.86194	23
7.2216	3.86187	27	7.22157	3.86194	18
7.22157	3.86188	23	7.22154	3.86193	29
7.22154	3.86187	28	7.22152	3.86193	19
7.22152	3.86187	21	7.22149	3.86192	14
7.2215	3.86187	27	7.22147	3.86193	16
7.22147	3.86187	20	7.22142	3.86192	15
7.22145	3.86187	21	7.2214	3.86193	24
7.22141	3.86188	19	7.22136	3.86193	29
7.22138	3.86188	21	7.22134	3.86193	39
7.22135	3.86187	33	7.22131	3.86194	31
7.22133	3.86187	37	7.22128	3.86193	35
7.2213	3.86188	44	7.22126	3.86193	36
7.22127	3.86187	26	7.22124	3.86193	57
7.22125	3.86186	25	7.22122	3.86192	54
7.2212	3.86186	50	7.22117	3.86193	35
7.22118	3.86187	35	7.22114	3.86192	35
7.22115	3.86187	25			
7.22111	3.86186	33			
7.22109	3.86186	31			

Table 5.4: Volumetric water content of soil in the cocoa farm during the dry season

Line 2			Line 5			Line 8		
Northing	Easting	VWC (%)	Northing	Easting	VWC (%)	Northing	Easting	VWC (%)
7.22204	3.86125	8	7.22204	3.86136	8	7.22209	3.86144	8
7.222	3.86125	8	7.22202	3.86135	9	7.22207	3.86142	8
7.22198	3.86127	2	7.22201	3.86136	10	7.22205	3.86142	6
7.22197	3.86126	9	7.22199	3.86136	8	7.22202	3.86145	7
7.22195	3.86126	6	7.22197	3.86136	8	7.22199	3.86144	8
7.22193	3.86127	7	7.22194	3.86137	12	7.22197	3.86142	9
7.22191	3.86125	8	7.22191	3.86136	11	7.22194	3.86143	8
7.22187	3.86125	20	7.22188	3.86135	10	7.22191	3.86143	8
7.22185	3.86125	26	7.22185	3.86136	12	7.22187	3.86143	8
7.22183	3.86124	20	7.22179	3.86135	11	7.22184	3.86143	9
7.22179	3.86127	18	7.22175	3.86133	8	7.22182	3.86143	10
7.22176	3.86124	17	7.22173	3.86137	9	7.22179	3.86144	7
7.22172	3.86125	16	7.22171	3.86135	8	7.22177	3.86143	8
7.2217	3.86128	14	7.22169	3.86136	9	7.22173	3.86143	10
7.22168	3.86126	15	7.22167	3.86136	9	7.22171	3.86143	12
7.22166	3.86124	7	7.22164	3.86137	14	7.22168	3.86142	12
7.22164	3.86125	12	7.22162	3.86135	8	7.22165	3.86142	11
7.22161	3.86127	11	7.22159	3.86134	11	7.22162	3.8614	6
7.22156	3.86126	12	7.22156	3.86134	14	7.22159	3.86142	8
7.22154	3.86124	16	7.22153	3.86134	13	7.22157	3.86141	6
7.22151	3.86124	13	7.22149	3.86135	13	7.22154	3.86141	13
7.22148	3.86125	11	7.22147	3.86135	11	7.2215	3.86141	12
7.22145	3.86124	13	7.22144	3.86136	14	7.22147	3.86141	8
7.22142	3.86123	11	7.22142	3.86135	15	7.22145	3.86141	8
7.22139	3.86124	18	7.22139	3.86132	17	7.22142	3.86141	8
7.22137	3.86123	13	7.22137	3.86131	22	7.2214	3.8614	12
7.22135	3.86125	12	7.22134	3.86131	16	7.22137	3.8614	10
7.22133	3.86122	15	7.22132	3.86132	14	7.22135	3.8614	10
7.22131	3.86121	8	7.22128	3.86134	16	7.22131	3.8614	13
7.22128	3.86121	9	7.22126	3.86132	14	7.22128	3.8614	11
7.22124	3.86123	7	7.22124	3.86131	11	7.22126	3.8614	11
7.22122	3.86123	8	7.2212	3.86132	8	7.22124	3.86143	16
7.22121	3.86122	10	7.22117	3.86132	10	7.22121	3.86141	13
7.22119	3.8612	10						

*VWC-Volumetric water content

Table 5.4 cont'd

Line 11			Line 14			Line 17		
Northing	Easting	VWC (%)	Northing	Easting	VWC (%)	Northing	Easting	VWC (%)
7.22208	3.86149	8	7.22205	3.86158	9	7.22206	3.86167	16
7.22206	3.8615	6	7.22202	3.86157	9	7.22203	3.86166	11
7.22204	3.8615	5	7.222	3.8616	9	7.22201	3.86167	10
7.22202	3.8615	5	7.22198	3.86158	9	7.22199	3.86166	11
7.22198	3.86151	4	7.22195	3.86158	10	7.22196	3.86167	11
7.22194	3.86148	8	7.22193	3.86158	10	7.22192	3.86166	8
7.22192	3.86151	8	7.22191	3.86159	9	7.22189	3.86167	9
7.2219	3.8615	9	7.22187	3.86159	8	7.22187	3.86167	6
7.22187	3.86151	10	7.22183	3.86159	8	7.22182	3.86166	8
7.22185	3.8615	8	7.2218	3.86158	9	7.2218	3.86166	9
7.22183	3.86151	13	7.22178	3.86159	8	7.22177	3.86165	7
7.2218	3.86152	13	7.22174	3.86159	8	7.22172	3.86166	5
7.22177	3.8615	9	7.22172	3.86158	8	7.22168	3.86166	5
7.22174	3.8615	8	7.22167	3.86158	9	7.22166	3.86166	9
7.22172	3.86149	6	7.22165	3.86158	12	7.22163	3.86166	9
7.22169	3.86151	5	7.22162	3.86158	11	7.2216	3.86166	5
7.22167	3.86149	4	7.22159	3.86158	9	7.22158	3.86165	5
7.22163	3.86151	8	7.22156	3.86158	8	7.22154	3.86166	8
7.2216	3.86151	6	7.22154	3.86158	7	7.22152	3.86166	7
7.22157	3.86151	7	7.22151	3.86158	6	7.2215	3.86166	8
7.22153	3.86151	8	7.22149	3.86158	9	7.22146	3.86166	9
7.22151	3.8615	8	7.22146	3.86157	8	7.22144	3.86166	8
7.22148	3.86151	9	7.22144	3.86158	7	7.2214	3.86166	7
7.22143	3.86151	10	7.22141	3.86157	8	7.22137	3.86166	6
7.22141	3.8615	10	7.22138	3.86158	9	7.22133	3.86166	5
7.22137	3.86149	11	7.22136	3.86158	9	7.2213	3.86165	8
7.22135	3.8615	8	7.22133	3.86156	7	7.22128	3.86165	5
7.22133	3.8615	8	7.2213	3.86157	8	7.22124	3.86166	4
7.2213	3.86148	10	7.22126	3.86158	9	7.22122	3.86165	8
7.22127	3.86148	9	7.22123	3.86158	8	7.22118	3.86164	6
7.22124	3.86149	14	7.22121	3.86157	8	7.22117	3.86165	4
7.2212	3.86149	13	7.22118	3.86156	7	7.22115	3.86166	5
7.22118	3.86149	14	7.22116	3.86156	7	7.2211	3.86165	10
7.22116	3.86148	18						

Table 5.4 cont'd

Line 20			Line 22		
Northing	Easting	VWC (%)	Northing	Easting	VWC (%)
7.22207	3.86173	9	7.22207	3.86181	12
7.22203	3.86174	9	7.22205	3.86181	9
7.222	3.86175	11	7.22203	3.86181	8
7.22198	3.86176	7	7.222	3.8618	10
7.22196	3.86176	3	7.22198	3.8618	8
7.22192	3.86176	8	7.22195	3.86181	4
7.2219	3.86176	8	7.2219	3.8618	8
7.22188	3.86174	7	7.22188	3.86181	7
7.22184	3.86175	9	7.22186	3.8618	7
7.2218	3.86175	8	7.22183	3.8618	11
7.22178	3.86175	8	7.2218	3.8618	11
7.22176	3.86175	9	7.22177	3.8618	9
7.22172	3.86175	10	7.22172	3.8618	10
7.2217	3.86175	9	7.22169	3.86179	9
7.22167	3.86174	14	7.22167	3.8618	9
7.22164	3.86174	13	7.22165	3.8618	13
7.22162	3.86174	11	7.22163	3.86179	8
7.22159	3.86174	15	7.2216	3.86179	11
7.22156	3.86174	12	7.22156	3.86179	9
7.22153	3.86174	11	7.22155	3.8618	9
7.22151	3.86174	11	7.22153	3.86179	11
7.22146	3.86174	10	7.2215	3.86179	11
7.22143	3.86174	12	7.22147	3.86179	8
7.2214	3.86174	11	7.22143	3.86179	8
7.22137	3.86174	11	7.22141	3.86179	9
7.22135	3.86173	11	7.22137	3.86179	9
7.22131	3.86173	8	7.22134	3.8618	12
7.22128	3.86173	9	7.22131	3.8618	10
7.22126	3.86173	10	7.22129	3.86179	8
7.22124	3.86173	8	7.22126	3.86179	9
7.22121	3.86173	7	7.22123	3.86178	10
7.22119	3.86173	9	7.22119	3.86179	14
7.22116	3.86173	11	7.22116	3.86179	14
7.22114	3.86173	9	7.22114	3.86178	13

Table 5.4 cont'd

Line 25			Line 27		
Northing	Easting	VWC (%)	Northing	Easting	VWC (%)
7.22201	3.8619	12	7.22199	3.86194	15
7.22199	3.8619	11	7.22196	3.86194	14
7.22197	3.86189	9	7.22193	3.86194	10
7.22195	3.86189	14	7.22191	3.86194	16
7.2219	3.86189	8	7.22188	3.86193	10
7.22188	3.86188	8	7.22186	3.86193	9
7.22186	3.86187	10	7.22183	3.86193	9
7.22183	3.86188	10	7.2218	3.86194	11
7.22181	3.86189	11	7.22177	3.86193	14
7.22179	3.86188	10	7.22174	3.86193	9
7.22177	3.86188	9	7.22171	3.86193	8
7.22174	3.86187	9	7.22169	3.86194	7
7.2217	3.86187	8	7.22165	3.86195	8
7.22168	3.86188	7	7.22161	3.86194	9
7.22164	3.86188	8	7.22159	3.86194	7
7.2216	3.86187	8	7.22157	3.86194	7
7.22157	3.86188	7	7.22154	3.86193	8
7.22154	3.86187	8	7.22152	3.86193	7
7.22152	3.86187	7	7.22149	3.86192	7
7.2215	3.86187	9	7.22147	3.86193	7
7.22147	3.86187	9	7.22142	3.86192	7
7.22145	3.86187	7	7.2214	3.86193	8
7.22141	3.86188	9	7.22136	3.86193	9
7.22138	3.86188	8	7.22134	3.86193	11
7.22135	3.86187	9	7.22131	3.86194	11
7.22133	3.86187	10	7.22128	3.86193	10
7.2213	3.86188	9	7.22126	3.86193	12
7.22127	3.86187	9	7.22124	3.86193	11
7.22125	3.86186	9	7.22122	3.86192	11
7.2212	3.86186	11	7.22117	3.86193	9
7.22118	3.86187	10	7.22114	3.86192	11
7.22115	3.86187	11			
7.22111	3.86186	11			
7.22109	3.86186	10			

Table 5.5: Electrical conductivity of soil in the kola farm during the wet season

Line 1			Line 4			Line 7		
Northing	Easting	EC (µS/cm)	Northing	Easting	EC (µS/cm)	Northing	Easting	EC (µS/cm)
7.22198	3.85993	27	7.22201	3.85983	52	7.22197	3.85979	30
7.22196	3.8599	30	7.22198	3.85982	68	7.22201	3.85974	35
7.22195	3.85991	53	7.22195	3.85983	71	7.22196	3.85975	33
7.2219	3.8599	54	7.22196	3.85983	73	7.22194	3.85973	47
7.22188	3.85988	32	7.22191	3.85981	65	7.22192	3.85976	30
7.22186	3.85989	40	7.22187	3.85982	36	7.22189	3.85975	49
7.22182	3.85988	24	7.22184	3.8598	39	7.22184	3.85974	46
7.22179	3.85989	50	7.2218	3.85981	43	7.22182	3.85975	70
7.22176	3.85988	62	7.2218	3.85981	28	7.2218	3.85973	37
7.22174	3.85989	41	7.22177	3.85981	36	7.22178	3.85973	31
7.22171	3.85987	32	7.22174	3.85981	28	7.22174	3.85973	27
7.22167	3.85986	33	7.22172	3.85979	41	7.2217	3.85973	33
7.22165	3.85986	46	7.22168	3.8598	43	7.2217	3.85972	28
7.22162	3.85986	116	7.22167	3.8598	56	7.22167	3.85973	28
7.22161	3.85988	48	7.22164	3.8598	43	7.22164	3.85976	58
7.22158	3.85988	38	7.22159	3.85978	39	7.2216	3.85972	63
7.22155	3.85986	66	7.22158	3.85981	50	7.2216	3.85973	50
7.22153	3.85985	54	7.22156	3.85979	67	7.22156	3.85973	63
7.22149	3.85988	31	7.22153	3.85979	62	7.22153	3.85973	46
7.22146	3.85985	29	7.22149	3.8598	63	7.22149	3.85973	27
7.22144	3.85988	62	7.22149	3.85981	65	7.22149	3.8597	22
7.2214	3.85988	56	7.22143	3.85981	76	7.22145	3.85973	19
7.22137	3.85988	62	7.22144	3.85982	63	7.22142	3.85972	33
7.22135	3.85987	65	7.22141	3.8598	64	7.2214	3.85972	16
7.22133	3.85987	52	7.22139	3.85981	54	7.22137	3.85972	37
7.22131	3.85987	51	7.22134	3.85979	71	7.22134	3.85973	37
7.22128	3.85987	17	7.22132	3.85979	34	7.22132	3.85972	42
7.22126	3.85989	35	7.2213	3.85978	45	7.22129	3.85971	27
7.22123	3.85988	35	7.22126	3.85979	37	7.22126	3.85972	47
7.2212	3.85988	17	7.22125	3.8598	93	7.22125	3.85971	29
7.22118	3.85987	33	7.22124	3.85978	48	7.22121	3.85974	26
7.22115	3.85987	37	7.22119	3.85979	52	7.22118	3.85972	32
7.22112	3.85985	52	7.22116	3.85978	47	7.22116	3.85974	43
7.2211	3.85986	48	7.22113	3.8598	46	7.22114	3.85974	12
7.22107	3.85987	70	7.22111	3.85978	70	7.2211	3.85975	27
7.22104	3.85987	45	7.22107	3.85978	69	7.22107	3.85974	28

*EC-Electrical conductivity

Table 5.5 cont'd

Line 10			Line 13			Line 16		
Northing	Easting	EC (µS/cm)	Northing	Easting	EC (µS/cm)	Northing	Easting	EC (µS/cm)
7.222	3.85964	37	7.22202	3.85958	53	7.22204	3.85952	82
7.22197	3.85965	42	7.222	3.85959	53	7.22202	3.85949	118
7.22195	3.85965	44	7.22197	3.85958	46	7.22198	3.8595	160
7.22191	3.85965	43	7.22195	3.85958	44	7.22195	3.8595	143
7.22188	3.85965	24	7.22191	3.85957	37	7.22193	3.8595	145
7.22186	3.85963	22	7.22188	3.85959	41	7.22191	3.85949	197
7.22185	3.85966	34	7.22188	3.85957	47	7.22189	3.85949	153
7.22181	3.85964	31	7.22183	3.85958	42	7.22186	3.85949	176
7.22179	3.85965	28	7.22179	3.85959	52	7.22183	3.8595	117
7.22175	3.85965	30	7.22178	3.85959	49	7.2218	3.8595	148
7.22174	3.85964	22	7.22175	3.85959	35	7.22177	3.85951	176
7.22173	3.85964	46	7.22173	3.85959	51	7.22174	3.85948	145
7.2217	3.85965	31	7.2217	3.85958	47	7.22171	3.85949	137
7.22168	3.85963	20	7.22168	3.85959	56	7.22169	3.85949	128
7.22166	3.85964	34	7.22164	3.85957	89	7.22167	3.8595	165
7.22161	3.85965	48	7.22162	3.85957	74	7.22165	3.85948	230
7.2216	3.85963	16	7.2216	3.85959	49	7.22161	3.85949	156
7.22158	3.85962	20	7.22159	3.85955	48	7.22158	3.85948	211
7.22156	3.85963	33	7.22155	3.85959	39	7.22156	3.85949	200
7.22151	3.85963	35	7.22151	3.85957	50	7.22153	3.85949	278
7.22148	3.85963	56	7.22148	3.85957	50	7.22151	3.85949	165
7.22149	3.85963	23	7.22145	3.8596	81	7.22146	3.85949	176
7.22144	3.85963	29	7.22143	3.85957	131	7.22145	3.85949	244
7.22142	3.85962	45	7.22142	3.85955	57	7.22141	3.85949	336
7.2214	3.85963	68	7.22138	3.85955	40	7.22138	3.85948	278
7.22137	3.85964	94	7.22135	3.85957	58	7.22136	3.85948	262
7.22134	3.85963	68	7.22132	3.85957	52	7.22134	3.85948	99
7.2213	3.85962	89	7.22129	3.85955	56	7.2213	3.85948	109
7.22129	3.85962	96	7.22128	3.85955	61	7.22128	3.85948	99
7.22128	3.85964	89	7.22126	3.85958	77	7.22126	3.85948	124
7.22125	3.85965	88	7.22124	3.85958	71	7.22124	3.85946	151
						7.22122	3.85949	145
						7.22121	3.8595	131

Table 5.5 cont'd

Line 16			Line 19			Line 21		
Northing	Easting	EC (µS/cm)	Northing	Easting	EC (µS/cm)	Northing	Easting	EC (µS/cm)
7.22204	3.85952	82	7.22204	3.85942	115	7.22204	3.85934	202
7.22202	3.85949	118	7.22203	3.85942	105	7.22201	3.85934	152
7.22198	3.8595	160	7.222	3.85941	111	7.222	3.85935	91
7.22195	3.8595	143	7.22196	3.85942	88	7.22197	3.85935	85
7.22193	3.8595	145	7.22195	3.85942	125	7.22193	3.85935	94
7.22191	3.85949	197	7.22192	3.85943	99	7.22191	3.85935	162
7.22189	3.85949	153	7.22188	3.85943	117	7.22188	3.85935	131
7.22186	3.85949	176	7.22187	3.85941	124	7.22187	3.85936	102
7.22183	3.8595	117	7.22184	3.85943	125	7.22184	3.85936	146
7.2218	3.8595	148	7.22181	3.85941	114	7.22182	3.85936	158
7.22177	3.85951	176	7.22179	3.85942	115	7.22178	3.85938	122
7.22174	3.85948	145	7.22175	3.85943	98	7.22176	3.85939	227
7.22171	3.85949	137	7.22173	3.85943	72	7.22172	3.85937	139
7.22169	3.85949	128	7.2217	3.85943	61	7.2217	3.85938	128
7.22167	3.8595	165	7.22168	3.85944	113	7.22167	3.85938	184
7.22165	3.85948	230	7.22165	3.85943	182	7.22165	3.85936	119
7.22161	3.85949	156	7.22163	3.85944	147	7.22161	3.85931	115
7.22158	3.85948	211	7.2216	3.85943	187	7.22158	3.85937	139
7.22156	3.85949	200	7.22155	3.85942	234	7.22155	3.85936	167
7.22153	3.85949	278	7.22153	3.85942	228	7.22153	3.85937	132
7.22151	3.85949	165	7.22151	3.85942	165	7.2215	3.85936	109
7.22146	3.85949	176	7.22149	3.85941	132	7.22149	3.85936	79
7.22145	3.85949	244	7.22146	3.8594	149	7.22146	3.85936	158
7.22141	3.85949	336	7.22143	3.8594	216	7.22143	3.85936	228
7.22138	3.85948	278	7.2214	3.8594	476	7.2214	3.85936	295
7.22136	3.85948	262	7.22139	3.8594	545	7.22138	3.85936	246
7.22134	3.85948	99	7.22136	3.8594	501	7.22135	3.85935	176
7.2213	3.85948	109	7.22133	3.8594	216	7.22131	3.85933	152
7.22128	3.85948	99	7.22129	3.85939	152	7.2213	3.85935	119
7.22126	3.85948	124	7.22127	3.85939	108	7.22128	3.85936	77
7.22124	3.85946	151	7.22124	3.85939	98	7.22125	3.85935	142
7.22122	3.85949	145				7.22123	3.85935	92
7.22121	3.8595	131				7.2212	3.85934	92

Table 5.6: Volumetric water content of soil in the kola farm during the wet season

Line 1			Line 4			Line 7		
Northing	Easting	VWC (%)	Northing	Easting	VWC (%)	Northing	Easting	VWC (%)
7.22198	3.85993	12	7.22201	3.85983	17	7.22197	3.85979	12
7.22196	3.8599	12	7.22198	3.85982	24	7.22201	3.85974	13
7.22195	3.85991	17	7.22195	3.85983	25	7.22196	3.85975	13
7.2219	3.8599	18	7.22196	3.85983	25	7.22194	3.85973	16
7.22188	3.85988	13	7.22191	3.85981	23	7.22192	3.85976	12
7.22186	3.85989	13	7.22187	3.85982	13	7.22189	3.85975	16
7.22182	3.85988	11	7.22184	3.8598	14	7.22184	3.85974	15
7.22179	3.85989	17	7.2218	3.85981	14	7.22182	3.85975	25
7.22176	3.85988	21	7.2218	3.85981	12	7.2218	3.85973	13
7.22174	3.85989	13	7.22177	3.85981	13	7.22178	3.85973	12
7.22171	3.85987	12	7.22174	3.85981	12	7.22174	3.85973	12
7.22167	3.85986	13	7.22172	3.85979	14	7.2217	3.85973	13
7.22165	3.85986	16	7.22168	3.8598	14	7.2217	3.85972	12
7.22162	3.85986	44	7.22167	3.8598	18	7.22167	3.85973	12
7.22161	3.85988	16	7.22164	3.8598	14	7.22164	3.85976	19
7.22158	3.85988	12	7.22159	3.85978	13	7.2216	3.85972	23
7.22155	3.85986	23	7.22158	3.85981	17	7.2216	3.85973	17
7.22153	3.85985	17	7.22156	3.85979	24	7.22156	3.85973	23
7.22149	3.85988	12	7.22153	3.85979	21	7.22153	3.85973	16
7.22146	3.85985	12	7.22149	3.8598	22	7.22149	3.85973	12
7.22144	3.85988	22	7.22149	3.85981	23	7.22149	3.8597	10
7.2214	3.85988	18	7.22143	3.85981	28	7.22145	3.85973	9
7.22137	3.85988	23	7.22144	3.85982	21	7.22142	3.85972	13
7.22135	3.85987	23	7.22141	3.8598	23	7.2214	3.85972	5
7.22133	3.85987	17	7.22139	3.85981	17	7.22137	3.85972	13
7.22131	3.85987	17	7.22134	3.85979	26	7.22134	3.85973	13
7.22128	3.85987	6	7.22132	3.85979	13	7.22132	3.85972	14
7.22126	3.85989	13	7.2213	3.85978	15	7.22129	3.85971	12
7.22123	3.85988	13	7.22126	3.85979	13	7.22126	3.85972	16
7.2212	3.85988	6	7.22125	3.8598	35	7.22125	3.85971	12
7.22118	3.85987	13	7.22124	3.85978	16	7.22121	3.85974	11
7.22115	3.85987	14	7.22119	3.85979	18	7.22118	3.85972	13
7.22112	3.85985	18	7.22116	3.85978	16	7.22116	3.85974	14
7.2211	3.85986	16	7.22113	3.8598	15	7.22114	3.85974	3
7.22107	3.85987	26	7.22111	3.85978	25	7.2211	3.85975	12
7.22104	3.85987	15	7.22107	3.85978	24	7.22107	3.85974	12

*VWC-Volumetric water content

Table 5.6 cont'd

Line 10			Line 13			Line 16		
Northing	Easting	VWC (%)	Northing	Easting	VWC (%)	Northing	Easting	VWC (%)
7.222	3.85964	13	7.22202	3.85958	18	7.22204	3.85952	30
7.22197	3.85965	14	7.222	3.85959	18	7.22202	3.85949	43
7.22195	3.85965	15	7.22197	3.85958	15	7.22198	3.8595	52
7.22191	3.85965	14	7.22195	3.85958	15	7.22195	3.8595	52
7.22188	3.85965	11	7.22191	3.85957	13	7.22193	3.8595	50
7.22186	3.85963	10	7.22188	3.85959	14	7.22191	3.85949	58
7.22185	3.85966	13	7.22188	3.85957	16	7.22189	3.85949	53
7.22181	3.85964	12	7.22183	3.85958	14	7.22186	3.85949	56
7.22179	3.85965	12	7.22179	3.85959	18	7.22183	3.8595	43
7.22175	3.85965	13	7.22178	3.85959	16	7.2218	3.8595	49
7.22174	3.85964	10	7.22175	3.85959	13	7.22177	3.85951	57
7.22173	3.85964	16	7.22173	3.85959	17	7.22174	3.85948	48
7.2217	3.85965	12	7.2217	3.85958	15	7.22171	3.85949	50
7.22168	3.85963	9	7.22168	3.85959	18	7.22169	3.85949	47
7.22166	3.85964	13	7.22164	3.85957	35	7.22167	3.8595	52
7.22161	3.85965	16	7.22162	3.85957	27	7.22165	3.85948	59
7.2216	3.85963	5	7.2216	3.85959	16	7.22161	3.85949	53
7.22158	3.85962	9	7.22159	3.85955	16	7.22158	3.85948	58
7.22156	3.85963	13	7.22155	3.85959	13	7.22156	3.85949	58
7.22151	3.85963	13	7.22151	3.85957	17	7.22153	3.85949	60
7.22148	3.85963	18	7.22148	3.85957	17	7.22151	3.85949	55
7.22149	3.85963	10	7.22145	3.8596	29	7.22146	3.85949	56
7.22144	3.85963	12	7.22143	3.85957	46	7.22145	3.85949	59
7.22142	3.85962	15	7.22142	3.85955	19	7.22141	3.85949	62
7.2214	3.85963	24	7.22138	3.85955	14	7.22138	3.85948	59
7.22137	3.85964	37	7.22135	3.85957	19	7.22136	3.85948	60
7.22134	3.85963	25	7.22132	3.85957	17	7.22134	3.85948	39
7.2213	3.85962	36	7.22129	3.85955	18	7.2213	3.85948	41
7.22129	3.85962	38	7.22128	3.85955	21	7.22128	3.85948	38
7.22128	3.85964	35	7.22126	3.85958	28	7.22126	3.85948	48
7.22125	3.85965	35	7.22124	3.85958	26	7.22124	3.85946	50
						7.22122	3.85949	50
						7.22121	3.8595	48

Table 5.6 cont'd

Line 19			Line 21		
Northing	Easting	VWC (%)	Northing	Easting	VWC (%)
7.22204	3.85942	43	7.22204	3.85934	58
7.22203	3.85942	39	7.22201	3.85934	54
7.222	3.85941	42	7.222	3.85935	35
7.22196	3.85942	34	7.22197	3.85935	30
7.22195	3.85942	48	7.22193	3.85935	37
7.22192	3.85943	38	7.22191	3.85935	55
7.22188	3.85943	44	7.22188	3.85935	47
7.22187	3.85941	47	7.22187	3.85936	38
7.22184	3.85943	46	7.22184	3.85936	52
7.22181	3.85941	40	7.22182	3.85936	51
7.22179	3.85942	44	7.22178	3.85938	47
7.22175	3.85943	38	7.22176	3.85939	59
7.22173	3.85943	26	7.22172	3.85937	48
7.2217	3.85943	22	7.2217	3.85938	47
7.22168	3.85944	41	7.22167	3.85938	57
7.22165	3.85943	56	7.22165	3.85936	44
7.22163	3.85944	52	7.22161	3.85931	44
7.2216	3.85943	56	7.22158	3.85937	48
7.22155	3.85942	59	7.22155	3.85936	54
7.22153	3.85942	58	7.22153	3.85937	48
7.22151	3.85942	53	7.2215	3.85936	44
7.22149	3.85941	48	7.22149	3.85936	29
7.22146	3.8594	52	7.22146	3.85936	54
7.22143	3.8594	58	7.22143	3.85936	59
7.2214	3.8594	62	7.2214	3.85936	63
7.22139	3.8594	61	7.22138	3.85936	60
7.22136	3.8594	62	7.22135	3.85935	54
7.22133	3.8594	59	7.22131	3.85933	51
7.22129	3.85939	49	7.2213	3.85935	46
7.22127	3.85939	42	7.22128	3.85936	28
7.22124	3.85939	39	7.22125	3.85935	51
			7.22123	3.85935	37
			7.2212	3.85934	35

Table 5.7: Electrical conductivity of soil in the kola farm during the dry season

Line 1			Line 4			Line 7		
Northing	Easting	EC (µS/cm)	Northing	Easting	EC (µS/cm)	Northing	Easting	EC (µS/cm)
7.22198	3.85993	27	7.22201	3.85983	41	7.22197	3.85979	30
7.22196	3.8599	22	7.22198	3.85982	37	7.22201	3.85974	27
7.22195	3.85991	32	7.22195	3.85983	52	7.22196	3.85975	23
7.2219	3.8599	36	7.22196	3.85983	34	7.22194	3.85973	25
7.22188	3.85988	28	7.22191	3.85981	46	7.22192	3.85976	27
7.22186	3.85989	34	7.22187	3.85982	38	7.22189	3.85975	32
7.22182	3.85988	26	7.22184	3.8598	29	7.22184	3.85974	28
7.22179	3.85989	35	7.2218	3.85981	32	7.22182	3.85975	25
7.22176	3.85988	40	7.2218	3.85981	24	7.2218	3.85973	23
7.22174	3.85989	37	7.22177	3.85981	25	7.22178	3.85973	28
7.22171	3.85987	23	7.22174	3.85981	24	7.22174	3.85973	25
7.22167	3.85986	33	7.22172	3.85979	34	7.2217	3.85973	34
7.22165	3.85986	60	7.22168	3.8598	41	7.2217	3.85972	27
7.22162	3.85986	59	7.22167	3.8598	32	7.22167	3.85973	30
7.22161	3.85988	33	7.22164	3.8598	26	7.22164	3.85976	38
7.22158	3.85988	31	7.22159	3.85978	21	7.2216	3.85972	35
7.22155	3.85986	31	7.22158	3.85981	45	7.2216	3.85973	33
7.22153	3.85985	32	7.22156	3.85979	45	7.22156	3.85973	31
7.22149	3.85988	23	7.22153	3.85979	34	7.22153	3.85973	24
7.22146	3.85985	24	7.22149	3.8598	27	7.22149	3.85973	15
7.22144	3.85988	38	7.22149	3.85981	38	7.22149	3.8597	12
7.2214	3.85988	39	7.22143	3.85981	43	7.22145	3.85973	22
7.22137	3.85988	39	7.22144	3.85982	41	7.22142	3.85972	29
7.22135	3.85987	37	7.22141	3.8598	51	7.2214	3.85972	26
7.22133	3.85987	39	7.22139	3.85981	32	7.22137	3.85972	32
7.22131	3.85987	40	7.22134	3.85979	53	7.22134	3.85973	29
7.22128	3.85987	29	7.22132	3.85979	27	7.22132	3.85972	27
7.22126	3.85989	28	7.2213	3.85978	32	7.22129	3.85971	18
7.22123	3.85988	30	7.22126	3.85979	17	7.22126	3.85972	30
7.2212	3.85988	19	7.22125	3.8598	42	7.22125	3.85971	21
7.22118	3.85987	32	7.22124	3.85978	30	7.22121	3.85974	27
7.22115	3.85987	36	7.22119	3.85979	34	7.22118	3.85972	22
7.22112	3.85985	34	7.22116	3.85978	27	7.22116	3.85974	16
7.2211	3.85986	42	7.22113	3.8598	28	7.22114	3.85974	13
7.22107	3.85987	41	7.22111	3.85978	32	7.2211	3.85975	18
7.22104	3.85987	29	7.22107	3.85978	27	7.22107	3.85974	23

*EC-Electrical conductivity

Table 5.7cont'd

Line 10			Line 13			Line 16		
Northing	Easting	EC (µS/cm)	Northing	Easting	EC (µS/cm)	Northing	Easting	EC (µS/cm)
7.222	3.85964	34	7.22202	3.85958	33	7.22204	3.85952	48
7.22197	3.85965	33	7.222	3.85959	34	7.22202	3.85949	45
7.22195	3.85965	37	7.22197	3.85958	35	7.22198	3.8595	59
7.22191	3.85965	36	7.22195	3.85958	27	7.22195	3.8595	58
7.22188	3.85965	24	7.22191	3.85957	21	7.22193	3.8595	76
7.22186	3.85963	19	7.22188	3.85959	27	7.22191	3.85949	95
7.22185	3.85966	28	7.22188	3.85957	39	7.22189	3.85949	74
7.22181	3.85964	23	7.22183	3.85958	33	7.22186	3.85949	68
7.22179	3.85965	26	7.22179	3.85959	40	7.22183	3.8595	72
7.22175	3.85965	25	7.22178	3.85959	29	7.2218	3.8595	71
7.22174	3.85964	20	7.22175	3.85959	27	7.22177	3.85951	62
7.22173	3.85964	35	7.22173	3.85959	31	7.22174	3.85948	77
7.2217	3.85965	26	7.2217	3.85958	33	7.22171	3.85949	72
7.22168	3.85963	15	7.22168	3.85959	37	7.22169	3.85949	53
7.22166	3.85964	24	7.22164	3.85957	46	7.22167	3.8595	74
7.22161	3.85965	28	7.22162	3.85957	44	7.22165	3.85948	73
7.2216	3.85963	16	7.2216	3.85959	45	7.22161	3.85949	83
7.22158	3.85962	17	7.22159	3.85955	38	7.22158	3.85948	80
7.22156	3.85963	21	7.22155	3.85959	34	7.22156	3.85949	89
7.22151	3.85963	22	7.22151	3.85957	34	7.22153	3.85949	116
7.22148	3.85963	24	7.22148	3.85957	40	7.22151	3.85949	81
7.22149	3.85963	21	7.22145	3.8596	45	7.22146	3.85949	77
7.22144	3.85963	27	7.22143	3.85957	60	7.22145	3.85949	87
7.22142	3.85962	27	7.22142	3.85955	35	7.22141	3.85949	130
7.2214	3.85963	39	7.22138	3.85955	32	7.22138	3.85948	80
7.22137	3.85964	51	7.22135	3.85957	35	7.22136	3.85948	69
7.22134	3.85963	41	7.22132	3.85957	41	7.22134	3.85948	62
7.2213	3.85962	55	7.22129	3.85955	36	7.2213	3.85948	63
7.22129	3.85962	52	7.22128	3.85955	44	7.22128	3.85948	48
7.22128	3.85964	48	7.22126	3.85958	43	7.22126	3.85948	49
7.22125	3.85965	39	7.22124	3.85958	56	7.22124	3.85946	50
						7.22122	3.85949	103
						7.22121	3.8595	66

Table 5.7 cont'd

Line 19			Line 21		
Northing	Easting	EC (µS/cm)	Northing	Easting	EC (µS/cm)
7.22204	3.85942	61	7.22204	3.85934	106
7.22203	3.85942	62	7.22201	3.85934	65
7.222	3.85941	54	7.222	3.85935	59
7.22196	3.85942	47	7.22197	3.85935	88
7.22195	3.85942	61	7.22193	3.85935	58
7.22192	3.85943	78	7.22191	3.85935	77
7.22188	3.85943	98	7.22188	3.85935	67
7.22187	3.85941	105	7.22187	3.85936	56
7.22184	3.85943	85	7.22184	3.85936	73
7.22181	3.85941	78	7.22182	3.85936	69
7.22179	3.85942	64	7.22178	3.85938	64
7.22175	3.85943	80	7.22176	3.85939	92
7.22173	3.85943	67	7.22172	3.85937	72
7.2217	3.85943	60	7.2217	3.85938	75
7.22168	3.85944	73	7.22167	3.85938	75
7.22165	3.85943	81	7.22165	3.85936	65
7.22163	3.85944	76	7.22161	3.85931	76
7.2216	3.85943	128	7.22158	3.85937	77
7.22155	3.85942	79	7.22155	3.85936	82
7.22153	3.85942	76	7.22153	3.85937	63
7.22151	3.85942	69	7.2215	3.85936	53
7.22149	3.85941	73	7.22149	3.85936	68
7.22146	3.8594	68	7.22146	3.85936	62
7.22143	3.8594	82	7.22143	3.85936	84
7.2214	3.8594	144	7.2214	3.85936	134
7.22139	3.8594	99	7.22138	3.85936	82
7.22136	3.8594	187	7.22135	3.85935	67
7.22133	3.8594	91	7.22131	3.85933	69
7.22129	3.85939	61	7.2213	3.85935	54
7.22127	3.85939	61	7.22128	3.85936	60
7.22124	3.85939	56	7.22125	3.85935	76
			7.22123	3.85935	57
			7.2212	3.85934	51

Table 5.8: Volumetric water content of soil in the kola farm during the dry season

Line 1			Line 4			Line 7		
Northing	Easting	VWC (%)	Northing	Easting	VWC (%)	Northing	Easting	VWC (%)
7.22198	3.85993	6	7.22201	3.85983	10	7.22197	3.85979	6
7.22196	3.8599	4	7.22198	3.85982	8	7.22201	3.85974	5
7.22195	3.85991	5	7.22195	3.85983	9	7.22196	3.85975	4
7.2219	3.8599	6	7.22196	3.85983	8	7.22194	3.85973	5
7.22188	3.85988	4	7.22191	3.85981	10	7.22192	3.85976	5
7.22186	3.85989	7	7.22187	3.85982	7	7.22189	3.85975	6
7.22182	3.85988	5	7.22184	3.8598	7	7.22184	3.85974	6
7.22179	3.85989	6	7.2218	3.85981	7	7.22182	3.85975	4
7.22176	3.85988	9	7.2218	3.85981	5	7.2218	3.85973	5
7.22174	3.85989	7	7.22177	3.85981	5	7.22178	3.85973	5
7.22171	3.85987	5	7.22174	3.85981	5	7.22174	3.85973	5
7.22167	3.85986	7	7.22172	3.85979	7	7.2217	3.85973	8
7.22165	3.85986	9	7.22168	3.8598	7	7.2217	3.85972	6
7.22162	3.85986	9	7.22167	3.8598	8	7.22167	3.85973	6
7.22161	3.85988	7	7.22164	3.8598	6	7.22164	3.85976	8
7.22158	3.85988	6	7.22159	3.85978	5	7.2216	3.85972	8
7.22155	3.85986	8	7.22158	3.85981	10	7.2216	3.85973	7
7.22153	3.85985	7	7.22156	3.85979	8	7.22156	3.85973	6
7.22149	3.85988	6	7.22153	3.85979	8	7.22153	3.85973	5
7.22146	3.85985	6	7.22149	3.8598	5	7.22149	3.85973	3
7.22144	3.85988	7	7.22149	3.85981	7	7.22149	3.8597	3
7.2214	3.85988	8	7.22143	3.85981	9	7.22145	3.85973	4
7.22137	3.85988	7	7.22144	3.85982	7	7.22142	3.85972	5
7.22135	3.85987	7	7.22141	3.8598	8	7.2214	3.85972	5
7.22133	3.85987	8	7.22139	3.85981	5	7.22137	3.85972	5
7.22131	3.85987	9	7.22134	3.85979	9	7.22134	3.85973	6
7.22128	3.85987	6	7.22132	3.85979	5	7.22132	3.85972	5
7.22126	3.85989	6	7.2213	3.85978	6	7.22129	3.85971	4
7.22123	3.85988	6	7.22126	3.85979	5	7.22126	3.85972	6
7.2212	3.85988	4	7.22125	3.8598	5	7.22125	3.85971	5
7.22118	3.85987	6	7.22124	3.85978	6	7.22121	3.85974	6
7.22115	3.85987	7	7.22119	3.85979	7	7.22118	3.85972	4
7.22112	3.85985	8	7.22116	3.85978	5	7.22116	3.85974	4
7.2211	3.85986	9	7.22113	3.8598	6	7.22114	3.85974	3
7.22107	3.85987	7	7.22111	3.85978	8	7.2211	3.85975	5
7.22104	3.85987	7	7.22107	3.85978	5	7.22107	3.85974	5

*VWC-Volumetric water content

Table 5.8 cont'd

Line 10			Line 13			Line 16		
Northing	Easting	VWC (%)	Northing	Easting	VWC (%)	Northing	Easting	VWC (%)
7.222	3.85964	6	7.22202	3.85958	6	7.22204	3.85952	7
7.22197	3.85965	5	7.222	3.85959	9	7.22202	3.85949	8
7.22195	3.85965	5	7.22197	3.85958	8	7.22198	3.8595	12
7.22191	3.85965	8	7.22195	3.85958	6	7.22195	3.8595	11
7.22188	3.85965	5	7.22191	3.85957	4	7.22193	3.8595	13
7.22186	3.85963	4	7.22188	3.85959	5	7.22191	3.85949	14
7.22185	3.85966	5	7.22188	3.85957	9	7.22189	3.85949	12
7.22181	3.85964	4	7.22183	3.85958	7	7.22186	3.85949	11
7.22179	3.85965	5	7.22179	3.85959	8	7.22183	3.8595	12
7.22175	3.85965	4	7.22178	3.85959	5	7.2218	3.8595	10
7.22174	3.85964	4	7.22175	3.85959	5	7.22177	3.85951	10
7.22173	3.85964	5	7.22173	3.85959	7	7.22174	3.85948	13
7.2217	3.85965	5	7.2217	3.85958	7	7.22171	3.85949	10
7.22168	3.85963	3	7.22168	3.85959	7	7.22169	3.85949	8
7.22166	3.85964	5	7.22164	3.85957	10	7.22167	3.8595	11
7.22161	3.85965	5	7.22162	3.85957	8	7.22165	3.85948	11
7.2216	3.85963	4	7.2216	3.85959	10	7.22161	3.85949	12
7.22158	3.85962	4	7.22159	3.85955	8	7.22158	3.85948	12
7.22156	3.85963	5	7.22155	3.85959	7	7.22156	3.85949	13
7.22151	3.85963	5	7.22151	3.85957	8	7.22153	3.85949	14
7.22148	3.85963	4	7.22148	3.85957	8	7.22151	3.85949	14
7.22149	3.85963	4	7.22145	3.8596	10	7.22146	3.85949	9
7.22144	3.85963	4	7.22143	3.85957	11	7.22145	3.85949	13
7.22142	3.85962	4	7.22142	3.85955	7	7.22141	3.85949	12
7.2214	3.85963	8	7.22138	3.85955	5	7.22138	3.85948	11
7.22137	3.85964	8	7.22135	3.85957	6	7.22136	3.85948	13
7.22134	3.85963	4	7.22132	3.85957	8	7.22134	3.85948	11
7.2213	3.85962	9	7.22129	3.85955	7	7.2213	3.85948	11
7.22129	3.85962	8	7.22128	3.85955	8	7.22128	3.85948	10
7.22128	3.85964	8	7.22126	3.85958	8	7.22126	3.85948	10
7.22125	3.85965	6	7.22124	3.85958	9	7.22124	3.85946	10
						7.22122	3.85949	12
						7.22121	3.8595	9

Table 5.8 cont'd

Line 19			Line 21		
Northing	Easting	VWC (%)	Northing	Easting	VWC (%)
7.22204	3.85942	9	7.22204	3.85934	14
7.22203	3.85942	9	7.22201	3.85934	10
7.222	3.85941	9	7.222	3.85935	9
7.22196	3.85942	7	7.22197	3.85935	11
7.22195	3.85942	8	7.22193	3.85935	8
7.22192	3.85943	11	7.22191	3.85935	12
7.22188	3.85943	13	7.22188	3.85935	10
7.22187	3.85941	15	7.22187	3.85936	10
7.22184	3.85943	11	7.22184	3.85936	11
7.22181	3.85941	12	7.22182	3.85936	10
7.22179	3.85942	11	7.22178	3.85938	9
7.22175	3.85943	11	7.22176	3.85939	11
7.22173	3.85943	12	7.22172	3.85937	10
7.2217	3.85943	8	7.2217	3.85938	11
7.22168	3.85944	11	7.22167	3.85938	12
7.22165	3.85943	12	7.22165	3.85936	12
7.22163	3.85944	11	7.22161	3.85931	11
7.2216	3.85943	12	7.22158	3.85937	10
7.22155	3.85942	11	7.22155	3.85936	11
7.22153	3.85942	11	7.22153	3.85937	11
7.22151	3.85942	8	7.2215	3.85936	7
7.22149	3.85941	11	7.22149	3.85936	8
7.22146	3.8594	9	7.22146	3.85936	9
7.22143	3.8594	11	7.22143	3.85936	11
7.2214	3.8594	15	7.2214	3.85936	13
7.22139	3.8594	13	7.22138	3.85936	11
7.22136	3.8594	11	7.22135	3.85935	12
7.22133	3.8594	12	7.22131	3.85933	9
7.22129	3.85939	11	7.2213	3.85935	9
7.22127	3.85939	9	7.22128	3.85936	8
7.22124	3.85939	9	7.22125	3.85935	10
			7.22123	3.85935	8
			7.2212	3.85934	8

Table 5.9: Thermal properties of soil in the cocoa farm during the wet season

Northing	Easting	Thermal conductivity ($Wm^{-1}K^{-1}$)	Volumetric heat capacity (mJ/m^3K)	Thermal diffusivity (mm^2/s)	Soil temperature (^0C)
Line 1					
7.22201	3.86123	1.549	1.276	1.214	25.2
7.22189	3.86123	1.656	1.512	1.095	25.81
7.22183	3.86122	2.14	2.071	1.033	24.97
7.22171	3.86121	1.499	1.51	0.993	25.13
7.22161	3.86122	2.107	2.185	0.964	24.89
7.22152	3.86121	1.885	2.498	0.755	26.13
7.22139	3.86121	1.821	3.456	0.527	25.14
7.22129	3.86119	1.514	1.67	0.907	24.97
7.22119	3.86121	2.398	3.08	0.778	26.02
Line 4					
7.22205	3.8613	2.058	2.164	0.951	25.26
7.22195	3.86132	2.314	2.131	1.086	25.04
7.22183	3.86132	2.129	2.323	0.916	24.95
7.22173	3.86131	1.812	2.109	0.859	24.6
7.2216	3.86132	1.645	2.277	0.722	25.94
7.2215	3.8613	2.023	2.982	0.678	26.6
7.22138	3.86127	2.024	2.011	1.006	25.73
7.22128	3.8613	2.176	2.554	0.852	27.46
7.22117	3.86126	1.931	2.437	0.792	26.96
Line 7					
7.22207	3.86141	2.046	2.896	0.706	26.69
7.22196	3.86141	2.02	2.131	0.947	25.93
7.22183	3.86141	2.004	2.382	0.841	25.42
7.22173	3.86142	2.118	2.216	0.955	25.52
7.22163	3.86139	1.909	2.401	0.795	26.96
7.22151	3.86138	2.307	2.693	0.855	27.63
7.22139	3.86138	2.297	2.771	0.829	26.31
7.22128	3.86138	2.535	2.876	0.881	26.77
7.22116	3.86138	2.216	2.551	0.869	25.21
Line 10					
7.2221	3.8615	2.209	2.272	0.972	26.91
7.22198	3.86147	2.016	2.388	0.844	27.28
7.22188	3.86147	1.677	2.026	0.828	27.29
7.22175	3.86146	2.187	2.903	0.753	26.29
7.22164	3.86147	1.342	2.47	0.543	25.76
7.22154	3.86145	2.103	1.914	1.099	26.53
7.22143	3.86146	2.143	2.686	0.798	26.7
7.22129	3.86146	2.323	2.852	0.815	26.08
7.22119	3.86146	1.845	2.516	0.733	26.19

Table 5.9 cont'd

Northing	Easting	Thermal conductivity ($Wm^{-1}K^{-1}$)	Volumetric heat capacity (mJ/m^3K)	Thermal diffusivity (mm^2/s)	Soil temperature (^0C)
Line 13					
7.22206	3.86154	2.023	2.136	0.947	25.85
7.22195	3.86154	2.18	2.887	0.755	26.66
7.22185	3.86155	2.082	2.484	0.838	27.25
7.22175	3.86154	1.893	1.809	1.046	26.26
7.22164	3.86155	1.706	2.143	0.796	26
7.22151	3.86155	1.562	1.954	0.799	26.17
7.22141	3.86154	1.72	2.541	0.677	25.56
7.22128	3.86154	1.998	1.913	1.045	25.74
7.22118	3.86153	1.808	1.946	0.929	25.52
Line 16					
7.22206	3.86163	2.319	2.799	0.829	25.23
7.22193	3.86164	2.431	2.508	0.969	25.5
7.22183	3.86163	2.328	2.302	1.011	25.58
7.22172	3.86164	2.379	2.142	1.11	25.52
7.2216	3.86164	2.259	2.108	1.072	25.21
7.22149	3.86163	2.365	2.508	0.943	24.85
7.22136	3.86163	1.926	1.99	0.968	24.9
7.22125	3.86163	1.948	1.909	1.021	25.56
7.22115	3.86162	1.873	1.764	1.062	24.59
Line 19					
7.22208	3.86171	2.121	2.638	0.804	25.88
7.22196	3.86173	2.437	2.574	0.947	25.96
7.22186	3.86171	1.988	2.015	0.987	25.62
7.22171	3.8617	2.321	2.519	0.921	25.32
7.2216	3.86172	2.248	2.651	0.848	25.78
7.22151	3.86171	2.306	2.744	0.841	25.53
7.22135	3.8617	2.259	2.737	0.825	24.87
7.22125	3.86171	1.448	1.954	0.741	24.91
7.22114	3.8617	2.003	2.061	0.971	24.75
Line 22					
7.22207	3.86181	2.079	2.521	0.825	26.39
7.22198	3.8618	2.196	2.315	0.948	26.2
7.22186	3.8618	1.732	1.59	1.089	26.41
7.22172	3.8618	2.15	1.993	1.079	25.07
7.22163	3.86179	2.292	2.451	0.935	24.89
7.22153	3.86179	2.3	4.578	0.502	25.22
7.22141	3.86179	2.42	2.433	0.995	24.84
7.22129	3.86179	2.03	2.649	0.766	25.63
7.22116	3.86179	2.201	2.231	0.987	25.26

Table 5.9 cont'd

Northing	Easting	Thermal conductivity ($Wm^{-1}K^{-1}$)	Volumetric heat capacity (mJ/m^3K)	Thermal diffusivity (mm^2/s)	Soil temperature (^0C)
Line 25					
7.22201	3.8619	2.515	2.821	0.892	26.24
7.2219	3.86189	2.22	2.386	0.931	25.53
7.22181	3.86189	2.643	2.151	1.229	26.29
7.2217	3.86187	2.21	2.797	0.79	25.35
7.22157	3.86188	2.258	1.466	1.54	25.11
7.22147	3.86187	2.479	2.459	1.008	25.68
7.22135	3.86187	2.126	1.31	1.623	25.69
7.22125	3.86186	2.185	2.581	0.847	25.25
7.22111	3.86186	1.927	1.89	1.02	25.2
Line 27					
7.22199	3.86194	2.42	2.738	0.884	25.31
7.22188	3.86193	2.24	2.326	0.963	25.5
7.22177	3.86193	2.33	2.174	1.072	25.69
7.22165	3.86195	2.412	2.533	0.953	25.18
7.22154	3.86193	2.329	1.812	1.285	25.4
7.22142	3.86192	2.293	1.587	1.445	25.59
7.22131	3.86194	2.326	1.167	1.994	26.21
7.22122	3.86192	2.715	4.322	0.628	24.95
7.2211	3.86191	2.169	1.815	1.195	25.56

Table 5.10: Thermal properties of soil in the cocoa farm during the dry season

Northing	Easting	Thermal conductivity ($Wm^{-1}K^{-1}$)	Volumetric heat capacity (mJ/m^3K)	Thermal diffusivity (mm^2/s)	Soil temperature (^0C)
Line 1					
7.22201	3.86123	1.6	1.897	0.843	26.65
7.22189	3.86123	0.807	1.196	0.647	28.05
7.22183	3.86122	2.018	2.407	0.838	26.24
7.22171	3.86121	1.476	1.711	0.863	27.05
7.22161	3.86122	2.213	3.5	0.632	26.65
7.22152	3.86121	1.84	2.477	0.743	28.23
7.22139	3.86121	1.813	4.233	0.428	26.72
7.22129	3.86119	1.001	2.041	0.49	27.05
7.22119	3.86121	1.166	2.172	0.537	29.45
Line 4					
7.22205	3.8613	1.035	1.519	0.681	26.76
7.22195	3.86132	1.745	2.324	0.751	26.8
7.22183	3.86132	1.497	2.156	0.694	26.59
7.22173	3.86131	2.251	2.195	1.025	26.89
7.2216	3.86132	1.529	2.253	0.679	27.79
7.2215	3.8613	1.984	2.988	0.664	29.26
7.22138	3.86127	1.205	1.94	0.621	28.77
7.22128	3.8613	1.997	2.261	0.883	28.68
7.22117	3.86126	1.469	2.381	0.617	29.11
Line 7					
7.22207	3.86141	1.282	1.49	0.86	29.19
7.22196	3.86141	1.672	2.961	0.565	27.4
7.22183	3.86141	1.73	1.626	1.064	27.18
7.22173	3.86142	1.07	1.561	0.686	28.03
7.22163	3.86139	1.556	1.805	0.862	30.43
7.22151	3.86138	1.849	2.548	0.726	31.55
7.22139	3.86138	1.329	2.232	0.596	30.32
7.22128	3.86138	1.42	2.164	0.656	30.14
7.22116	3.86138	1.663	1.787	0.93	27.56
Line 10					
7.2221	3.8615	1.796	1.946	0.923	29.01
7.22198	3.86147	0.896	1.059	0.846	33.71
7.22188	3.86147	1.507	2.019	0.746	30.67
7.22175	3.86146	1.735	1.847	0.939	27.56
7.22164	3.86147	1.205	1.87	0.645	27.49
7.22154	3.86145	0.959	1.474	0.65	29.89
7.22143	3.86146	1.44	2.448	0.588	30.23
7.22129	3.86146	1.534	1.66	0.925	29.17
7.22119	3.86146	1.852	2.119	0.874	29.54

Table 5.10 cont'd

Northing	Easting	Thermal conductivity ($Wm^{-1}K^{-1}$)	Volumetric heat capacity (mJ/m^3K)	Thermal diffusivity (mm^2/s)	Soil temperature (^0C)
Line 13					
7.22206	3.86154	1.493	1.753	0.852	29.62
7.22195	3.86154	1.155	1.751	0.659	29.16
7.22185	3.86155	1.397	1.583	0.882	29.78
7.22175	3.86154	1.767	2.244	0.787	28.45
7.22164	3.86155	1.223	1.287	0.95	27.46
7.22151	3.86155	1.551	1.366	1.135	27.3
7.22141	3.86154	2.075	1.653	1.255	28.08
7.22128	3.86154	1.959	3.662	1.959	28.57
7.22118	3.86153	1.916	1.781	1.076	28.75
Line 16					
7.22206	3.86163	0.714	1.472	0.483	26.82
7.22193	3.86164	1.179	1.66	0.71	29.51
7.22183	3.86163	1.492	1.703	0.87	27.69
7.22172	3.86164	1.033	1.887	0.547	27.95
7.2216	3.86164	1.427	1.827	0.782	27.67
7.22149	3.86163	1.363	1.769	0.77	27.34
7.22136	3.86163	1.545	2.016	0.766	27.1
7.22125	3.86163	1.506	1.427	1.056	28.15
7.22115	3.86162	1.119	1.84	0.608	26.95
Line 19					
7.22208	3.86171	1.229	1.738	0.707	29.15
7.22196	3.86173	1.224	1.489	0.836	29.83
7.22186	3.86171	1.307	2.631	0.497	27.55
7.22171	3.8617	1.039	1.606	0.647	27.31
7.2216	3.86172	1.082	2.799	0.386	28.19
7.22151	3.86171	1.342	3.054	0.44	28.8
7.22135	3.8617	1.31	2.426	0.54	27.24
7.22125	3.86171	1.533	2.308	0.664	28.08
7.22114	3.8617	1.06	2.679	0.396	27.24
Line 22					
7.22207	3.86181	1.192	1.976	0.603	29.21
7.22198	3.8618	1.246	2.069	0.602	28.23
7.22186	3.8618	0.837	1.207	0.693	30.4
7.22172	3.8618	0.969	1.33	0.729	28.15
7.22163	3.86179	1.352	1.964	0.688	27.08
7.22153	3.86179	1.718	1.93	0.89	28.53
7.22141	3.86179	0.919	1.975	0.465	26.9
7.22129	3.86179	1.56	2.113	0.738	27.88
7.22116	3.86179	1.706	2.051	0.832	27.3

Table 5.10 cont'd

Northing	Easting	Thermal conductivity ($Wm^{-1}K^{-1}$)	Volumetric heat capacity (mJ/m^3K)	Thermal diffusivity (mm^2/s)	Soil temperature (^0C)
Line 25					
7.22201	3.8619	1.701	2.016	0.844	27.78
7.2219	3.86189	1.321	1.674	0.789	27.06
7.22181	3.86189	1.411	1.064	1.329	28.36
7.2217	3.86187	1.23	3.494	0.352	27.14
7.22157	3.86188	1.84	2.695	0.683	26.84
7.22147	3.86187	1.254	2.606	0.481	27.83
7.22135	3.86187	1.02	1.755	0.581	28.17
7.22125	3.86186	1.425	1.483	0.96	26.77
7.22111	3.86186	1.026	1.884	0.545	27.83
Line 27					
7.22199	3.86194	1.182	1.598	0.74	28.34
7.22188	3.86193	1.279	2.083	0.614	29.48
7.22177	3.86193	1.507	1.558	0.967	27.84
7.22165	3.86195	1.01	0.993	1.017	27.53
7.22154	3.86193	1.609	2.094	0.768	27.63
7.22142	3.86192	0.7	0.876	0.8	27.66
7.22131	3.86194	1.112	2.914	0.381	27.34
7.22122	3.86192	1.559	2.157	0.723	27.01
7.2211	3.86191	1.134	3.234	0.351	27.55

Table 5.11: Thermal properties of soil in the kola farm during the wet season

Northing	Easting	Thermal conductivity ($Wm^{-1}K^{-1}$)	Volumetric heat capacity (mJ/m^3K)	Thermal diffusivity (mm^2/s)	Soil temperature (^0C)
Line 1					
7.22198	3.85993	1.433	1.754	0.817	25.42
7.22188	3.85988	1.959	1.917	0.979	25.86
7.22176	3.85988	1.624	2.056	0.79	25.6
7.22165	3.85986	1.076	1.881	0.572	25.53
7.22155	3.85986	1.932	2.401	0.805	25.75
7.22144	3.85988	1.977	2.085	0.948	26.11
7.22133	3.85987	1.905	2.225	0.856	25.92
7.22123	3.85988	2.071	2.73	0.759	26.46
7.22112	3.85985	1.889	2.086	0.905	26.43
Line 4					
7.22201	3.85983	1.655	1.995	0.829	25.92
7.22191	3.85981	1.903	1.93	0.986	26
7.2218	3.85981	1.782	2.155	0.827	26.44
7.22168	3.8598	2.16	2.478	0.872	26.23
7.22158	3.85981	1.847	2.524	0.732	26.12
7.22149	3.85981	2.23	2.643	0.844	25.98
7.22139	3.85981	2.202	3.003	0.733	25.96
7.22126	3.85979	1.614	1.976	0.817	26.64
7.22116	3.85978	1.577	2.029	0.777	26.59
Line 7					
7.22197	3.85979	1.333	2.566	0.519	25.96
7.22192	3.85976	1.509	2.265	0.666	26.26
7.2218	3.85973	1.074	1.639	0.655	26.72
7.2217	3.85972	1.278	1.857	0.688	26.65
7.2216	3.85973	1.123	1.673	0.671	26.66
7.22149	3.8597	1.181	1.397	0.845	29.04
7.22137	3.85972	1.252	2.262	0.553	26.86
7.22126	3.85972	1.455	3.431	0.424	27.31
7.22116	3.85974	1.5	2.267	0.662	27.54
Line 10					
7.222	3.85964	1.161	1.498	0.775	26.13
7.22188	3.85965	1.91	2.644	0.772	26.16
7.22179	3.85965	1.568	2.001	0.784	26.49
7.2217	3.85965	1.631	1.973	0.827	26.25
7.2216	3.85963	1.159	1.776	0.652	26.01
7.22148	3.85963	1.358	1.447	0.938	26.77
7.2214	3.85963	1.78	1.811	0.983	26.38
7.22129	3.85962	1.814	1.572	1.154	26.36

Table 5.11 cont'd

Northing	Easting	Thermal conductivity ($Wm^{-1}K^{-1}$)	Volumetric heat capacity (mJ/m^3K)	Thermal diffusivity (mm^2/s)	Soil temperature (^0C)
Line 13					
7.22202	3.85958	1.441	1.99	0.724	26.6
7.22191	3.85957	1.784	1.781	1.002	26.71
7.22179	3.85959	1.52	2.492	0.61	26.71
7.2217	3.85958	1.424	2.343	0.608	26.54
7.2216	3.85959	1.904	3.274	0.581	26.25
7.22148	3.85957	1.816	2.518	0.721	27.23
7.22138	3.85955	1.433	1.864	0.769	26.4
7.22128	3.85955	2.127	1.6	1.329	26.97
Line 16					
7.22204	3.85952	1.406	1.613	0.872	27.14
7.22193	3.8595	1.723	2.382	0.723	26.85
7.22183	3.8595	1.905	2.473	0.77	26.68
7.22171	3.85949	1.701	2.755	0.618	27.18
7.22161	3.85949	1.707	2.755	0.62	27
7.22151	3.85949	1.932	2.839	0.681	27.42
7.22138	3.85948	1.563	2.826	0.553	26.93
7.22128	3.85948	1.403	2.615	0.537	26.72
Line 19					
7.22204	3.85942	1.465	2.521	0.581	27.41
7.22195	3.85942	1.612	2.145	0.751	27.18
7.22184	3.85943	1.715	2.227	0.77	28.17
7.22173	3.85943	1.362	3.205	0.425	27.55
7.22163	3.85944	1.61	2.893	0.557	26.58
7.22151	3.85942	1.609	2.928	0.549	27.68
7.2214	3.8594	1.839	3.454	0.532	27.5
7.22129	3.85939	1.306	2.831	0.461	26.51
Line 21					
7.22204	3.85934	1.56	2.482	0.628	26.63
7.22193	3.85935	1.522	2.392	0.636	26.67
7.22184	3.85936	1.448	2.064	0.702	26.67
7.22172	3.85937	2.04	2.695	0.757	26.5
7.22161	3.85931	1.28	2.595	0.493	26.2
7.2215	3.85936	1.536	3.345	0.459	26.79
7.2214	3.85936	2.111	3.473	0.608	26.44
7.2213	3.85935	1.704	2.733	0.624	26.11

Table 5.12: Thermal properties of soil in the kola farm during the dry season

Northing	Easting	Thermal conductivity ($Wm^{-1}K^{-1}$)	Volumetric heat capacity (mJ/m^3K)	Thermal diffusivity (mm^2/s)	Soil temperature (^0C)
Line 1					
7.22198	3.85993	1.37	2.465	0.556	27.65
7.22188	3.85988	1.347	2.755	0.489	28.21
7.22176	3.85988	1.54	2.757	0.559	28.28
7.22165	3.85986	1.249	2.54	0.492	28.2
7.22155	3.85986	1.462	2.203	0.664	27.27
7.22144	3.85988	1.508	3.232	0.467	28.46
7.22133	3.85987	0.8	1.664	0.481	28.73
7.22123	3.85988	1.397	2.405	0.581	28.43
7.22112	3.85985	1.726	2.501	0.69	28.57
Line 4					
7.22201	3.85983	1.485	2.351	0.632	28.64
7.22191	3.85981	1.192	2.475	0.481	27.15
7.2218	3.85981	1.156	2.079	0.556	28.73
7.22168	3.8598	1.361	2.26	0.602	28.78
7.22158	3.85981	1.77	2.942	0.602	28.8
7.22149	3.85981	1.279	0.954	1.341	29.35
7.22139	3.85981	1.338	2.955	0.453	28.86
7.22126	3.85979	1.23	2.365	0.52	28.8
7.22116	3.85978	1.53	1.873	0.817	30.01
Line 7					
7.22197	3.85979	1.616	2.485	0.65	30.13
7.22192	3.85976	1.089	1.753	0.622	29.64
7.2218	3.85973	1.107	2.025	0.547	30.27
7.2217	3.85972	1.082	2.323	0.466	29.65
7.2216	3.85973	1.306	0.982	1.329	31.48
7.22149	3.8597	1.537	2.251	0.683	34.48
7.22137	3.85972	1.171	1.375	0.852	29.93
7.22126	3.85972	1.557	2.588	0.602	32.63
7.22116	3.85974	1.16	1.323	0.877	30.62
Line 10					
7.222	3.85964	1.224	2.077	0.589	31.47
7.22188	3.85965	1.568	1.991	0.787	32.12
7.22179	3.85965	1.199	1.798	0.668	34.16
7.2217	3.85965	1.063	1.517	0.701	31
7.2216	3.85963	1.002	0.863	1.161	29.83
7.22148	3.85963	1.098	1.684	0.652	31.75
7.2214	3.85963	1.424	1.908	0.747	29.68
7.22129	3.85962	1.812	1.402	1.294	32

Table 5.12 cont'd

Northing	Easting	Thermal conductivity ($Wm^{-1}K^{-1}$)	Volumetric heat capacity (mJ/m^3K)	Thermal diffusivity (mm^2/s)	Soil temperature (^0C)
Line 13					
7.22202	3.85958	1.43	1.675	0.854	32.12
7.22191	3.85957	1.302	1.891	0.688	32.02
7.22179	3.85959	1.339	2.173	0.616	30.8
7.2217	3.85958	1.529	1.485	1.028	31.26
7.2216	3.85959	1.49	2.04	0.73	31.21
7.22148	3.85957	1.43	1.742	0.821	32.8
7.22138	3.85955	1.674	1.609	1.04	31.27
7.22128	3.85955	0.758	1.523	0.498	33.08
Line 16					
7.22204	3.85952	1.197	2.043	0.586	28.62
7.22193	3.8595	1.409	2.604	0.541	27.27
7.22183	3.8595	1.694	3.279	0.517	28.17
7.22171	3.85949	1.683	2.217	0.759	28.26
7.22161	3.85949	1.468	2.102	0.699	28.44
7.22151	3.85949	2.039	2.497	0.816	28.24
7.22138	3.85948	1.477	1.791	0.825	29.17
7.22128	3.85948	1.792	1.926	0.931	28.99
Line 19					
7.22204	3.85942	1.688	2.129	0.793	28.83
7.22195	3.85942	1.655	2.122	0.778	27.72
7.22184	3.85943	0.888	1.204	0.738	29.37
7.22173	3.85943	1.869	2.081	0.898	30.12
7.22163	3.85944	1.546	2.186	0.707	28.66
7.22151	3.85942	1.22	0.76	1.605	30.89
7.2214	3.8594	1.346	2.492	0.54	28.55
7.22129	3.85939	1.734	2.312	0.74	29.38
Line 21					
7.22204	3.85934	1.124	2.22	0.506	28.51
7.22193	3.85935	1.217	2.254	0.54	28.83
7.22184	3.85936	1.686	2.224	0.758	29.34
7.22172	3.85937	1.447	1.658	0.873	29.25
7.22161	3.85931	1.298	1.287	1.009	28.55
7.2215	3.85936	1.187	1.278	0.929	31.68
7.2214	3.85936	1.326	2.361	0.561	29.03
7.2213	3.85935	1.573	2.448	0.643	31.55